Black Shales and massive sulfide deposist in the Iberian Pyrite Belt

REINALDO SÁEZ[1](*); CARMEN MORENO[1]; FELIPE GONZÁLEZ[1]; GABRIEL R. ALMODÓVAR[1]

[1]University of Huelva, Huelva, Spain, (*) saez@uhu.es

Introduction

Many massive sulfide deposits at the Iberian Pyrite Belt (IPB) are hosted by black shales. This relationship is well constrained in some of the major deposits at the province, including Neves-Corvo [1], Tharsis[2], Sotiel [3], and Aznalcóllar [4]. Geochemical environment during ore deposition has been atempted only at the Filon Norte deposit, within the Tharsis District [5][6]. New geochemical data from the black shales hosting the MS at Aznalcóllar and Sotiel show significant differences in terms of environmental conditions for ore generation. Considering the differences in metal content of each deposit, this could be noteworthy for exploration.

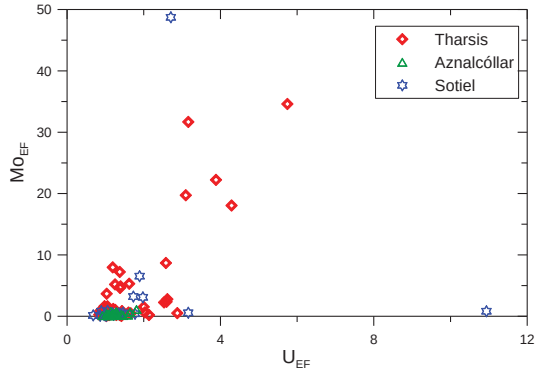

Figure 1: U_{EF} *vs* Mo_{EF} diagram for black shales hosting some IPB ore deposits. Cluster close to x-axis includes the Aznalcóllar and most of the Sotiel samples.

Inorganic geochemical proxies such V/Cr and V/V+Ni suggest general dixosic condition for Tharsis, Aznalcóllar and Sotiel. Recent studies enhance the role of U and Mo as proxies for paleo-environmental reconstructions [7]. Black shales data of these three dstricts on the U_{EF} - Mo_{EF} diagram (Fig. 1) point to disparate environmental conditions. The low absolute values as well as the absence of covariation for the Aznalcollar and Sotiel samples sugest general oxic botom water environents. At Tharsis, the positive correlation together with the dispersion of values sugest changing conditions fron oxic to strongly anoxic, and even euxinic conditions, for the depositional environment.

[1] Oliveira et al (2004) Mineralium Deposita, **39**, 422-436
[2] González et al (2002) Jour. Geol. Soc. London, **159**, 229-232
[3] González et al (2006) Geological Magazine, **143**, 821-827
[4] Almodóvar et al (1998) Mineralium Deposita, **33**, 111-136
[5] Tornos et al (2008) Economic Geology, **103**, 185-214
[6] Sáez et al (2011) Mineralium Deposita, **46**, 585-614
[7] Algeo & Tribovillard (2009) Chemical Geology, **268**, 211-225

This study is a contribution to research project P-S ANOXIA (CGL2011-30011)

Chemical U-Th-total Pb ages in recycled metamorphic terranes: the case of the South Carpathian basement units

GAVRIL SĂBĂU[1*] AND ELENA NEGULESCU[1]

[1]Geological Institute of Romania, Bucharest, Romania, g_sabau@yahoo.co.uk ([*] presenting author), elinegu@yahoo.com

Monazite chemical geochronology

Monazite geochronology has emerged as a reliable dating method for metamorphic ages, as monazite, at variance with other widely employed minerals of geochronological relevance, grows coevally with metamorphic assemblages and displays subsequent chemical and isotopic stability; even dating by chemical methods assuming isotopical equilibrium proved to be accurate enough. Yet, few data refer to metamorphic formations with complex history and thorough succesive overprints, for which the basement units of the South Carpathians represent a typical example.

Previous geochronological data and interpretation

The basement units of the South Carpathians are involved in intricate Variscan and Cretaceous thrust and wrench tectonics. Consisting mainly of medium-grade metamorphic rocks, all types of basement were traditionally considered Precambrian in age [1]. Extensive U-Pb zircon dating revealed Gondwanan provenance and protholith ages ranging from Early Proterozoic to Early Paleozoic [2]. Ar-Ar dating aimed to decipher the metamorphic history overwhelmingly indicated Variscan ages [3], sometimes at odds with cover-basement and intrusion – host-rock relationships. Therefore electron microprobe U-Th-Pb chemical chronology was attempted on rock units of the main basement complexes in order to elucidate the building blocks and temporal details of Variscan tectonometamorphic events.

Results and Conclusions

The age values derived from microprobe U-Th-Pb analyses revealed variable responses of monazite to polymetamorphic events, as well as frequent post-climactic records, resulting in age plateaus often joined by quasi-continuous spectra in case of reworked pre-Variscan complexes. Purely Variscan age patterns in rock units, also displaying microstructures and chemical zonation patterns consistent with a monometamorphic history, sandwiched between pre-Variscan terms, indicate frequent imbrication of reworked and juvenile metamorphic units during the Variscan thermotectonic events in the South Carpathian basement. The recorded evolution is consistent with complex interactions of migrating slivers that originate from the northern Gondwanan margin, up to the time of the Variscan collision. Accidental Alpine age values, mostly unrelated to pervasive metamorphic overprints, indicate low-temperature recrystallization domains in monazite, which call for caution in interpreting monazite age data.

[1] Kräutner *et al*. (1988) *in Zoubek (ed.) Precambrian in younger fold belts*, Wiley & Sons, 639-660. [2] Dallmeyer *et al.* (1998) *Tectonophysics* **290**, 111-135. [3] Balintoni *et al.* (2009) *Gondwana Research* **16**, 119-133.

Clumped and magnesium isotopes in corals: a comparison with traditional paleothermometers

SAENGER C[1*], THIAGARAJAN N[2], FELIS T[3], LOUGH J[4], HOLCOMB M[5], GAETANI G[6], COHEN AL[6], AFFEK HP[1] AND WANG Z[1]

[1]Yale University, New Haven, CT, USA, casey.saenger@yale.edu (* presenting author)
[2]California Institue of Technology, Pasadena, CA, USA.
[3]MARUM, University of Bremen, Bremen, Germany.
[4]Australia Institute of Marine Science, Townsville, Australia.
[5]University of Western Australia, Perth, Australia.
[6]Woods Hole Oceanographic Institution, Woods Hole, MA, USA.

Corals represent valuable paleoclimatic archieves that may record sub-annual sea surface temperature (SST) over many centuries. Despite strong correlations with SST, the interpretation of traditional proxies (i.e. $\delta^{18}O$, Sr/Ca) is not straightforward because variations in seawater composition and biological vital effects can overprint climatic signals. Evidence for vital effects include 1) proxy-SST calibrations that differ significantly from abiogenic relationships and 2) inter/intra-coral differences in proxy-SST calibrations. Carbonate clumped isotopes (Δ_{47}) and magnesium isotopes ($\delta^{26}Mg$) have emerged as new paleotemperature proxies that may be less prone to seawater variability and vital effects.

Based on the temperature dependent "clumping" of ^{13}C and ^{18}O into a single bond, Δ_{47} temperatures, at equilibrium, do not depend on the composition of the solution from which a carbonate forms. Furthermore, similar Δ_{47}-SST relationships in biogenic carbonates and inorganic precipitates argue against vital effects. However, early sub-annual coral Δ_{47} data deviates from the cannoical Δ_{47}-SST relationship and may reflect a vital effect [1]. We present a survey of Δ_{47} shallow water corals from the Atlantic, Pacific and Red Sea. Sub-annual Δ_{47} in two *Porites* corals shows a temperature sensitivity similar to abiogenic calibrations, but offset toward higher Δ_{47} values that underestimate SST by ~9°C. This effect cannot be attributed to laboratory artifacts or environmental variables such as salinity, but may result from fast coral calcification. Possible mechanisms for this apparent link to calcification will be discussed.

Like Δ_{47}, temperature dependent magnesium isotope fractionation [2] is unlikely to be affected by solution composition, suggesting it may also be a valuable paleo-thermometer. Sub-annual $\delta^{26}Mg$ variability in two *Porites* corals shows obvious annual cycles that are in phase with $\delta^{18}O$ and Sr/Ca, suggesting a temperature dependence not seen in previous bulk sampling [3]. However, the temperature sensitivity of coral $\delta^{26}Mg$ appears to be larger than abiogenic experiments raising the possibility of a vital effect. Potential sources for this discrepancy will be discussed.

[1] Ghosh et al. (2006) *Geochim. Cosmichim. Acta* **70**, 1439-1456.
[2] Wang et al. (2011) *AGU Fall Meeting* **PP51E-07**.
[3] Wombacher et al. (2011) *Geochim. Cosmichim. Acta* **75**, 5797-5818.

Was Mineral Surface Toxicty an Impetus for Evolution of Bacterial Extra-cellular Polymeric Substances (EPS)?

NITA SAHAI[1*], JIE XU[2], CHUNXIAO ZHU[3], NIANLI ZHANG[4], AND WILLIAM J. HICKEY[3]

[1]University of Akron, Akron, U.S.A., *sahai@uakron.edu
[2]George Washington University, Washington D.C., U.S.A., gail_xu_1982@hotmail.com
[3]University of Wisconsin, Madison, U.S.A., czhu3@wisc.edu, wjhickey@wisc.edu
[4]University of Michigan, Ann Arbor, U.S.A., nianliz@umich.edu

Bacterial community-living at the mineral-water interface is enabled by an extracellular, polymeric, biofilm matrix. Despite the energetic penalties of EPS production, biofilm formation capability likely evolved on early Earth because of several proposed crucial cell survival functions. The potential toxicity of mineral surfaces towards cells in promoting biofilm formation, however, has not been fully appreciated.

We examined here the effects of nanoparticulate oxides (amorphous SiO_2, anatase β-TiO_2, and γ-Al_2O_3) on EPS- and biofilm-producing wild-type strains and their isogenic knock-out mutants which are defective in EPS-producing ability. In particular, we used the Gram-negative wild-type *Pseudomonas aeruginosa* PAO1 and its EPS knock-out mutant *Δpsl*, and the Gram-positive wild-type *Bacillus subtilis* NCIB3610 and its EPS-knock-out mutant *yhxB*Δ. Results showed that (a) cell viability was lower in the presence of each oxide relative to its oxide-free control, (b) toxicity was mineral-specific, and could be related to surface charge and particle size, (c) toxic minerals could induce EPS production, (d) the amount of EPS generated in the presence of oxides was related to relative toxicity of the minerals, and (e) Gram-positive cells were less susceptible to mineral toxicity than Gram-negative cells. Taken together, these results indicated a previously unrecognized role for microbial extracellular polymeric substances (EPS) in shielding bacterial cells against the toxic effects of mineral surfaces.

The function of EPS proposed here is distinct from the previously proposed roles. It is likely that EPS played multiple functions, including our hypothesized role of protecting against mineral toxicity. Furthermore, not all minerals are toxic or benign, and toxicity depends on surface chemistry and particle size. Our results provide insight to the potential impact of nanoparticulate mineral surfaces in promoting increased complexity of cell surfaces, including EPS and biofilm formation, on early Earth.

The Role of Water Molecules in Stabilizing Amorphous Calcium Carbonate: A Computer Simulation Study

M. SAHARAY[1*], A. OZGUR YAZAYDIN[2], AND R. JAMES KIRKPATRICK[3]

[1]Department of Chemistry, Michigan State University, East Lansing, Michigan 48824, USA, saharaym@chemistry.msu.edu (* presenting author)

[2]Department of Chemical Engineering, University of Surrey, Guildford, GU2 7XH, United Kingdom, a.yazaydin@surrey.ac.uk

[3]College of Natural Science, Michigan State University, East Lansing, Michigan 48824, USA, rjkirk@cns.msu.edu

Session 18b. Nucleation, Growth, and Dissolution in Aqueous Environments: Elementary Processes and Atomistic Models

Amorphous calcium carbonate (ACC) is a critical transient phase in the inorganic precipitation of $CaCO_3$ and in bio- and biomimetic mineralization. Proteins known to be responsible for the biomineralization of, for instance, bird egg shells, bind to ACC nanoparticles and lower or remove the energy barrier to crystallization. The mechanisms of these processes are related to the structures of hydrous and anhydrous ACCs, but the details are poorly known. To advance fundamental molecular-level understanding of the bulk hydrous and anhydrous ACC, we studied these systems using both classical and quantum mechanical simulation methods. Car-Parrinello molecular dynamics (CPMD) simulations of calcium carbonate solvated in a bath of water molecules have been performed at a temperature of 300K to elucidate the microscopic structure, dynamics, and electronic properties of water molecules in the first two solvation shells of calcium carbonate. The reorientational dynamics of near-neighbor water molecules around Ca^{2+} and CO_3^{2-} ions are investigated through first- and second-order time correlation functions, and are in good agreement with nuclear magnetic resonance experiments. The intramolecular vibrations of CO_3^{2-} ion have also been examined through an analysis of the velocity autocorrelation function of the atoms and are compared with that of isolated $CaCO_3$ and existing vibrational spectra of calcium carbonate. In addition, classical molecular dynamics simulations of pre-nucleated ACC are carried out to understand the role of water molecules in stabilizing these clusters. Starting from a hydrous ACC model with a $CaCO_3/H_2O$ ratio of 1/1, we gradually reduced the water concentration of the system to completely dehydrated ACC. Simulation results using the DL_POLY software on the structure and dynamics of the constituent molecules due to drying will be presented.

Acknowledgements

We thank Prof. Richard J. Reeder and Prof. Brian Phillips for providing the atomic positions from the reverse Monte Carlo model of ACC [1].

[1] Goodwin, A. L.; Michel, F. M.; Phillips, B. L.; Keen, D. A.; Dove, M. T.; Reeder, R. J.(2010) *Chemistry of Materials* **22**, 3197.

New U-Pb ages for gabbro sills within the Ramah Group, northern Labrador: implications for Paleoproterozoic extension in Nain craton, and metallogeny

T. SAHIN[1*], M.A. HAMILTON[1], P.J. SYLVESTER[2], AND D.H.C. WILTON[2]

[1]University of Toronto, Geology, Toronto, Canada, tsahin@geology.utoronto.ca (* presenting author); mahamilton@geology.utoronto.ca

[2]Memorial University, Earth Sciences, St John's, Canada, psylvester@mun.ca; dwilton@mun.ca

Archean gneisses of the North Atlantic craton (NAC) in northern Labrador are unconformably overlain by three principal Paleoproterozoic supracrustal remnants – the mostly clastic Snyder/Falls Brook Group, the dominantly volcanic Mugford Group, and, furthest north, the chiefly sedimentary Ramah Group.

Ramah Group is an ~1700m thick cover sequence of lowermost siliciclastic quartz sandstone capped by a distinct supratidal dolomite horizon, together defining a west-facing shallow shelf sequence, overlain by euxinic, pyritic shales and mudstones and pyrite-chert associations (Nullataktok Formation). Upwards, this unit passes through a mixture of carbonate debris flow breccias, and then into voluminous turbiditic sandstones. Sills of diabase or gabbro extensively intrude the upper sedimentary units. The sills typically exhibit chilled margins, and are clearly transgressive to their host sediments. Sills reach up to ~100 m in thickness, though many are only a few meters thick, in many places with preserved primary layering. The entire sequence of sedimentary rocks and sills was deformed and (locally) metamorphosed to amphibolite facies, as part of an east-verging fold-and thrust belt on the east margin of the 1.78 Ga Torngat Orogen. The depositional age of the Ramah Group has only been bracketed only between its late Archean (ca. 2.5 Ga), Nain craton-derived detrital zircons, and Torngat deformation.

We have dated both gabbroic and ultramafic compositional variants of Ramah sills, from samples collected from thick sheets intruding the Nullataktok Formation. ID-TIMS U-Pb baddeleyite analyses yield identical ages of emplacement at 1888 ± 5 and 1887 ± 4 Ma. These represent the first precise U-Pb dates for extension-related mafic magmatism of this age in the NAC in Labrador, and provide a new minimum age for the host Ramah Group sediments. Mafic magmatism of this age is unknown in the Greenland portion of the craton, but is well represented in the Circum-Superior belt, including the ca. 1883 Ma Molson dyke swarm and Fox River sill of Manitoba (Molson Igneous Events), the 1890-1870 Ma Raglan-Expo-Katiniq sills of the Cape Smith belt, Ungava, and the 1884-1874 Ma mafic-ultramafic magmatism of the Labrador Trough.

By analogy with contemporaneous Circum-Superior sediment-sill complexes (Thompson, Birchtree, Raglan-Expo), Ramah Group may have potential for magmatic Ni-Cu-PGE sulfide deposits.

Ocean redox changes in the wake of the Marinoan glaciation

S. K. SAHOO[1]*, N. J. PLANAVSKY[2], B. KENDALL[3], X. WANG[4], X. SHI[4], A. D. ANBAR[3,5], T. W. LYONS[2] AND G. JIANG[1]

[1]Dept. Geoscience, Univ. Nevada, Las Vegas, NV, USA (*presenting author: sahoos@unlv.nevada.edu), and ganqing.jiang@unlv.edu
[2]Dept. Earth Science, Univ. California, Riverside, CA, USA noah.planavsky@email.ucr.edu and timothy.lyons@ucr.edu
[3]SESE, Arizona State Univ. Tempe, AZ, USA brian.kendall@asu.edu and anbar@asu.edu
[4]Sch. Earth Sc. & Res., Univ. Geosciences, Beijing, China wxqiang307@yahoo.com.cn and shixyb@cugb.edu.cn
[5]Dept. Chem/Biochem, Arizona State Univ. Tempe, AZ, USA

Metazoans first appeared in the fossil record shortly after the termination of the late Cryogenian (Marinoan) glaciation about 635 Myr ago [1]. It has been long hypothesized that an oxygenation event was the driving factor behind the rise and early diversification of metazoans [2], but there is little evidence for a direct link between animal and redox evolution. Here we report new geochemical data from early Ediacaran organic-rich black shales of the basal Doushantuo Formation in South China. These shales were deposited with a strong connection to the open ocean [3] and span the interval of the earliest metazoan fossil [1]. The temporal record of trace metal enrichments (particularly molybdenum) in euxinic shales currently provides one of the clearest signals for a significant redox shift in the Neoproterozoic [4,5]. However, prior to our study the oldest known occurrences of Phanerozoic-like trace metal enrichments are found near the end the Ediacaran (ca. 551 Ma) [4,5], long after the radiation of complex metazoans [1].

In contrast, we found very high, Phanerozoic-like, redox sensitive trace element (molybdenum, vanadium and uranium) abundances in euxinic shales (as identified by sedimentary Fe speciation) that were deposited between 635 and 630 Ma, within five million years of the Marinoan glaciation and coincident with the appearance of the earliest metazoan fossils. Moreover, highly negative pyrite sulphur isotope ($\delta^{34}S_{pyrite}$) values down to –35‰ from basinal samples also point toward an oxidizing ocean-atmosphere system. The isotope fractionation between pyrite and coeval sulphate in the deep basin section is >65‰—equivalent to the maximum fractionations observed in the Phanerozoic rock record [6]. As increase in the fractionation in the Neoproterozoic has been commonly linked to growth of the marine sulphate reservoir and surface oxidation [5], the large sulphur isotope fractionation, therefore, point toward a well oxidized ocean-atmosphere system. Our data provide the first direct evidence for a significant early Ediacaran postglacial oxygenation event. Our results support a casual link between one of the most severe glaciations in Earth's history, the oxygenation of the Earth's surface, and the earliest diversification of complex animals.

[1] Yin (2007) *Nature* **446,** 661-663. [2] Knoll (1999) *Science 284,* 2129-2137. [3] Jiang (2011) *Gondwana Research* **19**, 831-849. [4] Scott (2008) *Nature* **452**, 456-459. [5] Och (2011) *Earth-Science Reviews* **110**, 26-57. [6] Sim (2011) *Science* **333**, 74-77.

Radium interactions with iron (oxy)hydroxide minerals.

M. SAJIH[1*], N.D.BRYAN[1], D.J. VAUGHAN[2], M. DESCOSTES[3], V. PHROMMAVANH[3], KATHERINE MORRIS[1,2]

[1] Centre for Radiochemistry Research and Research Centre for Radwaste and Decommissioning and [2]Williamson Research Centre for Molecular Environmental Science, The University of Manchester, Manchester, M13 9PL. [3]AREVA NC - Business Group Mines, Direction R&D, BAL 3720C, Tour AREVA, 1, Place Jean Millier, 92084 Paris La Défense Cedex, France. (*correspondence: mustafa.sajih@ manchester.ac.uk)

Typically, radium is the most significant contributor to dose in mining effluents from legacy uranium mining operations. However, little is known regarding the uptake of Ra^{2+} by iron (oxy)hydroxide minerals under environmental conditions representative of the mining wastes. Here, we assess the behaviour of Ra^{2+} (and Ba^{2+} as a chemical analogue of Ra^{2+}) to provide surface complexation constants that will be used in the prediction of Ra^{2+} speciation, mobility and fate across a range of environmental conditions.

Radium and barium uptake onto ferrihydrite and goethite was studied in the concentration range nM to mM and from pH 5 - 10, conditions commonly found in legacy U-mine wastes. For ferrihydrite, uptake of Ra^{2+} at nM concentrations was strong at pH > 7. At higher concentrations (µM - mM) Ba^{2+} sorption to ferrihydrite was slightly weaker than that of Ra^{2+}. Experiments with goethite showed weaker binding for both metal ions in all systems studied. Ongoing experiments are exploring the reversibility of these systems. In addition, we are exploring the behaviour of Ra^{2+} during transformation of ferrihydrite to goethite, a process of potential importance in the impacted environments.
Surface complexation modelling has successfully simulated Ra^{2+} and Ba^{2+} sorption across the pH and concentration ranges studied. These data will be used in underpinning the safety case for legacy mining sites.

Ectomycorrhizal sclerotia formation and status of organo-mineral complex aluminum in low pH *Fagus* forest

NOBUO SAKAGAMI[1*] AND MAKIKO WATANABE[2]

[1]Ibaraki University, College of Agriculture, sakagami@ams.kuramae.ne.jp (* presenting author)

[2]Tokyo Metropolitan University, Department of Geography, m.wata@tmu.ac.jp

Sclerotia of ectomycorrhizal fungus *Cenococcum geophilum* are preserved in soils with *Cenococcum* mycorrhizae.[1] Ferricrocin is known as an ectomycorrhizal siderophore of *Cenococcum geophilum*.[2, 3] In our previous studies, we reported a characteristic concentration of aluminum in sclerotium and the relationship between aluminum (plus iron) content in sclerotia and active aluminum and iron in soils.[4, 5] Absorption of aluminum and iron may be an evidence of activity of *C. geophilum* associated with its siderophore. This fact harmonizes with microbial dissolution of aluminum and iron from minerals studied on ectomycorrhizal fungus.[6] In this study, we established 10 × 10-m quadrat beneath the *Fagus* forest in northeastern Japan, and then subdivided the plot using a 2 × 2-m grid. Thirty six surface soil samples were collected at each grid node.

The SEM-EDX observation (JSM-6610LV, JEOL) on distribution of elements in a cross section of soil aggregate including a sclerotium showed a slight accumulation of aluminum on soil surrounding sclerotium (Fig.1).

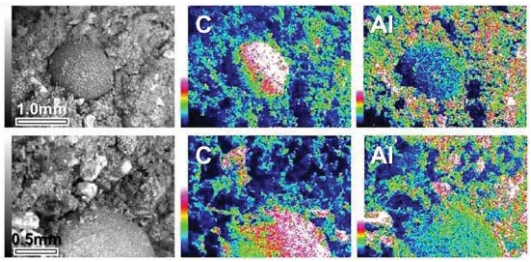

Figure 1: Distribution of C and Al in a cross section of soil aggregate including a sclerotium by SEM-EDX analysis.

According to the analytical results of the sclerotia content, and the status of aluminum in soil (dithionite-citerate, oxalate, pyrophosphate, ammonium acetate, and water extractable aluminum), we discuss the interaction between sclerotia formation and the status of soil aluminum. Furthermore, the interaction between soil and ectmycorrhizal activities in the investigated forest soils are noted regarding with micro topography, *Fagus* stands and floor vegetation.

[1] Trappe (1964) *Lloydia* **27**, 100-106. [2] Haselwandter & Winkelmann (2002) *BioMetals* **15**, 73-77. [3] Hoffland et al. (2004) *Front. Ecol. Env.* **2,** 258-264. [4] Watanabe *et al*. (2001) *Soil Sci. Plant Nutr*. **47**, 411-488. [5] Sakagami et al. (2007) *Proc. OMD 2007*, 402-403 [6] Watteau & Berthelin (1994) *Euro. J. Soil Biol.* **30**, 1-9.

Spectroscopic studies on sedimentary organic material

FANI SAKELLARIADOU

University of Piraeus, Maritime Studies Dept, Piraeus, Greece, fsakelar@unipi.gr

Introduction

Sediment samples from the Saronicos gulf, belonging to the Aegean Sea, were studied for the characterization of humic substances (HS) and dissolved organic matter (DOM). HS are significant sediment constituents performing in metal and toxic material scavenging and transport. Infrared and fluorescence spectroscopy were applied. DOM corresponds to the most active and mobile form of soil organic matter and the major soluble component of natural aquatic systems, with significant functions in the ecological and environmental system. DOM was studied by fluorescence spectroscopy.

Results and discussion

Spectroscopic methods on HS: The application of IR spectroscopy gives spectra with the characteristic peaks for hydroxyl, methyl, methylene, aromatic bond, carbonyl, carboxyl, phenol, alcohol, polysaccharide and silicate impurities. Conventional fluorescence spectroscopy [1] provides with emission spectra with maximum emission intensity at 415-427nm, excitation spectra with a major excitation peak at 355 to 330nm, and synchronous-scan excitation spectra with a very structured form; suggesting the presence of humic-like material with a marine origin.

Spectroscopic methods on DOM: Mono-dimensional emission spectra reveal one typical broad peak with a maximum between 442 and 439 nm. Excitation spectra show three peaks or shoulders at 330 nm, 351 nm, 377-381 nm, and a shoulder at 440 nm. Synchronous scan excitation spectra show one strongest peak at 340-345nm and another much lower or lower intensity peak or shoulder at 385-387nm. Therefore, it seems that fulvic acids, aquatic humic acids and natural organic matter are present. Higher humification index [2, 3], related to a more condensed nature, corresponds to areas with weaker seawater circulation [4]. Excitation/emission matrix spectra (EEMS) exhibit the peak M [5] corresponding to the marine humic fluorophore, strongly correlated with biological activity

[1] Senesi *et al.* (1991) *Soil Science* **152**(4), 259-271. [2] Ohno (2002) *Environ. Sci. and Technol.* **36**, 742-746. [3] Zsolnay *et al* (1999) *Chemosphere* **38**, 45-50. [4] Luciani *et al*. (2008) *Mar. Environ. Res.* **65**, 148-157. [5] Sakellariadou (2012) *IJOO* **6**, 27-43.

A coupled biomarker-genetic approach to understanding the $U^{k'}_{37}$ SST proxy in estuaries

JEFF SALACUP[1*], TIMOTHY HERBERT[1], WARREN PRELL[1]

[1]Brown University, Providence, RI, USA,
Jeffrey_Salacup@brown.edu (* presenting author)

Towards a mechanistic understanding of $U^{k'}_{37}$

The $U^{k'}_{37}$ SST proxy has been widely and successfully applied in the reconstruction of open ocean temperatures on centennial to orbital timescales and has proved an indispensable tool in our investigations of past climates. However, the utility of the $U^{k'}_{37}$ SST proxy is thought to break down in near shore settings experiencing more dynamic nutrient and salinity fluctuations. Given the importance of coastal systems, , knowledge of past local to regional SST variability is critical to habitat adaptation and restoration strategies. Furthermore, the rapid deposition of both marine and terrestrial organic and inorganic material in estuarine and coastal systems makes them valuable archives of high-resolution paleo-environmental information.

Here, we present the results of a 3-year-long monthly to sub-weekly resolved record of water column $U^{k'}_{37}$ and alkenone concentration (C_{37}total) and associated instrumental SST suggesting that while important and informative seasonal inconsistencies exist, especially during alkenone blooms, the integrated $U^{k'}_{37}$ signal preserved in Narragansett Bay sediments reflects mean annual instrumental SST. A subset of samples were analyzed for haptophyte-specific 18S ribosomal RNA (rRNA) to understand the composition of the alkenone-producing community during times of instrumental-$U^{k'}_{37}$ coherency and incoherency, alike. So far, the only alkenone-producing species detected in Narragansett Bay, *E.huxleyi* and *G.oceanica* - which dominate open-ocean production and form the foundation of the $U^{k'}_{37}$-SST calibration – were detected in the high salinity lower-Bay during the spring bloom of 2010. A second 'brackish' alkenone-producing population is suspected on the basis of high contributions of the $C_{37:4}$ alkenone in the low-salinity upper Bay.

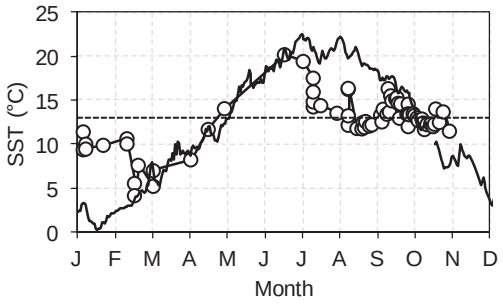

Figure 1. An example of the discrepancy between instrumental SST (solid line) and $U^{k'}_{37}$-inferred SST (open circles) from 2010. C_{37}total-inferred haptophyte blooms peaked in Feb and Aug during periods of maximum instrumental-$U^{k'}_{37}$ SST divergence. Black dashed line is the mean annual instrumental SST for Narragansett Bay for 2009-2011 (~13.4°C).

Fingerprinting uranium-bearing material: development and validation of methods

A. SALAÜN[1*], A. HUBERT[1], J. AUPIAIS[1], E. PILI[1], F. POINTURIER[1], S. DIALLO[1], A.-L. FAURE[1] AND P. RICHON[1].

[1]CEA, DAM, DIF, F-91297 Arpajon, France,
anne.salaun@cea.fr (*presenting author)

The nuclear forensics project

Many parameters such as trace elemental impurity patterns [1], uranium or oxygen isotopic compositions [2, 3] and anionic impurities [4] are known to be tracers of geographical origin of uranium-bearing materials. These parameters can allow to go back to a part of the history (industrial treatment or origin) of a seized nuclear material when they are used individually (Figure 1).

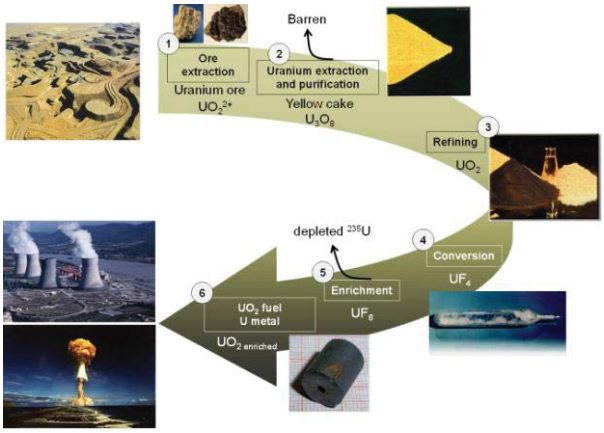

Figure 1: From ore to fuel: a variety of steps for uranium fingerprinting

But in some cases, they are not enough discriminating. We herein document a complete characterization of reference and unknown uranium ore concentrates for which REE, ($^{234}U/^{238}U$) and oxygen isotopic compositions were determined. This original approach which combined all three determinations covers a more global overview of such material.

Methods

A complete analytical procedure has been developed on a single sampling for trace-level determination of lanthanides and U isotopic composition in yellow cakes using ICP-MS, TIMS and PERALS (Photon Electron Rejecting Alpha Liquid Scintillation). The method was validated by the measurement of a reference material and will be applied for the analysis of unknown yellow cakes from various origins. Similarly, oxygen isotopic compositions of reference yellow cakes are currently under measurement by SIMS (Secondary Ion Mass Spectrometry) on particles and by fluorination on bulk samples.

[1] Varga (2010) *Radiochimica Acta* **98**, 771-778.
[2] Keegan (2008) *Applied Geochemistry* **23**, 765-777.
[3] Tamborini (2002) *Analytical Chemistry* **74**, 6098-6101.
[4] Badaut (2009) *J. Radioanal. Nucl. Chem.* **280**, 57-61.

Kinetic modeling of olivine carbonation reaction: study of the rate dependence on temperature and pCO_2 in open and closed systems

GIUSEPPE D. SALDI[1*], DAMIEN DAVAL[1,2] AND KEVIN G. KNAUSS[1],

[1]Lawrence Berkeley National Laboratory, Berkeley, CA, gdsaldi@lbl.gov (* presenting author); ddaval@lbl.gov; kgknauss@lbl.gov

[2] LHyGeS, CNRS UMR 7517, Strasbourg, France

Although both olivine dissolution and magnesite precipitation rates have been studied and modeled over a significant range of temperatures and aqueous chemical compositions, the mechanisms of the process that combines these two reactions have not been adequately described from a kinetic standpoint.

It was shown that the formation of a silica passivating layer at the interface between pristine olivine and aqueous solution can significantly slow down or even stop the dissolution of this mineral, thus hindering the attainment of the conditions necessary to initiate the carbonation reaction [1, 2]. Recent experimental measurements also indicate that magnesite precipitation can be the rate limiting step to forsterite carbonation in some other conditions [3].

To improve the understanding of mineral carbonation processes and provide new data that can contribute to its kinetic description we conducted a series of experiments in pure water from 90 to 180 °C, at a pCO_2 of 100 and 200 bar, using both the well characterized San Carlos olivine and a pure synthetic forsterite sample. Batch experiments were performed in flexible Au bags whereas steady-state carbonation rates were investigated at 150 °C by means of a mixed-flow Ti-reactor. The study of the chemistry of aqueous solution and the analysis of reacted olivine samples by XRD, SEM-EDX and Rockeval 6 allowed us to describe quantitatively the carbonation reaction as a function of pCO_2 and temperature. All experiments were characterized by the ubiquitous presence of a silica-rich layer at the olivine-aqueous solution interface. The nature of this layer changes as a function of temperature, and can lead to increasing rates of carbonation as magnesite precipitation rates increase with increasing temperature.

Comparison between the results obtained from two one-month-long batch and mixed-flow reactor experiments at 150 °C show that the extent of carbonation is limited by the saturation with respect to a silica polymorph, and possibly by the formation of secondary Mg-silicates. In the closed system, olivine to magnesite conversion rates are <1 %, whereas the extent of carbonation are significantly higher in the open system (8-9 % at least) and magnesite precipitation was found to be the rate limiting step of the reaction in this latter case.

The role of Fe in the passivating properties of the silica layer and its incorporation into the carbonate phase under reducing conditions is also being studied and some experimental results will be presented.

[1] Bearat et al. (2006) *Environ. Sci. Technol.***40**, 4802-4808. [2] Daval et al. (2011) *Chem. Geol.***284**, 193-209. [3] Saldi et al. (2012) *Geochim. Cosmochim. Acta*, doi:10.1016/j.gca.2011.12.005.

High precision 4-isotope Sulfur measurements using the CAMECA IMS 1280-HR

P. PERES, F. FERNANDES, M. SCHUHMACHER, P. SALIOT*

CAMECA, 29 quai des Grésillons, 92622 Gennevilliers Cedex, France, peres@cameca.com

Secondary Ion Mass Spectrometry (SIMS) technique provides direct in situ measurement of elemental and isotopic composition in selected µm-size areas of the sample. The CAMECA IMS 1280-HR is an ultra high sensitivity ion microprobe that delivers unequalled analytical performance for a wide range of SIMS applications: isotope ratio measurements, geochronology applications (U-Pb dating in Zircon), trace element analyses, particle screening measurements,...

Conventional Sulfur isotope studies focus on the two most abundant isotopes ^{32}S and ^{34}S. However, there has been an increasing interest in the minor ^{33}S (~0.7%) and ^{36}S (~0.02%) isotopes since mass independent fractionation effects have been discovered [1-3].

This paper presents 4-isotope Sulfur data obtained on standard and unknown pyrite samples. Measurements have been performed using a small 10µm Cs^+ beam spot, and high mass resolution conditions (~4,500) to resolve the hydride mass interferences. The four S isotopes have been collected simultaneously: ^{32}S, ^{33}S and ^{34}S on Faraday Cup detectors, and the low abundance ^{36}S (intensity ca. $2x10^5$ c/s) on an Electron Multiplier. The EM yield drift has been automatically monitored and corrected using a propriatery algorithm. More than 100 spot analyses have been performed in fully automated mode, with an analysis time of 4 minute/spot.

Data on the standard sample show that a precision < 0.2 permil (1SD) can be achieved for $\delta^{34}S$, $\delta^{33}S$ (and $\Delta^{33}S$). An excellent precision, < 0.3 permil (1SD), is also obtained for $\delta^{36}S$ (**Figure 1**) and $\Delta^{36}S$.

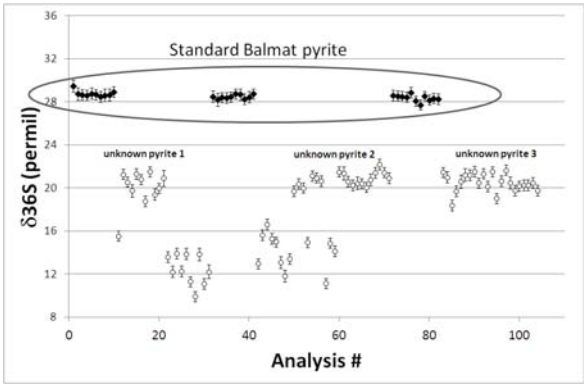

Figure 1: $\delta^{36}S$ data on standard and unknown pyrite samples.

This measurement protocol with multicollection configuration FC-FC-FC-EM allows to work with good spatial resolution (spot size ~10µm) and yields excellent precision for all Sulfur isotopes, including for the lowest abundance ^{36}S.

[1] Kamber and Whitehouse (2007) *Geobiology* 5, 5-17.
[2] Williford et al. (2011) *GCA* 75, 5686-5705.
[3] Whitehouse (2011) *Goldschmidt 2011 abstract*, 2155.

Ultra depleted mantle at the Gakkel Ridge

VINCENT SALTERS[1*], AFI SACHI KOCHER1, HENRY J.B.DICK[2]

[1]NHMFL and EOAS, Florida State University, Tallahassee, Florida, USA, salters@magnet.fsu.edu (* presenting author) [8pt font size]

[2]MG&G, Woods Hole Oceanographic Institution, Woods Hole, Massachusetts, USA, hdick@whoi.edu

The Gakkel Ridge is one of the slowest spreading ridge segments in the global ridge system and with some of the thinnest oceanic crust. In some locations there is little or no evidence for volcanic activity and oceanic mantle is directly exposed on the ocean floor. This provides an excellent opportunity to investigate the heterogeneity of the oceanic mantle in situ.

We have analyzed a number of peridotites from the western end of the Sparsely Magmatic Zone (3° to 28°E as well as samples further west up to 65°E) and found highly radiogenic Hf and Nd isotopic composition. All but five samples are more radiogenic in either Nd or Hf than MORB. Six samples lie in the extension of the OIB MORB array with ε_{Nd} up to 23.7 and ε_{Hf} up to 54.6. The remainder of the data (14 samples) lie above the OIB-MORB array and its extension with ε_{Nd} values up to 27.4 and ε_{Hf} values up to 291! These values are the most extreme values measured for oceanic mantle. This data confirms the ultra depleted nature of the Gakkel Ridge mantle [1] and its highly heterogeneous nature [2].

Since the Hf and Nd system is expected to behave similar during melting, melt can be added back in the peridotite until the Hf and Nd model age coincide. These calculations show that depleted Gakkel Ridge peridotites have very little melt extracted from them (<1%) and have model ages that ranges from 2.4Ga to future ages with most between 600Ma and 1.2 Ga. The MORB Hf-Nd isotope systematics indicate this depleted component (ReLish) is ubiquitous [3] but under-sampled in basalts due to its depleted character. The presence of ReLish decrease the amount of melt a heterogeneous parcel of mantle can yield during ascent and average melt rate can be much lower requiring depth of melting to start deeper.

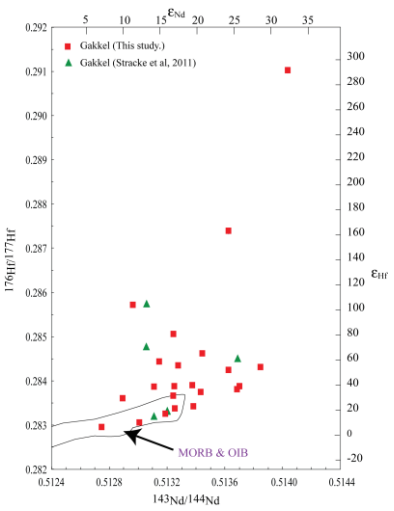

[1] Stracke, A, *et al*., *Earth Plan. Sci. Lett*, **308**, 359-368 (2011).

[2] Liu, C.Z., *et al*., *Nature*, 452, 311-315 (2008).

[3] Salters, V.J.M., et al., *Geochem. Geophys. Geosys*. 12, Q08001.

Integrated TIMS-TEA/LA-ICPMS constraints on pluton emplacement

K. SAMPERTON[1*], B. SCHOENE[1], J. COTTLE[2] AND J. CROWLEY[3]

[1]Princeton University, Department of Geosciences, Princeton NJ, USA, ksampert@princeton.edu (*presenting author)

[2]University of California–Santa Barbara, Department of Earth Science, Santa Barbara CA, USA, cottle@geol.ucsb.edu

[3]Boise State University, Department of Geosciences, Boise ID, USA, jimcrowley@boisestate.edu

Major conceptual and technical breakthroughs over the past decade have increased temporal and spatial resolutions for both ID-TIMS and LA-ICPMS. An outgrowth of this development is the ability to address whether zircon U-Pb ages can be assumed *a priori* to equate to the timing of pluton emplacement. We employ an integrated analytical regime coupling U-Pb TIMS-TEA with *in situ* LA-ICPMS trace element characterization in order to 1) assess intra-grain trace element zoning at the five micron scale and couple this with "bulk" geochemical and geochronological data, 2) fingerprint crystal populations within a single sample and better interpret age spread in high-precision datasets, and 3) characterize the temporal and geochemical evolution of magmas during ascent, mixing, and pluton assembly.

We apply this methodology to the 32-30 Ma Bergell Intrusion (N Italy), which preserves a spectacular 12-15 km crustal section through a single, continuous magmatic system, in addition to distinct process zones (pluton roof, floor, and feeder zone/tail). Preliminary U-Pb ID-TIMS zircon geochronology of CL-imaged grain fragments documents 400-500 kyr of zircon growth within individual hand samples ranging in composition from megacrystic granodiorite to tonalite. Precision on individual analyses of 10-20 ka (~0.05%) makes this duration easily resolveable. *In situ* trace element transects performed on the exact same minerals prior to ID-TIMS dating exhibit evolving core-to-rim REE and Hf abundances, which are interpreted to represent evolving magma composition and/or temperature. Variability in trace elements across single grains is often small compared to variation across many grains, necessitating high-precision ID-TIMS U-Pb geochronology in conjunction with the trace element data in order to evaluate long term (> tens of ka) trends in magma evolution, even in apparently autocrystic zircon populations. Geochemical transects were used to generate numerically modeled bulk trace element signatures and compared to TIMS-TEA data. The combination of these approaches produces trends strongly suggestive of closed system evolution of zircon chemistry through time for samples from ~15-20 km paleodepth.

While our data support TIMS-TEA as a viable analytical protocol, further work is required to understand the emplacement history of the Bergell. Expansion of our existing geochronologic/trace element dataset to include other dateable accessory phases indentified in Bergell samples, including monazite, allanite, and sphene, will be integrated with field observations and structural data in order to place robust constraints on such geochemical information. Our geochronological approach in the context of detailed geologic mapping will allow us to directly test competing models of Bergell emplacement (e.g., diapiric uprise vs. incremental assembly) by comparing the chronologies of different process zones (e.g., synmagmatically-deformed pluton floor vs. ballooning roof).

The role of fluids in the formation of REE (-Zr, Nb, Ta) deposits associated with alkaline plutons

IAIN M. SAMSON[1] AND ANTHONY E. WILLIAMS-JONES[2]

[1]University of Windsor, Department of Earth and Environmental Sciences, ims@uwindsor.ca

[2]McGill University, Department of Earth and Planetary Sciences

Mineral deposits in which a variety of rare elements, including REE, Zr, Ta, Nb, Be, and Ga, are concentrated are associated with alkaline to peralkaline plutons, typically in rift settings. Although, in general, there are common features among such deposits, the plutons can vary substantially in their internal character and structure, and their degree of Si saturation, from Si-oversaturated (e.g., Strange Lake, Quebec/Labrador) to Si-undersatured (e.g., Thor Lake, NWT, and Illimaussaq, Greenland). The former are characterized by alkaline granites and the latter by nepheline syenites. This variable magma character is reflected in a diverse primary rare element mineralogy. For example, at Strange Lake, Zr was mainly hosted by zircon and elpidite, Nb by pyrochlore and the REE by all three minerals. In contrast, in the Nechalacho deposit at Thor Lake, Zr and REE were hosted by zircon in the upper, miaiskitic, zone and by eudialyte in the lower, agpaitic, zone. Columbite is likely to have been the primary host for Nb. In both settings, the mineralization is characterized by higher HREE/LREE than other systems, such as those associated with carbonates.

The concentration of rare elements through fractional crystallization into pegmatites or by physical crystal accumulation was important in these deposits, however, hydrothermal fluids have played an important role in the subsequent transport and precipitation of rare elements. In particular, water-rock interaction and hydrothermal alteration have significantly modified the mineralogical character of the REE and Zr minerals, and this has increased the mineralogical diversity in such deposits, and resulted in upgrading and ease of beneficiation. The water-rock interaction history can be complex and multi-stage, leading to texturally and mineralogically complex assemblages in which pseudomorphing of early-formed minerals (both rare-element and non-rare element bearing) played a critical role in rare-element mineral precipitation.

The increasing availability of experimental data on the stability of aqueous rare element complexes is making modelling of the processes mentioned above easier, although a lack of data on mineral solubility remains a hindrance. Many models of deposit formation, both in silicic and carbonatitic environments, have employed fluoride complexes to facilitate element transport, with precipitation resulting from their destabilization as a consequence of the addition of Ca from host rocks or by fluid mixing, and the precipitation of fluorite. Although there is ample evidence for Ca metasomatism in the above-mentioned and other deposits, a true evaluation of this model is hindered by a lack of information on ligand concentrations, particularly fluoride. Furthermore, mineralogical and textural observations from these and other systems suggest that other complexation and precipitation models need to be considered.

Zircon, zircon everywhere: What caused the zircon superfertility of Grenville magmas?

SCOTT D. SAMSON[1]*, AARON SATKOSKI[2], DAVID MOECHER[3]

[1]Syracuse University, Earth Sciences, Syracuse, NY, USA, sdsamson@syr.edu (* presenting author)

[2]Syracuse University, Earth Sciences, Syracuse, NY, USA, amsatkos@syr.edu

[3]University of Kentucky, Earth and Environmental Sciences, Lexington, KY, USA, moker@uky.edu

A common assumption in many detrital zircon studies is that the abundance of zircon grains defining a particular age range directly corresponds to the area of exposed continental crust of that age. This is often not the case, however, as much modern alluvium and Paleozoic sandstone have large, sometimes exclusive, 1.3 – 1.0 Ga age peaks, a so-called Grenvillian signature. This is true even for sedimentary rocks very distal to exposed Grenville crust, such as Cambrian sandstone in California and clastic sediment in northwestern Canada. One of the reasons for the extreme abundance of ~ 1 Ga detrital zircon is that magmas associated with Grenville orogenic events contain unusually abundant, and often surprisingly large, zircon crystals. Large and abundant crystals will dominate the zircon budget of alluvium, particularly if sediment has been transported significant distances by major river systems.

A fundamental question about the Grenville Orogeny thus arises: what caused the magmas associated with the tectonic events to be so zirconium rich? One possibility is that the high Zr content, often > 500 ppm, is the result of a high abundance of zircon xenocrysts in the Grenvillian plutons. In this scenario the high Zr whole-rock contents would not be due to actual magmatic compositions but would reflect the total zircon crystal cargo of the intrusion. A second possibility is that the sources of Grenvillian magmas themselves were unusually Zr rich. A recent suggestion has been made that long-lived subduction beneath Laurentia may have significantly chemically enriched the Laurentian mantle lithosphere prior to Grenvillian magmatism. Furthermore, if Zr-enriched parent material was partially melted then the newly formed magma would be even higher in Zr content (assuming Zr distribution coefficients << 1). A third possibility is that unusually hot continental lithospheric conditions existed during the assembly of Rodinia. Very high temperature magmas can become very Zr-rich prior to reaching zircon saturation and thus can crystallize an abundant amount of zircon. These three, not necessarily mutually exclusive, hypotheses have yet to be thoroughly tested, despite their importance to an understanding of what might be one the most Zr-rich magmatic episodes in Earth history. But regardless of the cause, the role of zircon superfertility must be a primary consideration when using detrital zircon as a proxy for studies of continental crustal growth. Estimates of the amount of juvenile crust generated based on isotopic analysis of detrital zircon could be biased if variation in zircon fertility is not taken into consideration.

An experimental and field study on P, Si, As, Cr, V and Se binding to Fe- and Al-hydroxysulfates under oxic and anoxic conditions in acidic pit lakes: chemical *vs.* microbial controls

JAVIER SÁNCHEZ-ESPAÑA[1*], MARTA DIEZ ERCILLA[1], CARMEN FALAGÁN[1], IÑAKI YUSTA[2]

[1]Unidad de Mineralogía e Hidrogeoquímica Ambiental (UMHA). Instituto Geológico y Minero de España, Madrid, Spain, j.sanchez@igme.es (* presenting author)

[2] Unidad de Mineralogía e Hidrogeoquímica Ambiental (UMHA), Universidad del País Vasco (UPV-EHU), Bilbao, Spain, i.yusta@ehu.es

Introduction and scopes

The chemical composition of acidic mine pit lakes usually include trace elements which may form either oxyanions or some other anionic species, depending on pH-Eh conditions and sulfate concentration. Some elements (e.g., P, Si) are biogeochemically important, whereas others (e.g., As, Cr, V, Se) may be highly toxic to aquatic ecosystems. In the pit lakes of the Iberian Pyrite Belt (SW Spain), the fate and transport of most of these trace elements has been shown to be closely associated to the formation and (meta)stability of low-crystallinity solid phases like schwertmannite and hydrobasaluminite [1]. The present work reports recent field and experimental observations on the mobility of these elements through the water column, redoxcline and the sediment/water interfase.

Results and discussion

Schwertmannite is the most abundant mineral product of microbial Fe^{II} oxidation in the studied pit lakes (pH 2.2-3.1) [1]. Field and experimental evidence exists to support that As, Cr and P are temporaly immobilized by sorption on µm- to nm-scale schwertmannite colloids. Experimental data (including titrations under oxic and anoxic conditions) coupled to geochemical modeling, indicate that the most important retention mechanism is that of sorption of arsenate, chromate and phosphate anions to the positively charged, highly reactive schwertmannite surfaces. The process seems to be reversible, and these elements can be again released to the aqueous phase during settling to the underlying, anoxic part by either (i) microbial reductive dissolution, and/or (ii) schwertmannite aging (conversion to jarosite and/or goethite).

The behaviour of Si, V and Se appears to be more closely linked to the precipitation of hydrobasaluminite or an analogous Al phase. An evident discrepancy exists between the sorption behaviour observed under field and experimental conditions. Such discrepancy could be accounted for by recent microscopic (SEM-EDS) findings, which suggest a strong microbial control on Al precipitation and the associated sorption of Si and other elements. The role of acidophilic microbes in the Fe-Al co-precipitation at pH~4.0 represents a geochemically singular aspect which deserves further investigation.

[1] Sánchez-España, J., Yusta, I., Diez, M. (2011) *Applied Geochemistry* **26**, 1752-1774.

The density of carbonate and silicate melts in the upper mantle

CARMEN SANCHEZ-VALLE[1,*], SUJOY GHOSH[1], WIM J. MALFAIT[1], RITA SEIFERT[1], SYLVAIN PETITGIRARD[2] AND JEAN-PHILIPPE PERRILLAT[3]

[1]Institute for Geochemistry and Petrology, ETH Zurich, Zurich, Switzerland, carmen.sanchez@erdw.ethz.ch (* presenting author)

[2]ESRF, Grenoble, France.

[3]Laboratoire de Sciences de la Terre, UCB Lyon1-ENS Lyon-CNRS, Lyon, France

Although carbonate melts are volumetrically minor phases in the mantle, they may control the mobility of C and its residence time in the mantle, ultimately contributing to the gobal carbon cycle [1]. Carbonate melts are also considered as effective metasomatic agents because of their wetting properties, high migration rate and characteristic trace element enrichment [2]. The density of carbonate liquids is thus an important parameter to model their percolation through the mantle and evaluate their behavior as metasomatic agents and carbon reservoirs, but available data remains scarce at relevant P-T conditions and melt compositions [3,4].

In this contribution we report *in situ* invetigations of the density of carbonate liquids in the Mg-Fe binary and Mg-Fe-Ca ternary systems at upper mantle conditions (2 GPa and 1900 K). Density was determined from the X-ray absorption contrast between the samples and a diamond capsule used to contain the sample at high pressure and temperature conditions. Experiments were perfomed using a panoramic Paris-Edinbugh press at ID27 beamline of the ESRF. Pressure and temperature were determined from the X-ray diffaction patterns of hBN and Pt using the double-isochore method. The measurements provide preliminary constrains on the equation of state of carbonate liquids representative for natural carbonatites, including melt compositions produced by the partial melting of carbonated peridotites [5]. The results are combined with own recent data for the density of silicate melts (rhyolites and phonolites) and literature data for mantle minerals to discuss buoyancy relations in the upper mantle and their evolutions with pressure to better quantify the extraction of C-bearing liquids from residual rocks during partial melting and the ascent of melts through the mantle. Ultimately, we will discuss the role of carbonate-silicate liquids as metasomatic agents and carbon reservoirs.

[1]Dasgupta and Hirschmann (2010) *Earth Planet. Sci. Lett.* 2**98**, 1-13.
[2]Green and Wallace (1988) *Nature* **336**, 459-462.
[3]Dobson et al., (1996) *Earth Planet. Sci. Lett.* **143**, 207-215.
[4]Liu et al. (2007) *Contrib. Mineral. Petrol*. **153**, 55-66.
[5]Dasgupta and Hirschmann (2006) Nature **440**, 659-662.

Composition of SOM in the Canadian high Arctic

REBECCA L. SANDERS[1*], RACHEL L. SLEIGHTER[2], TULLIS C. ONSTOTT[3], LYLE G. WHYTE[4], PATRICK G. HATCHER[5], AND SATISH C. B. MYNENI[6]

[1]Princeton University, Department of Geosciences, rlsander@princeton.edu (* presenting author)
[2]Old Dominion University, Department of Chemistry and Biochemistry, rsleight@odu.edu
[3]Princeton University, Department of Geosciences, tullis@princeton.edu
[4]McGill University, Department of Natural Resoure Sciences, lyle.whyte@mcgill.ca
[5]Old Dominion University, Department of Chemistry and Biochemistry, phatcher@odu.edu
[6]Princeton University, Department of Geosciences, smyneni@princeton.edu

Permafrost underlies one fourth of the Earth's surface and contains approximately half of the global organic carbon (OC) in soils. Thawing and rapid losses of OC in the form of CO_2 and CH_4, associated with warming of arctic regions, raises serious concerns about the stability of OC in permafrost soils and its influence on the biogeochemical cycling in the surrounding Arctic Ocean. The composition of extractable OC in a soil profile collected from the McGill Arctic Research Station on Axel Heiberg Island in the Canadian high Arctic has been characterized using ultrahigh resolution mass spectrometry and nuclear magnetic resonance spectroscopy. The OC in this polar desert is oxygen-poor and highly enriched in lipids, because algae and detrital carbon from surrounding rocks are the main carbon sources. The OC is poor in lignin and protein in the high Arctic soils when compared to soils of other climates because of the lack of vascular plants. In addition, the OC composition of the whole soils was analyzed by carbon K-edge XANES, which indicated that the OC consisted of mostly aliphatic carbon as well as smaller contributions from unsaturated OC, carboxyls, and proteins. Most striking was the absence of oxygenated OC, which is often present as carbohydrates in polar region soils with more vegetation.

Such a contrasting composition of OC in Arctic soils may result in carbon losses from climate warming that may disagree with the widely-accepted models based upon the biogeochemistry of temperate soils. Heating experiments are currently underway to investigate how and to what extent the OC composition changes as a function of warming, indicative of how these soils may evolve as a result of climate change. Understanding how recalcitrant this highly aliphatic, oxygen-poor terrestrial carbon is will be critical to identifying its impact on the biogeochemical cycling in the surrounding Arctic Ocean.

Geochemistry of mercury and trace elements captured by activated carbons in a Canadian coal-fired power plant

HAMED SANEI[*1], FEIYUE WANG[2], FRANK HUGGINS[3]

[1]Geological Survey of Canada, Calgary, AB, T2L 2A7, Canada, hsanei@nrcan.gc.ca (* presenting author)
[2]Department of Chemistry, University of Manitoba
[3]Department of Chemical and Materials Engineering, University of Kentucky, Lexington, Kentucky, USA

Abstract

The coal-fired power plants in Canada are required to reduce the emission of Hg up to 80% by 2018 and beyond to meet the national and regional regulatory targets. Activated carbon (AC) is considered by industry as an efficient sorbent to capture Hg from the flue gas during the combustion process. A widespread use of AC is anticipated by the coal-fired power plants to reduce the emission of Hg and meet their regulatory obligations.

This study investigates the geochemistry of ESP fly ash and related feed coal samples during an experiment trial by a full-scale coal-fired power plant in Western Canada. Furthermore capturing efficiency and retention ability of 5 different commercial ACs were examined. While the significant amount of Hg is being captured by ACs, the ultimate fate of Hg after capture and possible environmental impacts related to handling and use of Hg-rich fly ash has been a major concern. This study investigates volatilization and leachability of Hg and other elements from the captured fly ash.

The results show that capturing ability varies depending on AC's injection rates, fly ash particle size sorting, and temperature of the flue gas. Thermal release of Hg from fly ash samples appears negligible up to a temperature of 80°C. De-volatilization of Hg begins beyond 80°C, showing a sudden increase after 120°C. The constant heating at 140°C resulted in a steady de-volatilization of Hg during the 8 hour experiment that suggests a slow release of Hg during long exposure to heat. We recommend further investigation of possible Hg de-volatilization at higher temperature with the samples being exposed for a longer period of time.

Mercury is mostly leachable under strong acid digestion suggesting strong chemical retention. However, <10% of the total captured Hg can be released under the more moderate chemical digestion. The retention ability tends to decrease significantly in fine-grained fly ashes. The fly ashes injected with high sulphur AC provided the strongest chemical retention for Hg. We conclude that the possible Hg-S binding associated with ACs not only provides the best Hg capture capacity, but also provides the strongest thermal and chemical retention ability.

Solid - Liquid Equilibria for the ternary $Na_2B_4O_7$ - NaBr - H_2O System at 348 K

SHIHUA SANG[1, 2]*, HUIYI NING[1], AND DAN WANG [1]

[1]College of Materials and Chemistry & Chemical Engineering, Chengdu University of Technology, Chengdu 610059, China.

* sangsh@cdut.edu.cn

[2]Mineral Resources Chemistry Key Laboratory of Sichuan Higher Education Institutions，Chengdu 610059, China

Introduction

Many salt lake brines on the Qinghai - Tibet plateau in China are well known for high concentrations of Li, K and B. Furthermore, a huge amount of underground gasfield brine was also discovered in China,such as Sichuan western basin. Sodium chloride, potassium, boron , bromine and sulfates are the major chemical component of the oilfield brine, which often accompanies Li, Sr and I. The ternary system $Na_2B_4O_7$ - NaBr - H_2O is a subsystem of the underground gasfield brines.

Results

The solid - liquid equilibria for the ternary system $Na_2B_4O_7$ - NaBr - H_2O at 348 K were measured experimentally using the method of isothermal solution saturation. On the basis of experimental data, the phase diagram of the ternary system was constructed. In the phase diagram of the ternary system $Na_2B_4O_7$ - NaBr - H_2O at 348 K(Figure 1), there are one invariant point E and two univariant curves E1E and E2E. The points E1 and E2 represent the solubility of the binary systems of $Na_2B_4O_7$- H_2O and NaBr - H_2O at 348K with mass fraction ($100w_b$) of 19.30 and 54.35, respectively. Curve E1E and E2E are the solubility isotherms of $Na_2B_4O_7 \cdot 5H_2O$ and NaBr, respectively. The invariant point E corresponds to the solution saturated with both NaBr and $Na_2B_4O_7 \cdot 5H_2O$. Phase equilibrium solids were NaBr and $Na_2B_4O_7 \cdot 5H_2O$ in the studied ternary system. The crystallization area of $Na_2B_4O_7 \cdot 5H_2O$ (E1ED field) in the phase diagram is obviously bigger than that of NaBr (E2EA field).

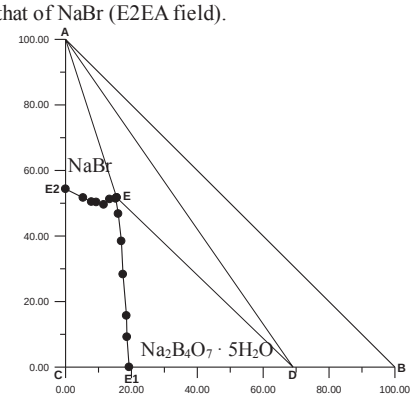

Figure 1 Phase diagram of the ternary system $Na_2B_4O_7$ - NaBr - H_2O at 348 K

Acknowledgements: This project was supported by the National Natural Science Foundation of China (No. 40973047) and the Youth Science Foundation of Sichuan Province, China (08ZQ026-017).

Use of two new Na/Li thermometric relationships for geothermal fluids in volcanic environments

BERNARD SANJUAN[1*], RAGNAR ASMUNDSSON[2], ROMAIN MILLOT[3]AND MICHEL BRACH[3]

[1] BRGM, Department of Geothermal Energy, Orléans, France, b.sanjuan@brgm.fr (* presenting author)

[2]Tiger Energy Services, Taupo, New Zealand, ragnar.asmundsson@tigerhd.com

[3]BRGM, Department of Metrology, Monitoring and Analysis, Orléans, France, r.millot@brgm.fr, m.brach@brgm.fr

Thermometers such as Silica, Na/K, Na/K/Ca, Na/K/Ca/Mg or $\delta^{18}O$ (H_2O-SO_4), based on empirical or semi-empirical laws derived from chemical equilibrium reactions between water and minerals in the deep reservoirs, are commonly used in geothermal exploration in order to estimate the reservoir temperatures. Unfortunately, these estimations are not always concordant because of processes which can perturb the chemical composition of the fluids during their ascent up to the surface (water mixing, fluid cooling, etc.). Given these discordances, auxiliary thermometers such as Na/Li, based on statistical relationships, were also developed. As Li is rather lowly reactive, the use of this thermometer can give more reliable temperature estimations. Presently, three different Na/Li relationships ([1], [2]) are mainly available according to the fluid salinity and the geological environment (volcanic/granitic and sedimentary rocks).

This study carried out in the framework of the European HITI project (HIgh Temperature Instruments for supercritical geothermal reservoir characterization and exploitation) with the collaboration of ISOR Iceland Geosurvey proposes two new Na/Li thermometric relationships. The first concerns the fluids derived from high-temperature seawater-basalt interaction processes existing in the oceanic ridges and rises as well as in the emerged rifts such as those of Iceland (Reykjanes, Svartsengi and Seltjarnarnes geothermal fields) and Djibouti (Asal-Ghoubbet and Obock geothermal areas). It can be expressed as follows:

$$\text{Log (Na/Li in mol/l)} = 920/(T°K) + 1.105 \quad (r^2 = 0.994).$$

The second relationship, developed using dilute fluids collected only from Icelandic geothermal wells in the 100-325°C range, surprisingly close to that determined by Fouillac and Michard (1981) for volcanic saline fluids at temperatures ≥ 200°C, is:

$$\text{Log (Na/Li in mol/l)} = 1786/(T°K) - 0.936 \quad (r^2 = 0.976).$$

The uncertainty on temperature estimation is ± 25°C for both relationships. These results confirm that the Na/Li ratios not only depend on temperature but also on other parameters. The nature of the reservoir rocks and fluid seems to be the most influent one. Some literature case studies and thermodynamic considerations suggest that the Na/Li ratios could be controlled by chemical equilibrium reactions involving different mineral assemblages where illite and micas would be, however, always present.

[1] Fouillac Ch. and Michard G. (1981) *Geothermics,* **10**, n°1, 55-70. [2] Kharaka and Mariner (1989) *Naeser and McCulloch Eds, Springer-Verlad, New York,* 99-117.

Carbonated basalts at depth: density, compression mechanisms, and potential buoyancy

C. SANLOUP[1*], C. CRÉPISSON[2], G. MORARD[3], H. BUREAU[3], G. PROUTEAU[4] AND S. PETITGIRARD[5]

[1]University of Edinburgh, Edinburgh, UK, chrystele.sanloup@ed.ac.uk (* presenting author)
[2]Ecole Normale Supérieure, Paris, France, celine.crepisson@ens.fr
[3]Université Pierre et Marie Curie – Paris 6, Paris, France
[4]ISTO, Orléans, France
[5]European Synchrotron Radiation Facility, Grenoble, France

Introduction

The alkali basalt composition was chosen as representative of two potentially relevant contexts : alkali basalts dragged in the Japanese sea have been interpreted as originating from the asthenosphere [1,2], and their high vesicularity suggested high CO_2 content in the pre-eruptive melt. Also, primitive alkali basalts are generated in subduction contexts, as the one used here (Stromboli [3]) and as such, could have contributed to the formation of cratonic roots.

Experiments

In situ density and structural measurements were collected using respectively x-ray absorption and x-ray diffraction techniques. High P-T conditions up to 7 GPa were generated using the Paris-Edinburgh press at the european synchrotron (ESRF, ID27 beamline) and the cell-assembly described in [5]. Recovered quenched samples were analyzed by EPMA and Raman spectroscopy to check for CO_2 content and speciation.

Density measurements as a function of pressure show a higher compressibility than for non-carbonated basalts. Structural data, as expressed by pair distribution function of the melt, show an increased coordination number of Al. Such effect had been proposed based on viscosity measurements at modest P [6,7], and seems emphasized at higher P.

Density of the carbonated alkali basalt is then compared to seismological and petrological values of the density for surrounding rocks to check for potential neutral buoyancy at depth.

[1] Hirano (2001) *GRL* **28**, 2719-2722. [2] Hirano (2006) *Science* **313**, 1426-1428. [3] Pichavant et al. (2009), *J. Pet.* **50**, 601-624. [4] [5] Van Kan Parker et al. (2010) *High Pressure Res.* **30**, 332-341. [6] Brearley (1989) *GCA*, **53**, 2609-2616.[7] White (1990) *JGR* **95**, 15683-15693.

Interpretation of helium isotopes in modern hydrothermal systems

Y. SANO[1] AND T. P. FISCHER[2, 3]

[1]Atmosphere and Ocean Research Institute, University of Tokyo, Kashiwanoha, Chiba 277-8564, Japan (*correspondence: ysano@aori.u-tokyo.ac.jp)
[2]Division of Earth Sciences, National Science Foundation, Arlington, VA 22230, USA
[3]Department of Earth and Planetary Sciences, University of New Mexico, Albuquerque, NM87131-1116, USA

Many reviews and textbooks on terrestrial helium isotopes have been published since the discovery of mantle helium in 1969. This work focuses on the interpretation of helium isotopes of fluid samples in modern hydrothermal systems. In hot spot regions such as Hawaii, Yellowstone and Iceland, helium isotopes of fluid samples are generally higher than MORB-type He (8.0+/-1.5) Ra where Ra is the atmospheric ratio of 1.4×10^{-6}. Seismic tomography data of the three regions show that a continuous low-velocity anomaly is imaged from the surface to at least the surface of the lower mantle [1-3]. The plume-type He may be derived from the lower mantle. In the other hot spot regions such as Afar, Canary and Reunion, the thermal conduit associated with mantle upwelling extends to depths greater than 500 km. There is a weak positive correlation between maximum helium isotopes and the buoyance flux except for Hawaii. Graham [4] compiled 658 MORB glass data and reported that the more than 90% of helium isotopes are lying between 6.5-9.5 Ra. Hydrothermal fluids in MOR shows the helium isotopes varying from 7.2 Ra to 9.2 Ra with the average of (8.09+/-0.49) Ra, identical to that of the global average of MORB. The average ^{3}He/heat ratios is calculated (8.6+/-3.8) x 10^{-18} mol/J world-wide. When we take into account of a global axial heat flow in MOR [5], the total ^{3}He flux would become (2.8+/-1.2) atom/cm^2/s, a little smaller than the well-established value of 4 atom/cm^2/s [6]. Helium isotope data of subduction zones were compiled by Hilton et al [7]. Now additional data are available in the Kamchatka, Izu-Bonin, Ryukyu-Taiwan, Sangihe arc in Indonesia and Central American system. The cir-cum Pacific helium data are summarized as follows: (a) helium isotopes vary significantly from 0.01 Ra to 10.1 Ra and the rage is much larger than that of MOR-type He. (b) The highest value of 10.1 Ra observed in the Vanuatu islands suggests the contribution of plume-type He. (c) The second highest values (8.8-8.9) Ra are found in the Colombian Andes and Sunda arc systems, falling within the range of MOR-type He. (d) Relatively lower values (6.5–7.0) Ra are observed in the Ecuadorian, Peruvian and Chilean Andes and the eastern Sunda/Banda arc, slightly lower than that of MOR-type. There is no apparent correlation between the maximum value of arc segments and the magma production rate or the taper angle of the slab.

[1] J. Lei and D. Zhao (2006) *EPSL* **241**, 438-453. [2] H. Yuan and K. Dueker (2005) *GRL* **32**, L07304. [3] J. Ritsema and R. Allen (2003) *EPSL* **207**, 1-12. [4] D. Graham (2002) in *Noble Gases, Reviews in Mineral. Geochem.* **Vol. 47**, 247-317. [5] C.R. German and K.L. Von Damm (2004) in *Treatise Geochem.* **Vol. 6**, 181-222. [6] H. Craig et al. (1975) *EPSL* **26**, 125-132. [7] D. Hilton et al. (2002) in *Noble Gases, Reviews in Mineral. Geochem.* **Vol. 47**, 319-370.

Comparative study of synthetic and natural iron sulfates and oxides by Raman spectroscopy

ANTONIO SANSANO[1*], JESUS MEDINA[2], FERNANDO RULL[3], PABLO SOBRON[4]

[1]Unidad Asociada UVA-CSIC Centro de Astrobiologia, Spain, sansanoca@cab.inta-csic.es

[2] Unidad Asociada UVA-CSIC Centro de Astrobiologia, Spain, medina@fmc.uva.es

[3] Unidad Asociada UVA-CSIC Centro de Astrobiologia, Spain, rull@fmc.uva.es

[4] Space Science and Technology, Canadian Space Agency, Canada, Pablo.Sobron@asc-csa.gc.ca

The study of iron minerals, in particular, sulfates and oxides of evaporitic characteristics, has carried a great interest in the last years, not only for their direct application in the analysis of mine drainage, also in their application to the study of the mineralogy of Mars surface. The jarosite discovery[1], as well as of other hydrated sulfates[2] in the surface of the red planet carried out by MERs represent an important focus of interest for the study of the evolution and the geodynamics of the planet and their possible astrobiological implications.

The use of quick and precise techniques, susceptible of being boarded in missions to other planets, is revealed as an important aspect when carrying out so much analysis of synthetic materials as collected materials from different geologic analogs. In particular, Raman spectroscopy as part of the payload of the mission Exomars[3] and that it will be launched in the 2018 to Mars, shows up like a very powerful technique when analyzing in-situ and in a non destructive way the molecular composition of the analyzed materials, besides giving us a quite precise idea of structural aspects that could be extrapolated in reference to their possible genesis.

In this work we present the results of the application of this technique to materials synthesized in laboratory also to materials extracted in diverse campaigns to different Martian analogs as are Rio Tinto River and El Jaroso Ravine, both in Spain[4]. On one hand, the use of materials of synthetic origin provides us so much patterns for reference use and also an approach to the necessary conditions for the formation of one or another compound, in a controlled way. On the other hand, the materials picked up in the natural localizations give us a real panoramic of how they are distributed and this materials become in the geochemical conditions that surround them. This allows us to compare them among and with the synthetic ones being been able to extract conclusions about the conditions of their origin, their structural characteristics and being able to formulate hypothesis on their formation process and could be extrapolated by methods of the analysis in situ in Mars, of the materials that there are.

[1] Klingelhöfer et al. (2004), Science, 306, 1740-1745 [2] Johnson et al. (2007) JGR, V34, L13202 [3] Rull et al (2006) Spect.Now. v18, 18-21 [4] Rull et al. (2008) LPSC XXXIX, #1616.

Multiple sulphur isotope evidence for an oceanic sulphate concentration decrease in the Marinoan glaciation aftermath

P. SANSJOFRE [1*], P. CARTIGNY[1], M. ADER[1], R. TRINDADE [2] AND A. NOGUEIRA[3]

[1] Equipe de Géochimie des Isotopes Stables, Institut de Physique du Globe de Paris, Sorbonne Paris Cité, Univ Paris Diderot, UMR 7154 CNRS, F-75005 Paris, France, sansjofre@ipgp.fr (* corresponding author)

[2] Departamento de Geofisica IAG, Universidade de São Paulo, Brazil, rtrindad@iag.usp.br

[3] Instituto de Geociências, Universidade Federal do Pará, Bélem, Brazil, anogueira@ufpa.br

In order to better contrain the sulphur cycle in the aftermath of the Marinoan Glaciation, we performed sulphur isotope composition analysis ($\delta^{33}S$ - $\delta^{34}S$ - $\delta^{36}S$) of Ediacarian carbonates, on both Carbonate Associated Sulphate (CAS) and pyrite. Samples come from Carmelo quarry (Mato Grosso, Brazil) where 20m of white dolomicrite (Mirassol d'Oeste Formation) directly cover the glacial sediments related to the Marinoan glaciation (~635Ma). This dolomicrite is overlying by 150m of Guia Formation limestone's which begin with 40 meters of carbonate-rich siliciclastic material evolving to pure carbonate intercalated with thin layers of marls.

Results show an increase in both $\delta^{34}S_{pyr}$ and $\delta^{34}S_{CAS}$ upward along the section. $\delta^{34}S_{pyr}$ and $\delta^{34}S_{CAS}$ vary from -10‰ to +26‰ and from +16 to +51‰ respectively. Our $\delta^{34}S_{CAS}$ data are relatively high compared to present day oceanic sulphate value (+21‰), but they are in agreement with previous data reported for the same time period. $\Delta^{33}S$ data show values close to 0‰ (0.03 ± 0.02‰) at the base of the section and significatively higher values in the upper part, up to +0.16 ± 0.02‰.

For steady-state ocean sulphur concentration, an increase in the isotopic values can be partially explained by an increase in pyrite burial rate together with a higher $\delta^{34}S_{sulphate}$ input. However this model cannot account neither for the extremely high values of $\delta^{34}S_{CAS}$ nor for the $\Delta^{33}S$ signal. We thus developped a non steady state model in which we take into account the effect of Rayleigh distillation on $\delta^{34}S_{CAS}$, $\delta^{34}S_{pyr}$ and $\Delta^{33}S$ values. Results show that the increase in both $\delta^{34}S$ (CAS and pyrite) and $\Delta^{33}S$ are well explained by a decrease of ~50% in the oceanic sulphate concentration. We thus propose that the post-Marinoan ocean experienced a decrease in sulphate concentration which could result from an increase in sulphate consumption by BSR relative to the net riverine sulphate delivery input.

Membrane-dependent microbial inhibition during CO_2 sequestration: Implications for the alteration of subsurface community composition

EUGENIO-FELIPE U. SANTILLAN[1*], CHRISTOPHER R. OMELON[1], TIMOTHY M. SHANAHAN[1], AND PHILIP C. BENNETT[1]

[1]University of Texas Austin, Austin, TX, USA
efu.santillan@utexas.edu (* presenting author)

Background

When CO_2 is stored in deep saline aquifers, many geochemical changes will occur due to CO_2 dissolution [1]. High PCO_2 will also perturb the existing microbial communities that influence the geochemistry of the reservoir through their metabolic activities.

The CO_2 molecule itself is toxic to microorganisms. It is easily permeable through cell membranes changing membrane fluidity, the proton pump, and intracellular pH [2]. Adaptations that slow the diffusion of CO_2 into the cell, like biofilms and thick cell walls, will be selected for in the new environment.

In this study, we assessed the tolerance of several representative organisms to high PCO_2 based on their membrane morphologies: the Gram-negative bacterium *Shewanella oneidensis*, the Gram-positive bacterium *Bacillus subtilis* sp0A mutant, the Gram-positive endospore forming bacterium *Geobacillus stearothermophilus*, and the methanogenic archaeon *Methanothermobacter thermoautitrophicus*.

Results and Conclusions

Results show the Gram-negative organism is the most susceptible to CO_2 toxicity surviving a maximum pressure of 25 atm for 2 hours. However, when grown in the presence of a mineral, survival time increases beyond 8 hours due to biofilm formation. Archaea can withstand 50 atm of CO_2 for 8 hours and Gram-positive endospores can handle 50 atm of CO_2 for at least 24 hours potentially due to thick and rigid cell membrane or wall compositions.

Images taken by transmission electron microscopy show all experimental organisms have a threshhold tolerance to CO_2. We observed clumping of cytoplasmic contents at differing CO_2 pressures suggesting CO_2 plays an effect in altering intracellular activity. Lipid profiles of the bacteria also show a decrease in concentrations of monounsaturated or of short-chained fatty acids during CO_2 exposure indicating CO_2 causes a loss in cell viability.

Our findings suggest that during CO_2 sequestration, biofilms, Gram-positive endospores, and methanogens are organisms that will survive in the new environment. Because each organism varies in their CO_2 tolerance, regions surrounding the CO_2 plume may eventually form where different organisms are most active This in turn can have effects on mineral precipitation catalyzed on cell membranes and the geochemistry of the greater subsurface.

[1] Kharaka et al. (2006) *Geology* **34**, 577-580. [2] Hong and Pyun (1999) *Journal of Food Science* **64**, 728-733.

In situ remediation and pedogenesis in bauxite residue ('red mud')

TALITHA SANTINI[1,2*], MARTIN FEY[1], AND ANDREW RATE[1]

[1]University of Western Australia, Perth, Australia,
talitha.santini@uwa.edu.au (* presenting author)
[2]McMaster University, Hamilton, Canada

Introduction

'*In situ*' approaches to tailings management typically address unfavourable properties of the tailings after deposition in storage areas by surface application of treatments. In the case of bauxite residue, *in situ* remediation means selecting treatments that will aid in lowering pH from values of >12 to <9, lowering electrical conductivity from values of >4 dS/m to <1 dS/m, and that will stimulate biological activity in the initially sterile tailings. Treatments including sewage sludge, tillage, green waste, dredge spoil, and topsoil were applied at a bauxite residue ('red mud') storage area in Corpus Christi, Texas.

Results and discussion

Rainfall leaching (for 40 years) prior to amendment removed excess soluble salts, but not all residual sodalite ($Na_8(AlSiO_4)_6Cl_2$) and calcite ($CaCO_3$) which slowly dissolve and continue to buffer pH at values >8. Substantial replacement of Na^+ with Ca^{2+} has occurred on cation exchange sites, particularly in surface residue layers. Calcite dissolution, facilitated by rainfall leaching and organic acids and $CO_{2\,(g)}$ from plant roots, may provide Ca^{2+} for this exchange.

Bauxite residue pore water was high in Al, Ca, Fe, Na, and Si. Formation of gravel in the residue was attributed to precipitation of aluminosilicate coatings on surfaces exposed to the atmosphere during drying and cracking of residue (Figure 1). Some pores in the gravel contained nordstrandite or bayerite (both $Al(OH)_3$). Given that silicate inhibits crystallisation of aluminium hydroxides from solution [1], it appears that the aluminosilicate coatings formed first, lowering Si content of pore water, which then allowed precipitation of nordstrandite/ bayerite inside the gravel pores after further drying.

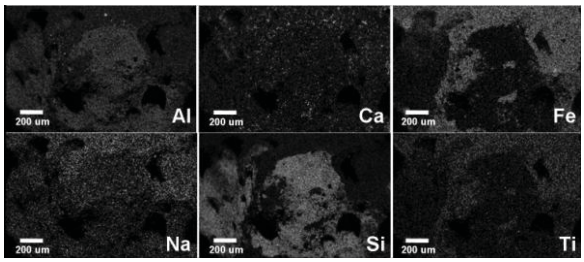

Figure 1: Element maps from gravel with aluminosilicate coating.

Sewage sludge was more effective than dredge spoil or topsoil in lowering bauxite residue pH, and increasing total N and extractable NH_4^+. Sewage sludge outperformed other treatments in terms of generating a suitable soil-like medium for plant cover, and addressing high pH and lack of plant nutrients such as organic C and N, K, Mg, and P in bauxite residue. Applied treatments can influence bauxite residue chemistry and mineralogy, and improve soil formation and *in situ* remediation.

Sr and Nd isotope composition of the Alcáçovas calc-alkaline rocks (Ossa-Morena Zone, Portugal)

JOSÉ F. SANTOS[1]*, PATRÍCIA MOITA[2], JONI MARQUES[1]

[1]Geobiotec / Dep. Geociências, Univ. Aveiro, Portugal, jfsantos@ua.pt*

[2]Centro de Geofísica / Dep. Geociências, Univ. Évora, Portugal

The Alcáçovas area is located in the SW sector of the Ossa-Morena Zone (OMZ), close to a major fault that separates this geotectonic unit from the South Portuguese Zone (SPZ). Along this boundary, in the OMZ, testimonies of low-K tholeiitic and calc-alkaline magmatism are common and have been interpreted as being related to the operation of a subduction zone between OMZ and SPZ during the Variscan cycle [1]. Two main igneous lithologies, both displaying calc-alkaline compositions, can be found in the studied area: gabbro-diorites and dacitic-rhyolitic porphyries [2,3]. Outcrop conditions have not yet allowed to establish unequivocally the sequence of magma emplacement. In previous geochronological studies on the porphyries, whole-rock Rb-Sr dates and K-Ar ages cluster around 320 Ma [4,5,6].

According to field observations, sometimes felsic dykes cut mafic rocks, but there are also gradual transitions from gabbroic to tonalitic compositions, within bodies mapped as gabbro-diorite, revealing that different melts coexisted.

In this study, rock samples of both gabbro-dioritic bodies and porphyries were analysed for Rb-Sr and Sm-Nd isotopes. Considering the whole set of samples, no isochron was obtained, showing that they can not be simply related by crystal fractionation processes.

Rb-Sr data of porphyries from a single quarry (at Lameira, 7 km to the SW of Alcáçovas) give 323±16 Ma (MSWD=1.9; initial $^{87}Sr/^{86}Sr$=0.7097±0.0018). Taking into account that the rocks of the Lameira outcrop show strong hydrothermal alteration, this date must be viewed as a consequence of a very efficient redistribution of mobile elements during aqueous fluid circulation and, as such, it places a minimum limit to the actual magmatic age

The plot of compositions of the gabbro-dioritic bodies, including their transitions to tonalites and the associated felsic dykes, in the ε_{Nd}-$^{87}Sr/^{86}Sr$ diagram, define an almost perfect hyperbole (from εNd_{323} = +3.9 and $^{87}Sr/^{86}Sr_{323}$ = 0.7058 to εNd_{323} = -3.8 and $^{87}Sr/^{86}Sr_{323}$ = 0.7085), as expected in a mixture between mantle-derived melts and crustal materials. In the same diagram, samples from the Lameira quarry show an almost constant εNd_{323}, between -2.4 and -2.9, and $^{87}Sr/^{86}Sr_{323}$ varying from 0.7092 to 0.7106. Therefore, the Lameira porphyries could represent a member of the same mixture, with the Sr signature modified by hydrothermal fluids with a stronger crustal component.

Funding: FCT through projects Petrochron (PTDC/CTE-GIX/112561/2009) and Geobiotec (PEst-C/CTE/UI4035/2011).

[1] Santos et al. (1990) *Comun. Serv. Geol. Portugal* **76**, 29-48.
[2] Gonçalves et al. (1992) *Not. Expl. Carta Geol. Torrão*, 86 pp.
[3] Caldeira et al (2007) *Comun. Geol. INETI* **94**, 05-28.
[4] Andrade (1974) *Mem. Not. Univ. Coimbra* **78**, 29-36.
[5] Coelho et al. (1986) *Ciências da Terra UNL* **8**, 65-72.
[6] Priem et al. (1986) *Comun. Serv. Geol. Portugal* **72**, 03-07.

Correlation of magnetic susceptibility with $\delta^{18}O$ data in magnetite- and ilmenite-type granites from Iberian massif

HELENA SANT'OVAIA[1*], HELENA MARTINS[1], JOSÉ CARRILHO LOPES[2], JOANA MACHADO[1] AND FERNANDO NORONHA[1]

[1] DGAOT, Centro de Geologia, F.C. Univ. Porto, Portugal, hsantov@fc.up.pt (* presenting author)

[2] Centro Geologia Univ. Lisboa; Dep. Geoc., E.C.T. Univ. Évora, Portugal (carrilho@uevora.pt)

The relationship between oxygen isotopic values and magnetic susceptibility composition on 11 Variscan Portuguese granites has been investigated. Whole-rock oxygen-isotope ($\delta^{18}O$) values for Vieira do Minho (VM), Vila Pouca de Aguiar (VPA), Chaves, Castelo Branco (CB), Manteigas and Serra da Estrela (SE) granitoids, were compiled from bibliography [1,2,3,4], and $\delta^{18}O$ for Santa Eulalia Plutonic Complex (SEPC) were obtained by laser fluorination at the Stable Isotopic Laboratory of Salamanca. Magnetic susceptibility (Km) values were obtained with a Kappabridge equipment from Toulouse University and Geology Centre, Porto University [2,5,6,7,8]. In this study is shown that there is a significant inverse correlation between Km and $\delta^{18}O$. *Magnetite*-type granites (Manteigas granodiorite and SEPC external facies) have Km>10^{-3} SI and low $\delta^{18}O$ values ranging from 8.9 to 10.3‰ instead those of *ilmenite*-type (all the other granites) have Km≤10^{-4} SI and are $\delta^{18}O$ enriched (9.3 to 13.5‰). The *I*-type granites (VM, VPA, Chaves, Manteigas and SEPC external facies) show lower average $\delta^{18}O$ (10.2‰) and higher Km values (100x10^{-6} SI) than the *S*-type granites (SE and CB) with $\delta^{18}O$ = 12.6‰ and Km = 65x10^{-6} SI.

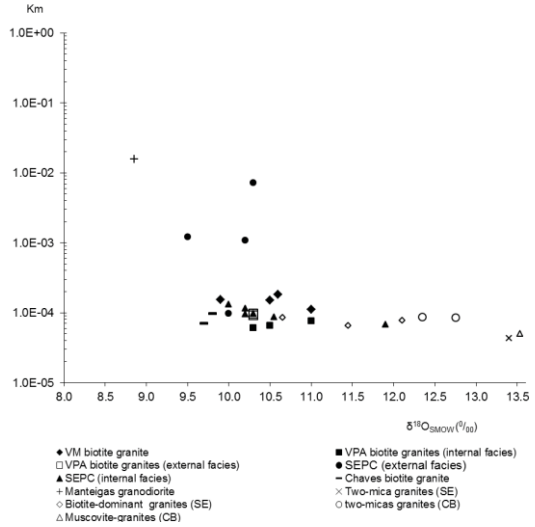

Figure 1: Semi-log plot of Km (in Si units) versus $\delta^{18}O$.

This work has been financially supported by PTDC/CTE-GIX/099447/2008 (FCT-Portugal, COMPETE/FEDER).

[1] Martins *et al.* (in prep.) [2] Martins *et al.* (2009) *Lithos* **111**, 142-155. [3] Antunes *et al.* (2008) *Lithos* **103**, 445-465. [4] Neiva *et al.* (2009) *Lithos* **111**, 186-202. [5] Sant'Ovaia *et al.* (2010) *JSG* **32**, 1450-1465. [6] Sant'Ovaia *et al.* (2000) *TRSE, ES* **91**, 123-127. [7] Sant'Ovaia *et al.* (2008) *33rd IGC* CD. [8] Sant'Ovaia *et al.* (2011) *Min. Mag.* **75**, 3, 1795.

Dissolved iron in the vicinity of the Kerguelen Islands, Southern Ocean, during the KEOPS 2 experiment

G. SARTHOU[1*], F. QUÉROUÉ[1,2,3], F. CHEVER[1], A.R. BOWIE[2], P. VAN DER MERWE [2], E. BUCCIARELLI[1], M. FOURQUEZ [4], S. BLAIN[4]

[1]LEMAR, UMR 6539 CNRS UBO IRD IFREMER, Place Nicolas Copernic, F-29280 Plouzané, France (* presenting author: Geraldine.Sarthou@univ-brest.fr)
[2]Antarctic Climate and Ecosystems CRC, University of Tasmania, Hobart, Tasmania, Australia
[3]Institute for Marine and Antarctic Studies, University of Tasmania, Hobart, Tasmania Australia
[4]LOMIC, UMR 7621 CNRS UPMC, avenue du Fontaulé, 66650 Banyuls sur mer, France

During KEOPS 2 (KErguelen Ocean and Plateau compared Study 2, Oct.-Nov. 2011), the distribution of dissolved Fe was investigated in the upper 1300 m in the vicinity of the Kerguelen Islands. Samples were analysed on board by flow injection analysis and chemiluminescence detection, with a detection limit of 0.02 ± 0.02 nM (n=13). A clear enrichment was observed above the Plateau. Indeed, the highest concentrations (2-4 nM) were observed at the most coastal station, east of the Kerguelen Islands. Then concentrations decreased eastward with the lowest values in an anti-cyclonic structure (0.06 nM at sea-surface and 0.3-0.4 nM at depth). A similar behaviour was observed at our reference station in the HNLC area, west of the Kerguelen Islands. In the polar front region, concentrations increased with values around 0.3-0.4 nM at sea-surface and 0.6-0.7 nM at depth. On-board incubations on natural plankton communities clearly showed a strong iron limitation at our reference station, a moderate one in the anti-cyclonic structure and no limitation above the Plateau.

Sorption of borate on calcined products of natural dolomite

Keiko Sasaki[1*], Yukiho Hosomomi[2], and Xinhong Qiu[3]
[1]Kyushu University, Earth Resources Engineering, Fukuoka, Japan, keikos@mine.kyushu-u.ac.jp (* presenting author)
[2] Kyushu University, Earth Resources Engineering, Fukuoka, Japan, y-hosomomi11@mine.kyushu-u.ac.jp
[3] Kyushu University, Earth Resources Engineering, Fukuoka, Japan, q-q11@mine.kyushu-u.ac.jp

Introduction

Boron is a dynamic trace element that can affect the metabolism or utilization of numerous substances involved in life processes, and also one of the most difficult elements to immobilize in aquatic environments [1]. Natural dolomite was modified to provide as a sorbent for borate. Calcination condition was investigated at 700 °C ~900 °C under air and reducing atmosphere.

Results and Conclusion

Calcite ($CaCO_3$) and magnesian calcite (Ca, Mg)CO_3 were included as impurities as well as dolomite ($CaMg(CO_3)_2$) in the specimen. Increasing with calcination temperature, sequential decarbonation was confirmed by XRD, that is, transformation of dolomite into magnesia and calcite at 700 °C, transformation of magnesian carbonate into magnesia and calcite at 800 °C, and transformation of calcite into lime at 900 °C. Surface molar ratio of Ca/Mg decreased from 1.6 to 0.6 independently of calcination temperatures. Sorption isotherm of borate at 25 °C was compared with calcined products under different conditions. In calcination under air, the greatest sorption density of borate was found with calcined product at 700 °C (Fig. 1). BET type of sorption isothedrm curve suggests that removal of borate is expected to occur through destructive sorption of MgO in calcined products. However, under reducing conditions the greatest sorption density was observed with calcined product at 900 °C.

Removal mechanism of borate is principally co-precipitation with $Mg(OH)_2$ in hydration nof MgO. The above result suggests the surface of magnesia (MgO) was more significantly affected by CO_2 in a process of decarbonation at higher temperature, and that higher crystalinity of MgO is more reactive in hydration.

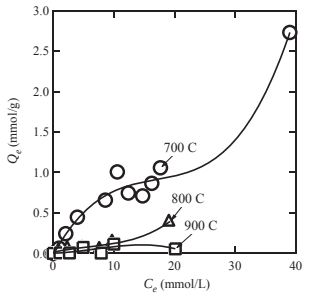

Figure 1: Sorption isotherm of borate at 25 °C on calcined products of natural dolomite at 700 °C ~900 °C under air.

[1] Sasaki *et al.* (2011) *J. Hazard. Mater.*, **185,** 1440-1447.

Experimental studies on carbon isotope fractionation in the deep Earth

M. SATISH-KUMAR [1*], TAKASHI YOSHINO[2], SHOGO MIZUTANI[1], HAYATO SO[3], AND MUTSUMI KATO[4]

[1]Department of Geosciences, Shizuoka University, Shizuoka, Japan smsatis@ipc.shizuoka.ac.jp
[2] ISEI, Okayama University, Misasa, Japan
[3]Asahi Diamond Industrial Co. Ltd, Mie, Japan
[4]Graduate School of Sciences, Chiba University, Chiba, Japan

Carbon is the fourth most abundant element in the solar system. It has a key role in the melting phase relations of mantle rocks [1] and metallic core [2]. Carbon further acts as an agent of mass transfer in the form of mobile carbonate-rich melts [1]. An efficient tool to understand the carbon cycle, both in the shallow and deep Earth environments, is by using carbon isotopic composition. However, our understanding of carbon isotopic composition of deep Earth is very limited. Here we present results of experimental determination of partitioning of carbon isotopes at high-pressure high-temperature conditions, in systems analogous core formation environment and carbonate melting in the mantle conditions.

High-pressure experiments were performed using a Kawai type multi-anvil high-pressure apparatus at the ISEI, Okayama University, Misasa, Japan. Two types of starting materials were used. First type is a mixture of Fe + 9.0wt% C with known carbon isotopic composition. Second set of experiments were carried out in the Mg-Si-C-O system, where San Carlos enstatite and olivine was mixed with graphite and magnesite. Experiments were carried out at a pressure of 5 and 10 GPa at temperature conditions between 1200 ºC and 2100 ºC. Carbon isotope measurements were carried out using an IRMS.

The distribution of carbon isotopes between iron carbide melt and graphite/diamond at high-pressure high-temperature conditions shows the presence of large and measurable carbon isotope fractionation in the Fe-C system. These results were also consistent with the carbon isotope distribution between graphite and cohenite (Fe_3C) in iron meteorites. A temperature-dependent fractionation of carbon isotopes between iron carbide melt and graphite/diamond, as reported in [3], is believed to have created a "^{12}C-enriched core" with a significant difference in the distribution of carbon isotopes between the carbon core and bulk silicate Earth during accretion and differentiation of early Earth. In order to further characterize the carbon movement in the mantle, the carbon isotope systematics during melting of carbonated mantle in the presence of graphite/diamond were investigated in the Mg-Si-C-O system. Preliminary results indicate that carbon isotopes show considerable partitioning between graphite/diamond and carbonate melt at temperatures and pressures corresponding to upper mantle conditions. We attempt to discuss the carbon isotope systematics in the mantle and core based on our experimental results.

[1] Dasgupta & Hirschmann (2006) *Nature*, **440**, 659-662 [2] Dasgupta & Walker (2009) *Geochimica Cosmoshim. Acta,* **72**, 4627-4641 [3] Satish-Kumar et al., (2011) *Earth Planet. Sci. Lett.* **310**, 340-348

δ^{26}Mg of brachiopod shells and the composition of past seawater

S. SAULNIER[*1], C. ROLLION-BARD[1], C. LECUYER[2], N. VIGIER[1] AND M. CHAUSSIDON[1]

[1]CRPG-CNRS, BP 20, Vandoeuvre-lès-Nancy, France, saulnier@crpg.cnrs-nancy.fr (* presenting author)
[2]Laboratoire de Géologie de Lyon, CNRS, Université Claude Bernard Lyon 1, Villeurbanne, France.

The Mg isotope composition of marine carbonates can provide information on the dynamics of the Mg cycle through geological times (e.g. [1]). Brachiopods were extensively used for tracking both physicochemical conditions and secular isotopic variations of past oceans (e.g. [2]). Articulated brachiopods shells are made of low-Mg calcite, which is relatively resistant to most diagenetic processes [3]. However, significant intravariability in oxygen and carbon isotope ratios have been shown for several species, mainly due to kinetic and metabolic effects operating during calcite formation (e.g. [4]).

Magnesium, oxygen and carbon isotopes were measured in various fragments of a fossil *Terebratula scillae* (2.1 Ma) in order to test whether brachiopod shells could constitute valuable proxies of the seawater Mg isotope composition. The external parts of the shell, including the primary layer and external contamination were physically removed before analyses. Mg isotope ratios were measured by MC-ICP-MS Neptune *Plus*, with an external 2σ error of 0.15‰. Oxygen and carbon isotope ratios were measured by IRMS, with an 2σ error of 0.04‰.

The ventral and dorsal valves have similar isotope compositions and variability: δ^{26}Mg ranges from -2.95 to -2.02 ‰, δ^{18}O ranges from 2.57 to 3.15‰ and δ^{13}C ranges from 1.12‰ to 2.00‰. No correlation is observed with Mg/Ca ratio. A negative trend can be observed between δ^{26}Mg and δ^{18}O. The lowest δ^{26}Mg values correspond to isotope equilibrium determined for inorganic calcite relative to seawater Mg (Saulnier et al., submitted), and are systematically observed in the fragments located at the outer parts of the shell. This suggests that the outermost parts of brachiopod shells can be used to track the Mg isotope composition of past seawter. This aspect will be tested by studying ancient brachiopods with geological ages spanning from 0 to 54 Ma.

[1] Higgins and Schrag (2010) *GCA* **74**, 5039-5053. [2] Veizer et al. (1999) *Chem. Geol.* **161**, 58-88. [3] Brand and Veizer (1980) *J. Sedimt Petrol.* **50**, 1219-1236. [4] Auclair et al. (2003) *Chemical Geology* **202**, 59-78

Diffusion chronometry and seismology: insights into eruption precursors

KATE SAUNDERS[1*], JON BLUNDY[1], RALF DOHMEN[2] AND KATHY CASHMAN[1]

[1]Department of Earth Sciences, University of Bristol, Bristol, UK, Kate.Saunders@bristol.ac.uk (* presenting author)

[2]Institut für Geologie, Mineralogie und Geophysik, Ruhr-Universtät Bochum, Germany

Timescales of magmatic processes are key to our understanding of active volcanic systems, yet remain one of the most poorly constrained variables. Today many active volcanoes are monitored through a combination of seismicity, ground deformation, gas emissions and geodetic methods. In some instances these methods can be used to track magma movement in the crust prior to eruption, but not every magma pulse of magma results in an eruption.

Petrological methods can interrogate the products of recent eruptions. Zoned volcanic crystals potentially perserve a record of magmatic processes during the lifetime of a crystal from nucleation to eruption. As the magma evolves, changes in the composition, water content, temperature or pressure will result in renewed growth of a different composition generating zoned crystals. In particular, diffusion chronology (relaxation of elements across compositional interfaces) enables us to calculate a time series, precisely dating the perturbations that occur in the magma chamber prior to eruption. These petrologically determined times series can be correlated with time series generated through geophysical techniques from the same eruption to ascertain links to pre-eruptive processes.

Mount St. Helens produced a series of well studied and characterised eruptions during 1980-86. Orthopyroxene is an ubiqitous crystal phase throughout the eruption sequence. Over 500 orthopyroxene crystals from nine of the eruptions have been investigated through a combination of back-scattered electron imaging and major element chemistry by electron probe microanalyser. This revealed multiple orthopyroxene crystal populations of both unzoned and zoned crystals. Zoned crystals populations were further sub-divided into: (1) normal zoned crystals (Fe-rich rims); (2) reversed zoned crystals (Mg-rich rims); (3) oscillatory zoned crystals. Diffusive chronometry of Mount St. Helens zoned orthopyroxene reveals that the majority of rim growth occurred within two years prior to eruption. Episodes of magma mixing identified in the petrological rocord are temporally correlated with the recorded seismicity indicating both tectonic and degassing driven seismic events occurred.

Molecular- and pore-scale response of uranium to advective geochemical gradients in heterogeneous sediments

KAYE S. SAVAGE[1*], WENYI ZHU[1], MARK O. BARNETT[2], C. TYLER WOMBLE[1] AND JAN E. PATTON[1]

[1]Wofford College Environmental Studies, Spartanburg SC, USA, savageks@wofford.edu (* presenting author), zhuw@wofford.edu, womblect@email.wofford.edu, pattonje@email.wofford.edu

[2]Dept. Civil Engineering, Auburn University, AL, USA, barnem4@auburn.edu

Experimental approach

Column experiments were devised to investigate the role of changing fluid composition on mobility of uranium through a sequence of geologic media. Fluids and media were chosen to be relevant to the ground water plume emanating from the former S-3 ponds at the Oak Ridge Integrated Field Research Challenge (ORIFC) site. Synthetic ground waters were pumped upwards at 0.05 mL/minute for 21 days through layers of quartz sand alternating with layers of uncontaminated soil, quartz sand mixed with illite, quartz sand coated with iron oxides, and another soil layer. Increases in pH or concentration of phosphate, bicarbonate, or acetate were imposed on the influent solutions after each 7 pore volumes while uranium (as uranyl) remained constant at 0.1mM. A control column maintained the original synthetic groundwater composition with 0.1mM U. Pore water solutions were extracted to assess U retention and release in relation to the advective ligand or pH gradients. Following the column experiments, subsamples from each layer were characterized using microbeam X-ray absorption spectroscopy (XANES) in conjunction with X-ray fluorescence mapping and compared to sediment core samples from the ORIFC, at SSRL Beam Line 2-3.

Results

U retention of 55 – 67 mg occurred in phosphate >pH >control >acetate >carbonate columns. The mass of U retained in the first-encountered quartz layer in all columns was highest and increased throughout the experiment. The rate of increase in acetate- and bicarbonate-bearing columns declined after ligand concentrations were raised. U also accumulated in the first soil layer; the pH-varied column retained most, followed by the increasing-bicarbonate column. The mass of U retained in the upper layers was far lower.

Speciation of U, interpreted from microbeam XANES spectra and XRF maps, varied within and among the columns. Evidence of minor reduction to U(IV) was observed in the first-encountered quartz layer in the phosphate, bicarbonate, and pH columns while only U(VI) was observed in the control and acetate columns. In the soil layer, the acetate and bicarbonate columns both indicate minor reduction to U(IV), but U(VI) predominated in all columns. In the ORIFC soils, U was consistently present as U(VI); sorption appears to be the main mechanism of association for U present with Fe and/or Mn, while U occurring with P appears in discrete particles consistent with a U mineral phase. U in soil locations with no other elemental associations shown by XRF are likely uranium oxide phases.

A silicon isotopic record of long term changes in continental weathering

PAUL S. SAVAGE[1,2]*, R. BASTIAN GEORG[3], HELEN M. WILLIAMS[4] & ALEX N. HALLIDAY[1]

[1]Department of Earth Sciences, University of Oxford, Oxford, UK
[2]Department of Earth and Planetary Sciences, Washington University, St. Louis, MO, USA (* presenting author; savage@levee.wustl.edu)
[3]WQC, Trent University, Peterborough, Ontario, Canada
[4]Department of Earth Sciences, Durham University, Durham, UK

High precision MC-ICP-MS analyses of a suite of globally sourced clastic sediments suggest that the Si isotope system behaves more conservatively than other stable isotope tracers (i.e. Li, Mg, O) during continental weathering. This is contrary to expectation, as previous studies have shown that Si isotopes can be significantly fractionated toward lighter compositions during formation of secondary phases [1]. Nevertheless, Si isotopes in shales do not correlate with canonical proxies for weathering. Instead, good negative correlations between $\delta^{30}Si$ values and insoluble element concentrations (Nb, Hf, TiO_2) indicate that intensive chemical weathering is required before resolvable negative Si isotopic fractionation occurs in such lithologies.

On this basis, Si isotope variations in the long-term clastic sedimentary record could be used to provide a reliable proxy for investigating long term changes in the degree of reworking of continental crust and/or the intensity of continental weathering. When there is extensive formation and exposure of continental material (the Si in which has not undergone prior weathering), erosion should produce sediment with Si isotopic compositions similar to igneous continental crust [2]. If the availability of new crustal material is reduced, then the sedimentary record will become increasingly dominated by reworking of pre-existing lithologies, which will drive the Si isotope compositions to lighter values over time.

Such a hypothesis has been tested here using the post-Archaean Australian shale (PAAS) suite [3]. These samples are ideal, as they were all sourced from the same continental mass (Australia and, before, Gondwanaland) and have a wide range of depositional ages, from 1500Ma to 200Ma. The data display an enrichment in isotopically light Si with time, which appears to relate to increasing Nd crustal residence age [4]. As such, sediment derived from sources dominated by recycling of older crustal lithologies display the lightest isotopic compositions, as predicted. There is also evidence, however, that incorporation of authigenic marine lithologies can complicate this simple relationship.

Extremely negative Si isotopic compositions in Archaean shales (also sourced from Gondwanaland) cannot be explained by long-term continental weathering, as they were deposited when new continental crust dominated the budget. This could, therefore, reflect more intense weathering, due to more aggressive climatic conditions, early in Earth history.

[1] Ziegler et al., (2005) *GCA*, **69(19)**, pp 4597–4610
[2] Savage et al., (2011) *Mineralogical Magazine*, **75(3)**, pp 1803
[3] Nance and Taylor, (1976), *GCA*, **40**, pp 1539-1551
[4] Allègre and Rousseau, (1984) *EPSL*, **67**, pp 19-34

Improved calibration technique for magnetite analysis by LA-ICP-MS

D. SAVARD[1]*, S.-J. BARNES[1], S. DARE[1], G. BEAUDOIN[2]

[1]Université du Québec à Chicoutimi, Chicoutimi (Qc), Canada, G7H 2B1 *ddsavard@uqac.ca
[2]Université Laval, Québec (Qc), Canada

Oxide minerals such as magnetite and chromite are becoming popular in the field of geochemical exploration because the wide variety of trace elements present could potentially be used in provenance studies [1]. The method of analysis used is commonly LA-ICP-MS because it provides limits of detections down to ng/g levels when the analytical parameters can be optimized. No matrix-matched reference materials (RM) are available at the moment for *in-situ* calibration. Artificial glasses could be used to calibrate but only Fe can be used as an internal standard because of the inhomogeneous distribution of most of the other elements in magnetite. [2] proposed using NIST-610 to calibrate. However, the Fe content in NIST-610 is low at c.a. 0.05% while Fe in magnetite is c.a. 72%, thus limiting the use of NIST-610 to a beam >25µm, with a maximum precision of R^2<0.85 when results are compared to EMPA analysis of natural magnetite. [3] proposed the combination of 5 iron-rich RM to cover the elements of interest. Based on the elements for which EMPA results are available this calibration is satisfactory. However, this technique is time consuming and reduces the space available in the ablation cell.

We have found that USGS glasses GSE-1g and GSD-1g provide an accurate calibration for a beam size down to 4µm. The glasses are produced from natural basaltic material, containing c.a. 10% Fe, doped with a wide variety of trace elements. Figure 1 shows a good correlation between working values and those obtained at LabMaTer (UQAC) using a 193nm Resonetics M-50 laser and Aglilent 7700X ICP-MS. GSE-1g was used to calibrate while GSD-1g was used to monitor the precision and accuracy of the calibration. A natural magnetite from the Bushveld, BC-28 [4], was used as a quality control RM. Based on EMPA data, the calibration technique is also suitable for chromites, ilmenites and other Fe-rich oxides.

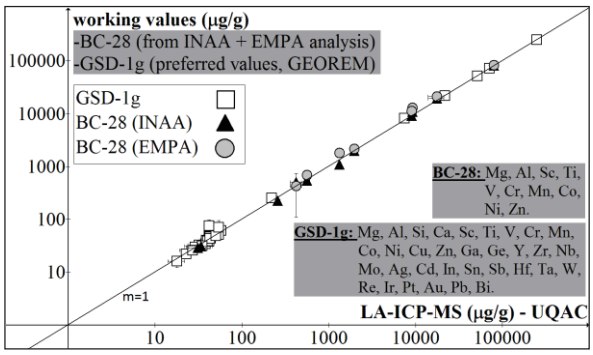

Figure (1): Accurate LA-ICP-MS calibration for magnetite analysis using GSE-1g as calibrant, GSD-1g and BC-28 as quality controls, and ^{57}Fe as internal standard.

[1] Dupuis C. and Beaudoin G. (2011) *Miner. Deposita* **46**:319-335. [2] Nadoll P. and Koenig A.E. (2011) *JAAS* **26**:1872-1877. [3] Savard *et al.* (2010) *Geoch. Cosmo. Acta* **74** (12):A914. [4] Barnes S.-J. *et al.* (2004) *Chem. Geol.* **208:**293-317.

How mobile is selenium in claystone? Insights given by radiochemistry and X-ray absorption spectroscopy

S. SAVOYE[1*], M.L. SCHLEGEL[1], B. FRASCA[1,2]

[1] CEA DANS/DPC, L3MR & LISL, Gif sur Yvette, France, sebastien.savoye@cea.fr (* presenting author), michel.schlegel@cea.fr

[2] University of Paris-Sud, France, benjamin_frasca@yahoo.fr

Introduction

The transport in the Callovo-Oxfordian clay formation of Se under its more oxidised forms, *i.e.* Se(IV) and Se(VI), was studied by means of batch and diffusion experiments [1], carried out at lab in N_2/CO_2 glovebox for mimicking as much as possible the physico-chemical conditions prevailing in-situ. A radiochemical approach using HTO, ^{36}Cl and ^{75}Se, as tracers, was supplemented by a non-radioactive one, for which the solid was investigated by X-Ray Absorption Spectroscopic (XAS) methods.

Results and Discussion

Results showed that Se(VI) diffused almost like ^{36}Cl, with little affinity towards clayey rocks (Rd < 0.02 mL g^{-1}). Conversely, the batch and diffusion-experiments revealed that Se(IV) exhibited a much stronger affinity towards the Callovo-Oxfordian claystone, in inverse correlation to initial Se concentration. Values of Rd were estimated, ranging from 10 to about 200 mL g^{-1} for $[Se(IV)]_{ini}$ decreasing from 10^{-3} to 10^{-6} mol L^{-1}. This behaviour could not be reproduced only with a simple model, especially for the pristine samples (diffusion experiments), since Se showed a secondary maximum ~ 2 mm under the surface, both in the radioactive and stable diffusion cells (Figure 1). The determination of the selenium oxidation state by XAS revealed that the total Se profile was clearly the sum of the contribution of (i) Se(IV), exhibiting a relative regular diffusion profile and of (ii) the more reduced selenium species (Se(red) ~ Se (0), Se(-I) and/or Se(-II)), especially located at about 2 mm from the interface (Figure 1).

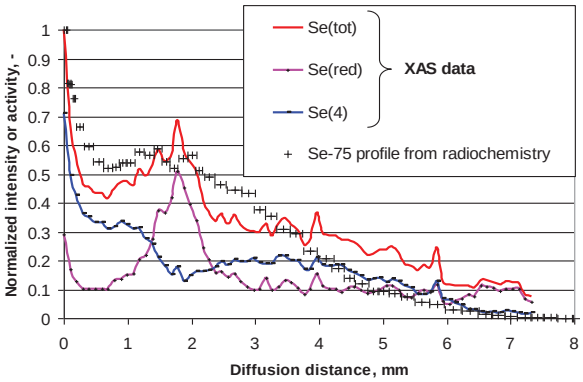

Figure 1: Distribution of the Selenium species along the rock profile obtained by XAS and comparison with radiochemistry data

The origin of the selenium distribution linked to some reduction processes was discussed regarding the mineralogy and the physico-chemical conditions prevailing in the pores.

[1] Savoye *et.al.* (2010) *Environ. Sci. Techn.* **44**, 3698-3704.

Retention of melt in granulite terrains

EDWARD SAWYER

Université du Québec à Chicoutimi, Sciences de la terre, ewsawyer@uqac.ca

Introduction

Previous work [1] showed that metagreywacke protoliths in the Ashuanipi Subprovince in northern Quebec produced approximately 600000 km^3 of granitic melt during granulite facies anatexis. Virtually all that melt was extracted from where it formed, leaving behind an Opx + Bt + Pl ± Qz residuum. What became of that melt?

Results

Fieldwork shows that very little of the anatectic melt collected into leucosomes, but a significant proportion remained in the granulite terrain as secondary diatexite migmatite. Melt accumulated in regional-scale dilatant sites. Field, geochemical and microstructural studies indicate that the secondary diatexite plays an important role in the evolution of granitic magma. Their microstructure and whole rock geochemistry indicates that a small proportion have the composition appropriate for the initial, anatectic melt. Most have compositions (supported by field relations) indicative of significant contamination by their melt-depleted wall rocks; contamination by the peritectic phase (Opx) alone is not sufficient. The microstructure (form and composition) of the feldspar-crystal framework in the diatexite reveals a wide range of responses to deformation during solidification. In places, meter-sized patches of leucocratic monzogranite occur in the diatexite and indicate local fractional crystallisation. However, most of the secondary diatexite represents an accumulation of plagioclase from which the fractionated melt has been removed. Kilometre-sized bodies of leucocratic monzogranite in the terrain represent part of the volume of fractionated melt that separated from the secondary plagioclase-rich cumulate diatexite, the balance moved to higher crustal levels.

Conclusions

Granulite terrains are much less depleted in melt than analysis of the residual rocks alone indicates. Large amounts of anatectic melt may be retained and melt from different source rocks can accumulate in the same sites. These sites represent a key reservoir in the deep crust where the composition of granite magma is established. Fractional crystallisation and general contamination exert a greater control on composition than source rock composition, or entrainment of peritectic phases.

[1] Guernina & Sawyer (2003) *Journal of Metamorphic Geology* **21**, 181-201-pp.

Geochemical investigations of the intrabasaltic palaeosols (bole beds) from Deccan Traps, India in deducing the palaeoclimatic conditions

MOHAMMED RAFI SAYYED [1*] AND SAJID HUNDEKARI[2]

[1]Geology Department, Poona College, Camp, Pune, India, mrgsayyed@yahoo.com (* presenting author)
[2] Geology Department, Poona College, Camp, Pune, India, sajid_hundekar@yahoo.com

Geochemical analysis of the intrabasaltic bole beds (palaeosols) occurring in the parts of Deccan Volcanic Province (India) was applied in deducing the palaeoenvironmental conditions prevailed during their formation. The bole beds the study area occur as red or green couloured clayey intercalations between the basaltic lava flows and show distinct environmental conditions during their formation when compared with the modern soils. In general red boles show higher weathering intensity, much leaching of the bases than the green boles while modern soils show moderate weathering but quite high leaching of the bases. The Weathering Potential Index (WPI) however suggests higher weathering in red boles, moderate in green boles and lesser in the modern soils. The Parkers Weathering Index (PWI) and calcination values indicate an enrichment of calcium during the formation of green boles thereby indicating aridity. Red boles were formed under higher rainfall but lesser temperature (more hydrolysis) than the green boles (less hydrolysis) while modern soils were formed under much higher rainfall and comparatively low temperature (strong hydrolysis). Iron species ratio, Product Index and FeO/Mgo values suggest that red boles were formed under strongly oxidizing but lesser acidic conditions while green boles were formed under less oxidizing but higher acidic conditions. The modern soils however indicate not much oxidizing but alkaline conditions. More retention of original mafic components in red boles and felsic components in green boles indicate selective dissolution of mafic components from green boles in more acidic fluids. Less hydrolysis and more calcination in green boles (than red boles) point towards more arid conditions during their formation than the red boles. However modern soils were formed under considerably humid conditions. The values of salinization indicate that the red boles were formed under fairly leached but relatively poorly drained conditions than the green boles while modern soils formed under quite intensely leached but poorly drained conditions. In conclusion the red boles were formed as a result of intense weathering under strongly oxidizing, acidic, more humid (more hydrolysis) environment with fairly leached but relatively poorly drained conditions than the green boles, suggestive of distinct weathering regimes. As a whole the palaeoclimates during the bole bed formation were quite different than the Holocene as the conditions were rather arid, fairly drained more acidic and strongly oxidizing with comparatively lesser rainfall but higher temperature. Although there is lack of age of control it is believed that the modern soil formation from Deccan traps represent much longer geomorphic history than the time lapsed during the formation of individual bole bed. In view of this, much intense weathering under stronger oxidizing conditions and more acidic conditions yet more aridity than the Holocene indicate catastrophic climatic conditions during the bole bed formation which can be related to the perturbations due to Deccan volcanic activity.

Inter-hemispheric patterns of Holocene Glacier and Temperature Change

JOERG M. SCHAEFER[1*], AARON PUTNAM[1,] GEORGE DENTON[2], DAVID BARRELL[3], ROBERT FINKEL[4], TOBY KOFFMAN[2], CHRISTIAN SCHLUECHTER[5], IRENE SCHIMMELPFENNIG[1], ROSEANNE SCHWARTZ[1], SUMMER RUPPER[6]

[1] Lamont-Doherty Earth Observatory, Palisades, NY-10964, USA, schaefer@ldeo.columbia.edu (* presenting author)
[2] University of Maine and Climate Change Institute, Orono, ME 04469, USA
[3] GNS Science, Dunedin, New Zealand
[4] University of California, Berkeley, USA
[5] University of Berne, Switzerland
[6] Brigham Young University, Provo, Utah, USA

Glacier and Temperature Change

Glaciers are among the most sensitive recorders of climate change, making them highly valuable as paleo-climate recorders and, at the same time, highly vulnerable to ongoing climate change.
Using independent lines of argument from glaciology, glacial geology and climate science, we make the case that glaciers in temperate climate zones are pre-dominantly driven by temperature change and, in turn, form sensitive thermometers.

Holocene Temperatures from glacier and marine records

Recent progress in the method of cosmogenic nuclide surface exposure dating now affords for precise reconstructions of glacier fluctuations throughout the Holocene and up to present day. In combination with detailed mapping of the paleo-snowline, a measure of past glacier extent, relative to today's snowline, we present comprehensive records of glacier advances in southern and northern mid-latitudes during the Holocene, and deduce regional Holocene temperatures. We compare these terrestrial temperature records with near-by and far field marine temperature estimates to better understand the inter-hemispheric patterns of Holocene temperatures.

We finally discuss implications and potential of these data sets for improving climate models.

Modeling of concentrations in major elements of subsurface and deep waters in the Ringelbach granitic research catchment (Vosges, France)

T. SCHAFFHAUSER[1*], F. CHABAUX[1], B. FRITZ[1], B. AMBROISE[1], A. CLEMENT[1] AND Y. LUCAS[1]

[1]LHYGES, Université de Strasbourg/EOST, CNRS, France (*correspondence: thiebaud.schaffhauser@etu.unistra.fr)

For constraining the nature of water-rock interactions occuring within granitic watersheds and exploring the potential relationships existing between subsurface and deep waters a geochemical study combined with a modeling approach has been undertaken in the small Ringelbach granitic catchment (Vosges, France). Concentrations of major elements were measured in water samples from the main springs emerging within the catchment as well as from two 150-m deep boreholes (deep waters) drilled through the whole weathering profile of the granite bedrock.

The coupled transport/reaction model KIRMAT [1] has been used in this study to discuss and constrain the main spatial and temporal geochemical variations observed in these different waters. It combines geochemical reactions, including clay precipitation [2], and 1D mass transport equations to simulate the reactive transport of a fluid through a rock along a given water pathway.

In the case of the Ringelbach watershed, we have simulated the transfer of rainwaters along different water pathways, from very permeable surficial arenic formation to almost impermeable deep fresh granite. Simulations point out that the initial chemical signature of rainwater is rapidly lost during its transfer through the substratum due to the weathering of rock-forming minerals. Furthermore, simulations indicate that the geochemical characteristics of spring waters and deep waters are mainly controlled by two different water pathways within the substratum: high-rate downslope subsurface flow for the springs, and very low flows through the whole granitic massif for borehole waters. These results suggest therefore that spring waters and deep waters are largely disconnected in the Ringelbach catchment.

[1] Gérard *et al.* (1998) Chemical Geology, **151**, 247–258.
[2] Fritz *et al.* (2009) GCA, **73**, 1340-1358.

The construction of the Alpine Adamello batholith as recorded by zircon

U. SCHALTEGGER[1*], C. BRODERICK[1], A. SKOPELITIS[1], D. FLOESS[2], A. ULIANOV[2], O. MÜNTENER[2], L. BAUMGARTNER[2], P. BRACK[3] AND P. ULMER[3]

[1]Earth and Environmental Sciences, University of Geneva, Switzerland, urs.schaltegger@unige.ch (*presenting author)
[2]Institute of Mineralogy and Geochemistry, University of Lausanne, Switzerland
[3]Institute of Geochemistry and Petrology, Swiss Federal Institute of Technology ETH, Zürich, Switzerland

Batholiths are formed by incremental melt addition over time scales spanning millions of years. They consist of composite plutons, which are formed through individual melt pulses that cool over a 10 to 100 ka timescale.

Careful laser ablation ICP-MS and CA-ID-TIMS zircon geochronology on the Adamello Batholith in Northern Italy not only reveals these different timescales, but also allows reconstruction of some of the batholith-forming processes: (a) The entire batholith grows from 43 to 33 Ma through melts derived from an increasingly crust-contaminated arc-type source; (b) single mappable plutons are compositionally more or less heterogeneous and consist of a number of melt pulses; (c) each pulse intruded and cooled as a single unit over timescales of several 10 to 100 ka; (d) the Val Fredda pluton in the southernmost Re di Castello unit shows bimodal magmatism with gabbroic melts injecting into tonalite mushes and sharing some 100 ka of crystallization and cooling; (e) the subsequent pulses of diorites and tonalites of the Lago della Vacca pluton are recognized to tap the same source mushes and continuously recycle the crystal cargo [1], while in the case of more evolved tonalites of the Central Adamello unit the pulses consist of fractionated residual melt without inheritance of crystal cargo.

Chemical-abrasion, high-precision ID-TIMS zircon dating also revealed that mapped units show a significant age spread with clear geographic trends interpreted as accretion of pulses that are not discernible in the field. The trace element and Hf isotopic composition of dated zircon is a paramount tool to trace fractionation of major and accessory minerals during zircon crystallization, mixing of melts with different source components or of mixing ante- or xenocrystic crystal cargo into a melt batch [2] In this way, zircon provides a means to trace the thermal and magmatic evolution of deeper crustal reservoirs. Additional titanite U-Pb data may help to quantify the rate of high-temperature cooling down to the solidus or, alternatively, trace prolonged heat advection followed by partial remelting and homogenization of subsequent melt batches, as seen in the Lago della Vacca unit.

[1] Schoene et al. (in press) *Earth Planet. Sci. Lett.* [2] Schoene et al. (2010) *Geochim. Cosmochim. Acta* **74**, 7144-7159.

Estimating isotope fractionation driven by nuclear size

E. A. SCHAUBLE[1*], S. GHOSH[2], B. A. BERGQUIST[2]

[1]UCLA, Los Angeles, CA, USA schauble@ucla.edu (* presenting author)

[2]U. Toronto, Toronto, ON, Canada

Mass-independent fractionation (MIF), where isotope abundance variations are disproportionate in mass, can have several causes. The nuclear field shift effect, proposed by Jacob Bigeleisen to explain mass independent uranium isotope signatures observed in chemical exchange experiments, stems from slight perturbations in chemical bond strengths caused by variation the volume and shape of nuclei[1]. It is unique in being a thermodynamically driven MIF mechanism that persists at conditions of equilibrium isotope exchange, and is truly independent of isotopic mass. Theoretical calculations have so far been limited to fairly small molecules, atoms and ions, in part because relativity becomes important for electrons interacting closely with nuclei, necessitating an approximate solution of the Dirac equation for electronic structure modeling. Methods for estimating isotopic fractionation factors in more complex materials are needed in order to understand recent detections of nuclear volume signatures in evaporating liquid metals, ores, and sediment, and to guide future studies. In this study we have developed procedures for cross-calibrating calculations made with relativistic electronic structure theory against less computationally intensive models.

Our initial goal was to calculate the equilibrium fractionation between liquid mercury liquid and mercury vapor to compare with experiment[2]. We observed a strong correlation ($R^2 \approx 0.9$) between a) relativistically estimated nuclear volume fractionation and b) the Mulliken population of 6s electrons in Hg-bearing species calculated with methods that incorporate relativistic effects only in the generation of a mercury pseudopotential. This is consistent with the strong correlation between atomic polar tensor charges and fractionation observed previously[3]. Based on the slope of the correlation (~1.5‰ in $^{202}Hg/^{198}Hg$ per 6s electron at 295 K), and estimated ~70-80% occupation of 6s orbitals in liquid mercury[4], we estimate 0.5-0.9‰ nuclear volume fractionation of $^{202}Hg/^{198}Hg$ between liquid and vapor, liquid being enriched in neutron-rich isotopes, and a positive $\Delta^{199}Hg$ signature of 0.1-0.2‰ in vapor. Including mass dependent fractionation effects, a total liquid-vapor $^{202}Hg/^{198}Hg$ fractionation of 0.7-1.3‰ is calculated, in good agreement with experimental results.

Plane-wave density functional theory methods, which can be applied to crystalline solids and liquids (within a periodic boundary condition approximation), appear to similarly show strong correlation with relativistic estimates of nuclear-volume fractionation. This suggests that it may be possible to estimate equilibrium MIF signatures in a wide variety of complex, geochemically interesting materials.

[1] Bigeleisen, 1996, JACS 118:3676. [2] Estrade et al. 2009, GCA 73: 2693; Ghosh et al, in press, Chem. Geol. [3] Wiederhold et al. 2010, Env. Sci. Tech. 44:4191. [4] Mattheiss et al. 1977, Phys. Rev. B 16:624.

The Rofna Porphyry Complex: Combining LA-ICPMS and CA-TIMS U-Pb ages on zircons.

THOMAS SCHEIBER[1*], BENJAMIN D. HEREDIA[1], JASPER BERNDT[2], AND O. ADRIAN PFIFFNER [1]

[1] Institute of Geological Sciences, University of Bern, Switzerland, scheiber@geo.unibe.ch, benjamin.heredia@geo.unibe.ch, pfiffner@geo.unibe.ch

[2] Institut für Mineralogie, Universität Münster, Germany jberndt@uni-muenster.de

The Rofna Porphyry Complex (RPC) in the northern part of the Suretta nappe of the Penninic zone in eastern Switzerland, is mainly composed of two different lithologies: porphyritic rock types and augengneisses (Fig. 1). The augengneisses are cross-cut by porphyritic rocks and have been traditionally interpreted as Ordovician intrusives [1] without having any radiometric age control. Our field observations indicate that (a) the augengneisses show homogenous penetrative deformation whereas the porphyritic rocks reveal variable degrees of Alpine deformation, and (b) the augengneisses occur structurally above the porphyritic rocks (Fig. 1).

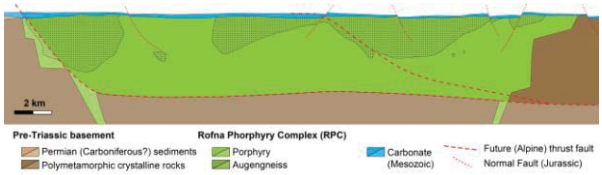

Figure 1: Restored section of the frontal part of the Suretta nappe - a feasible pre-Alpine constellation at the time of Jurassic rifting.

The magmatic event emplacing the porphyry has already been dated by ID-TIMS at 268.3 ± 0.6 Ma, which is a mean $^{206}Pb/^{238}U$ age of two nearly concordant multigrain fractions [2]. In order to constrain the age relationship between the different RPC rock types, we performed U-Pb LA-ICPMS measurements on zircons. In the augengneiss two age populations can be observed: One showing little spread at 311 Ma, and another younger one with a larger spread from 250 to 288 Ma. For the porphyritic rocks there is only one cluster of LA-ICPMS ages yielding an age range from 260 to 278 Ma.

Our new data suggest that the augengneisses are not the result of Ordovician magmatism, but may be related to the Variscian orogeny. The younger population in the augengneisses overlaps with the intrusion age of the porphyry and could either be the result of zircon neoformation or partial resetting of the U-Pb system.We therefore interpret the RPC as a composite late-Variscan and post-Variscan intrusive complex, where the pophyritic rocks followed pre-existing magma conduits, replenishing and disrupting the older augengneiss body at a shallow crustal level. High precision CA-TIMS data will provide further control of the emplacement relationships between these metamorphosed magmatic rocks.

[1] Spicher (1980) *Geological map of Switzerland*, 1:500.000. [2] Marquer, Challandes & Schaltegger (1998) *Schweiz. Mineral. Petrogr. Mitt.* **78**, 397-414.

Iron isotopes as a tracer in an acid-sulfate soil system

K. SCHEIDERICH[1*], J. KIRBY[1], P. SHAND[1,2]

[1]CSIRO Land and Water, Urrbrae, Australia, kate.scheiderich@csiro.au (*presenting author)
[2]Flinders University, Adelaide, Australia

Iron isotopes have been extensively studied in many systems and the fractionation factors are at least experimentally well understood for many common processes on earth's surface, including Fe-oxide mineral formation, precipitation reactions, and biological transformations such as microbially-mediated reductive dissolution of hematite. In complex environments, these well-undestood fractionations can be applied to assess the transport and speciation of Fe. However, only a few attempts have been made to understand the fractionations occuring in sulfur-rich systems, and these have been limited to acid mine drainage and hydrothermal vents. Salt marshes, tidal flats, and terrestrial floodplain environments, though well studied from the perspective of nutrients, trace metal cycling, and light stable isotopes (particularly C and S), have received little attention, yet are Fe-rich as a result of Fe monosulfide and pyrite formation.

Here we examine Fe isotope fractionation and Fe speciation in acid sulfate soil profiles and sediments from the Murray River system (South Australia), in order to gain an understanding of processes, pathways and biogeochemical cycling of Fe and associated metals through this environment. Inland acid sulfate soils are present in most fresh and saline wetland systems in the Murray-Darling Basin, largely due to the build-up of sulfide minerals during high pool levels. This situation has existed since the installation of locks in the 1930's. Prolonged recent drought led to oxidation of sulfide minerals and soil acidification with severe impacts on the local soil ecosystem. However, in the floodplain soils, desiccation of pyrite-laded, organic rich sediment allows Fe oxidation, then re-flooding events release acid to the river. Prelimary results from two oxidized soil samples of have a small range of light, near-zero δ^{57}Fe values. However, significant fractionation has been observed between primary sulfide minerals and their oxidation products in other acid sulfate soils in Australia. This is consistent with previously observed isotope fractionation between oxidized Fe minerals precipitated from Fe-rich sulfidic mine drainage [1, 2]. Additional data regarding the exact Fe mineral phases present in the soils, as well as sequential extractions of these phases and isotopic analysis of the extracts may provide additional constraints on Fe translocation in these environments.

[1] Egal, M., Elbaz-Poulichet, F., Casiot, C., Motelica-Heino, M., Négrel, P., Bruneel, O., Sarmiento, A., Nieto, J. (2008) *Chemical Geology* **253**, 162-171. [2] Herbert, R., Shippers, A. (2008) *Environ. Sci. Technol*. **42**, 1117-1122.

Coupled geochemical processes limiting phytosiderophore-promoted iron uptake from soils

W.D.C. SCHENKEVELD[1*], E. OBURGER[2], Y. SCHINDLEGGER[3], A. REGELSBERGER[3], S. HANN[3], M. PUSCHENREITER[2] AND S.M.KRAEMER[1]

[1]Universität Wien. Dept. of Environmental Geosciences, Althanstrasse 14, 1090 Wien, Austria, schenkw6@univie.ac.at (* presenting author)
[2]University of Natural Resources and Life Sciences, Dept. of Forest and Soil Sciences, Tulln, Austria
[3]University of Natural Resources and Life Sciences, Dept. of Chemistry, Wien, Austria

Graminaceous plant species (grasses) exude multidentate complexing agents called phytosiderophores (PS) for the purpose of iron aquisition, in particular under conditions of iron deficiency stress. Upon release from the root surface, the ligands diffuse into soil solution and solubilize iron from iron bearing phases in the soil, forming iron complexes which are taken up at the root surface.

Although the mechanism of action of PS has been intenisively studied, this was mostly done in hydroponics or in soil suspensions with a low soil to solution ration that did not allow to investigate coupled geochemical processes. The aim of the current project is to quantitatively understand the geochemical and geophysical processes limiting PS promoted iron uptake.

In the present work the rate of iron mobilization from various soils by the PS deoxymugineic acid (DMA) was examined in batch experiments, both with and without addition of a sterilant (sodium azide) to prevent biodegradation of the DMA ligand. Both clay and sandy soils, differing in iron availability were included.

Fe mobilization corresponded with 10 to 60% of the added DMA. The extent to which Fe was mobilized positively correlated with Fe availability parameters (e.g. DTPA-extractable Fe) and negatively correlated with the clay content of the soils. Especially in soils of low Fe availability, Fe mobilization was strongly compromised by the mobilization of competing cations like Cu, Zn, Ni and Co.

In absence of sterilant, all metal-DMA complexes were removed from solution within 4 days. Depending on the soil, Fe mobilization reached a maximum after 0.25 to 8 hours.. Except for one soil, maximum Fe mobilization was not dependent on sterilant addition. Also when sterilant was added, FeDMA concentrations eventually decreased, indicating that processes other than biodegradation significantly compromise the FeDMA concentration.

These results strongly indicate that for improving the understanding of plant iron acquisition, the kinetics and thermodynamics of coupled rhizosphere processes need to be studied coherently.

Fe electron transfer and atom exchange at mineral/water interfaces

M. SCHERER*[1], D. LATTA[2], T. PASAKARNIS[1], A. NEUMANN[1], M. BARGER[1], K. ROSSO[3], AND C. JOHNSON[4]

[1]Civil and Environmental Engineering, University of Iowa, Iowa City, IA 52242(*correspondence: michelle-scherer@uiowa.edu)

[2] Molecular Environmental Science Group, Biosciences Division, Argonne National Laboratory, Argonne, IL 60439, USA

[3]Chemical and Materials Science Division, Pacific Northwest National Laboratory, Richland, Washington 99352

[4]Dept. of Geoscience, University of Wisconsin-Madison, Madison WI 53706

Electron and ion exchange reactions at mineral/water interfaces influence the composition of natural waters, the biogeochemical availability of nutrients, and the environmental fate of heavy metals and contaminants. A new conceptual model is emerging to describe the reaction of aqueous Fe(II) at the mineral/water interface that couples oxidation and reduction reactions between spatially separated surface sites connected through the bulk mineral via either electrical conduction, atom diffusion, both, or some other yet unknown mechanism [1, 2]. We are collaborating to combine ^{57}Fe Mössbauer spectroscopy, Fe isotope tracer experiments, and molecular modeling to investigate Fe electron transfer at mineral surfaces and the rates and mechanism of Fe atom exchange.

We are exploring these processes in commonly occurring Fe oxides and Fe-containing clay minerals over a range of environmentally relevant conditions. Here we provide a summary of what we have learned so far, as well as present new findings investigating whether cation substitution influences the rate of atom exchange, and whether similar reactions will occur in clay minerals, as well as between aqueous Fe(III) and Fe(II) containing minerals.

[1] Gorski and Scherer (2011) *Aquatic Redox Chemistry* **1071**, 315-343.
[2] Yanina and Rosso (2008) *Science* **320**, 218-222.

Effect of Ce(III) oxidation by Mn(IV) on its use as a paleo-redox proxy

JOHAN SCHIJF[1*] AND KATHLEEN S. MARSHALL[2]

[1]University of Maryland Center for Environmental Science, Chesapeake Biological Laboratory, Solomons, MD, USA, schijf@cbl.umces.edu (* presenting author)

[2]University of Maryland Center for Environmental Science, Chesapeake Biological Laboratory, Solomons, MD, USA, marshall@cbl.umces.edu

Research outline

Marine sedimentary cerium (Ce) anomalies are due to enhanced Ce sorption with respect to the strictly trivalent REEs as it is oxidized from Ce(III) to more reactive Ce(IV). They are often interpreted as indicative of oxidizing conditions, specifically the presence of free oxygen, in the bottom water of ancient ocean basins at the time of sediment deposition. Such an interpretation could be complicated if Ce(III) were oxidized in the absence of free oxygen, as has been shown to occur on the surface of manganese oxides. We performed sorption experiments under anaerobic conditions with yttrium and the REEs in 0.5 M NaCl on pure synthetic Fe(III) and Mn(IV) oxides, plus three synthetic ferromanganese oxides containing 25, 50, and 90 mol% Mn. All precipitates were found to be X-ray amorphous and to contain Mn(IV) only.

REE sorption on the pure Fe and Mn oxides is well described with a non-electrostatic surface complexation model (SCM) that accounts for the higher acidity of hydroxyl groups on the Mn oxide, for monodentate and bidentate binding of the REEs by these groups, and for the binding of REE–hydroxide complexes at elevated pH [1,2]. REE sorption on ferromanganese oxides is moreover adequately described with a linear combination of the pure Fe and Mn oxide SCMs that reflects the proportion of each phase in the mixture. A clear presence, respectively absence, of Ce anomalies indicates that Ce(III) is oxidized on Mn oxide at all experimental pH values (4–8), but never on Fe oxide. The extent of oxidation on ferromanganese oxides is similar to that on pure Mn oxide, even at the lowest Mn content.

Below pH ~ 5.5 the Ce anomaly in pure Mn oxides is independent of pH, suggesting that the oxidation reaction involves direct transfer of an electron from Ce(III) to Mn(IV). Above pH ~ 5.5 the Ce anomaly has a linear pH dependence and the oxidation reaction may involve the species $CeOH^{2+}$, or otherwise require the presence of H_2O or OH^-.

Conclusions

Laboratory experiments of REE sorption on pure Fe and Mn oxides and on ferromanganese oxides with a wide range of Mn contents, in 0.5 M NaCl at T = 25°C, demonstrate that Ce(III) is oxidized under anaerobic conditions at the Mn oxide surface and thus probably by Mn in ferromanganese oxides, not by Fe. Hence, marine sedimentary Ce anomalies are not a reliable proxy of the presence of free oxygen in the deep paleo-ocean wherever Mn oxides abound in the watercolumn or on the seafloor. At the very least, such records should be interpreted with appropriate caution.

[1] Schijf & Marshall (2011) *Marine Chemistry* **123**, 32-43.
[2] Marshall & Schijf (2012) *Chemical Geology*, in review.

Microbially-mediated isotopic fractionation of selenium : Relevance for biogeochemical processes in the geological record

KATHRIN SCHILLING[1*], THOMAS M. JOHNSON[2], ROBERT SANFORD[2] AND PAUL R. D. MASON[1]

[1]Utrecht University, Utrecht, The Netherlands, k.schilling@uu.nl (* presenting author)

[2]University of Illinois at Urbana-Champaign, Urbana, IL, USA

The terrestrial and marine evolution and preservation of life are sensitive to changes in redox conditions. Selenium as an redox-sensitive element can provide information about the oxyengenation history of the ocean and atmosphere. Microbial reduction of Se-oxyanions causes isotopic fractionation, and stable Se isotope ratios can be used as a novel tool to detect biological Se cyling in the geological record. In addition, Se isotope ratios, in the geological record as well as in modern environments, may fingerprint specific metabolisms. However, our knowledge about microbially-mediated Se isotopic fractionation is limited due to lack of experimental studies under environmentally relevant Se and electron-donor concentrations. Here we determine new pure culture Se isotopic fractionation factors and investigate their dependence on experimental conditions including selenium and electron-donor concentrations. Results are given as magnitudes of isotopic fractionation, ε (ε=1000*(α-1)[‰]; α = $(^{82}Se/^{76}Se)_{Reactant}/(^{82}Se/^{76}Se)_{Product}$. We aim to investigate metabolically diverse microorganisms, including *Desulfitobacterium* st. Viet1*, Geobacter sulfurreducens* PCA*, Pseudomonas stutzeri* KC, *Aneromyxobacter dehalogenans* FRCW, and *A. dehalogenans* FRC-R5.

The pure cultre of *Desulfitobacterium* Viet1 coupled the reduction of 44μM Se(VI) with oxidation of lactate under strictly anaerobic conditions. This reduction yielded an ε Se(VI)→Se(0) = 9.4±0.3‰ (n=2) . This ε is higher than those previously reported for *Bacillus selenitireducens*, *Bacillus arsenicoselenatis* and *Sulfurospririllum barnesii* [1] and could be useful in explaining very high $\delta^{82/76}$Se values (up to −12.77‰) observed in high-selenium carbonaceous shales from Yutangba deposit, China [2]. Further experiments will determine the ε's for microbial Se reduction under electron-donor rich and electron-donor poor conditions. The results of this study will be useful in interpreting the measured Se isotope ratios in the rock record and may reflect the distribution of microorganisms in modern and ancient Earth.

[1] Herbel (2000) *Fractionation of selenium isotopes during bacterial respiratory reduction of selenium oxyanions* **64#**, 3701-3709.
[2] Wen (2007) *Large selenium isotopic variations and its implication in the Yutangba Se deposit, Hubei Province, China* **52#**, 2443-2447.

Geochemistry and thermobarometry of postglacial Llaima tephras

JULIE C. SCHINDLBECK[1] (*), ARMIN FREUNDT[1], STEFFEN KUTTEROLF[1], KAREN STREHLOW[1]

1 GEOMAR, Kiel, Germany, jschindlbeck@geomar.de(*)

Llaima is a large active stratovolcano in the Southern Volcanic Zone in Chile. Field work in 2011 revised the postglacial stratigraphy after Naranjo&Moreno (1991) and led to the subdivision into units I to V. Postglacial activity started 13.500 years ago with caldera-forming eruption of two mafic ignimbrites (unit I). These are overlain by a sequence of three basaltic-andesitic to two dacitic lapilli fallout deposits and reworked tuffaceous sediments (unit II). At ~8600 cal BC a large Plinian eruption emplaced a compositionally zoned dacitic to andesitic fallout tephra (unit III) that became capped by subsequent andesitic surge deposits (unit IV) when the eruption became unstable. The following unit V represents a time interval of ~7000 years during which at least 30 basaltic to andesitic ash and lapilli fallout deposits with intercalated tuffaceous sediments and paleosols were emplaced.

Bulk-rock, mineral and glass chemical analyses constrain the vertical compositional changes of Llaima tephras. Tephra compositions switch between a calc-alkaline differentiation trend (unit I) and a more tholeiitic trend (units II-IV), with samples of unit V varying between both trends, indicating a strong control of $f(O_2)$ (and $P(H_2O)$) on the relative timing of Fe-Ti oxide fractionation. Moreover, iron rich fayalites that are in equilibrium with the glass composition occur in units II and III with calculated T-$f(O_2)$ close to the FMQ suggesting that late-stage fayalite precipitation involved crossing of the FMQ boundary. The younger unit V tephras and historical compositions define a second differentiation trend relatively enriched in K_2O, Rb, Ba and Zr; this is not the results of changing source conditions but can be explained by a stronger early olivine fractionation in the respective magmas.

Thermobarometric calculations based on amph, cpx-liq, plag-liq, ol-liq and Fe-Ti-oxide compositions constrain changing magma chamber positions over time. Storage depths were 14 - 19 km for unit I andesite and and varied between 10 to 17 km for unit II andesites and dacites. The compositionally zoned eruption of units III and IV withdrew dacite magma from ~10 km depth but andesite from a deeper level of 13-15 km. Storage depths of unit V andesitic magmas ranged from 6 to 15 km. Based on temporally changing storage depths and differentiation paths, a 4-stage evolution of the postglacial magmatic system of the Llaima volcanic complex is proposed.

Characterization of U-bearing phases at a U-tailings facility in Sask. Canada

MICHAEL SCHINDLER*[1], JENNIFER DUROCHER[1] AND TOM KOTZER[2]

[1] Laurentian University, Department of Earth Sciences mschindler@laurentian.ca (*presenting author) ; jl_durocher@laurentian.ca

[2] Cameco Corporation, Senior Environmental Geochemist tom_kotzer@cameco.com

Uranium mobility around radioactive waste products such as mine tailings is a growing environmental concern. The characterization of particular U-bearing solid phases in the surface and subsurface around U-mine tailings facilities is essential in understanding and controlling the mobility of uranium [1]. The Key Lake milling facility located in Saskatchewan, Canada, has the world's largest annual U production capacity (25 million pounds U_3O_8) where it processes various grades of U-ore (maximum grade 18%, average grade 4%) from local operations [2]. In general, the ore is crushed; U is dissolved and leached using sulfuric acid and finally extracted and purified using ammonium sulfate and ammonia gas treatments [3]. Mining and milling waste products including tailings (1983-1996) and a portion of the acidic leachates and raffinates are stored in the engineered on-site Above Ground Tailings Management Facility (AGTMF) [4]. The occurrence, paragenesis and chemical composition of U-bearing phases at the AGTMF were examined, in both unconsolidated as well as epoxy impregnated samples to a maximum depth of 10 cm, using Scanning Electron Microscopy, X-ray Diffraction, Raman Spectroscopy, Laser Ablation ICP-MS, X-ray Photoelectron Spectroscopy and synchrotron-based micro-X-ray Fluorescence Spectroscopy. Uranium-bearing phases were observed as micro-sized coatings and included phases belonging to the zippeite group as well as the autunite group. Detailed mineralogical and chemical characterization of the tailings also indicated the presence of β-U_3O_8 (Fig. 1a) and U-bearing gypsum (Fig. 1b).

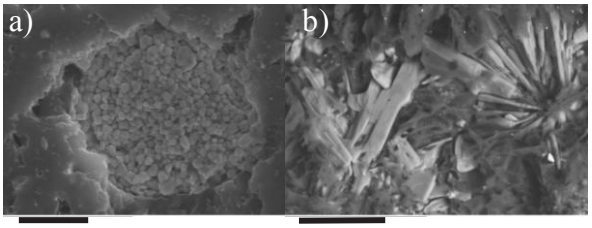

Figure 1: Backskatter electron images of (a) a cluster of β-U_3O_8 and (b) uranium-bearing gypsum.

Pb-isotope measurements and Raman spectra suggest that β-U_3O_8 is an alteration product of uraninite ore rather than a product of the milling process or bacterial reduction. LA-ICP-MS analyses of the gypsum crystals showed surprisingly high U-concentrations which were attributed to nanometre-scale intergrowths and coatings.

[1] Buck *et al.* 1996. *Environmental Science & Technology* **30,** 81. [2] Gandhi 2007. *Geological Survey of Canada,* open file **5005,** *Sask. Industry and Resources,* open file **2007-11.** [3] Cameco 2010. Key Lake Extension Project [4] Jarrell 2004. *IAEA-TECDOC-1419*. 45-74.

The Last Stages of Terrestrial Planet Formation: Dynamical Friction and the Late Veneer

H. E. SCHLICHTING[1,*], P. H. WARREN[1], Q.-Z. YIN[2]

[1]Dept. of Earth & Space Sciences, UCLA 595 Charles E. Young Drive East, Los Angeles, CA 90095 (hilke@ucla.edu) (* presenting author)

[2]Department of Geology, University of California Davis, One Shields Avenue, Davis, CA 95616 (qyin@ucdavis.edu)

The final stage of terrestrial planet formation consists of the cleanup of residual planetesimals after the giant impact phase. Dynamically, a residual planetesimal population is needed to damp the high eccentricities and inclinations of the terrestrial planets to circular and coplanar orbits after the giant impacts stage. Geochemically, highly siderophile element (HSE) abundance patterns inferred for the terrestrial planets and the Moon suggest that a total of about 0.01 $M_\oplus$ of chondritic material was delivered as 'late veneer' by planetesimals to the terrestrial planets after the end of giant impacts. Here we combine these two independent lines of evidence for a leftover population of planetesimals and show that: 1) A residual population of small planetesimals containing 0.01 $M_\oplus$ is able to damp the high eccentricities and inclinations of the terrestrial planets after giant impacts to their observed values. 2) At the same time, this planetesimal population can account for the observed relative amounts of late veneer added to the Earth, Moon and Mars provided that the majority of the accreted late veneer was delivered by small planetesimals with radii ≤10 m. These small planetesimal sizes are required to ensure efficient damping of the planetesimal's velocity dispersion by mutual collisions, which in turn ensures sufficiently low relative velocities between the terrestrial planets and the planetesimals such that the planets' accretion cross sections are significantly enhanced by gravitational focusing above their geometric values. Specifically we find, in the limit that the relative velocity between the terrestrial planets and the planetesimals is significantly less than the terrestrial planets' escape velocities, that gravitational focusing yields a mass accretion ratio Earth/Mars ~ $(\rho_\oplus/\rho_{mars})(R_\oplus/Rmars)^4$ ~17, which agrees well with the mass accretion ratio inferred from HSEs of 12-23. For the Earth-Moon system, we find a mass accretion ratio of ~ 200, which, as we show, is consistent with the mass accretion ratio inferred from HSE abundances of 150-700. We conclude that small residual planetesimals containing about ~ 1% of the mass of the Earth could provide the dynamical friction needed to relax the terrestrial planets' eccentricities and inclinations after giant impacts, and also may have been the dominant sources for the relative and absolute amounts of late veneer added to Earth, Moon and Mars. We argue that the terrestrial planets volatile elements were also delivered by the late veneer in order to account for the ~4.4Ga old terrestrial hydosphere and early felsic crust of granitoids reflected in Hadean zircons [1]. [1] Harrison (2009) *Annual Review of Earth Planet. Sci.* **37,** 479–505.

Nanoscale microstructure and texture patterns of bivalve nacre

W. W. Schmahl[1], E. Griesshaber[1], H. S. Ubhi[2]

[1]Department of Earth and Environmental Sciences, LMU München, Germany, wolfgang.schmahl@lrz.uni-muenchen.de

[2]Oxford Instruments, Halifax Road, High Wycombe, UK, Singh.Ubhi@oxinst.com

Biological hard tissues are hierarchical composites. EBSD is one of the best methods available for structural characterization of biological tissues, since it provides microstructure imaging and crystal orientation determination on several hierarchical levels. While the conventionally used 20 kV acceleration voltage yields EBSD with a spatial resolution in the micrometer range, high resolution, low kV (8 to 15) EBSD renders a 100-400 nm step resolution. This enables the investigation of nanostructures such as orientation patterns in the nacreous parts of biological skeletons.

We could map orientation patterns of calcite with high resolution, low kV (8 to 15) EBSD. This rendered measurements with 100-400 nm step resolution and enabled for the first time the investigation of biological nanostructures, especially orientation patterns in nacre and the nacreous parts of biological skeletons. The investigated specimens are the nacreous portions of the oyster *Crassostrea gigas* and of the bivalve *Mytilus edulis.* Further, we investigated the shells of *Elliptio crassidens*, *Cristaria plicatus* (composed entirely of nacreous aragonite) and the pearl of the freshwater mollusk *Hyriopsis cumingii*. The aragonite nanoplatelets are untwined single crystals that assemble to platelets. Stacks of almost equally oriented platelets form clusters with distinct orientations. Within a cluster the orientation goes across the platelets, while neighbouring platelets that belong to different clusters often form twin related orientations (rotation by 60 degrees around the c-axis). The normal to the platelets is the c-axis (setting: a=4.96 Å, b=7.97 Å, c=5.75 Å). The size of the correlated clusters and the abundance of twin relationships between adjacent platelets varies significantly between the investigated mollusk species.

For *Crassostrea gigas*, *Cristaria plicatus* and the pearl of *Hyriopsis cumingii* one crystal orientation dominates, such that the overall texture pattern has a 3D single crystal like appearance. For *Mytilus edulis* and *Elliptio elliptio* the three twin orientations are of similar abundance.

3D STXM tomography of Fe(II)-oxidizing bacteria

GREGOR SCHMID[1*], LIKAI HAO[1], ANDREAS KAPPLER[1], MARTIN OBST[1]

[1]University of Tuebingen, Germany, Center for Applied Geoscience, gregor.schmid@uni-tuebingen.de (* presenting author) likai.hao@uni-tuebingen.de, andreas.kappler@uni-tuebingen.de, martin.obst@uni-tuebingen.de

In pH-neutral environments ferrous iron can be oxidized under anoxic or microoxic conditions by Fe(II)-oxidizing bacteria. Different microbial metabolisms of Fe(II) oxidation and biomineralization of these bacteria have been identified and characterized so far. Initial Fe(III) mineral precipitation in the periplasm and subsequently cell encrustation was observed with the mixotrophic, nitrate-reducing, Fe(II)-oxidizing *Acidovorax* sp. strain BoFeN1 isolated from anoxic littoral sediments from Lake Constance, Germany [1]. Iron mineral precipitation in vicinity to the cell was shown for the phototrophic, anaerobic Fe(II)-oxidizing *Rhodobacter* sp. strain SW2 [2]. Also, under microaerophilic conditions iron minerals can be deposited within extracellular polymeric structures such as twisted stalks or sheats which are extruded by microaerophilic *Gallionella* strains [3].

To further our understanding of the different mineralization patterns and mechanisms of Fe-biomineralization, we investigated BoFeN1, SW2 and an environmental biofilm containing twisted stalks (similar to those observed for *Gallionella* strains) from an abondoned silver mine in Germany. We conducted conventional soft X-ray scanning transmission microscopy (STXM) in combination with angle-scan tomography measurements allowing for a 3D reconstruction. The advantage of STXM is the combination of high spatial resolution (≈10 nm) with the possibility of identifying and quantifying cell components such as proteins and lipids, extracellular polymeric substances (EPS) and iron minerals. Therefore, we acquired image sequences across the C1s, O1s and Fe2p absorption edges for BoFeN1, SW2 and an environmental biofilm containing twisted stalks. Compositions maps of the macromoleculars components were obtained by linear combination fits of reference spectra of proteins, lipids, polysaccharides and iron minerals. The association of the Fe-phases with the organic components of the cell-mineral aggregates was then analyzed quantitatively in 3D by correlation analysis.

Our results confirmed that iron is precipitated within the periplasm of BoFeN1, in contrast to SW2 and the environmental biofilm where the iron precipiates are closely asscociated with organic expolymers.

[1] Miot (2009) *Geochim. Cosmochim. Ac.* **73**, 696-711.
[2] Kappler (2004) *Geochim. Cosmochim. Ac.* **68**, 1217-1226.
[3] Chan (2004) *Science* **303**, 1656-1658.

Interpretation of Lu-Hf garnet geochronology by investigation of HREE zoning profiles

ALEXANDER SCHMIDT [1a*], MATTHIAS KONRAD-SCHMOLKE [1b]

1 Institute of Earth- & Environmental Science, University of Potsdam, Germany

[a] alexander.schmidt@geo.uni-potsdam.de (* presenting author)

[b] mkonrad@geo.uni-potsdam.de

Garnets are well suited for Lu-Hf and Sm-Nd geochronology, and a growing number of studies now focus on the Lu-Hf system for evaluating the evolution of different types of metamorphic rocks, because of the difference in the ages obtained by the two isotope systems (Lu-Hf dating early, Sm-Nd dating late growth). However, the interpretation of ages obtained for garnets by the Lu-Hf system is not always straightforward due to the ambiguity in the explanation of observed sharp Lu-peaks in garnet cores. Garnet strongly controls the Lu (and other HREE) budget of many metamorphic rocks, and also more often than not inherit information obtained during pro- and retrograde growth through enrichment of Lu & HREE in early formed cores. The mere occurrence of sharp Lu peaks in garnet cores in rocks of (ultra)high-pressure and high-temperature conditions indicates a resistance to metamorphic resetting, therefore attesting to the suitability of Lu-Hf garnet geochronology for complex metamorphic rocks.

In this study we concentrated on the Lu & HREE distribution in garnets from different metamorphic rocks to evaluate the modes of incorporation during growth and also processes of resetting of these growth profiles. We also investigated the impact of these growth profiles on the Lu and Hf isotopic composition of different garnet zones, trying to determine growth rates of garnets, and how this will affect the Lu-Hf ages obtained for bulk-garnet separates. This includes both a model approach to assess the influence of several garnet growth events on bulk garnet ages, as well as the "in-situ" (small portions of a garnet zone cut-out/drilled-out) measurement of the isotopic composition in suitable garnet grains.

As more garnets from different types of rocks are being analysed for their potential Lu growth profiles our understanding of how to interpret the obtained ages is improving, especially when we compare Lu-Hf ages with geochronology of other minerals based on other isotope systems. Hence a larger database will shed light on the discussion of e.g. which mineral best yields an age estimate for prograde, peak and retrograde conditions in a metamorphic rock.

Experimental study on the pseudobinary H_2O+$NaAlSi_3O_8$ at 600–800 °C and to 2.5 GPa

CHRISTIAN SCHMIDT[1*], ANKE WATENPHUL[2], ANKE WOHLERS[1], AND KATHARINA MARQUARDT[1]

[1] GFZ German Research Centre for Geosciences, Potsdam, Germany, christian.schmidt@gfz-potsdam.de (* presenting author), anke.wohlers@gfz-potsdam.de, katharina.marquardt@gfz-potsdam.de

[2]Hamburger Synchrotronstrahlungslabor HASYLAB at Deutsches Elektronen-Synchrotron DESY, Hamburg, Germany, anke.watenphul@desy.de

There are still uncertainties in phase relations in the high-temperature portion of P-T diagrams for H_2O+$NaAlSi_3O_8$ (e.g., [1]). Dissolution of albite in H_2O is usually considered to be congruent or nearly congruent [2], although many experiments showed formation of the aluminous solids paragonite (e.g., at 500–650 °C, 0.5–0.9 GPa [2], at 500 °C, 0.2–0.7 GPa and 600 °C, 0.4–0.8 GPa [3], and at 700°C, 1–1.5 GPa [4]) and corundum (e.g., at 800 °C, 0.7–2 GPa [4]). However, some of these P-T conditions intersect that of the critical curve [5] along which no solid phase can be present. For information to resolve this conflict, we conducted experiments on several pseudobinary mixtures between 39 and 54 wt% $NaAlSi_3O_8$, i.e., near the critical composition [5]. The system was studied by optical observation and Raman spectroscopy using a hydrothermal diamond-anvil cell [6]. Synthetic zircon was used as Raman spectroscopic pressure sensor [7].

At the start of each run, the assemblage silicate glass and aqueous fluid was heated to 600 °C. Then, the resulting melt and aqueous fluid were held at this temperature until a solid had formed. Jadeite grew rapidly at $P \geq 2$ GPa. In experiments at pressures to 1.06 GPa, albite nucleated within a minute to a few hours. Paragonite formed at 1.64 GPa in an experiment with 54 wt% $NaAlSi_3O_8$ and at 1.09 GPa at 39 wt% $NaAlSi_3O_8$. Upon heating, paragonite was still present at and above the temperature of homogenization of silicate melt and aqueous fluid to a single fluid phase, whereas albite always showed the expected melting at temperatures less than that of melt and aqueous fluid homogenization.

Our data indicate that the high-pressure portion of the critical curve [5] is a metastable extension at $T < 760$ °C, at which paragonite is stable. Furthermore, the formation of a substantial fraction of paragonite at intermediate bulk $NaAlSi_3O_8$ concentrations implies that the aqueous fluid must have a peralkaline composition, which in turn enhances the solubility of high field strength elements. The obtained data for the P-T location of the critical curve based on the determined isochores are close to or at slightly higher pressure than those reported in ref. [5].

[1] Hayden & Manning (2011) *Chem. Geol.* **284**, 74-81. [2] Shmulovich *et al.* (2001) *Contrib. Mineral. Petrol.* **141**, 95-108. [3] Davis (1972) PhD diss., Penn. State Univ. [4] Antignano & Manning (2008) *Chem. Geol.* **255**, 283-293. [5] Shen & Keppler (1997) *Nature* **385**, 710-712. [6] Bassett *et al*. (1993) *Rev. Sci. Instrum.* **64**, 2340-2345. [7] Schmidt *et al*. (2011) *Min. Mag.* **75** (3), 1819.

The arc delaminate: a geochemical reservoir twice the size of the continental crust

MAX W. SCHMIDT[1*]. OLIVER JAGOUTZ[2]

[1]Dep. Earth Sciences, ETH Zurich, Switzerland, max.schmidt@erdw.ethz.ch (* presenting author)
[2]Dep. Earth Atmos. Planet. Sciences, MIT, Cambrige, USA, jagoutz@mit.edu

Most primitive melts in arcs are basaltic in composition but the continental crust or arc average is andesitic. To evolve from a primitive basalt to an andesitic composition, cumulates have to be fractionated and, if gravitationally unstable, can be delaminated. Such lower crustal cumulates are exposed in the Kohistan arc (N Pakistan) in a 10 km section through dunites, wehrlites, websterites, cpx-bearing garnetites and hornblendites, and garnet gabbros. We have compiled primitive melts for nine island arcs from the literature and fitted these with the bulk Kohistan arc [1] or average bulk continental crust [2] and the Kohistan cumulates. By average, ~15 wt% wehrlite + ~20% garnet hornblendite + ~35% garnet gabbro complement ~30% arc or continental crust and explain very well (r^2~2) the evolution from a tholeiitic/calc-alkaline primitive high-Mg basalt to the continental crust. The bulk delaminate has 44-48 wt% SiO_2, total alkalis of 1.1-1.4 wt% and an X_{Mg} of 0.67-0.69. Mass fractions derived from major elements were employed to compare trace elements: cumulates+crust deviate on average only by 25-30% from primitive melts, with the biggest deviations on the subduction-added traces. Relative to the continental or arc crust, the delaminate mass results to 1.8-2.5 times that of the continental crust.

The delaminates have ρ=3.2-3.5 g/cm^3 and V_P=7.9-8.2. At the base of the crust, they are thus difficult to distinguish seismically. Once reaching a critical thickness, they may sink into the deeper mantle where they form a geochemical reservoir twice the size of the continental crust. With respect to primitive mantle, the delaminate is enriched in Ba, K, Sr, and P and REE with LREE<HREE. The delaminate reservoir would develop highly unradiogenic Pb over time and would counterbalance the radiogenic MORB and OIB reservoirs. Delamination of twice as much material as remains in the arc crust increases the flux of primitive melt in arcs threefold. This places the magma production rate at arcs (per km arc length) slightly above that at mid-ocean ridges indicating that global fluxes and magmatic heat loss need to be revised.

[1] Rudnick R.L., Gao S. (2003) *Treatise of Geochemistry* **3**, 1-64.
[2] Jagoutz O. Schmidt M.W. (2012) *Chem.Geol.* doi:10.1016/j.chemgeo.2011.10.022

Structural changes on dehydration of amorphous calcium carbonate

MILLICENT P. SCHMIDT[1*], BRIAN L. PHILLIPS[1], ANDREW J. ILOTT[2], AND RICHARD J. REEDER[1]

[1]Stony Brook Unviersity, Geosciences, Stony Brook, NY USA millicentpschmidt@gmail.com (* presenting author), brian.phillips@sunysb.edu, rjreeder@stonybrook.edu
[2]Stony Brook Unviersity, Chemistry, Stony Brook, NY USA andyilott@gmail.com

Introduction and Methods

Amorphous calcium carbonate (ACC) is a common transient precursor to biogenic calcium carbonate, but the transformation and stabilization mechanisms remain unknown. Studies have shown that the calcium carbonate biomineralization pathway for two different biogenic ACC samples follows the progression of hydrated ACC ➔ anhydrous ACC ➔ calcite, aragonite and/or vaterite.[1][2] In this study, we present a structural analysis and comparison of hydrated and partially-dehydrated, synthetic ACC applying novel synthesis techniques to examine the under-studied first transformation step in the biomineralization pathway.

ACC was synthesized using three different methods and then partially-dehydrated by heating to temperatures below the crystallization temperature (ca. 185 °C or 330 °C depending on the synthesis method).[3][4] Hydrated and partially-dehydrated ACC samples were analyzed by X-ray absorption fine structure (XAFS) spectroscopy, pair distribution function (PDF) analysis from X-ray total scattering, FT-IR spectroscopy, thermal analysis, and nuclear magnetic resonance (NMR) spectroscopy.

Results and Conclusions

Thermal analysis showed total mass losses averaging 10% (46% loss of total water) with dehydration to 115 °C (16% and 75%, respectively for heating to 150 °C). XAFS and total scattering results showed no evidence of significant structural changes with heating, suggesting that the effects of dehydration relate primarily to the water component in ways that are largely insensitive to the X-ray based techniques. FT-IR spectra show a loss of structural water as evidenced by decreases in the intensity of the O-H bending and stretching bands at 1630 and 3300 cm^{-1}, respectively. The ^{1}H NMR spectra of hydrous ACC, obtained indirectly via ^{13}C-detection, contain signals from three principal hydrogen environments: a broad spinning sideband envelope from rigid structural water, a narrow peak near +5 ppm from restrictedly mobile water, and a small narrow peak at +0.2 ppm due to hydroxyl. Dehydration of ACC leads to a reduction in signal intensity from both rigid and mobile water that increases with increased dehydration temperature but with little change in their relative proportions. No significant change in the intensity of the hydroxyl peak was observed in samples heated up to 200 °C. The retention of some restrictedly mobile water and lack of change in the PDFs from X-ray total scattering in dehydrated ACC suggest that thermal dehydration does not significantly disrupt the calcium-rich framework of the ACC [5].

[1] Radha (2010) *PNAS*, **107**, 16438-16443. [2] Politi (2008) *PNAS*, **105**, 17362-17366.[3] Koga (1998) *Thermochim. A.* **318.** 239-244. [4] Faatz (2004) *Adv. Mater.* **16** 996-1000. [5] Goodwin (2010) *Chem. Mater.* **22.** 3197-3205.

Actinide sorption and reactivity at the muscovite-aqueous interface

M. SCHMIDT[1, 2,*], S. S. LEE[1], R. E. WILSON[1], K. E. KNOPE[1], P. FENTER[1], L. SODERHOLM[1]

[1]Chemical Sciences and Engineering Division, Argonne National Laboratory, Argonne, IL, USA

[2]Current Address: Institute for Nuclear Waste Disposal, Karlsruhe Institute for Technology, Karlsruhe, Germany, moritz.schmidt@kit.edu (* presenting author)

Introduction

We present recent findings regarding the interaction of tri- and tetravalent actinides (Th, Pu) with the charged (001) basal plane of muscovite. *In situ* crystal truncation rod measurements and resonant-anomalous x-ray reflectivity were applied to investigate structures in the near-interface region under varying solution conditions (ionic strength, actinide concentration, chemical speciation of the actinide, background electrolyte).

Results

The results show a broad variety of potential forms of interaction, that strongly depends on the actinides' aqueous chemistry. The strongly hydrated cations do not shed their hydration layers upon sorption, but remain as extended outer sphere complexes [1]. In this sorption state the cations are highly concentrated in the near-interface region, and also highly mobile which allows for subsequent reactions (e.g. polymerization) between sorbed species to occur. In the case of plutonium this interfacial reactivity has been found to dominate the sorption behavior.

The results are expected to provide valuable input to the ongoing discussion about potential nuclear waste repository strategies as well as enrich the molecular level understandifng of the actinides' environmental geochemistry in general.

[1] Lee (2010) *Langmuir* **26,** 16647-16651.

Unraveling the chemical space of extreme natural environments and chondritic organic matter

PHILIPPE SCHMITT-KOPPLIN[1*], ZELIMIR GABELICA[2], NANCY HINMANN[3], MICHAEL GONSIOR[4] , WILLIAM COOPER[5], REGIS GOUGEON[6], MOURAD HARIR[1], NORBERT HERTKORN[1]

[1]Helmholtz Zentrum Muenchen, Analytical BioGeoChemistry, Germany schmitt-kopplin@helmholtz-muenchen.de

[2] Université de Haute Alsace, Lab. GSEC, France

[3] Uniersity of Montana, Missoula, USA

[4] University of California, Irvine, USA

[4] Linköping university, Linköping, Sweden

[6] Université de Bourgogne, Institut Jules Guyot, France

Natural organic matter (NOM) occurs in soils, freshwater, marine and hydrothermal environments, in the atmosphere and represents an exceedingly complex mixture of organic compounds that collectively exhibits a nearly continuous range of properties (size-reactivity continuum). The fate NOM in the bio- and geosphere is governed according to the rather fundamental restraints of thermodynamics and kinetics. In these intricate materials, the "classical" signatures of the (geogenic or ultimately biogenic) precursor molecules, like lipids, glycans, proteins and natural products have been attenuated, often beyond recognition, during a succession of biotic and abiotic (e.g. photo- and redox chemistry) reactions. NOM incorporates the hugely disparate characteristics of abiotic and biotic complexity.

Numerous descriptions of organic molecules present in organic chondrites (COM) have improved our understanding of the early interstellar chemistry that operated at or just before the birth of our solar system. However, all molecular analyses were so far targeted toward selected classes of compounds with a particular emphasis on biologically active components in the context of prebiotic chemistry. Here we demonstrate that a non-targeted molecular analysis of the solvent-accessible organic fraction of Murchison extracted under mild conditions allows one to extend its indigenous chemical diversity to tens of thousands of different molecular compositions and likely millions of diverse structures. This molecular complexity, which provides hints on heteroatoms chronological assembly, suggests that the extraterrestrial chemodiversity is high compared to terrestrial relevant biological and biogeochemical-driven chemical space.

(ultra)High resolution analytical approaches will be presented in their application to unravel the chemical nature and organic signatures in biosystems [1], geosystems [2-4] with a focus on extreme environments such as hydrothermal and meteoritic origins [5] with a special focus on sulphur organic compounds.

[1] Rosselló-Mora et al. (2008) Nature – ISME Journal **2**, 242-253

[2] Schmitt-Kopplin *et al* (2010) Anal. Chem. **82**, 8017–8026.

[3] Gonsior et al (2011) Water Research **45(9)**, 2943-2953.

[4] Schmitt-Kopplin *et al.* (2011) Biogeosciences Discuss. **8**, 11767-11793.

[5] Schmitt-Kopplin *et al* (2010) *PNAS* **107(7)**, 2763-2768.

Multi-scale geochemical time series constraints on Archean lithosphere formation

BLAIR SCHOENE[1]* AND C. BRENHIN KELLER[1]

[1]Princeton University, Princeton, NJ, 08544 USA, bschoene@princeton.edu*, cbkeller@princeton.edu

Robsust comparisons of lithosphere formation processes in the Archean, Proterozoic and Phanerozoic require: 1) geochronology of adequate resolution to sequence magmatic and stuctural processes with precision relevant to tectonic processes (~1 Ma), which has been difficult in older terranes; 2) an unbiased and continuous assessment of secular change in, for example, petrologic processes through Earth history.

Recent advances in chemical abrasion ID-TIMS U-Pb geochronology permit sub-million year precision on $^{207}Pb/^{206}Pb$ dates of single closed system Archean zircons. Applied to the pristine ca. 3.2 Ga Usutu magmatic system in the eastern Kaapvaal craton, such high-precision geochronology permits evaluation of geochemical evolution during piecewise batholith construction over <20 Ma. Combined with structural data and placed into the context of the adjacent Barberton greenstone belt, these constraints are used to construct a model where regional subhorizontal contraction occurred synchronous with emplacement of an evolving magmatc system. The temporal resolution provided by this work is unprecedented in Archean systems, and allows direct comparison with Phanerozoic arc- and plume-related magmatic systems.

In order to reconstruct billion-year records of secular variation in the continental rock record, we have compiled a database of over 70,000 igneous samples from various sources, each with age, spatial coordinates, and major and trace element data. Monte Carlo simulations with weighted bootstrap resampling significantly reduces sample collection and temporal biases, and allows precise estimation of mean global igneous geochemistry for 3.8 Ga. Both low SiO_2 (basalts) and evolved high SiO_2 rocks show statistically significant trends through time, the former being consistent with decreasing mantle melt fraction in the present and the latter showing increased importance of deep crustal fractionation/partial melting and TTG production in the Archean. Mean values of many geochemical proxies from both SiO_2 ranges show step functions near 2.5 Ga. These data support a model linking high degree mantle melting and lower crustal delamination and TTG production as being more important in the Archean; this process is largely independent of driving plate tectonic models but can be used to inform them.

Our geochemical dataset can be directly linked with geophysical models estimating crustal and lithospheric thickness, heat flow, and seismic velocities. Doing so reveals correlations between, for example, mean crustal thickness and mean geochemistry of continental igneous rocks, that change through time. This secular variation can provide a connection between the formation of continental lithosphere and magma production and evolution, and be used to inform tectonic models for specific terranes. Conversely, inferences from long term average records must be consistent with detailed structural, geochronological, and geochemical studies of preserved crust.

Was more continental crust destroyed than created during Phanerozoic time?

DAVID W. SCHOLL[1]* and ROBERT J. STERN[2]

[1]University of Alaska Fairbanks, USA, dscholl@usgs.gov
[2]University of Texas, Dallas

Introduction

It is easy to study what exists but not what has disappeared, so it is generally assumed that the volume of continental crust has increased with time. Field observations can be used to estimate how much new, (juvenile) mantle-derived continental and island arc (CIA) crust is generated and how much CIA material is lost (recycled) to the mantle. Greatest additions (via arc magmatism) and losses (via sediment subduction and subduction erosion) occur at ocean-margin and crust-suturing (collisional) subduction zones (SZs). Lesser volumes are added to plate interiors at rifted margins and hotspots and removed by lower crust delamination.

Estimated Phanerozoic Gains and Losses

The best estimates for additions and losses come from geophysical, geological, and drilling studies of modern SZs and, less reliably, from fossil Cenozoic and older ones. We have estimated that long-term average gains and losses for the Phanerozoic are similar at ~3.2 km^3/yr (i.e. 3.2 AU--Armstrong Units) [1]. These estimates, which do not include a term for

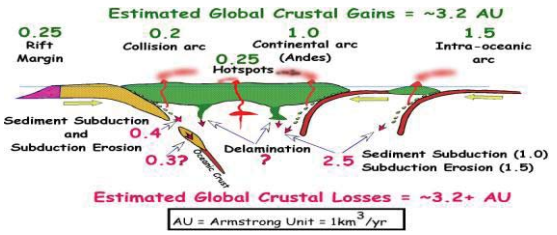

crustal foundering, are comparable to, but distinctly lower than, those of Clift et al. [2] (additions <5 AU, losses ~4.9 AU) or losses (5.25 AU) assessed by C. R. Stern [3]. The range of these estimates usefully captures our present understanding and uncertainty. Losses are least constrained for deeply subducted continental crust, for example Africa, Arabia, India, and northern Australia today, and at older collisional SZs, and by crustal delamination.

Plausible Net Phanerozoic Crustal Loss

It seems likely that at crust-suturing SZs estimated losses of deeply subducted CIA crust (based chiefly on two examples, the Paleoproterozoic Wopmay orogen of NW Canada and the Cenozoic Melanesian orogen of New Guinea), could easily be higher than our [1] estimate of 0.3 AU, and certainly a loss must be considered for our un-estimated volume of lower crust delamination. In consideration of these concerns, the uncorrected-for component of remelted older crust in continental (Andean) arc magma, and the higher volumes of recycled crust estimated by Cliff et al. [2] and C. R. Stern [3], it is plausible that during at least the Phanerozoic the net product of gains and losses has been to reduce Earth's inventory of CIA crust.

[1] Stern and Scholl (2010) Inter. Geology Rev. **52**, 1–31. [2] Cliff, Vannucchi, & Morgan (2009) Earth Sci. Rev. **97**, 80-104. [3] C.R. Stern (2011) Gondwana Research **20**, 284-308.

Spatial and temporal trends of iron and iron isotope cycling in the Peruvian oxygen minimum zone

FLORIAN SCHOLZ[1*], CHRISTIAN HENSEN[1], SILKE SEVERMANN[2], ANNA NOFFKE[1], BRIAN HALEY[3], JAMES MCMANUS[3], RALPH SCHNEIDER[4] AND KLAUS WALLMANN[1]

[1]Helmholtz Centre for Ocean Research Kiel (GEOMAR), Kiel, Germany, fscholz@geomar.de (* presenting author), chensen@geomar.de, anoffke@geomar.de, kwallmann@geomar.de

[2]Institute for Marine and Coastal Sciences (IMCS), Rutgers University, New Brunswick, NJ, USA, silke@marine.rutgers.edu

[3]College of Earth Ocean and Atmospheric Sciences (CEOAS), Oregon State University, Corvallis, OR, USA, bhaley@coas.oregonstate.edu, mcmanus@coas.oregonstate.edu

[4]Institute for Geosciences (IfG), Kiel University, Kiel, Gernany, schneider@gpi.uni-kiel.de

Iron (Fe) is a key element in the global ocean's biogeochemical framework because of its essential role in numerous biological processes. A poorly studied link in the oceanic Fe cycle is the reductive release of Fe from sediments in oxygen depleted ocean regions - the oxygen minimum zones (OMZs). Changing rates of Fe release from OMZ sediments may have the potential to modulate ocean fertility which has far-reaching implications considering the high amplitude oxygen fluctuations throughout earth history as well as the ongoing ocean deoxygenation projected for the near future. In order to explore spatial and temporal trends of Fe cycling in OMZs, we present here Fe isotope and speciation data for surface sediments from a transect across the Peruvian upwelling area, one of the most pronounced OMZs of the modern ocean.

Because of continuous dissimilatory Fe reduction and diffusive loss across the benthic boundary, sediments within the OMZ are strongly depleted in reactive Fe components, and the little reactive Fe left behind has a heavy isotope composition. In contrast, surface sediments below the OMZ are enriched in reactive Fe, with the majority being present as Fe oxides with comparably light isotope composition. This lateral pattern of Fe depletion and enrichment indicates that Fe released from sediments within the OMZ is reoxidized and precipitated at the oxycline. First-order calculations suggest that the amount of Fe mobilized within the OMZ and that accumulated at the boundaries are largely balanced. Therefore, benthic Fe fluxes in OMZs should be carefully evaluated prior to incorporation into global models, as much of the initially released Fe may be reprecipitated prior to vertical or offshore transport.

First XRF core scanning results for partly laminated piston cores from the OMZ boundaries reveal downcore oscillations in the content of reactive Fe and redox-sensitive trace metals that are attributed to past changes in OMZ extension. Ongoing work on these cores will focus on their dating and the downcore investigation of Fe and trace metal records in order to better understand past Fe cycling within the Peruvian OMZ and potential interactions with climate variability.

Lung Fluid-Mineral Interaction: Experimental Challenges and Outcomes

MARTIN A. SCHOONEN[1*], ANDREA HARRINGTON[1]

[1]Stony Brook University, Department of Geosciences martin.schoonen@stonybrook.edu (*presenting author) Andrea.Harrington@stonybrook.edu

Introduction

The inhalation of mineral dust can potentially lead to lung disease. Perhaps the best-known examples are exposure to asbestos, quartz, and coal, which can lead to mesothelioma, silicosis, and coal workers' pneumoconiosis, respectively. Despite clear causal evidence, the mechanisms by which mineral particles induce these diseases remain, in part, unknown. Geochemists are in a position to contribute to a better understanding of the mechanisms by which particles induce disease by conducting experimental studies to determine mineral biodurability and their ability to generate reactive oxygen species (ROS). Biodurability is an important factor as it expresses how long a particle is expected to remain in the lung after inhalation on the basis of its solubility in lung fluid. ROS are intermediate species in the reduction of molecular oxygen. Hydrogen peroxide and hydroxyl radical are the two most important ROS. Recent work shows that minerals, such as pyrite and olivine, produce hydrogen peroxide and hydroxyl radical when dispersed in water. Hydroxyl radical is particularly detrimental to human health.

While there is a wealth of data on the dissolution of minerals in water and some data is available on ROS formation in mineral slurries, few experiments have been conducted in a lung fluid proxy. A promising avenue of research is to conduct mineral dissolution experiments in Simulated Lung Fluid (SLF). There is, however, no single, standard recipe for SLF. One approach is to create a "simple" SLF solution that contains a phosphate buffer and several inorganic salts and organic acids. This formulation captures the essentials in terms of pH and ionic strength, but lacks complexity due to the absence of proteins, lipids and other macromolecules.

A comparison of pyrite dissolution rate in water and a simple SLF showed a drastic decrease in rate of dissolution in SLF. Addition of Survanta™, a bovine pulmonary surfactant, showed little or no change in rate, suggesting that the addition of the natural mixture of lipids, proteins and other biomolecules had no effect on dissolution rate. On the other hand, the addition of Survanta™ did lead to a rapid decrease of hydrogen peroxide in the slurry.

Conclusion

It is possible for Geochemists to contribute to a better understanding of lung diseases triggered by inhalation of mineral dust by conducting experiments with well-characterized minerals in SLF. While the addition of complex biomacromolecules is likely to affect the stability of hydrogen peroxide and possibly hydroxyl radical, dissolution rate data obtained in simple SLF are probably good biodurability indicators. The speciation of ROS is affected by the presence of complex biomolecules. It is possible that their presence promotes reactions that consume hydrogen peroxide and/or hydroxyl radicals.

Towards a consistent quantitative description of mineral precipitation and dissolution rates

J. SCHOTT[1*], E. H. OELKERS[1], P. BÉNÉZETH[1], Q. GAUTIER[1], O.S. POKROVSKY[1], G. JORDAN[2], AND G.D. SALDI[3]

[1]Université de Toulouse & CNRS, GET, Toulouse, France, jacques.schott@get.obs-mip.fr (*presenting author)
[2]Ludwig-Maximilians-Universität München, Germany
[3]Lawrence Berkeley Laboratory, Earth Science Div., Berkeley, USA.

Knowledge of the mechanisms and rates of mineral dissolution and precipitation, especially at close to equilibrium conditions, is essential for describing the temporal and spatial evolution of natural and industrial processes including weathering, diagenesis, hydrothermal deposit formation, CO_2 sequestration, and radioactive waste disposal. The Surface Complexation approach (SC) combined with Transition State Theory (TST) provides an efficient framework for describing mineral dissolution over wide ranges of solution composition, chemical affinity, and temperature. There has been a large debate for several years, however, about the comparative merits of SC/TS versus classical growth theories for describing mineral dissolution and precipitation at near to equilibrium conditions. The paucity of combined microscopic and macroscopic rate measurements on identical samples has prevented reconciliation of the surface coordination chemistry and crystal growth approaches.

This study considers recent results obtained in our laboratory on quartz, brucite, gibbsite, boehmite, kaolinite, magnesite, dolomite, and hydromagnesite dissolution and precipitation at near to equilibrium conditions via the combination of complementary techniques including batch and mixed flow reactors, hydrogen-electrode concentration cell (HECC), potentiometric titration cell, and hydrothermal atomic force microscopy (HAFM). Results show that the dissolution and precipitation of hydroxides, kaolinite and hydromagnesite powders of relatively high surface area closely follow SC/TST rate laws with a linear dependence of both dissolution and precipitation rates on fluid saturation state even at close to equilibrium ($\Delta G < 500$ J/mol) conditions. This occurs because sufficient reactive sites are available for dissolution and growth (kink, steps, edges) allowing reactions to proceed via the direct and reversible detachment/attachment of reactants at the surface. In contrast, for quartz and magnesite crystals, whose surfaces contain much fewer active sites, crystal growth (and dissolution) rates at near equilibrium conditions exhibit either a parabolic (defect assisted nucleation, spiral growth) or linear (attachment/detachment at reactive sites) dependence on saturation state depending on the treatment of the crystals before the reaction. For example, after extended dissolution (a process that creates active sites) both quartz and magnesite crystals exhibit transient linear growth rates. SC/TST rate laws can thus be applied only to those minerals that have abundant reactive sites density. It follows that determination of the active site density and origin (screw dislocations, preexisting steps…) on mineral surfaces is critical to identifying the mechanism and thus the rate equations that can describe quantitatively mineral dissolution and precipitation rates as a function of fluid composition in natural and industrial processes.

Intact polar tetraether lipids in the Arabian Sea water column and sediments: Implications for TEX_{86} paleothermometry

STEFAN SCHOUTEN[1,*], SABINE LENGGER[1], ANGELA PITCHER[1], ELLEN C. HOPMANS[1], LAURA VILLANUEVA[1] AND JAAP S. SINNINGHE DAMSTÉ[1]

[1]Royal Netherlands Institute for Sea Research, PO Box 59, Den Burg, Texel, The Netherlands. stefan.schouten@nioz.nl (* presenting author)

The TEX_{86} is an increasingly used paleotemperature proxy and relies on the fact that temperature affects the number of cyclopentane moieties in thaumarchaeal membrane lipids (glycerol dibiphytanyl glycerol tetraether lipids, GDGTs). In living Archaea, these lipids are present as intact polar lipids (IPL) with sugar- and/or phosphate-containing head groups attached to the core lipids (CL). Most studies on TEX_{86}, however, have up to now examined (fossil) CL GDGTs rather than IPL GDGTs, derived from living Archaea.

In this study, we examined the distribution and TEX_{86}-values of CL and IPL GDGTs in both the water column and sediment cores of the Arabian Sea, which contains a pronounced oxygen minimum zone. The depth profiles of crenarchaeol core lipid with a phosphohexose or dihexose head group match profiles of (expressed) genes specific for ammonia-oxidizing Thaumarchaeota. However, crenarchaeol with a hexose head group did not match the genetic depth profiles, suggesting that this IPL is partially of fossil origin. Furthermore, the concentration profiles of core lipid crenarchaeol and IPL-derived crenarchaeol showed a second peak in their abundance within the core of the OMZ which was not found in the archaeal gene concentration profiles. This representing additional evidence for a fossil contribution to the IPL pool, specifically for the glycosidic GDGTs. TEX_{86} values of both fossil core lipid and IPL-derived GDGTs increased from surface waters to the core of the OMZ, below which they decreased again, and did not correlate with *in situ* temperature. TEX_{86} values of IPL-derived GDGTs did correlate well with the relative amount of glycosidic GDGTs and were consistently higher than that those of CL GDGTs.

We subsequently isolated IPL GDGTs from Arabian Sea sediments to determine cyclopentane distributions and TEX_{86} of the individual IPL GDGTs. We observed strong differences in GDGT-composition amongst head groups: GDGT-2 and -3 (numbers indicate the number of cyclopentane moieties) are predominantly present as glycolipids, while GDGT-1 is predominantly present as phosphoglycolipid. A similar observation is made for IPL GDGTs of enriched Thaumarchaeota, i.e. GDGT-0, -1 and crenarchaeol predominantly occurring as CL of phosphoglycolipids, and GDGT-2, -3 and -4 as CLs of dihexose GDGTs [1]. As a consequence, in enrichment cultures, the TEX_{86} shows a relation with the relative amount of dihexose GDGTs, i.e. increasing TEX_{86} with increasing amount of dihexose GDGTs.

Our results thus suggests that head group composition of IPL GDGTs in Thaumarchaeota and selective preservation of glycosidic GDGTs during diagenesis may strongly impact TEX_{86} values of produced GDGTs in deep marine waters.

[1] Schouten S., et al. (2008) *Geochim Cosmochim Acta* **74**, pp. 3806 - pp. 3814.

Arsenic in soils from poultry litter application

MADELINE E. SCHREIBER[1]*

[1]Department of Geosciences, Virginia Tech, Blacksburg, VA 24061 USA (*presenting author, mschreib@vt.edu)

Introduction

The use of organoarsenicals in poultry feed additives has raised a concern about air, water and soil quality in regions of poultry production. This study examined the impact of poultry litter application on the distribution of As and other trace elements in soils. Soils from fields with varying litter applications in the Shenandoah Valley, Virginia, a region of intense poultry production, were collected, digested and analyzed for trace elements of interest. Data were statistically analyzed to examine relationships between litter application rates and trace element concentrations.

Methods

Sixteen cores were collected from the Frederick series, a well-drained silt loam. Sites were selected to represent soils with different histories of litter use: no litter use (control), and low, moderate and high litter use. The three litter amended sites had the following estimated litter application rates: 1.5 tons/acre/year (low), 3 tons/acre/year (moderate) and 6 tons/acre/year (high). At each site, four locations were chosen randomly for soil core collection. Soils in 15 cm increments were collected the surface to 120 cm depth. A total of 128 soil samples were collected for analysis. Soil samples were dried and ground, measured for particle size, organic matter and pH. Subsamples were digested for both Mehlich-extractable elements and acid-extractable elements (As, P, K, Ca, Mg, Zn, Cu, Fe). Statistical analysis was conducted on the dataset using several techniques, including correlation analysis, 1-way ANOVA comparison of means, and principal component analysis using JMP.

Results and Conclusions

Statistical analysis revealed that As does not concentrate in litter-amended soils, in contrast to litter-derived species P, Cu and Zn. While P, Cu, and Zn concentrations decrease with depth in the soil profile, As concentrations increase with depth in all soils and are correlated with iron and clay content, suggesting that As is adsorbed to iron oxides and clays, even in control soils that have not received litter application. At the highest litter application rate (20,000 kg/hectare/year; equivalent to 6 tons/acre/year), an As litter concentration of 40 mg/kg, a soil density of 1.6 m^3/kg, and a 30 year period of litter application, As concentrations in the top 20 cm of litter-amended soil are predicted to be only 4.5 mg/kg above background concentrations, assuming conservative behavior. This low level of As may be difficult to detect, especially in heterogeneous soils. Transport of As in due to competitive desorption by phosphate and DOC, complexation, or adsorption onto mobile particles may also contribute to the lack of observed accumulation of As in soils.

Growth of *Streptomyces mirabilis* P16B1 in heavy metal contaminated soil and impact to Soil Organic Matter formation

EILEEN SCHÜTZE(*)[1], MICHAEL KLOSE[1],DIRK MERTEN[2], SANDOR NIETZSCHE[3], MATTHIAS KÄSTNER[4], ERIKA KOTHE[1]

1 Institute for Microbiology - Microbial Phytopathology, Friedrich-Schiller-University, Neugasse 25, D-07745 Jena, Germany, (Email: eileen-schuetze@web.de)
2 Institute of Geosciences, Friedrich-Schiller-University, Burgweg 11, D-07749 Jena, Germany
3 Centre of Electron Microscopy, Friedrich-Schiller-University Jena, Ziegelmühlenweg 1, D-07740 Germany
4 Helmholtz Centre for Environmental Research - UFZ, Department of Bioremediation, Permoserstraße 15 , D-04318 Leipzig, Germany

It has been shown that streptomycetes are a dominant group of bacteria in heavy metal contaminated soil and that growth of soil bacteria had positive effects on bioremediation, on bioavailability of metals in soil and on biogeochemical cycles.

The former uranium mining site Wismut in Eastern Thuringia, Germany, shows extreme environmental conditions such as scant nutrients, intense salt load and low pH, followed by high metal content. Such habitats only can be colonized by microbes which are adequately adapted. Actinobacteria isolated from this hostile environment show high resistances against a range of heavy metals like nickel, cobalt, cadmium or zinc. Growth of *Streptomyces mirabilis* P16B1 was investigated in mesocosms of contaminated soil from the especially nickel and zinc contaminated sample sites K7 (WISMUT area Ronneburg, Germany). As control uncontaminated soil PaO (paradise parc Jena, Germany) was used. Heavy metal sensitive *S. lividans* TK24 was used as control in both types of soil as well as dead biomass from both used strains. This experiment gave insight in growth and contribution to soil organic matter (SOM) formation of the strain, as well as its impact to heavy metal availability. Scanning electron microscopy and XRD analysis were used to detect the mycelium, spore production, as well as dead bacterial biomass and its attachment to soil particles as patchy fragments. The metal content of soil from the samples was determined by SE methods and MS. Superoxide-dismutase (SOD)-production of *S. mirabilis* P16B1 under natural conditions was detected via native PAGE and qualitative SOD-staining as well as quantitative Assay with extracted protein. Auxine production and siderophore production were measure via MS.

It could be shown that inoculation with the strain has an effect of SOM formation in soil, as well as heavy metal availability in mobile and specifically adsorbed fraction. Due to Fenton reaction and elevated concentration of heavy metals SOD expression could be seen as an important resistance factor of strains. Auxine and siderophore production by streptomycetes could be shown directly in soil. Thereby application of extremely heavy metal resistant strains from WISMUT area for microbial enhanced phytoremediation could be recommended.

Marine terrace soils along the west coast of North America: a weathering archive?

MARJORIE SCHULZ[1*], COREY LAWRENCE[1], DAVE STONESTROM[1], TOM BULLEN[1], JENNIFER HARDEN[1], ART WHITE[1], JOHN FITZPATRICK[1] AND CARRIE MASIELLO[2]

[1]US Geological Survey, Menlo Park, California, USA, mschulz@usgs.gov (* presenting author), clawrence@usgs.gov, dastones@usgs.gov, tdbullen@usgs.gov, jharden@usgs.gov, afwhite@usgs.gov, jfitzpat@usgs.gov

[2]Rice University, Houston, Texas, USA, masiello@rice.edu

Soil chronosequences provide a framework for understanding the influence of time on soil and ecosystem properties. To simultaneously examine how landscapes of different ages will respond to future climate shifts, we can compare landscapes across age and climate. North America's west coast has a significant precipitation gradient (wet in the north, dry in the south), supporting a gradation of ecosystems from northern temperate rainforests, through mixed forests, semi-arid Mediterranean chaparral and southern desert ecosystems. Marine terraces occur up and down the west coast of North America; each flight of stair-like terraces is a chronosequence. The soils of coastal marine terraces in the west provide a "climosequence of chronosequences" ideally suited to examine the interactions of landscape age and climate on soil and ecosystem resistance and resilience to climate change.

Building on work at the Santa Cruz (CA) marine terraces, we are developing a network of terrace chronosequences along the west coast. Past work at the Santa Cruz terraces examined soil development and elemental cycling in detail. Ongoing work on these terraces includes field, laboratory, and modeling efforts to understand carbon cycling. Our future work will extend the methods we have refined at Santa Cruz to other well-established North American marine terrace chronosequences.

We hypothesize that soil properties, processes, and rates on west coast terraces might be meaningfully assigned to climate zones as well as age of soil formation. Comparison of results from different marine terrace chronosequences will require addressing several important questions linking the paleohistory of soil formation with contemporary soil properties: The central question is what memories of past climate do soils possess, and how can we measure them? This problem requires multidisciplinary discussions, inspiration, and work. Soil properties that turn out to be indicative of distinctive climate-ecosystem combinations are potentially useful as references for judging the timing and extent of change in other soils. For example, data from the Santa Cruz chronosequence suggests that the isotopic fractionation of Fe may indicate past chaparral or forested ecosystems in soils currently occupied by coastal prairies. We hope to establish which soil properties change most with climate, and by utilizing multiple time sequences of soils, to bracket the timing of the changes. In this way the potential of naturally occurring archives recorded in marine terraces along North America's west coast can be used to address questions about future effects from climate change.

The case of p-Process ^{180}W heterogeneities in Iron Meteorites

T. SCHULZ[1,3*], C. MÜNKER[1,2], S. PETERS[1,2]

[1] Institut für Geologie und Mineralogie, Universität Köln, Germany

[2] Steinmann Institut, Universität Bonn, Germany

[3] Department für Lithosphärenforschung, Universität Wien, Austria toni.schulz@univie.ac.at (* presenting author)

Introduction

For most elements, in particular for r- and s-process isotopes, the abundances of non-radiogenic isotopes appear to be fairly homogeneous in the early solar system. This is likely to reflect efficient homogenisation of materials in the protoplanetary disk. However, a notably small number of elements are reported to display distinct anomalies, interpreted as being nucleosynthetic. Due to their low abundances, only few studies so far have measured heavy p-process isotopes [e.g. 1]. The low abundances of these neutron deficient nuclides reflect their particular formation conditions [e.g. 2]. Our recently presented ^{180}W measurements in iron meteorites reported clearly resolvable anomalies of up to ~+700ppm [3], interpreted to be of nucleosynthetic origin. However, recent studies [4] argued that such non-radiogenic stable W isotope anomalies may reflect analytical artifacts, resulting from molecular interferences. We therefore conducted replicate measurements of the Cape York IIIAB iron meteorite using modified analytical protocols.

Methods

Tungsten measurements were conducted using the Neptune multicollector ICP-MS at the University Bonn that is equipped with high sensitivity 10^{12} Ohm amplifiers for measuring ^{180}W and the ^{178}Hf interference monitor. Measurements were run in low- and high resolution and by using different sampler cones, including so-called "Jet Cones" with wider aperture. About 6g of Cape York metal was dissolved and loaded onto conventional anion exchange columns. Following modified elution procedures, W was purified from the 6 g sample, and AMES standard solutions were processed as well. For multiple measurements of AMES W standard solutions we obtained external reproducibilities of ±80 ppm (2σ r.s.d). ^{178}Hf intensities were typically an order of magnitude lower than required for accurate ^{180}Hf interference corrections.

Results and Discussion

Our preliminary results confirm a clearly resolvable ^{180}W anomaly for Cape York. Using standard and Jet-cone setups we obtained ^{180}W values of about ~+350ppm and typical ^{182}W and ^{184}W signatures in low- and medium resolution. In high resolution we could reproduce the ^{180}W excess using standard cones, but an offset of as much as 4500ppm using Jet-cones, which can be attributed to anomalous mass bias behaviour potentially reflecting matrix effects. Terrestrial W isotope compositions obtained with standard cones for all AMES W solutions which were processed during column chemistries and for terrestrial metals from reduced basalts provide further support for a nucleosynthetic origin of the measured anomalies.

Conclusions

Evidence for ^{180}W heterogeneities in iron meteorites is provided from (1) systematic excesses in ^{180}W between different iron meteorite groups [3], (2) offsets from the respective group averages for long exposed meteorites due to cosmogenic burn-out of ^{180}W [3]) and (3) analytical evidences presented here. Our results call for further studies evaluating mass bias behaviour in modified ("Jet Cone") interface devices in MC-ICPMS systems.

[1] Fehr M.A. et al. (2005) **69**, 5099-51112. [2] Woosley S.E. and Howard W.M. (1978) ApJS, **36**, 285. [3] Schulz T. And Münker C. (2010), 73rd Met.Soc., #5116. [4] Holst J.C. et al. (2011), Workshop Hawaii. LPI Contr. **1639**, p. 9065.

Oxalate-promoted formation of saponite at 60°C and 1 atm pressure

DIRK SCHUMANN[1*], HYMAN HARTMAN[2], DENNIS D. EBERL[3], KELLY S. SEARS[4], REINHARD HESSE[1], HOJATOLLAH VALI[1,4]

[1]Earth & Planetary Sciences (McGill), Montreal, Canada, dirk.schumann@mail.mcgill.ca*

[2]Biomedical Engineering (MIT), Cambridge, USA, hymanhartman@hotmail.com

[3]USGS, Boulder, USA, ddeberl@usgs.gov

[4]FEMR (McGill), Montreal, Canada, hojatollah.vali@mcgill.ca

Introduction and Results

In carbonaceous chondrites there is a strong correlation between the occurrence of clay minerals and the presence of polar organic molecules (*e.g.* oxalic acid) [1][2]. Oxalic acid in the aqueous alteration phase of these meteorites could have enhanced the alteration of olivine and orthopyroxene to form Mg- and Fe-rich phyllosilicates [2]. It has also been proposed that clay minerals might have caused an enrichment of chiral "left"-handed amino acids like isovaline in these meteorites [3]. It is therefore important from the point of view of prebiotic chemistry whether oxalic acid might have catalyzed the formation clay minerals.

In this study we tested whether oxalate catalyses the crystallization of saponite from a silica gel powder at 60ºC and ambient pressure. For comparison in a second experiment NaOH solution was used instead of oxalate. Low magnification TEM images showed clusters of well developed globular aggregates consisting of packets of saponite crystals in the oxalate experiment and poorly crystallized saponite from the NaOH solution. High-resolution TEM lattice-fringe images of the ultrathin sections of the saponite globules treated with octadecylammonium (n_C=18) cations revealed the presence of 2:1 layer structures having variable interlayer charges: (1) short sequences of low-charge 2:1 silicate layers with an interlayer spacing of 13 to 14 Å and (2) sequences of higher charge 2:1 silicate layers having highly expanded interlayers of 25 to 33 Å. The difference in interlayer expansion results from the variation in the substitution of Al^{3+} for Si^{4+} within the tetrahedral sheets of the saponite crystallites. The Si/Al ratio seems to be passed on from layer to layer by heritage which is demonstrated by the regular interlayer expansion within the packets.

Conclusions

This study (i) showed the strong catalytic effect of oxalate on the nucleation and growth of saponite at low temperatures and pressure in contrast to NaOH, (ii) established the composition and structure of the 2:1 silicate layers of the saponite, and (iii) evaluated the replicating capability of the saponite. This study does not only offer an explanation for the formation of clay minerals in carbonaceous chondrites but may also explain the origin of clay minerals in other systems that contain oxalic acid associated with endolithic and epilithic (*e.g.* lichen) communities.

[1] Becker & Epstein (1982) *GCA* **46**, 97-103. [2] Hartman *et al.* (1993) *Origins of Life and Evolution of Biosphere* **23**, 221-227. [3] Pizzarello *et al.* (2003) *GCA* **67**, 1589-1595.

Transformations of mercury, arsenic and selenium in river sediments contaminated with coal ash: Field and laboratory studies

G. SCHWARTZ[1*], A. DEONARINE[1], L. RUHL[2], A. VENGOSH[2], G. BARTOV[3], T. JOHNSON[3], H. HSU-KIM[1]

[1]Duke University, Department of Civil and Environmental Engineering, Durham, NC, USA, grace.schwartz@duke.edu *

[2]Duke University, Division of Earth and Ocean Sciences, Durham, NC, USA

[3]University of Illinois at Urbana-Champaign, Department of Geology, Urbana, IL, USA

Coal combustion products, including coal ash, represent the largest industrial waste stream in the United States and contain elevated levels of toxic elements such as mercury (Hg), arsenic (As), and selenium (Se). Much of this waste is stored in unlined holding ponds and landfills that are not always monitored for their discharge to adjacent waters. Moreover, these holding ponds are susceptible to failures such as the disaster at the Tennessee Valley Authority (TVA) Kingston Fossil Plant in 2008 that caused more than 1 billion gallons of coal ash slurry to spill into the adjacent Emory River. In such cases, the fate of toxic elements associated with coal ash is greatly influenced by environmental conditions such as redox potential and microbial activities that induce transformations and leaching of contaminants. Here, we investigated the mobilization of coal ash contaminants in sediments through a field study of the river system surrounding the TVA coal ash spill site and also through laboratory sediment slurry experiments to understand how river conditions could facilitate mobilization of trace elements and production of methylmercury (MeHg). In the field survey, we sampled the sediments and surface water at the spill site during a two year period after the spill event. The results indicated elevated levels of MeHg in the river sediments near the spill site. The mercury originating from the coal ash demonstrated a stable Hg isotope signature that was different from the mercury originating from historical sources to this ecosystem. Thus, the isotope data suggested that the coal ash was stimulating MeHg production in the river sediments near the TVA site (either by providing Hg or other substrates for methylating bacteria). In the laboratory experiments, we cultured anaerobic sediment slurries to determine how the addition of coal ash could influence porewater chemistry and Hg speciation. The microcosms were prepared using sediment and surface water from a location several miles upstream of TVA spill site and cultured in an anaerobic chamber. A selection of the slurries was amended with coal ash obtained from the TVA Kingston Plant. Preliminary results of the sediment slurry incubations showed that the coal ash increased the amount of dissolved As and Se in the slurries at the initial time point. Over 4 days of incubation, dissolved As continued to increase while dissolved Se decreased in the slurries. These results suggested that arsenic was converting from As(V) to more soluble As(III) species in the slurries while selenium was converting from oxidized forms (e.g. selenate or selenite) to less soluble, reduced forms (e.g. elemental Se, selenide). The concentration of dissolved sulfate also decreased during the experiment, consistent with low redox potential in the slurries. While MeHg was observed in all slurry samples, the effect of coal ash on Hg speciation was mixed, with the coal ash providing a stimulating effect for MeHg production in some slurries and no effect in others. Further work will include sediment-coal ash slurries with more active microbial growth conditions. Overall, our field and laboratory studies highlight the need to consider environmental conditions in assessing the potential hazards of contaminants associated with coal ash.

Age of the Bushveld Complex

JAMES S. SCOATES[1*], COREY J. WALL[1], , RICHARD M. FRIEDMAN[1], JILL A. VANTONGEREN[2], AND EDMOND A. MATHEZ[2]

[1]Pacific Centre for Isotopic and Geochemical Research, Earth and Ocean Sciences, Vancouver, BC, Canada, jscoates@eos.ubc.ca, cwall@eos.ubc.ca, rfriedman@eos.ubc.ca

[2]Geology and Geophysics, Yale University, New Haven, CT, USA, jill.vantongeren@yale.edu

[3]American Museum of Natural History, New York, NY, USA, mathez@amnh.org

Determining the precise age of the Bushveld Complex, the world's largest layered intrusion located in the northern Kaapvaal craton of South Africa, has been a longstanding problem. The age and duration of magmatism associated with the complex is critical for establishing the genetic relations among its different rock units (Rustenburg Layered Suite, overlying Rooiberg Group felsic volcanic rocks, intrusive Rashoop Granophyres) and timing of formation of its world-class ore deposits (Cr-PGE-V). We report chemical abrasion ID-TIMS U-Pb zircon results (all ages reported as weighted $^{207}Pb/^{206}Pb$ averages) for 8 samples from the layered mafic rocks of the complex and the roof. These results demonstrate that the Bushveld Complex spans an ~7 million year interval from 2061 to 2054 Ma with major magma emplacement at ca. 2060 and 2055 Ma. In the mafic rocks of the Rustenburg Layered Suite, the ages overlap within analytical uncertainty at ca. 2055-2056 Ma for a diorite from the top of the Upper Zone ~50 m below the roof (2056.52 ± 0.81 Ma) and for two samples, ~300 km apart in the Western and Eastern limbs, from the PGE-rich Merensky Reef at the top of the Upper Critical Zone (2055.30 ± 0.61 Ma; 2056.13 ± 0.70 Ma, revised from [1]). These results are consistent with rapid filling, crystallization, and cooling of the upper 2/3 of the intrusion [2]. Ages for felsic rocks in the roof above the level of the Upper Zone diorite in the Eastern Limb range from 2054-2056 Ma, including a granodiorite mixed with hornfels or "leptite" (2054.83 ± 0.86 Ma), a granophyre from the Rashoop Granophyre Suite (Stavoren: 2055.70 ± 1.0 Ma), and a granite from the Nebo/Lebowa granites (2054.23 ± 0.79 Ma). These ages indicate that mafic and felsic rocks of the Bushveld Complex are broadly coeval and support the proposal that some of the original magma volume in the intrusion was expelled to form the Upper Rooiberg Group lavas or Rashoop granophyres [3]. Below the Merensky Reef, there is a shift to older ages at ca. 2060 Ma. Results for two samples at different locations of footwall pyroxenite immediately below the UG-2 chromitite (Eastern Limb), ~380 m below the Merensky Reef, are 2060.5 ± 1.4 Ma and 2059.8 ± 1.2 Ma. It has long been recognized that initial Sr isotope ratios in both plagioclase and whole rocks increase sharply at the Merensky Reef over a few metres due to the emplacement of a compositionally distinctive magma batch [4]. The U-Pb geochronological results of this study indicate an age gap of perhaps as much as 5 million years between the uppermost Upper Critical Zone (UG-2 chromitite) and the Merensky Reef and overlying Main and Upper zones. The lowermost mafic-ultramafic rocks of the Bushveld Complex (Lower Zone and Critical Zone) appear to result from an earlier phase of magmatism at ca. 2060 Ma, coeval with the nearby 2060 Ma Phalaborwa carbonatite [5]. After a hiatus, now marked by the level of the Merensky Reef, the major volume of the Bushveld Complex was emplaced at ca. 2055 Ma.

[1] Scoates & Friedman (2008) *Econ. Geol.* **103**, 465-471. [2] Cawthorn & Walraven (1998) *J. Petrol.* **39**, 1669-1687. [3] VanTongeren *et al.* (2010) *J. Petrol.* **51**, 1891-1912. [4] Kruger & Marsh (1982) *Nature* **298**, 53-55. [5] Wu *et al.* (2011) *Lithos* **127**, 309-322.

Paleoproterozoic collapse in seawater sulfate and subsequent shallowing of the methane cycle in marine sediments

C. T. SCOTT[1*], B. WING[1], A. BEKKER[2], N. PLANAVSKY[3], P. MEDVEDEV[4], S. M. BATES[3], M. YUN[2], T. W. LYONS[3]

[1]Department of Earth and Planetary Sciences, McGill University, Montreal, Canada, clinton.scott@mcgill.ca

[2] Department of Geological Sciences, University of Manitoba, Manitoba, Canada

[3]Departmet of Earth Sciences, University of California, Riverside, USA

[4] Institute of Geology, Karelian Research Center, RAS, Petrozavodsk, Russia

The initial accumulation of atmospheric oxygen, referred to as the Great Oxidation Event or GOE, is fairly well-constrained to between 2,450 and 2,320 Ma. However, the magnitude and duration of that rise in oxygen is subject to debate. It is also not clear how the dynamic oxidation of the early Paleoproterozoic transitioned into the environmental stasis of the Boring Billion. In order to examine the history of Paleoproterozoic surface oxidation, we used a combination of pyrite multiple-sulfur (^{32}S, ^{33}S and ^{34}S) and organic carbon isotopes from marine black shales. We analyzed the (1) 2,320 Ma Rooihoogte and Timeball Hill Formations, from which the GOE is dated; (2) the 2,200 to 2,100 Ma Sengoma Argillite Formation, deposited during the peak of the Lomagundi carbon isotope excursion in an open-marine setting on the Kaapvaal craton; and (3) the Upper Zaonega Formation of the Ludikovian Series, Russian Karelia, deposited in a marine basin between 2,100 and 2,000 Ma, in the immediate aftermath of the Lomagundi carbon isotope excursion.

Pyrite S isotopes display large ^{34}S-^{32}S fractionations (>30‰) relative to seawater sulfate, indicating that a large marine sulfate reservoir (2-20 mM) developed as an immediate result of the GOE and persisted for nearly 250 Ma. In the aftermath of the Lomagundi carbon isotope excursion, pyrite sulfur isotope fractionations drop to <15‰, suggesting a rapid collapse of the marine sulfate reservoir to <200 μM. These low-sulfate conditions persisted for at least 600 Ma. Thus, it appears that the high oxidation state of the atmosphere-ocean system that developed as the immediate result of the GOE was largely lost by 2,000 Ma and did not return until the Ediacaran period. Accordingly, the Boring Billion is best described as a long-lived redox regime that was intermediate between those of the Archean and the early Paleoproterozoic, rather than between the early Paleoproterozoic and the Phanerozoic.

Organic carbon isotopes record a secular shift to more negative values at ca. 2,050 Ma, which is tightly coupled to the positive excursion in pyrite S isotopes. We interpret this carbon isotope excursion as an enhancement in the biological methane cycle in marine sediments as a result of the crash in seawater sulfate. As seawater sulfate concentrations dropped, methanogenesis operated closer to the sediment-water interface, setting up conditions suitable for subsequent methanotrophy and incorporation of ^{13}C-depleted biomass into the marine sedimentary organic carbon pool.

Formation and evolution of cores in asteroids: clues from iron meteorites

EDWARD R. D. SCOTT

University of Hawai'i, Honolulu, HI 96821, USA, escott@hawaii.edu

In 12 out of 14 groups of iron meteorites, chemical variations are consistent with fractional crystallization of single pools of molten Fe-Ni-S (e.g., Ir is inversely correlated with Ni and varies by factors of 10^{1-4}) [1]. These irons have W isotopic compositions indicating they were isolated from Hf-bearing rock <1 Myr after CAI formation [2]. By contrast, irons in groups IAB and IIE do not show fractional crystallization trends (e.g. Ir is uniform), they contain abundant silicate inclusions including chondritic fragments, and their W isotopic compositions indicate more recent metal-silicate exchange. This suggests that most irons come from cores of asteroids that accreted <1 Myr after CAIs when ^{26}Al was abundant enough to form molten cores. Irons in groups IAB and IIE probably come from bodies that accreted later when there was insufficient ^{26}Al to allow metallic pools to form cores.

Irons from cores of differentiated asteroids should have cooled more slowly than irons from metallic pools. However, fractionally crystallized irons show fast cooling rates, e.g., 60-300 °C/Myr for IIIAB irons, 100-6600 °C/Myr for IVA irons, and 500-5000 °C/Myr for IVB irons [3-5]. These cooling rates are incompatible with cooling in cores of asteroids that were melted by ^{26}Al for two reasons. 1) Each group has a wide range of cooling rates whereas metallic cores should have cooled almost isothermally as metal conducts heat much more rapidly than silicate. 2) Bodies that were small enough to have cooled at these rates would have had radii of <10 km and could not have been melted by ^{26}Al. In addition, the 4565 Myr Pb-Pb age of a IVA iron [6] is incompatible with conventional models for fully differentiated asteroids which require cooling over tens to hundreds of Myr. The metallic cores supplying most iron meteorites must have cooled rapidly with little or no insulating mantle.

Impacts between asteroids at current impact velocities of ~5 km/s cannot efficiently remove silicate mantles from cores. However, impacts at lower speeds during accretion can disrupt projectiles impacting at grazing angles and speeds comparable to mutual escape velocities [7]. Repeated collisions under these conditions may have allowed core material to cool with little or no silicate insulation. Low-velocity collisions during accretion may also explain the presence of rock fragments in the IAB and IIE iron meteeorites.

The diversity of melted and unmelted asteroids and meteorites may result from formation of iron meteorites and achondrites from planetesimals that accreted near the terrestrial planets whereas chondrites accreted later in the asteroid belt [8]. Grazing impacts eviscerated differentiated asteroids so that fragments were lofted into the asteroid belt. Planetary accretion may have been a very inefficient process so that the differentiated asteroids represent the construction debris [7].

[1] Goldstein et al. (2009) *Chemie der Erde* **69**, 293-325. [2] Kleine et al. (2009) *GCA* **73**, 5150-5188. [3] Yang & Goldstein (2006) *GCA* **70**, 3197-3215. [4] Yang et al. (2008) *GCA* **72**, 3043-3061. [5] Yang et al. (2010) *GCA* **74**, 4493-4506. [6] Blichert-Toft et al. (2010) *EPSL* **296**, 469-480. [7] Asphaug (2010) *Chemie der Erde* **70**, 199–219. [8] Bottke et al. (2006) *Nature* **439**, 81-824.

Microscopy based detection and analysis of carbon nanocomposites in commercially available baseball bats

KEANA SCOTT[1*], CHRISTOPHER MARVEL[2], STEPHAN STRANICK[1] AND JOHN HENRY SCOTT[1]

[1]National Institute of Standards and Technology, Gaithersburg, MD, USA, keana.scott@nist.gov (* presenting author), stephan.stranick@nist.gov, johnhenry.scott@nist.gov

[2]Lehigh University, Bethlehem, PA, USA, cjm312@lehigh.edu

The number of consumer products incorporating polymer nanocomposites has rapidly increased in recent years [1]. Especially in sport equipment, the enhanced material properties such as high strength, high toughness and low density of these nanocomposites are effectively translated into a lighter equipment with improved performance characteristics. Although much work has been done in developing and characterizing these nanocomposite materials and nanofillers (nano-tubes, -particles, -fibers, etc.), characterization and lifecycle studies of nanocomposites in their product condition have been lacking. However, several recent studies have examined nanocomposite degradation and disposal products and explored their environmental impacts. Nguyen et al. have shown that surface exposure of carbon nanotube (CNT) network can result from the photodegradation of polymer matrix under UV exposure of CNT-polymer nanocomposites [2]. Wohlleben et al. have evaluated nanocomposite fragments for the nanofiller release and their in-vivo toxicity [3].

In this study, we examined two different types of commercially available baseball bats that incorporate CNT-polymer nanocomposites into their structures. Several different microscopy techniques were used to identify and analyze the CNTs in the bat and in the release fragments from two different use scenarios (normal and recycle/disposal). The normal use scenario included abrasion of the bat surface with different grades of polishing cloth and sand paper, simulating normal wear and tear. The recycle/disposal scenario included sawing and ripping the bat pieces. The cross-sectional samples of the bats were used to identify the locations of CNT nanocomposites and confirm the presence of CNTs in these materials. The bat surfaces and the release fragments from the two use scenarios are examined for the particle size distribution, release particle morphology and presence of loose or exposed CNTs. The preliminary results from the normal use scenario showed no loose or exposed CNTs in the wear particles or the abraded bat surfaces. The bulk of the release fragments from the sawing and ripping operation were mm to μm sized fragments. However, albeit in very low level, several types of nano-sized particles and fibers, including some that showed morphology consistent with polymer coated CNTs, were also detected in the release fragments. Additional work is in progress to characterize and quantify the nano-sized debris from the disposal scenario.

[1] http://www.nanotechproject.org/inventories/consumer/
[2] Nguyen et al. (2009) *Proc. Eur. Weathering Symposium* **11**, 149-161.
[3] Wohlleben et al. (2011) *Small* **7**, 2384-2395.

Constraining the composition of basinal brines in the Athabasca basin from individual fluid inclusion analysis in quartz overgrowths

RYAN SCOTT[1*], GUOXIANG CHI[2]

[1]University of Regina, Regina, Canada, ryan.dj.scott@gmail.com (* presenting author)
[2]University of Regina, Regina, Canada, guoxiang.chi@uregina.ca

Constraining the geochemical composition of basinal brines in the Athabasca basin is crucial in understanding the role of diagenetic fluids during the formation of high-grade unconformity-type uranium deposits. In order to characterize the diagenetic fluids before they were involved in mineralization, samples must be collected distally from mineralization or alteration zones. The Rumpel Lake drill core, which is located far away from known mineralization, is an excellent target for this type of analysis.

Isolated and clustered fluid inclusions in quartz overgrowths in the Athabasca Group sandstones (Fig. 1) were selected for analysis. Unlike minerals in veins, quartz overgrowths cannot be separated for bulk fluid inclusion analysis, therefore individual inclusions were analyzed with the heating-freezing, decrepitation SEM-EDS and cryogenic Raman spectroscopic methods [1, 2]. Ice-melting temperatures range from -37.5 to -11.0°C, suggesting that $CaCl_2$ may be present in addition to NaCl. Raman spectra obtained from frozen fluid inclusions show peaks that are comparable to published data for mixed NaCl-$CaCl_2$ systems (Fig. 1) [1]. SEM-EDS analysis shows that the decrepitates of the inclusions are composed of NaCl+KCl+$CaCl_2$±$MgCl_2$. These results are generally consistent with the proposals that the Athabasca basinal brines were derived from seawater evaporation [3], and indicate that some calcium in the basinal fluids found in uranium deposits may have been derived from fluid-rock interactions within the basin, rather than solely from the basement.

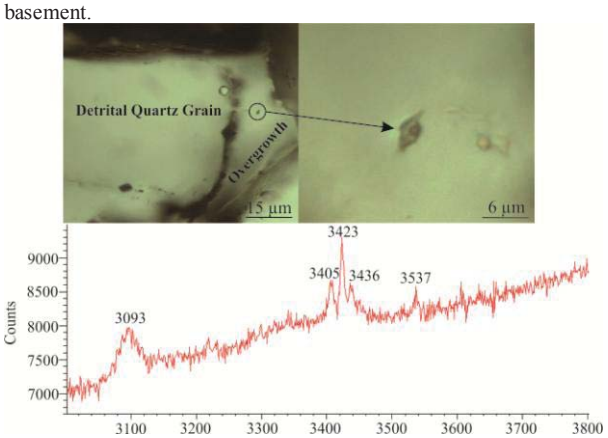

Figure 1: Upper: Isolated fluid inclusion located in the quartz overgrowth. Lower: Raman spectra of the depicted fluid inclusion homogeneously frozen to -185°C.

[1] Samson and Walker (2000) *The Canadian Mineralogist* **38**, 35-43. [2] Savard and Chi (1998) *Economic Geology* **93**, 920-931. [3] Richard *et al.* (2011) *Geochimica et Cosmochimica Acta* **75**, 2792-2810.

Vegetation collapse on Flores 69,000 years ago: A consequence of the Toba super-eruption, or a volcanic disaster closer to home?

NICK SCROXTON[1*], MICHAEL K. GAGAN[1], IAN S. WILLIAMS[1], JOHN C. HELLSTROM[2], HAI CHENG[3], LINDA K. AYLIFFE[1], GAVIN B. DUNBAR[4], WAHYOE S. HANTORO[5], HAMDI RIFAI[6], AND BAMBANG W. SUWARGADI[5]

[1]Research School of Earth Sciences, The Australian National University, Canberra, Australia, nick.scroxton@anu.edu.au (* presenting author), michael.gagan@anu.edu.au, ian.williams@anu.edu.au, linda.ayliffe@anu.edu.au,
[2]School of Earth Sciences, The University of Melbourne, Parkville, Australia, j.hellstrom@unimelb.edu.au,
[3]Institute of Global Environmental Change, Xi'an Jiatong University, Xi'an, China, cheng021@unm.edu,
[4]Antarctic Research Centre, Victoria University of Wellington, Wellington, New Zealand, gavin.dunbar@vuw.ac.nz,
[5]Research Center for Geotechnology, Indonesian Institute of Sciences, Bandung, Indonesia, whantoro@gmail.com, bambang.suwargadi@gmail.com,
[6]Department of Physics, State University of Padang, Padang, Indonesia, hamdi_unp@yahoo.com,

A large ~8‰ positive $\partial^{13}C$ excursion has been identified at 69,000 years BP in the speleothem archive from Liang Luar cave, Flores, Eastern Indonesia. The excursion, by far the largest in 92,000 years of record, begins abruptly, lasts for over 500 years, and only fully recovers to background $\partial^{13}C$ after 800 years. At its peak the excursion approaches bedrock values and we therefore interpret this event as massive vegetation destruction in western Flores followed by progressive recovery.

The excursion is coeval with the largest spike in concentration of elemental sulphur in the speleothem across this interval, measured using in situ, 30µm scale Sensitive High Resolution Ion Microprobe (SHRIMP) analysis. Atmospheric volcanic sulphate is introduced to the cave system through dissolution in rain and then groundwater. The concentration of sulphate in speleothems serves as a relatively new proxy for volcanic activity.

Taken together, the $d^{13}C$ and sulphur records indicate that this outstanding century-scale event represents massive vegetation loss in western Flores in the aftermath of a major volcanic eruption. Could the Toba super-eruption be the cause of this major event in the history of Flores? We will present $\partial^{18}O$, $\partial^{13}C$ and sulphur concentration records from Flores and nearby Sulawesi detailing the relative timings of the isotopic and concentration changes in order to separate the effects of local eruptions on Flores from the remote volcanic impact of the Toba super-eruption.

Proxy Recognition of Volcanic Ash and Eolian Dust: Implications for Climate Records, Tectonics, and Nutrient Cycling

RACHEL P. SCUDDER[1](*), RICHARD W. MURRAY[1], STEFFEN KUTTEROLF[2], JULIE C.SCHINDLBECK[2]

[1]Department of Earth Sciences, Boston University, Boston, MA, USA, rscudder@bu.edu (* presenting author), rickm@bu.edu
[2]GEOMAR, Kiel, Germany, skutterolf@geomar.de, jschindlbeck@geomar.de

Delivery of aluminosilicate material to the oceans in the form of eolian dust and volcanic ash is controlled by a number of geologic and climate mechanisms. This material can provide a record of physical processes (e.g., tectonics, climate, volcanology) and is also an important part of biogeochemical cycling (e.g., nutrient delivery). In the NW Pacific Ocean, large inputs of volcanic ash from convergent arc systems (e.g., Izu-Bonin, Marianas, Kamchatka) and eolian dust from China are related to the tectonic evolution of volcanic arcs and Cenozoic climate.

Differentiating eolian dust from altered and unaltered volcanic ash, and distinguishing both from primary authigenic phases, is difficult [1]. This is further complicated due to the presence of a large, relatively unrecognized component of volcanic ash that is mixed into the bulk sediment ("dispersed" ash). This dispersed ash is quantitatively significant and is an under-utilized source of critical geochemical and tectonic information [2]. For example, volcanic ash may provide as much bioavailable nutrients (e.g., Fe) to the surface water as does the eolian sources [3]. Because all these phases are aluminosilicates with a small compositional range, distinguishing between them to a precise degree is best achieved by a combination of chemical and quantitative multivariate statistical treatments [2].

We here extend our earlier study of ODP Site 1149 by presenting an enhanced data set that allows higher resolution study of volcanic input to the Izu-Bonin system. Our new expanded study confirms the presence of a significant dispersed ash component at Site 1149 [2]. The aluminosilicates are likely composed of four end members, i.e., loess and three other ash components. Geochemical signatures (e.g., K_2O, Fe_2O_3) of the dispersed ash can be exploited to provide insight into the clay mineralogy (i.e., smectite), which is involved in the hydrologic budget of subducting sediments. We will also present results from discrete ash layers as compared to the dispersed ash.

[1] Ziegler et al., (2007) *EPSL* **254,** 416-432. [2] Scudder et al., (2009) *EPSL* **284**, 639-648. [3] Olgun et al., (2001) *Global Biogeochem. Cycles* **25,** GB4001.

Hydrochemical analyses to evaluate groundwater system in Horonobe Area, Hokkaido, Japan

M. SEGUCHI [1*], M. OHOKA[1], M. NAKAMURA[1], Y. ICHIKAWA[1], R. SAKAI [2], M. MUNAKATA[2], J.-I. ISHIBASHI[3]

[1]OYO Corporation, 2-2-19 Daitakubo, Minami, Saitama, Japan (seguchi-mariko@oyonet.oyo.co.jp)
[2]Nuclear Safety Reserch Center , Japan Atomic Energy Agency, Tokai-mura, Naka-gun, Ibaraki-ken, Japan (sakai.ryutaro@jaea.go.jp)
[3] Faculty of Science, Kyushu University, Fukuoka 812-8581, Japan (ishi@geo.kyushu-u.ac.jp)

For the safety assessment of a geological disposal of radioactive waste, it is important to establish validation method for estimating regional groundwater flow system.

In this study, first we collected more than 200 data of saline waters which were analyzed by JAEA and other organizations. And in order to indicate the mixing ratio of saline waters from different origins, the multivariate analyses were carried out based on the M3 (Multivariate, Mixing and Mass-balance) model developed by SKB (Laaksoharju et al., 1999) . We analyzed on these data in three cases where chemical components combinations are different. These combinations are as follows: 1.Cl^-, δ D, δ ^{18}O (the components which are not involved in water-rock reaction) 2. Na^+, K^+, Ca^{2+}, Mg^{2+}, Cl^- (the components involved in water-rock reaction) 3. Na^+, K^+, Ca^{2+}, Mg^{2+}, Cl^-, δ D, δ ^{18}O (all components) .

We tried to construct a hydrochemical model in the region where Neogene to Quaternary marine sedimentary rocks are deposited. The Wakkanai formation and the overlying Koetoi formation which consist of siliceous and diatomaceous mud-stones are the main targets of our study.

As the result of the multivariate analyses, four types of endmembers were extracted. They are: 1. surface water , 2. Cl-poor water (HDB-5) , 3. Cl-rich saline water (HDB-7), 4. Ca-rich saline water((HOKUSHIN R-1). Spatial plotting of these endmembers shows that high concentration part of HDB-5 water is distributed in deeper region where abnormal formation pressures were measured, and HDB-7 water is more rich in western site. This result suggests that in this area, there are some types of deep groundwaters which flow in different directions.

This study is regulatory support research funded by the Nuclear and Industrial safety Agency, Ministry of Economy, Trade and Industry, Japan.

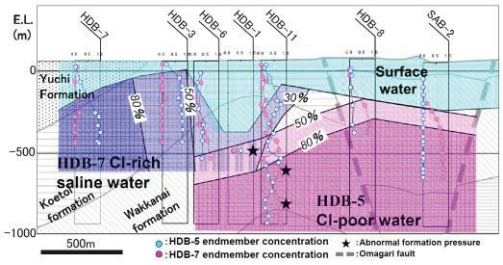

Figure 1: Projecting distribution of the endmenbers

[1] Laaksoharju et al., (1999) *Applied Geochemistry* **14#**, 861-871.

Interactions of U(VI) with archaea: what is different than with bacteria?

SONJA SELENSKA-POBELL[1*], THOMAS REITZ[1], AND MOHAMED MERROUN[2]

[1]Institute of Resource Ecology, HZDR, Dresden, Germany, s.selenska-pobell@hzdr.de (* presenting author)
[2]University of Granada, Granada, Spain, merroun@ugr.es

Archaea, in contrast to the diverse and dense bacterial populations, occur in uranium mining wastes in low numbers and belong mostly to particular crenarchaeal groups, some of them not yet cultured [1,2]. On the example of the termoacidophilic crenarchaeon *Sulfolobus acidocaldarius*, indigenous for many uranium contaminated wastes [3,4], we demonstrate that archaea tolerate substantially lower concentrations of U(VI) than bacteria and that they interact with this radionuclide in a significantly different way. One of the reasons for this behaviour is the unusual cell wall structure of the representatives of *Crenarchaeota* which is restricted to a single proteinaceous surface layer (S-layer), that is in contrary to the complex, rather thick, and rich on metal-binding ligands cell wall structure of bacteria. Due to the extreme acidic and mechanic stability of the *S. acidocaldarius* S-layer, it was possible to produce empty cells (ghosts) consisting only of the outermost S-layer membrane and to study their interactions with U(VI) at highly acidic (pH 1.5 and 3.0) and at moderate acidic (pH 4.5 and 6.0) conditions. Applying a set of modern spectroscopic techniques such as Time-Resolved Laser-induced Fluorescence (TRLF), X-ray Absorption, and Fourier-Transformed Infrared (FT-IR) we were able to demonstrate that at highly acidic conditions the *S. acidocaldarius* S-layer does not play any protective role against the toxic U(VI). At these conditions low amounts of uranium are bound mainly by the phosphate groups of the cytoplasma membrane [5]. This finding is in distinction to the results obtained with S-layers of the bacterial isolates recovered from uranium mining wastes. The S-layers of the latter bind significant amounts of U(VI) and strongly contribute to the remarkable uranium resistance of their hosts [6]. The high capability of the mentioned bacterial S-layers to bind U(VI) was atributed to the fact that they are phosphorylated [6]. This feature is unusual for both bacterial and archaeal S-layers and is not the case for the S-layer of *S. acidocaldarius* [6, 7]. At moderate acidic conditions (pH 4.5), typical for most uranium mining wastes, the studied archaeal S-layer ghosts, again in contrast to the bacterial ones, bind insufficient amounts of U(VI) exclusively via the carboxylic groups of their carboxylated amino acid residues [7]. At pH 6.0, which is substantially above the growth optimum of *S. acidocaldarius*, the permeability of its cells is increased due to the pH stress and possibly also to the presence of U(VI). As a result uncontrolled uptake of U(VI) as well as release of phosphorylated biomolecules and also of orthophosphate occurs. These processes result initially in formation and precipitation of mixed uranyl phosphate phases. With time most part of U(VI) is biomineralized in inorganic mineral phases. The efficacy of the biomineralization processes is, however, much lower then those published for bacteria, possibly due to the lower amount of polyphosphatic bodies in the studied archaeon [8]. We suggest that the limited presence of archaea in uranium wastes is related to their lower resistance to U(VI) which is determined by their cell wall structure and possibly also by some particular physiological and biochemical characteristics.

[1] Rastogi (2009) *Microbial Ecology* **58**, 129-139. [2] Reitz (2007) FZR-Report **459,** 42. [3] Marsh (1983] *FEMS Microb. Lett.,* **17**, 311-315. [4] Groudev (1993) FEMS Microb. Rev., **11**, 260-268. [5] Reitz (2010) *Radiochim Acta* **98**, 249-257. [6] Merroun (2005) *Appl. Environ. Microbiol.* **71**, 5532-5543. [7] Reitz (2011] *Radiochim Acta* **99,** 543-553. [8] Remonselez (2006) *Microbiology*, **152**, 59-66.

Novel Thermochronometric Techniques Applied to the Lavrion Detachment, Lavrion Peninsula, Attica, Greece

SPENCER SEMAN[1*], KONSTANTINOS SOUKIS[2], DANIEL STOCKLI[1], EMMANUEL SKOURTSOS[2], HARALAMPOS KRANIS[2]AND STYLIANOS LOZIOS[2]

[1]University of Texas at Austin, Jackson School of Geoscience, Texas, USA, spencer.seman@utexas.edu (*)
[2]National and Kapodistrian University of Athens, Athens, Greece,

The Lavrion Peninsula (SE Attica) is situated at the western boundary of the Attic-Cycladic Crystalline Complex (ACCC). The ACCC underwent blueschist to eclogite facies metamorphism during the Eocene followed by a greenschist facies overprint coincident with broad regional extension during the Miocene. This extension is generally attributed to the process of slab rollback and led to the formation of crustal scale detachments in the Aegean. In Lavrion, the dominant structure is a sub-horizontal detachment which juxtaposes lower plate rocks of the Kamariza Unit against the Lavrion Unit of the upper plate. Both units are dominated by greenschist facies calc-schists and marbles. The Lavrion Detachment (LD) is defined by a mylonitic zone which displays a top-to-SSW sense of shear. This is consistent with the overall sense of shear of the larger West Cycladic Detachment System (WCDS) exposed on the islands of Kea, Kythnos, Serifos and Makronisos directly to the east of the Lavrion Peninsula The LD, therefore, may represent the western most exposure of the larger WCDS. Exhumation of lower plate rocks along the WCDS on Kea, Kythnos, and Serifos occurred between 5-8Ma, 11-15Ma, and 5-8Ma, respectively[1]. In order to further constrain timing of movement on the LD and how it correlates to the WCDS, (U-Th)/He dating was conducted to understand the low temperature evolution of the lower plate and proximal upper plate rocks. Many upper and lower plate rocks (e.g. low grade calc-schists and marbles) of the LD are not conducive to traditional low temperature thermochronometric techniques so this study will employ titanite (U-Th)/He dating coupled with zircon and apatite (U-Th)/He where appropriate lithologies are present. Titanite is a common phase in greenschist facies calc-schists and possesses a closure temperature similar to zircon, making it an ideal chronometer for this study.[2]

[1] Grasemann (2012) *Lithosphere* **Volume 4**, 23-39.
[2] Reiners (1999) *Geochimica et Cosmochimica Acta* **Volume 63**, 3845-3859.

Modeling reactive transport of biogenic uraninite and its re-oxidation by Fe(III)-(hydr)oxides

S. S. ŞENGÖR[1*], J. GRESKOWIAK[2], H. PROMMER[3]

[1]Southern Methodist University, Dallas, USA, (* correspondence: sssengor@gmail.com)
[2]University of Oldenburg, Oldenburg, Germany
[3]CSIRO Land and Water, Wembley, Australia

Uranium contamination in the subsurface is a global problem in surface and groundwater, soils, sediments and related ecosystems due to its chemical and radioactive toxicity to human and ecosystem health. A promising strategy for in-situ remediation of U-contaminated subsurface is through stimulating iron and/or sulfate reducing indigenous bacterial species to catalyze the reduction of soluble U(VI) to insoluble U(IV) – uraninite (UO_2), typically accomplished by amending the groundwater with an organic electron donor. Thus, uraninite is generally regarded as the most desirable end product of this bioreductive process due to its low solubility, and hence stability under reducing conditions. However, it has recently been shown that once the electron donor is entirely consumed, the biogenic uraninite can be can be reoxidized (and remobilized) by Fe(III)-(hydr)oxides, which may potentially impede the cleanup efforts. Therefore, it is vital to understand the governing factors that control the redox behavior of the bioreduced uraninite with respect to uranium fate, transport, and long-term stability. Based on the experiments [1], a suitable biogeochemical reaction network was developed to integrate the experimental data and simulate these interactions in subsurface environments focusing on the role of sulfide, Fe(II), Fe(III) (hydr)oxides, and the effect of nanoscale particle size on the stability of biogenic uraninite and its reoxidation [2]. Model results showed that the oxidation of sulfide by Fe(III) directly competed with UO_2 reoxidation as thermodynamically, Fe(III) oxidizes sulfide preferentially to UO_2. The re-oxidation of UO_2 is thus shown to depend on the relative rates of UO_2 and sulfide oxidation by Fe(III), as well as to the activity of Fe(II) in solution [2]. The developed reaction network and the interplay that emerges between flow, physical transport and reactions has been further studied in 2-D numerical experiments that were based on the setting found at the South Oyster site, Eeastern Virgina [3]. These simulations included surface complexation of U(VI) and Fe(II) onto Fe(III) oxides, microbial sulfate reduction using acetate with reductive dissolution of ferrihydrite and considered a highly heterogeneous property distributions.

[1] Sani *et al.* (2004) *Geochim. Cosmochim. Acta* **68**, 2639–2648.
[2] Spycher *et al.* (2011) *Geochim. Cosmochim. Acta* **75**, 4426-4440 .
[3] Scheibe *et al.* (2006) *Geosphere* **2**, 220-235.

Biological productivity in the Subarctic North Pacific and Bering Sea: A proxy evaluation

SASCHA SERNO[1,2*], GISELA WINCKLER[1,3], ROBERT F. ANDERSON[1,3], CHRISTOPHER T. HAYES[1,3], HAOJIA REN[1], RAINER GERSONDE[4] AND GERALD H. HAUG[2,5]

[1]Lamont-Doherty Earth Observatory, Palisades, NY, USA, sserno@ldeo.columbia.edu (* presenting author), winckler@ldeo.columbia.edu, boba@ldeo.columbia.edu, cth@ldeo.columbia.edu, hren@ldeo.columbia.edu
[2]DFG-Leibniz Center for Surface Process and Climate Studies, Potsdam University, Potsdam-Golm, Germany
[3]Department of Earth and Environmental Sciences, Columbia University, New York, NY, USA
[4]Alfred Wegener Institute for Polar and Marine Research, Bremerhaven, Germany, Rainer.Gersonde@awi.de
[5]Geological Institute, ETH Zürich, Zürich, Switzerland, gerald.haug@erdw.ethz.ch

The Subarctic North Pacific (SNP) is one of the three principal HNLC (high nutrient low chlorophyll) regions in the modern ocean where biological production is limited. More than 20 years ago, John Martin and co-workers suggested that phytoplankton growth in the SNP is limited by iron which is mainly brought in by atmospheric eolian dust input from East Asian dust sources [1].

Productivity proxies (e.g., opal, carbonate, biogenic barium) show discrepancies in their interpretation from sediment cores in the SNP and Bering Sea for the last ~150 kyr. We will present results from a spatial survey of core-top sediments from 37 stations of the INOPEX cruise, with an extensive coverage of the whole SNP and Bering Sea. We will map and compare results from different productivity proxies (^{230}Th-normalized fluxes of opal, carbonate and biogenic barium) to evaluate the efficiency of the different proxies to reconstruct the spatial pattern in primary and export production with strong gradients across the SNP, as shown in studies of annual primary productivity estimated from the climatology of satellite ocean color observations [2] and of biological drawdown of pCO_2 [3]. Further, comparison with results from sediment trap studies will help to identify possible preservation problems for the different productivity proxies. First results indicate a good correlation between opal fluxes and published data of biological drawdown of pCO_2 in the northwestern and northeastern SNP. Results from this core-top study will be crucial for our ultimate goal to test the dust fertilization hypothesis over the last deglaciation using different dust flux and biological productivity proxies in sediment cores from the SNP.

[1] Martin and Fitzwater (1988) *Nature* **331**, 341-343. [2] Gregg et al. (2003) *GRL* **30**, 1809, doi:10.1029/2003GL016889. [3] Takahashi et al. (2002) *DRS II* **49**, 1601-1622.

The iron isotopic imprint of benthic iron release in suspended particles from the African oxygen minimum zone

SILKE SEVERMANN[1], DANIEL OHNEMUS[2] AND PHOEBE J. LAM[2]

[1]Institute for Marine and Coastal Sciences (IMCS), Rutgers University, New Brunswick, NJ, USA, silke@marine.rutgers.edu

[2]Woods Hole Oceanographic Insitution, 266 WOODS HOLE RD, Woods Hole, MA 02543

Continental margin sediments are increasingly being recognized as an important source of bioavailable iron to the open ocean. Benthic iron fluxes are particularly high in oxygen deficient ocean regions, such as the major Oxygen Minimum Zones (OMZs) off the African and South American west coasts. In these highly productive regions of the oceans, benthic (diagenetic) iron sources may be of similar importance to atmospheric iron sources. Iron isotopes are emerging as a powerful tool to trace the influence of reducing margins as a supply of iron to the open ocean. Redox recycling of reactive iron in the organic-rich shelf sediments imparts a characteristically light iron isotope signature on the benthic iron efflux. Aerosol iron, in contrast, typically resembles crustal material and shows no distinct isotope fractionation relative to average igneous rock. To examine the isotopic imprint of benthic iron release in oxygen deficient ocean regions we have measured the iron concentrations and isotope composition of suspended particles along two transects through the southern African OMZ at 13°S and 26°S. Dissolved and particulate iron concentrations are strongly elevated along the northern transect, which passes near the core of the OMZ. This pattern of high iron concentrations at intermediate depth suggests significant release of iron from the shelf sediments at bottom water oxyen concentrations <40μM. Despite this strong benthic release signal, iron isotope compositions of highly reactive Fe (0.5 M HCl leach at 60°C overnight) does not vary significantly from 0 ‰. At the southern sites, in contrast, overall sediment iron fluxes are smaller, but isotope compositions as low as -0.54 ‰ ($\delta^{56/54}$Fe, normalized to igneous rocks) are consistent with a diagenetic iron source from suboxic or anoxic sediments. Previous porewater studies have revealed a reversal in iron isotope fractionation during progression from suboxic/anoxic to sulfidic early diagentic reactions, potentially producing an iron efflux with isotope compositions close to 0 ‰ or even slightly positive. Consequently, rather than invoking an atmospheric signal at the northern site, we suggest a greater role for sulfides in the reduction and release of Fe^{2+} in the most oxygen-depleted regions of the OMZ. Light particulate isotope compositions at the southern site suggests that a significant proportion of dissolved Fe^{2+} is adsorbed or forms authigenic iron phases, and that particles are potentially an important vector for the transfer of reduced iron from the shelf to the open ocean. Results from this study provides a useful framework for the investigation of particles and their ispotope composition in the forthcomming GEOTRACES Pacific Section, which cosses the Peru OMZ.

Disturbance of the U/Pb and Th/Pb chronometers during low-T alteration of monazite.

A.-M. SEYDOUX-GUILLAUME[1*], J.-M. MONTEL[2], B. BINGEN[3], V. BOSSE[4], PH. DE PARSEVAL[1], J.-L. PAQUETTE[4], E. JANOTS[5] AND R. WIRTH[6]

[1] GET, UMR 5563 CNRS - Université Paul Sabatier - IRD, 14 avenue Edouard Belin, 31400 Toulouse, France. anne-magali.seydoux@get.obs-mip.fr
[2] G2R, CNRS, Ecole Nationale Supérieure de Géologie, Nancy-Université, BP 70239, 54056 Vandoeuvre-les-Nancy, France
[3] Geological Survey of Norway, 7491 Trondheim, Norway
[4] Clermont Université, CNRS UMR 6524, Université Blaise Pascal and IRD, 5 rue Kessler, 63038 Clermont-Ferrand France
[5] ISTerre BP 53, 38041 Grenoble CEDEX 9, France
[6] Helmholtz-Zentrum Potsdam, Deutsches GeoForschungsZentrum, Telegrafenberg, D-14473 Potsdam, Germany

Low-temperature alteration of monazite is documented in three centimetric monazite crystals from Norway (Arendal), Madagascar (Ambato), and Srilanka. The three crystals have different chemical compositions, especially regarding U, Th, Y and Pb contents and have ages ranging from 491 to 900 Ma. Optical and Electron microscope (SEM and TEM) images and electron microprobe analyses (EPMA) show that all of them share the same texture, suggesting an alteration reaction following which unaltered monazite (Mnz1) reacts to form a secondary, Th-U(-Y)-depleted, high-Th/U-monazite (Mnz2) associated with variable proportions of thorite ($ThSiO_4$), thorianite (ThO_2) and xenotime (YPO_4), depending on the initial composition of Mnz1. Images reveal variably intense fracturing, with cracks filled with Th-rich +/- Fe-rich phases. Monazite-xenotime thermometry demonstrates that Mnz1 interacted with a low temperature fluid. The alteration process is interpreted to follow a mechanism of fluid-present coupled dissolution-precipitation. Chemical dating with EPMA show no isochron age difference between primary and secondary monazite, except for the Ambato monazite, where altered domains are apparently older (750 Ma). U/Pb and Th/Pb isotope dating using LA-ICP-MS give dates consistent with EPMA dates, in pristine zones. However, in Mnz2, the systems are disturbed. In the case of Srilanka and Arendal, only $^{232}Th/^{208}Pb$ dates give a reasonable estimate of alteration age, respectively 450 and 864 Ma. U/Pb systems are disturbed due to common Pb contamination (up to 40%) and U fractionation relative to Th, responsible for depletion of U in altered monazites (and increase of Th/U). In contrast, for the Ambato monazite, both U/Pb and Th/Pb systems were affected and give inconsistent older dates for altered zones. This is attributed to significant common Pb contamination (up to 80%), also affecting all Pb isotopes and explained why electron probe ages were disturbed as well. Secondly disturbance results from Th-U-silicate contamination during measurement, due to the presence of high density of nano-phases and nano-fractures filled with Th-U-silicates, only visible using TEM. Finally, these results demonstrate the important role of radiation damage effects, in particular swelling-induced fracturing, and the essential role of porosity and cracks, which allow fluid (charged with elements) migration through the sample during this process.

Micron-scale imaging of the distribution of bio-available metals (Fe, Zn, Ni, Co) in modern and ancient microbial mats

MARIE CATHERINE SFORNA[1]*; PASCAL PHILIPPOT[1]; MARK VAN ZUILEN[1], ANDREA SOMOGYI[2], KADDA MEDJOUBI[2], PIETER VISSCHER[3] AND CHRISTOPHE DUPRAZ[3]

[1]Institut de Physique du Globe de Paris, Sorbonne Paris Cité, Paris, France; sforna@ipgp.fr (*presenting author)
[2]Synchrotron SOLEIL, Saint-Aubin, Gif sur Yvette, France
[3]Department of Marine Sciences, University of Connecticut, Groton, Connecticut, USA

Metals are essential micronutrients for all living organisms since they are used as structural elements or as catalytic centers in enzymes. Some, like Fe, are universally used, while others, such as Ni or Co, have a more limited biological function. Yet, they can be associated with enzymes that catalyze specific types of metabolism (e.g. N-assimilation). The evolution of these metalloenzymes likely reflects the variable paleogeochemistry of metals throughout Earth history. However, in addition to direct uptake for biological use, metals can be incorporated in bacterial exopolymer (EPS) constituting the biofilm matrix in microbial mats. The high chemical reactivity of such surfaces is ideal for metal cation scavenging, and thus leads to metal enrichment during diagenesis. Therefore, in order to use metals as tracers of past biological activity in the ancient rock record, knowledge of the mechanisms of metal uptake in living and diagenitically-modified microbial mats is required.

Here we present a study of the distribution of metals in modern and ancient stromatolites. These structures, ubiquitous in the rock record for the last 3.5Ga, have the potential to preserve biosignatures and are an excellent target for studies of metal tracers. We focused our study on 2.7Ga old stromatolites from the Tumbiana Formation (Western Australia) and on three modern stromatolites from the Bahamas (Storr's Lake, Big Pond and Highborne Cay).

In order to detect metal variation in the laminated organic fraction of stromatolite structures we used synchrotron-based scanning X-ray fluorescence technique. It was applied at the X-ray fluorescence microscopy line of the Australian Synchrotron. We used the Maia detector which consists of 384 detectors-elements. This permitted to perform multielemental imaging of ~cm sample areas with 2µm spatial resolution.

In modern stromatolites organic layers are enriched in metal with a general distribution of Fe, Zn >> Ni and Co. This enrichment becomes higher with increased degree of diagenesis. Indeed, the top of Big Pond's stromatolite contains high organic content linked to a low Fe content whereas the bottom shows lower organic content (diagenetic effect) and higher Fe content. Modern stromatolites, then, show clear evidence of early diagenesis where metals such as Fe, Zn display strong affinity for the organic layers. The ancient stromatolites from the Tumbiana Formation also show a strong metal enrichment in the organic fractions. In organic layers, Fe >Ni, Co > As, V, Ti > Zn are presents. Disseminated organic globules also show this general metal distribution. This could be evidence for pervasive fluid diagenesis in organic layers and of the preservation of the early diagenesis in organic globules. The high metal content in these samples confirms the strong affinity for organic fractions incorporating more and more type of metals with time.

Experimentally Determined Fe Isotope Fractionation between Metal and Silicate

ANAT SHAHAR[1*], MARY F. HORAN[2], JULIANA MESA GARCIA[1,3], TIMOTHY D. MOCK[2], VALERIE J. HILLGREN[1] AND LIWEI DENG[1]

[1]Geophysical Laboratory, Carnegie Insitution of Washington, Washington, D.C. , USA, ashahar@ciw.edu (* presenting author)
[2]Department of Terrestrial Magnestism, Carnegie Insitution of Washington, Washington, D.C., USA,
[3]EAFIT University, Medellin, Antioquia, Colombia

There has been much work done on quantifying the iron isotopic fractionation of naural samples but the mechanism(s) responsible for the measured fractionations is still largely unknown. Iron is not striaghtforward to understand because of its differing redox states and compatibility constraints. In this study we aim to understand the mechanism(s) responsible for iron isotope fractionation by performing high pressure and temperature experiments. We have varied the composition, temperature, and duration of the experiments. In particular we have examined the iron isotopic fractionation between metal and silicate with and without the influence of sulfur to represent a possible core formation model for Earth and Mars.

Experiments were conducted in a ½ inch piston cylinder apparatus at temperatures ranging from 1600°C – 1800°C at 1 GPa and for times ranging from 5 to 240 minutes. The run products were characterized, mechanically separated, dissolved and purified by anion exchange before introduction into a Nu Plasma II MC-ICPMS for isotopic analyses. It is crucial in these experiments to prove isotopic equilibrium so microprobe analyses, the three-isotope technique, and textures of run products were all utilized. Of the 50+ experiments conducted so far, fewer than 10% have passed all the requirements for isotopic equilibrium. However, in the experiments in which we are confident that equilibrium was achieved we find that there is a small but resolvable equilibrium iron isotopic fractionation factor between metal and silicate at high temperature, with the metal phase more enriched in $^{57}Fe/^{54}Fe$ than coexisting silicate.

Determining whether there is an equilibrium iron isotope fractionation between metal and silicate is central to understanding the Fe isotope signatures found within different meteorites and planetary bodies. The initial set of experiments duplicate the magnitude and direction of data from pallasite meteorites with higher $^{57}Fe/^{54}Fe$ in the metal than in coexisting olivine. And extrapolation of our results to the temperature of the Earth during core formation (~3000 K) results in an iron isotopic fractionaton of 0.08‰ between the core and mantle. By adding sulfur to the second set of experiments we can test how sensitive the iron isotopic fractionation is to a change in the surrounding ions as well as provide an analog to Mars.

Behavior of accessory minerals during Paleoproterozoic (1.9 Ga) weathering processes, Beaverlodge Ridge, NWT, Canada

PAUL SHAKOTKO*[1], LUKE OOTES[2] AND YUANMING PAN[1]

[1]University of Saskatchewan, Geological Sciences
phs090@mail.usask.ca
yup034@mail.usask.ca
[2] NWT Geoscience Office, Yellowknife, NT
luke_ootes@gov.nt.ca

Abstract

A well-preserved 1.9 Ga regolith that formed from a quartz-feldspar porphyry of dacitic composition at Beaverlodge Ridge, NWT, Canada, is overlain by a quartz arenite and has been overprinted by a greenschist facies regional metamorphism. Continental reconstruction placed Beaverlodge Ridge near the equator and thus tropical paleolatitude conditions at ~ 1.8 Ga [1]. The maximum AI and PIA values of 77 and 96, respectively, indicate heavy weathering during the formation of the Beaverlodge Ridge regolith. While Si, Fe, K, Ca, and Ti display an upward increase towards the unconformity, Na and Mg have been removed from the profile. Aluminum, Mn, and P remain relatively constant throughout the profile. These major element trends are inconsistent with other Paleoproterozoic regoliths (Gall, 1994; Pan and Stauffer, 2000) and are also inconsistent with a modern-day dacite weathering profile (Shangyi et al., 2007). Both of these show an upward loss in Ca. Subsequent analysis of the weathering rinds of porphyry in the quartz arenite shows a depletion in Ca relative to the altered porphyry. This suggests that the upward increase in Ca observed in the porphyry might be due to later overprinting events.

Electron microprobe analysis and back-scattered electron imaging reveal that accessory minerals such as zircon, allanite, and fluoroapatite in the Beaverlodge Ridge regolith are well preserved, whereas Fe and Ti oxides such as magnetite and rutile often display extensive weathering and show evidence of surface weathering such as etching and pitting. Zircon grains are sub- to euhedral, whereas allanite grains are anhedral. Fluoroapatite occurs in two different morphologies: 1) distinctly zoned, sub- to euhedral grains with overgrowth rims that often containing monazite inclusions within or adjacent to these overgrowths, and 2) lacking growthzones and monazite inclusions. Further morphological and compositional analyses of accessory minerals are underway to examine their roles in controlling the major and trace elements in the Beaverlodge Ridge regolith. These results are expected to shed new light on the oxic atmosphere ca. 1.9 Ga and lead to a greater understanding of GOE.

References

[1] Hou et al. (2008) Gondwana Research. **14**, 395-409.
Gall, (1994) Precambrian Research. **68**. 115-137.
Pan and Stauffer, (2000) American Mineralogist. **85**, 898-911.
Shangyi et al. (2007) Chinese Journal of Geochemistry. **26**, 4, 434-438.

OSMIUM CONTAMINATION OF SEAWATER SAMPLES STORED IN POLYETHYLENE BOTTLES

M. SHARMA[1]*, C. CHEN[1,2], T. BLAZINA[1,3] AND, K. LANDAU[1]

[1]Dept of Earth Sciences, Dartmouth College, Hanover, NH 03755 USA Mukul.Sharma@dartmouth.edu (* presenting author)
[2]Halliburton, 1805 Shea Center Dr, Suite 400 Highlands Ranch, CO 80129 USA
[3]Eawag, Überlandstrasse 133, 8600 Dübendorf, Switzerland.

A low blank-high yield procedure for the accurate determination of seawater osmium concentration and isotope composition has been developed. The resulting improvement in the detection limit reveals a subtle but significant temporal increase in the concentration of samples obtained during the GEOTRACES expeditions. This increase in Os concentration is accompanied by a decrease in the $^{187}Os/^{188}Os$ ratio of the water indicating contamination of waters from the storage bottles. These samples were stored in HDPE bottles. In comparison, analyses of another aliquot of water stored in a Teflon bottle show no Os contamination. Extending our analyses further to samples collected in LDPE bottles during SAFe expedition we find that the water has been contaminated. Additional investigations reveal that LDPE bottles could contribute large amounts of Os with an $^{187}Os/^{188}Os$ ratio that is distinctly lower than seawater. We also find that an acidified melted snow sample stored in an acid washed Teflon bottle is not contaminated after two years of storage. We conclude that the acidified seawater samples need to be stored in Teflon bottles for accurate and precise estimate of Os concentration and isotope composition. Consideration of reliable Os isotope data indicates that Os is not a conservative element and that the $^{187}Os/^{188}Os$ ratio of the surface water of the interior of the north Atlantic and north Pacific gyres is ~2-3% lower than that of the deep oceans. Additional analyses from the recently completed GEOTRACES cruise in the Atlantic are underway and will be presented.

Evidence of transport of Composition B colloids/nano-colloids in range soils

PRASESH SHARMA[1,*], MELANIE MAYES[1], AND GUOPING TANG[1]

[1]Oak Ridge National Lab, Subsurface Sciences Group, sharmap@ornl.gov (*presenting author), mayesma@ornl.gov and tangg@ornl.gov

Abstract

Munition constituents (explosive particles such as Composition B or simply Comp B) distributed heterogeneously at operational range sites from low-order denotations may be the source of contamination of TNT, RDX and HMX to underlying aquifers. Comp B consists of ~59% RDX, 40% TNT and 1% HMX. Mobility of these compounds in soils/groundwater may occur via dissolution of Comp B and/or via transport of Comp B particles/colloids. To determine this, we collected soils from the E horizon of Massachusetts Military Range (MMR) where RDX and TNT contamination was recently observed. Column experiments were conducted where Comp B particles (<2 μm) were applied on top of the MMR-E soil filled column and leached with background solution of 1 mM NaCl. Effluents were collected every hour and separated into two aliquots: 1) <1 μm (or total), 2) dissolved (<2nm) fractions. Each aliquot was analysed with HPLC to quantify TNT, RDX and HMX. Difference between the <1 μm and <2 nm fraction denotes the amount of TNT, RDX and HMX in the colloidal/nano-colloidal fraction.

Results showed that up to ~80% of TNT and between 40-50% of RDX and HMX in the system were transported in colloidal/nano-colloidal (>2 nm -1 μm). While comparing the breakthrough in <1 μm fractions, the breakthrough of RDX was the fastest followed by HMX and then TNT. While comparing breakthrough of dissolved vs colloidal/nano-colloidal fractions, the breakthrough of the colloidal fraction for TNT, RDX and HMX was relatively faster than the dissolved fraction. Using ATR-FTIR spectroscopy we were also able to identify Comp B colloids in column effluents.

Results conclude that: 1) Comp B particles may move as colloids/nano-colloids in soils, 2) Faster breakthrough of RDX and HMX suggests lower binding affinity whereas TNT binds more strongly to the soil matrix regardless of particle size and 3) The faster breakthrough of TNT, RDX and HMX in <1 μm fraction compared to the dissolved fraction suggests that Comp B colloids/particles may move in the subsurface with less retardation compared to dissolved TNT, RDX and HMX.

The results, for the first time, show evidence of colloidal transport of munition constituents in column systems. Transport of Comp B as colloids should thus be considered while studying contaminated field sites such as MMR. Current results will be compared with column experiments in which Comp B will be applied to intact MMR-E columns collected from the same site. Intact columns may contain fractures and macropores likely to enhance the propagation of colloidal phases.

Precise, accurate measurement of U-Th isotopes in a single solution by ICP-MS

REGINA MERTZ-KRAUS[1], KENNETH R. LUDWIG[1], AND WARREN D. SHARP[1*]

[1]Berkeley Geochronology Center, Berkeley, USA, rmertz@bgc.org, kludwig@bgc.org, wsharp@bgc.org (*presenting author)

U-series isotope measurements by ICP-MS commonly utilize separate runs for U and Th, and standard-sample bracketing to determine corrections for mass fractionation and ion counter yield. Here we present an approach where all information necessary to calculate a sample's age (aside from background/baseline levels) is determined while analyzing a single solution containing both U and Th. Such an internally calibrated procedure reduces any bias caused by distinct behavior of samples versus standards (e.g., matrix effects), eliminates drift, and offers simplicity of operation, calculation of preliminary ages in real time, and simplified analysis of errors and their sources. Hellstrom [1] developed a single-solution, internally calibrated technique for an ICP-MS with multiple ion counters (Nu Plasma), but to our knowledge such a technique has not been available previously for an ICP-MS with a single ion counter. We use a Thermo Neptune *Plus* multi-collector ICP-MS with eight movable Faraday cups and a fixed center cup/ion counter equipped with a high abundance-sensitivity filter (RPQ). We use Faraday cups to measure all masses except 230 and 234, which are generally measured on the ion counter with the RPQ detuned (i.e., set 50 volts below the acceleration voltage). Analyses are dynamic, with sequential axial masses of circa 229, 230, 233, 234, and 239. ^{238}U is maintained in cups throughout the analysis to avoid reflections and is used to normalize signal instabilities related to sample introduction. Each analysis has a three-part structure in which 1) background/baseline levels, 2) sample composition, and 3) peak-tails are sequentially measured. In step 1, multiplier dark noise/Faraday baselines plus background intensities at each mass are determined while aspirating running solution. During sample measurement in step 2, ion counter yields for Th and U are determined using signals of 300-500 kcps for ^{229}Th and ^{233}U by measuring ^{229}Th/^{238}U and ^{233}U/^{238}U ratios with the minor masses first on the ion counter and then in cups. Mass bias can be determined using the ^{233}U/^{236}U ratio of the spike, allowing the sample's ^{238}U/^{235}U ratio to be measured. In step 3, we monitor peak-tails at half-mass positions (229.5, 231.5, 234.5) and on mass 237 while aspirating sample solution. Tail measurement requires a distinct cup configuration to maintain 238 in the cups; however, no sample is consumed during automated cup reconfiguration.

We monitor the accuracy of ^{234}U/^{238}U ratios using CRM 145, which gives a weighted mean atom ratio of $(5.2899 \pm 0.0021) \times 10^{-5}$ (all errors 2 SEM), consistent with published and reference values. The reproducibility of ^{230}Th/^{238}U ratios is monitored using the Schwartzwalder Mine secular-equilibrium standard (SM). We detect no bias in ^{230}Th/^{238}U or ^{234}U/^{238}U ratios measured for SM at beam intensities ranging over a factor of four, consistent with accurate correction for IC yields. Aladdin's cave coral (AC-1), analyzed to check our method on carbonate, yields a mean age of 124.42 ± 0.37 ka, in agreement with published values. We are currently applying the method to corals, speleothems, pedogenic coatings, and tufas.

[1] Hellstrom (2003) *J. Anal. At. Spectrom.* **18**, 1346–1351.

Using ^{222}Rn, water isotopes and major ions to investigate a large alpine through-flow lake

GLENN D. SHAW[1*], AND ELIZABETH WHITE[1]

[1]Montana Tech of the University of Montana, Geological Engineering, Butte, MT USA, gshaw@mtech.edu (* presenting author)

Session 22a. Tracing Groundwater Variability

Geochemical and isotopic tracers in groundwater and surface water studies in montane catchments have become increasingly popular because monitoring wells are often sparse and terrain is complex (e.g. fractures and folds), which makes physical hydrogeologic methods difficult to characterize quantitatively. In this study several geochemical tracers (^{222}Rn, δ^2H, δ^{18}O, and major ions) were collected spatially in Georgetown Lake, Granite County Montana, a large montane lake with a surface area of 1489 ha. The geochemistry of nearby precipitation, surface water, and groundwater was also characterized to assess the chemistry of source waters mixing with the lake. Physical and chemical measurements were used to i) construct a water balance for the lake, ii) characterize groundwater flow locations and amounts with the lake, and iii) develop a conceptual model for geologic controls on groundwater-lake interactions. Stable isotopes were used in an endmember mixing analysis to separate the relative fractions of source waters mixing with the lake, a physical water budget was used to quantify the difference between groundwater inflows and outflows, and a radon mass balance was used to characterize the groundwater flow locations and amounts to the lake.

Results from the stable isotopes show three endmembers mix with the lake. They are precipitation (39%), groundwater (26%), and a strongly evaporated endmember (35%). The evaporated endmember is most likely groundwater and/or surface water that later evaporated after entering the lake. The physical water budget suggests little difference between groundwater inflows and outflows, but could not be used to quantify groundwater inflow or outflow amounts. The radon mass balance suggests that groundwater inflows to the lake are substantial. Based on the physical water budget, this implies that groundwater outflows are also significant and the lake is a through-flow lake. Radon measurements also show that nearly all of the groundwater inflows occur along the eastern side of the lake, which is underlain by carbonate bedrock. The western portion of the lake (~75% area) is underlain by western dipping Precambrian metasedimentary bedrock. The steep dip and limited groundwater elevations suggest that the western portion of the lake is losing. It appears that groundwater enters through fractures, caverns, and shallow alluvium from the carbonates, and groundwater exits through the western dipping bedding planes and fractures in the metasedimentary rocks.

The use of ^{222}Rn for determining groundwater discharge locations and amounts provides a simple, but crucial, method for developing the conceptual model in this study. The spatial measurements of ^{222}Rn elucidate groundwater interactions that could not be assessed by geology, water levels and physical water budgets alone. Even conservative water isotope mass balances were limited in characterizing the nature of groundwater-lake interactions.

The crystallization of Amorphous Calcium Carbonate (ACC), and the effects of magnesium and sulfate

SAM SHAW[1*], PIETER BOTS[1], JUAN-DIEGO RODRIGUEZ-BLANCO[1], CLIVE WOOD[1,2], ANDREW P. BROWN[2] AND LIANE G. BENNING[1]

[1]Earth Surface Science Institute, School of Earth and Environment, University of Leeds, Leeds, UK, s.shaw@see.leeds.ac.uk (* presenting author)

[2]Institute for Materials Research, University of Leeds, Leeds, UK

Many organisms use transient ACC during biomineralization, as a means to control the particle shape/size and structure (e.g. calcite, aragonite or vaterite) of the crystalline calcium carbonate formed. For example, sea urchin larvae produce highly elongated single crystals of calcite by the controlled deposition and transformation of ACC [1]. Organisms also adjust or control the crystallization pathway using inorganic ions, organic molecules and/or membrane structures. Resolving the mechanisms and kinetics of ACC crystallization in abiotic systems, and evaluating the role of inorganic additives (e.g. Mg and SO_4) is key to underpinning our understanding of biologically-controlled calcium carbonate formation. In particular, the pathway of crystallization from disordered hydrated ACC to fully crystalline calcite needs to be quantified.

Using *in situ* small and wide angle X-ray scattering (SAXS/WAXS) at fast time resolution (1 sec.) we studied the crystallization of ACC to vaterite/calcite in the absence and presence of variable Mg and SO_4 concentrations. We show that pure ACC crystallizes via a multi-stage process [2]. Firstly, hydrated and disordered ACC forms, then rapidly transforms to more ordered and dehydrated ACC; in conjunction with this, vaterite forms via a spherulitic growth mechanism. This is followed by Ostwald ripening of the vaterite particles, and finally transformation to calcite via a surface controlled growth mechanism. The presence of Mg in ACC significantly reduced the rate of crystallization and led to the direct formation of calcite (Mg = 10%), or various Ca-Mg-CO_3 polymorphs (Mg > 10%), including monohydrocalcite and dolomite (T>60°C) [3]. The presence of SO_4 did not alter the overall ACC crystallization mechanism, but reduced the rate of vaterite nucleation, growth and ripening due to surface adsorption [2]. Also, SO_4 dramatically increased the stability of vaterite compared to the pure system (i.e. stable for hours/days).

These results provide a comprehensive mechanistic description of the abiotic ACC crystallization pathway, with the final crystalline product being controlled by the initial ACC composition (e.g., Mg or SO_4 content). These abiotic crystallization mechanisms are similar to those observed in marine organisms [1], where it has been shown that secondary calcite nucleates within ACC, a process comparable to the secondary (vaterite) and tertiary (calcite) nucleation and growth observed in our systems.

[1] Killian *et al.* (2009) *J. Am. Chem. Soc.* **131,** 18404-18409. [2] Bots *et al* (2012) *J. Am. Chem. Soc* (Submitted). [3] Rodriguez-Blanco et al (2012a,b) *Geochim. Cosmochim. Acta*. (In Review)

Bioaccessibility and bioavailability of arsenic-bearing mine wastes via the inhalation pathway

SHDO, S.M.[1*], MOLINA, R.[2], BRAIN, J.[2] KIM, C.S.[1]

[1] Schmid College of Science, Chapman University, Orange, CA 92866, USA

[2]Harvard School of Public Health, Boston, MA 02114, USA

Due to extensive processing of ore from gold and silver mines in the Mojave Desert, CA, elevated concentrations of associated toxic metal(loid)s including arsenic (As) are often mobilized by the transport of mine wastes into surrounding communities. The fine-grained fraction of mine waste particles can readily become airborne and inhaled. making their bioaccesibility and bioavailibility extremely relevant.

Bulk samples were collected from a number of mines throughout the Mojave Desert and sieved to obtain fine size fractions. The size fraction was then ground using a ball mill to a size fraction (≤2.5 μm in particle diameter). The bioaccessibility of As as a function of pH was examined in phagolysosomal simulant fluid (PSF) Finally, the bioavailability of As was analyzed *in vivo* by intratracheally instilling the material.

Results from four different mine sites indicate that the mine wastes showed similar trends of arsenic dissolution within PSF, with the percent As released decreasing from pH 1.8-4.2 and then slightly increasing pH 5 (Figure 1). The As solubility at low pH is likely due to the dissolution of As-bearing mineral phases while the solubility at higher pH is likely due to the desorption of As sorbed to Fe-oxides. The *in vivo* studies will provide organ-specific bioavailability information which can be correlated with results from the PSF experiments.

This information will help to determine the operational pH for a PSF extraction that most accurately the *in vivo* outcome, with the eventual goal of developing a predictive bench-top bioaccessibility assay that can be used to estimate bioavailability of arsenic in mine wastes as introduced through the inhalation pathway.

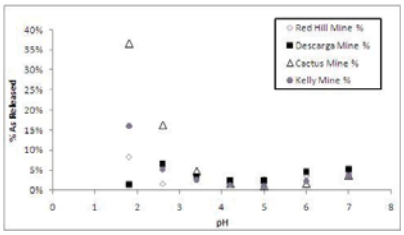

Figure 1: Percentage As released vs. pH

Extensive life on land ~1.1 Ga ago

NATHAN D. SHELDON[1*] AND MICHAEL T. HREN[2]

[1]Department of Earth and Environmental Sciences, University of Michigan, Ann Arbor, MI, USA, nsheldon@umich.edu* (presenting author)

[2]Department of Earth and Planetary Sciences, University of Tennessee, Knoxville, TN, USA, mhren@utk.edu

The precise timing of life's move onto land in the Precambrian, along with the extent of the terrestrial biosphere, is poorly constrained, with only a sparse record before the Neoproterozoic, known primarily from paleokarsts [1]. A recent study by Strother and colleagues [2] described the earliest non-marine eukaryotes from the ~1 Ga old lacustrine Diabaig Formation (Torridon Group, Scotland). Penecontemporaneous lakeshore and alluvial deposits well away from marine shorelines from Scotland also record microbially induced sedimentary structures [3]. Thus, at least locally, a significant and potentially diverse terrestrial biosphere was present, but the extent of the Mesoproterozoic terrestrial biosphere remains an open question.

Here, we present sedimentological and isotopic evidence for an extensive terrestrial biosphere preserved in sediments that are part of the ~1.1 Ga old Midcontinent Rift (MCR) of North America. The active rifting phase of the MCR was short-lived, from 1109 to 1087 Ma [4], and clastic sediments were deposited both as intrabasaltic units and as post-emplacement units. Rifting ceased due to Grenvillian compression to the East, which resulted in a partial re-closure of the rift. Penecontemporaneous intrabasaltic units from both sides of the rift in Minnesota and Michigan record a variety of sedimentary environments including paleosols [5-6], braid plains, alluvial fans, and lacustrine units; sites are currently >150 km apart, a distance that would have been significantly larger prior to the tectonic reversal caused by the Grenvillian compression. The sedimentary units have never been deeply buried or experienced any significant metasomatic alteration [5-6]. Microbially induced sedimentary structures including abraded Kinneyia, pustulose mound structures, multi-directional wave ripples, textured bedding planes, and stromatolites were recently documented [7]. Organic matter is also preserved on both sides of the rift in paleosols and microbial mat structures, as detrital carbon in laminated fluvial sediments, and occluded with the carbonate of lacustrine stromatolites in Michigan. "Clumped isotope" (Δ_{47}) analyses of stromatolitic carbonate range from 0.513–0.603 (± 0.004), which indicates carbonate formation temperatures of 35–60°C (±4°C), and that there was no significant post-burial heating of the preserved organic matter. $\delta^{13}C_{org}$ values range from -29.6 to -24.0‰, suggesting C fixation by photosynthesis. Some $\delta^{13}C_{org}$ depth profiles through paleosols indicate diffusive enrichment comparable to modern soils, which suggests that the microbial communities were present both at the soil surfaces and subsurface. Together, these various lines of evidence indicate an extensive terrestrial biosphere by ~1.1 Ga ago.

[1] Horodyski & Knauth (1994) *Science* **263**, 494-498. [2] Strother *et al*. (2011) *Nature* **473,** 505-509. [3] Prave (2002) *Geology* **30,** 811-814. [4] Ojakangas *et al*. (2001) *Sed. Geol.***141-142**, 421-442. [5] Mitchell & Sheldon (2009) *Precam. Res.* **168**, 271-283. [6] Mitchell & Sheldon (2010) *Precam. Res.* **183**, 738-748. [7] Sheldon (in press) *SEPM Special Paper*

Origin of the acidic rocks of the Early Permian Panjal Traps, Kashmir, India

J. GREGORY SHELLNUTT[1*], GHULAM M. BHAT[2], KUO-LUNG WANG[3], MICHAEL E. BROOKFIELD[4], JAROSLAV DOSTAL[5], AND BOR-MING JAHN[6]

[1]National Taiwan Normal University, Department of Earth Science,
jgshelln@ntnu.edu.tw (* presenting author)

[2]University of Jammu, Department of Geology
bhatgm@jugaa.com

[3]Academia Sinica Institute of Earth Sciences
kwang@earth.sinica.edu.tw

[4]Department of Environmental, Earth and Ocean Sciences University of Massachusetts at Boston
mbrookfi@hotmail.com

[5]Saint Mary's University, Department of Geology
jarda.dostal@stmarys.ca

[6]National Taiwan University, Department of Geosciences
bmjahn@ntu.edu.tw

Abstract

The Panjal Traps of northern India represent a significant outpouring of mafic and felsic volcanic rocks during the Early Permian and are synchronous with the opening of the Neotethys Ocean. Previous studies have suggested that the felsic volcanic rocks are derived by differentiation of mafic magmas. Dacites and rhyolites collected from the lower-middle portion of the volcanic pile near Pampore, Kashmir are peraluminous (ANCK > 1.0) in composition. Their whole rock I_{Sr} values are variable (I_{Sr} = 0.69307 to 0.71825) and indicate open system behavior of either Rb or Sr or both whereas their Nd isotopic compositions ($\varepsilon Nd_{(T)}$ = -8.6 to -8.9) are nearly uniform. The $\varepsilon Nd_{(T)}$ values and trace element (Th/Nb_{PM} > 4; Nb/U < 10; Th/Ta > 8) ratios suggest the rocks are derived from the crust. Major and trace elemental modeling suggest the likely source was from the middle crust rather than the lower or upper crust. Furthermore, the felsic Panjal Traps have trace element compositions similar to some felsic volcanic rocks and A-type granitic rocks from other large igneous provinces (e.g. Karoo, Parana and CAMP) and that they were likely derived by partial melting of an ancient crustal (i.e. T_{DM} = 1836 to 1937 Ma) source which experienced multiple episodes of crustal recycling. In contrast to other LIP felsic volcanic rocks, the acidic Panjal Traps are unique in that they were not derived from a mafic mantle source material. The heat required to melt the crust was likely due to the continuous injection of contemporaneous basaltic magmas which formed the majority of the mafic Panjal Traps.

Biogeochemistry Improves Prediction of Metal Bioaccessibility of Yard Soils in Tar Creek, USA

YONGMEI SHEN*, SUZIE SHDO, EMILY R. ESTES[1], AMI R. ZOTA[2], DANIEL J. BRABANDER[3], AND JAMES P. SHINE[1]

[1] Harvard School of Public Health, Boston, USA,
yshen@hsph.harvard.edu,
shdo100@mail.chapman.edu,
eestes@fas.harvard.edu,
jshine@hsph.harvard.edu

[2] University of California San Francisco, San Francisco, USA,
ZotaAR@obgyn.ucsf.edu

[3] Geosciences Department of Wellesley College, Wellesley, USA,
dbraband@wellesley.edu

Introduction

Heavy metal contamination in soils is ubiquitously observed due to mining, smelting, and industrial processes. Current approaches to determine the risk of metals via oral ingestion from soils are through operationally defined in-vivo or in-vitro tests. In addition, regulatory agencies often assume a default value as the bioavailable proportion of total metal. However, metal bioavailability in soil varies greatly based on their chemical forms, retention and releasing process, as well as exposure pathways. In order to better assess risks, it is necessary to bridge the gap between geochemistry, bioaccessibility and risk assessment of metals.

Method

In-vitro simple bioaccessibility extraction tests (SBET) and sequential extractions were conducted on yard soil samples collected from the Tar Creek Superfund Site, OK, a former lead and zinc mining area. In addition, we conducted SBET and sequential extraction on pure phase metal minerals and metal minerals spiked in a reference soil to determine the role of both speciation and soil matrix effects on metal bioaccessibility. X-ray absorption spectroscopy techniques were also used as a supplementary tool on a subset of yard soil samples. We applied statistic models to predict metal bioaccessibility in soils given metal distribution in the soil matrix.

Conclusion

Sequential extraction enables one to identify direct and potential hazardous metal fractions in soil in terms of being bioaccessible. Compared with total metal content, taking into account metal speciation in soil improves the estimation of the extent of bioaccessibility to different extents for different metals (Pb, Mn, Zn, Cd, Cu). The results help figure out the profound effects of mineralogical composition of metals, soil properties and particle size on determining metal bioaccessibility. Based on the results, site-specific metal biogeochemistry information might be able to be utilized to make metal bioavailability assessment more accurate.

Uranium adsorption by *Shewanella oneidensis* MR-1 in the presence of $NaHCO_3$

LING SHENG *, JEREMY B. FEIN

Civil Engineering and Geological Sciences, University of Notre Dame, Notre Dame. * lsheng@nd.edu (* presenting author)

There have been several previous studies that have measured the adsorption behavior of U(VI) onto non-metabolizing bacteria in experiments either devoid of dissolved CO2 or in systems open to the atmosphere. There is considerable evidence for extensive adsorption of U(VI) above pH 6-7 where the aqueous uranyl-tricarbonate aqueous complex dominates the aqueous budget of uranium. However, there is considerable uncertainty regarding the identity and thermodynamic stability of the bacterial surface complexes that cause this adsorption. It is particularly important to determine these parameters in order to model the effect of bacterial adsorption of U(VI) in a range of natural or engineered carbonate-bearing aqueous systems.

In order to constrain the stoichiometry and stability of the important U(VI)-bacterial surface complexes, we measured the adsorption of 60 ppm aqueous U(VI) as a function of $NaHCO_3$ concentration in solution from 0.0 to 30.0 mM. Experiments were conducted in 0.1 $NaClO_4$ to buffer ionic strength, and pH was varied from 3 to 9 in order to vary the extent of protonation of bacterial surface sites so that the sites that are important in U(VI) binding could be identified. All the experiments were conducted open to the atmosphere. The observed extents of U(VI) adsorption are independent of $NaHCO_3$ concentration in the system below pH 5. Above pH 5, the extent of adsorption decreases with increasing $NaHCO_3$ concentration, but the observed extent of adsorption in each case is greater than that predicted assuming only aqueous uranyl-carbonate complexation and neglecting ternary uranyl-carbonate-bacterial complexation.

We used a non-electrostatic surface complexation approach to model the adsorption data. The data require the existence of at least two uranyl-carbonate-bacterial surface complexes, and we use the observed adsorption measurements to constrain values for the stability constants for each of these complexes. The modeling results suggest the presence of additional uranyl-carbonate bacterial surface complexes than have been previously identified under conditions with elevated carbonate concentrations. These complexes can control the U(VI) adsorption behavior in systems with high carbonate concentrations and hence our results can be used to predict the extent of U(VI) adsorption onto bacteria in a range of natural and engineered systems.

Environmental monitoring of tungsten in Fallon, Nevada

PAUL R. SHEPPARD[1*], GARY RIDENOUR[2], AND MARK L. WITTEN[3]

[1]University of Arizona, Laboratory of Tree-Ring Research, Tucson, AZ USA, sheppard@ltrr.arizona.edu (* presenting author)
[2]Physician, Fallon, NV USA, docridenour@charter.net
[3]Odyssey Research, Tucson, AZ USA, mlwitten@yahoo.com

Environmental Monitoring in Fallon

Fallon, Nevada, USA, experienced a cluster of childhood leukemia beginning in 1997 [1]. Extensive research was conducted in Fallon by multiple entities to determine what might have caused this childhood leukemia cluster. For our part, we employed multiple techniques of environmental monitoring for metals in Fallon, including chemistry of airborne dust, lichens, surface dust, surfaces of tree leaves, and tree rings [2].

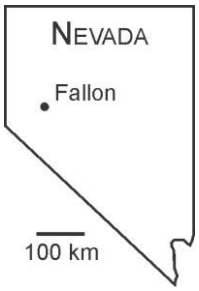

Figure 1: Map showing location of Fallon, Nevada, USA

Results

Tungsten and cobalt were elevated in airborne dust of Fallon relative to comparison towns. Tungsten and cobalt were elevated in lichen tissues within Fallon relative to desert sites outside of town. Surface dust showed tungsten and cobalt concentrations peaking just northwest of the center of Fallon relative to the outskirts of town. Leaf surfaces confirmed this spatial pattern of tungsten and cobalt peaking just northwest of the center of Fallon. Tree rings, a technique that emphasizes temporal resolvability, showed tungsten increasing in central Fallon by the mid to late 1990s, coinciding roughly with the onset of the cluster of childhood leukemia. Tree rings also showed high inter-tree variability in tungsten and cobalt across sampled trees within Fallon relative to comparison towns.

Conclusion

Fallon is distinctive by experiencing a cluster of childhood leukemia and having elevated airborne tungsten and cobalt. Linkage between a disease and an environmental condition cannot be made from environmental data alone. However, the co-occurrence in Fallon of elevated airborne tungsten and cobalt and a cluster of childhood leukemia logically should prompt biomedical research to evaluate the potential linkage between leukemia and the combined exposure to airborne tungsten and cobalt.

[1] Steinmaus et al. (2004) *Environmental Health Perspectives* **112**, pp. 766-771. [2] Sheppard, Ridenour, & Witten (2009) pp. 141-156 in *Airborne Particulates*, Cheng & Liu (Eds.), Nova Science Publishers, New York.

Multisite Surface-Complexation of Zn and Cu on Goethite

DAVID M SHERMAN*[1], DAVID MOORE

[3]School of Earth Sciences, University of Bristol, Bristol, BS8 1RJ, UK dave.sherman@bris.ac.uk (* presenting author)

Goethite (α-FeOOH) is the paradigm mineral for the scavenging of metals in terrestrial environments. The structure of goethite is based on edge-sharing FeO_6 octahedra which form double chains along the **b**-direction (using space-group setting Pnma); the double chains are linked to each other via corner-sharing in the **a**- and **c**-directions. At the nano-scale, goethite forms long needles along the **b**-direction with the {101} surfaces being dominant (Fig 1). The {101} surfaces have singly coordinated surface oxygens which can complex to metals via the formation of a bidentate double corner-sharing (2C) complex. However, the goethite needles are terminated by a {210} surface; on this surface, Zn and Cu could bind by forming an edge-sharing 2E complex (Fig. 2). The {210} surfaces comprise only a few per-cent of the surface area of goethite but we can infer that the {210} surfaces would be much more reactive than the {101} surfaces. We hypothesise that sorption of metals such as Zn and Cu to goethite will first take place on the more reactive {210} surface. However, since this surface only comprises a few percent of the total surface area the sorption capacity of the {210} surface will be limited to ~0.01wt % Cu or Zn.

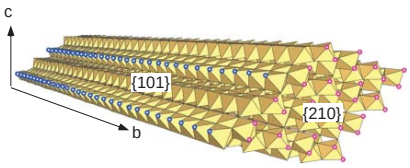

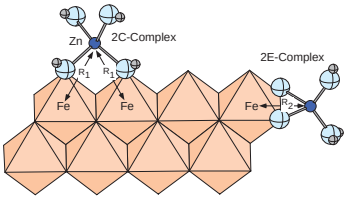

We have measured the sorption of Cu and Zn to goethite as a function of surface loading (0.008 to 0.8 wt. %). We find that our sorption edges can only be simultaneously modelled if we invoke several different surface complexes. For both Cu and Zn, the strong edge-sharing 2E complex on the {210} surface dominates at loadings < 0.01 wt. %. The weaker double corner-sharing 2C complex on the {101} surface dominates at loadings near 0.1 wt. %. Above 0.1 wt. %, both Cu and Zn form polynuclear complexes. Previous EXAFS studies of Cu [1] and Zn [2], at surface loadings > 0.1 wt %, only resolved 2C and polynuclear complexes of Zn or Cu on the {101} surface. However, at more environmentally relevant surface loadings, the 2E complexes on the {210} surface should be dominant. More powerful synchrotron sources (e.g., I20 at Diamond) will enable us to confirm the existence of the 2E complexes, at least for Zn.

[1] Peacock, L., & Sherman, D. M. (2004). *Geochimica et Cosmochimica Acta*, *68*(12), 2623-2637. [2] Trivedi, P., Axe, L., & Tyson, T. A. (2001). *Journal of Colloid and Interface Science*, *244*(2), 230-238.

Mercury in precipitation, sediments, and largemouth bass in FL: Insights using mercury stable isotopes

LAURA S. SHERMAN[1]* AND JOEL D. BLUM[2]

[1]University of Michigan, Earth and Environmental Sciences, Ann Arbor, MI, USA, lsaylors@umich.edu (*presenting author)

[2](Same as 1), jdblum@umich.edu

Mercury (Hg) concentrations in precipitation and fish are elevated across Florida (FL), U.S.A.[1] However, it is difficult to determine the specific biogeochemical pathways by which fish aquire Hg. Recent studies suggest that newly deposited Hg can be more bioavailable than Hg in sediments and that this Hg can rapidly enter aquatic food webs.[2] To gain insight into the sources of Hg to fish in FL, we analyzed Hg stable isotope ratios in precipitation, lake sediments, and largemouth bass collected across central FL.

We sampled surface sediments from freshwater lakes in central FL that are impacted by a mixutre of local and regional Hg sources. These surface sediments displayed a wide range of δ^{202}Hg values from -1.19 to -0.46‰ (mean = -0.72‰, 1 s.d. = 0.24‰, n = 18) and did not display significant mass-independent fractionation (MIF). Largemouth bass collected from a subset of these lakes displayed a range of δ^{202}Hg values and significant positive MIF (Δ^{199}Hg up to 4.43‰). We suggest that this MIF is due to photochemical degredation of methylmercury[3] prior to uptake into the food web. By using an experimentally derived fractionation relationship[3], we estimated δ^{202}Hg values of the fish methylmercury prior to photochemical processing and uptake. These δ^{202}Hg values were consistently offset from those of the corresponding sediments by 0.50‰ (1 s.d. = 0.14‰, n = 8). In addition, δ^{202}Hg values in the sediments were found to be correlated with the calculated δ^{202}Hg values for the fish methylmercury (r^2 = 0.47). These data suggest that methylmercury in the fish originates in large part from Hg in the sediments, which represents a mixture of historic Hg and modern atmospheric Hg. Prior to uptake by fish, non-photochemical processes[4, 5] cause an increase in δ^{202}Hg of ~0.50‰ and photochemical demethylation causes further increases in δ^{202}Hg values as well as large increases in Δ^{199}Hg values.

To examine the impact of a single, isolated source of Hg deposition on these relationships, we collected precipitation samples, lake sediments, and largemouth bass near a large coal-fired power plant in Crystal River, FL. These precipitation samples were uniquely characterized by large negative δ^{202}Hg values (mean = -2.56‰, 1 s.d. = 1.10‰, n = 28).[6] However, we did not observe similarly negative δ^{202}Hg values in sediments or fish collected in the area. Instead, δ^{202}Hg values of sediments and fish from the Crystal River area were comparable to those of the other lakes and were similarly offset and correlated. If emissions from the power plant have been isotopically consistent through time, this suggests that these emissions are not more rapidly bioavailable and are instead mixed with Hg in sediments prior to uptake by largemouth bass.

[1] Hand and Friedemann (1990) Florida Department of Environmental Regulation Report, 57pp. [2]Harris et al. (2007) *PNAS* **104**, 16586-16591. [3] Bergquist and Blum (2007) *Science* **318**, 417-420. [4] Rodríguez-González et al. (2009) *Environ. Sci. Technol.* **43**, 9183-9188. [5] Kritee et al. (2009) *Geo. Cosmo. Acta* **73**, 1285-1296. [6] Sherman et al (2012) *Environ. Sci. Technol* **46**, 382-390.

Natural Fe fertilization mechanisms in the Amundsen Sea Polynya, Antarctica

ROBERT M. SHERRELL[1,2]*, SILKE SEVERMANN[1,2], MARIA LAGERSTRÖM[1], KATHERINE ESSWEIN[1], KURIA NDUNGU[3], PER ANDERSSON[4], SHARON STAMMERJOHN[5], PATRICIA YAGER[6]

[1]Rutgers University, Institute of Marine and Coastal Sciences sherrell@marine.rutgers.edu (* presenting author) lagerstrom@marine.rutgers.edu kesswein@marine.rutgers.edu
[2]Rutgers University, Department of Earth and Planetary Sciences silke@marine.rutgers.edu
[3]Stockholm University, Applied Environmental Science kuria.ndungu@itm.su.se
[4]Swedish Museum of Natural History Per.Andersson@nrm.se
[5]INSTAAR, University of Colorado Sharon.Stammerjohn@Colorado.EDU
[6] University of Georgia, Sch. of Marine Programs pyager@uga.edu

The polynya of the Amundsen Sea, West Antarctica, is the most productive region of the Antarctic Shelf (~40 mg/m3 Chl-a in Dec. 2010), and is a test case for natural Fe fertilization, in stark contrast to the Fe-limited Antarctic Circumpolar Current (ACC) that borders this shelf region. ASPIRE (Amundsen Sea Polynya International Research Expedition, field work completed 2010-11), is an multidisciplinary study with a core emphasis on the mechanisms and pathways of bioavailable Fe delivery to the polynya euphotic zone. Candidate Fe sources include atmospheric deposition, upwelling of Modified Circumplar Deep Water, sea ice melting, glacier and iceberg melting, and inputs from shallow sediments. Samples for dissolved and particulate (>0.45um) trace metals and for Nd isotopes were collected at 35 stations in Dec. to early Jan. using a Geotraces-type CTD-rosette and in-situ pumps. Dissolved Fe (dFe) concentrations varying widely, and generally increase with depth. High values (up to 2nM) occur in near-bottom (~700m) waters of the western bathymetric trough and in the outflow from under the Dotson ice shelf (1nM at 150-600m). Lowest values (<0.1nM) are found in surface waters of the most productive central polynya region. Suspended particulate Fe (pFe), ranging 5-60nM, exceeds dissolved Fe throughout. Leachable fractions (LpFe; 25% acetic acid) range 0.2-16nM (2-35% of pFe), are lowest in the euphotic zone and highest in two important regions: at 50-600m where glacial meltwater-influenced flow emanates from under the ice shelf, and at ~300m adjacent to a drifting iceberg encountered in the southern polynya. Euphotic zone leachable Fe/P ratios are generally >10 mmol/mol, suggesting Fe-replete phytoplankton at most stations. Strikingly, Fe/P is very high (>1000 mmol/mol) and nearly identical at 50-150m in both the ice shelf and iceberg stations, suggesting that these are regions of injection of potentially bioavaible glacially-sourced LpFe into the upper water column. Dissolved Nd isotopes (<0.2um), a quasi-conservative tracer of continental sources, support the importance of glacial terrigenous inputs, with values as low as -6.0 at the ice-shelf outflow station (compare to adjacent ACC at ~ -8.0), tracing Fe inputs from radiogenic source rocks to shelf waters.

Inputs of dissolved and especially of labile particulate Fe resulting from flow under glacial ice-shelves are a major source of bioavailable Fe fueling productivity in the Amundsen Sea polynya.

Network of Terrestrial Subsurface sites in Precambrian Shields: Insights for Early Earth and Mars

B. SHERWOOD LOLLAR[1]*, T.C. ONSTOTT[2], T.L. KIEFT[3], L. LI[1], E. VAN HEERDEN[4], G.F. SLATER[5], D.P. MOSER[6], G. LACRAMPE-COULOUME[1], G. HOLLAND[7] AND C.J. BALLENTINE[7]

[1]University of Toronto, Toronto, Canada, bslollar@chem.utoronto.ca (* presenting author)
[2]Princeton University, Princeton, USA, tullis@princeton.edu
[3]New MexicoTech, Socorro, NM, USA, tkieft@nmt.edu
[4]University of Free State, Bloemfontein, South Africa, vheerde@ufs.ac.za
[5]McMaster University, Hamilton, Canada, gslater@mcmaster.ca
[6]Desert Research Institute, Las Vegas, USA, Duane.Moser@dri.edu
[7]University of Manchester, UK, chris.ballentine@manchester.ac.uk

Like the Lost City Hydrothermal Vents or Rainbow field, at depths of 2-3 km below the Earth's surface, saline fracture waters in the Precambrian Shields of Canada, Fennoscandia and South Africa are some of the most H_2 –rich on the planet and hence an important setting to investigate the planet's habitability – but significantly under investigated compared to the higher temperature hydrothermal systems and marine analog sites. The deep fracture waters host some of the deepest microbial communities yet identified on the planet: a low biomass, low biodiversity ecosystem subsisting at maintenance rates far from the photosphere – dominated by H_2-utilizing sulphate-reducing bacteria and H_2 derived from radiolysis and serpentinization [1,2]. These subsurface sites represent a critical environment in which to determine whether the types of chemolithotrophic life recognized at the vents are supported in the much larger segments of the Earth's crust where lower temperatures and hence slower rates of water-rock reaction prevail.

The tectonically quiescent, ancient fractured rock subsurface is directly relevant to single plate planets such as Mars, where surface expressions of volcanism such as hydrothermal vents are unlikely. Many of the investigated sites are located in northern regions in areas of continuous or semi-continuous permafrost, providing the opportunity to investigate psychrophilic life and hence as analogs for potential extinct or extant life on the icy planets and moons. Unlike high temperature seafloor systems like Lost City, where rapid fluid circulation and mixing means that the products of water-rock reaction such as H_2 rapidly diffuse away, the hydrogeologically isolated fracture waters in Precambrian Shield rock provide virtual "time capsules" in which, despite the slower rates of reaction, the products of water rock reaction and potential substrates for microbial life can accumulate and build up high concentration gradients over geological long time scales. The deepest and oldest fracture networks have residence time estimates derived from noble gas studies on the order of tens of millions of years [3], preserving a geochemical and microbial environment minimally impacted by hydrogeological mixing with the surface. They may provide a window into a different aspect of the Earth's biodiversity, but most significantly may preserve a more deeply branched and potentially evolutionarily older component of the Earth's life history with important implications for the origin and radiation of life on Earth. The deepest fracture water may even provide the opportunity to investigate controls on the biotic-abiotic transition and limits to life in the deep Earth.

[1] Lin et al. (2006) *Science* **314,** 479-482.
[2] Chivian et al. (2009) *Science* **322,** 275-278.
[3] Lippmann-Pipke et al. (2011) *Chemical Geology* **283,** 287-296.

High pressure constraints core formation from x-ray nanoscale tomography

YINGXIA SHI[1]*, WENDY L MAO[1, 2], LI ZHANG[3], WENGE YANG[4], YIJIN LIU[2], JUNYUE WANG[4]

[1]Stanford University, Stanford, USA, yingxias@stanford.edu*
[2]SLAC National Accelerator Laboratory, Menlo Park, USA
[3]Carnegie Institution of Washington, Washington, D. C., USA
[4]Argonne National Laboratory, Argonne, USA

Core-formation represents the most significant differentiation event in Earth's history. Percolation of liquid iron-rich alloy through a crystalline silicate matrix has been suggested as a possible core formation mechanism, especially for the differentiation of planetesimals during the early history of our solar system, since radioactive decay of short-lived isotopes in the small accreting bodies cannot provide enough heat to form extensive melting (i.e. magma ocean) [1-2]. Previous experimental results looking at dihedral angles in silicate metal samples synthetized at elevated pressures and temperatures suggest that percolation is unlikely to be an efficient mechanism in our planet [3-4]. However, experimental conditions in previous work have been limited in upper mantle conditions (<30GPa). Moreover the measurement of dihedral angles using transmission electron microscopy or backscattered electron microscopy may not generate satisfactory statistics. Nanoscale x-ray computed tomography (nanoXCT) has exciting potential as an accurate probe to study the 3D connectivity and permeability of core forming melts in crystalline silicates. Using a laser-heated diamond anvil cell, experimental conditions over the entire pressure-temperature range in the lower mantle can be accessed. In this study, we compressed and heated the mixture of iron-rich alloy + orthopyroxene, and then used a focused ion beam (FIB) to mill the quenched samples to extract a portion for nano-XCT. Pilot studies from our group using 3D nano XCT have demonstrated the ability to image the detailed morphology of the iron-alloy and silicates, along with details of Fe-FeS eutectic intergrowth patterns, which help to distinguish the relative Fe content in Fe and FeS. Data resulting from the combination of these techniques could improve our understanding of planetary core-forming processes.

[1] Keil *et al* (1997) *Meteoritics and Planetary Science* **32**, 349-363.

[2] Rubie, *et al* (2007) *Evolution of the Earth* **9**, 51-90.

[3] Shannon & Agee (1996) *Geophysical Research Letters* **23,** 2717-2720.

[4] Terasaki *et al* (2008) *Earth and Planetary Science Letters* **273**, 132-137.

Lead Adsorption on Iron-amended Composts

ZHENQING SHI,*[1] YEEWEI CHAN[1], AND JAMES HARSH[1]

[1]Washington State University, Pullman WA, USA, zhenqing.shi@wsu.edu (* presenting author)

Biosolids high in Fe have been shown to reduce the bioavailability of soil Pb both to plants and, when ingested or inhaled, to humans. We characterizing an Fe-rich compost that was developed to serve the same role as Fe-rich biosolids. The objectives of this work are (1) to determine the effectiveness of this material in lowering the bioavailability of Pb in soils (2) to characterize the nature of the reactive sites and their mechanism of metal sequestration. In this study, we (1) determine the capacity for Pb as a function of Fe concentration and Fe source, (2) assess the ability of Fe-compost to transform Pb in contaminated soils to highly recalcitrant states, and (3) model the distribution of Fe between organic- and Fe-sites.

Batch experiments were conducted to study the capacity of the iron-amended compost to adsorb Pb, including adsorption isotherms at various pH and adsorption edges at various initial Pb concentrations. For some selected experiments, the compost samples with varying iron contents were used to evaluate the effect of iron-amendment. Generally, the iron-amended composts showed high Pb adsorption capacity (> 3% Pb in composts), suggesting high concentrations of reactive organic matter and iron oxides in these compost samples. Lead adsorption increased with Fe concentration, suggesting that Fe sites played a role in increased adsorption.

The ability of iron-amended composts to sequester Pb in contaminated soils was investigated by incubating two contaminated soils with the compost samples at the field moisture content. We are evaluating the extractability of Pb in these treated soils with sequential extraction methods.

The preliminary modeling results with WHAM VI described the Pb adsorption results well using humic material and iron oxides as adsorbents. The modeling results also suggested that organic matter dominated adsorption at high Pb concentrations and adsorption to iron oxides was greatest at lower Pb concentrations. We are currently calibrating the model parameters with more data and comparing the performance of different speciation models, such as SHM and CD-MUSIC. We hope to acquire a quantitative understanding of the roles of both organic matter and iron minerals on Pb sequestration by the composts.

Uranium isotope fractionation associated with biostimulation experiments at the Old Rifle mill site

ALYSSA E. SHIEL[1]*, PARKER LAUBACH[1], THOMAS M. JOHNSON[1], CRAIG C. LUNDSTROM[1], KENNETH H. WILLIAMS[2] AND PHILIP E. LONG[2]

[1]Dept. of Geology, University of Illinois at Urbana–Champaign, Urbana, IL USA; ashiel@illinois.edu (*presenting author)
[2]Lawrence Berkeley National Laboratory, Berkeley, CA USA

Microbial and geochemical factors controlling subsurface U mobility are evaluated in the U contaminated aquifer at the former U mill site in Rifle, CO USA. Biotic reduction of U(VI) is induced by the injection of acetate (electron donor) into the contaminated aquifer and is used to immobilize U as U(IV). Experimental plots consist of monitoring wells both upgradient and downgradient of an injection gallery. The 2010–11 experiment (Plot C) was designed to isolate the impacts of reduction and sorption processes. Previous work has shown large shifts in $^{238}U/^{235}U$ (hereafter discussed as $\delta^{238}U$) accompany U(VI) bioreduction ($\Delta^{238}U = 1.05‰$) [1]. We provide the results of a more detailed study to increase confidence in the use of $\delta^{238}U$ as an indicator of U(VI) reduction and seek to apply this method to bioremediation experiments in which groundwaters are treated with acetate only or both acetate and bicarbonate (desorbs U from aquifer solids). In addition, this data set gives us, for the first time, $\delta^{238}U$ measurements during rebound of U(VI) concentrations as reduction wanes. This is particularly important as the long-term success of this remediation technique depends on the stability of sequestered U(IV).

We present groundwater U(VI) concentration and $\delta^{238}U$ results for two wells downgradient of the injection gallery; one of the wells (CD-01) was amended with acetate and the other (CD-14) with both acetate and bicarbonate. Preinjection values for the two wells are identical to those upgradient, within the uncertainties. For CD-01, the acetate injection upgradient led to a dramatic drop in [U(VI)] (from 165 to 10.6 ppb) and $\delta^{238}U$ (from 0.03 to -1.32‰), resulting from the preferential removal of ^{238}U as reduced U(IV). An excursion to greater $\delta^{238}U$ values during the period when [U(VI)] was at a minimum may be related to a contribution of relatively heavy U from nano-colloidal U(IV) in the filtered groundwater. After the amendment ceased, the groundwater [U(VI)] and $\delta^{238}U$ returned to approximately preinjection values. Lack of an increase of $\delta^{238}U$ above preinjection values is consistent with advection of U(VI) from upgradient, rather than reoxidation of U(IV), as the primary source.

For CD-14, a large increase in the [U(VI)] was induced by the bicarbonate injection (up to 415 ppb), while no change was observed in $\delta^{238}U$. This is in agreement with previous Rifle field experiments that revealed the absence of significant U isotope fractionation with adsorption–desorption of U(VI) [2]. The acetate injection led to a dramatic decrease in the [U(VI)] and $\delta^{238}U$ values (to 15 ppb and -1.19‰). The recovery of [U(VI)] and $\delta^{238}U$ is much slower for CD-14. Despite the return of [U(VI)] to preinjection values by the end of the field season, sustained U isotope fractionation (-0.43‰) is observed.

[1] Bopp *et al.* (2010) *Environ. Sci. Technol.* **44**, 5927–5933. [2] Laubach et al. (2010) *GSA Abstracts with Programs* **42**, 231.

Dissolved rhenium and molybdenum in rivers

ALAN SHILLER[1]*

[1]University of Southern Mississippi, Stennis Space Center, MS, USA, alan.shiller@usm.edu

Various workers have reported dissolved concentrations of Re and Mo in rivers and have generally concluded that sulfide weathering is the dominant source of these elements. This is based both on the well-known association of these elements with Black Shales as well as correlation with fluvial sulfate. We have examined the dissolved concentrations of Re and Mo in the Yukon River Basin in Alaska, the Loch Vale watershed, the lower Mississippi River, and the East Pearl River (Miss.). We find that fluvial sulfate correlates nearly 1:1 with estimates of non-carbonate calcium, suggesting that the fluvial Re- and Mo-sulfate correlations are not necessarily conclusive of a sulfide source. We also observe significant seasonal variability of Mo and sometimes Re in some rivers, suggestive of seasonal redox effects on element mobilization and transport.

Electrolyte Ion Adsorption at the Hematite/Water Interface: Cryogenic X-ray Photoelectron and Electrochemical Impedance Spectroscopic Studies

KENICHI SHIMIZU[1]*, ANDREY SHCHUKAREV[1], ANDRZEJ LASIA[2], JOSEPHINA NYSTRÖM[1], PAUL GELADI[3], BRITTA LINDHOLM-SETHSON[1], JEAN-FRANÇOIS BOILY[1]

[1]Department of Chemistry, Umeå University, Sweden, kenichi.shimizu@chem.umu.se (*presenting author)
[2]Department of Chemistry, University of Sherbrooke, Canada
[3]Unit of Biomass Technology and Chemistry, Swedish University of Agrecultural Sciences, Sweden

Hematite (α-Fe_2O_3) is a commonly occurring mineral in natural environments and its (electro)chemical attributes are of great importance to various geochemical and technological settings. A fundamental understanding of reactions taking place on hematite surfaces is particularly important in this regard. In this study, electrolyte ion adsorption and electrostatic potential development across the hematite/water interface are respectively probed by cryogenic X-ray photoelectron spectroscopy (XPS) and by electrochemical impedance spectroscopy (EIS).

Cryogenic XPS measurements are carried out on colloidal hematite particle surfaces equilibrated in 50 mM aqueous solutions of monovalent ions (Na^+, K^+, Rb^+, Cs^+, NH_4^+, F^-, Cl^-, Br^-, I^-) at pH 2-11. Results consistently reveal coexisting cations and anions both below and above the point of zero charge of hematite. Inverse correlation between pH dependent surface loadings and hydrous ionic radii is observed in both alkali metal ($Na^+ > K^+ > Rb^+ \approx Cs^+$) and halide ($F^- > Cl^- \approx I^- > Br^-$) ions. Ammonium ion sorption occurs through surface-bound NH_3 species (*e.g.* ≡Fe-OH···NH_3) shifting the protonation constant of the cation from pK = 9.3 in bulk solution to pK = 8.4 at the interface.

Hematite single crystal electrodes with various crystallographic orientations are used to obtain the pH dependence of electric surface potentials in NaCl and NH_4Cl solutions. Three distinct interfacial processes, space charging, electrical double layer, and adsorption of proton and/or electrolyte ions, are extracted by fitting experimental impedance data using an equivalent circuit model (Fig. 1). Double layer capacitance values vary with pH and exhibit a minimum at pH around 8.7, close to the point of zero charge of this mineral. This capacitance-pH behavior closely resembles that of the interfacial concentrations of electrolyte ions on colloidal hematite particles obtained by XPS. Our results reveal systematic effects of pH and electrolyte ion identity on the intrinsic activity of hematite surfaces.

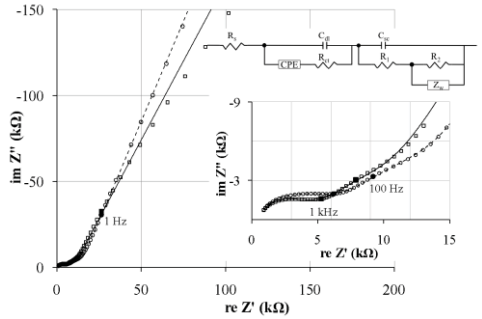

Fig. 1 *Complex plane plots of hematite in 0.1 M NaCl (pH 3.8, ○) and NH_4Cl (pH 3.5, □), including an equivalent circuit model.*

The Structure and reactivity of iron-organic matter coprecipitates

MASAYUKI SHIMIZU[1*], MARTIN OBST[2], ANDREAS KAPPLER[3], THOMAS BORCH[1,4]

[1]Department of Soil and Crop Sciences Colorado State Univervity, Fort Collins, U.S., masayuki.shimizu@colostate.edu (* presenting author)
[2]Center for Applied Geoscience Eberhard Karls University Tuebingen, Tuebingen, Germany, martin.obst@uni-tuebingen.de
[3]Center for Applied Geoscience Eberhand Karls University Tuebingen, Tuebingen, Germany, andreas.kappler@uni-tuebinge.de
[4]Department of Chemistry Colorado State University, Fort Collins, U.S., thomas.borch@colostate.edu

Introduction

Iron (Fe) (oxy)(hydr)oxides can have large specific surface areas and reactive functional groups, which make them important sorbents for soil nutrients, contaminants, and organic matter (OM). Thus, Fe oxides play a critical role in stabilizing soil organic matter. In the natural environment, pure Fe oxides, such as ferrihydrite, are rarely formed. For instance, OM can be incorporated in the ferrihydrite structure via coprecipitation, likely resulting inboth structual and reactivity changes. Despite the high natural abundance of Fe-OM coprecipitates, only few studies have attempted to determine their reactivity and characterize their chemical and physical properties. In this study, we synthesized Fe-OM coprecipitate with various methods, such as hydrolysis vs. oxidation and with different composition of OM, such as humic acid or fulvic acid. We then characterized the morphology, structure, and reactivity of these coprecipitates to gain new insight into how OM controls the biogeochemical cycling of Fe oxides.

Results and Conclusion

X-ray diffractometry (XRD) analysis indicated that coprecipitated OM did not change the crystal structure of 2-line ferrihydrite. Electrophoretic mobility (EM) analysis was conducted to study the impact of coprecipitated OM on the zeta potential of suspended Fe oxide particles between pH 5 and 9. The EM measurements clearly showed that the addition of OM resulted in more negatively charged partiles of coprecipitates compared to ferrihydrite. Particles with higher C/Fe ratios were more negatively charged than particles with lower C/Fe ratios. Scanning transmission X-ray microscopy (STXM) was used to obtain both two and three dimensional chemical maps of the Fe-OM coprecipitates as well as information about the most likely bounds formed between specific C and Fe surface functional groups. The STXM analysis indicated that Fe and C are evenly distributed within particles and that carboxylic-C may play an important role in complexation with Fe oxides. Complementary techniques, such as X-ray absorption spectroscopy, Mössbauer spectroscopy, TEM, SEM, specific surface area analysis were also conducted for the additional characterization. Our results indicate that both the ferrihydrite morphology and reactivity is strongly influenced when coprecipitated with soil organic matter.

Elucidating the Deep Sulfur Cycle: A Progress Report of Techniques and Findings

N. SHIMIZU*[1] AND C. W. MANDEVILLE [2]

[1] Woods Hole Oceanographic Institution, Woods Hole, USA, nshimizu@whoi.edu
[2] USGS, Reston, USA, cmandeville@usgs.gov

We have developed a SIMS method for in-situ determination of sulfur isotopic composition in silicate glasses has been developed, using a Cameca IMS 1280 ion microprobe. Calibrations were carried out for instrumental mass fractionation against well-documented natural and synthetic glasses with $\delta^{34}S$ ranging from -6 to +12‰. $\delta^{34}S$ in silicate glasses can be obtained with internal and external precisions ranging 0.4 – 0.7‰ (2σ). Accuracy is controlled by bracketing unknowns by repeated analyses of standards.

We used this method to determine ranges of natural variability in sulfur isotopic compositions in olivine-hosted melt inclusions from MORB, IAB and OIB to investigate how deep recycling of sulphur from oxidized and reduced surface reservoirs influences the sulfur isotopic compositions of mantle-derived melts. We found that (1) $\delta^{34}S$ of undegassed basalt MIs from arcs are most commonly heavy; Galunggung (Indonesia) ranging up to +10.7‰, Krakatau (Indonesia) to +8.8‰, and hydrous and highly oxidized (SO_4/total S =1) MIs from Augustine (Alaska) to +17.2‰, reflecting efficient recycling of oxidized sulfur into mantle wedge melting regions; and (2) Olivine-hosted melt inclusions from MORB and OIB display large variations in individual lavas; -10 to +10‰ for primitive FAMOUS MIs, -5 ~ +5‰ for depleted MIs from17°N (MAR), -6 ~ +2‰ for 26 – 29°N (MAR), among others, and MIs from 1960 Kilauea picrite range from -10 to -2‰. The variations are largest for MIs in Fo 90 – 91 olivines and appear to diminish as Fo decreases to Fo 82, reflecting the presence of large sulfur isotopic variability on local scales in the mantle and the effect of averaging during mixing of melt fractions prior to eruption of lavas.

It is evident that isotopic variations characterizing surface reservoirs survive during deep recycling. Elucidating co-variations with radiogenic isotopes and trace element abundance patterns will require a systematic approach to obtain sample suites that represent mantle endmember components.

U-Pb zircon ages of Early Archean gneisses from northern Labrador

M. SHIMOJO[1]*, S. YAMAMOTO[1], K. MAKI[2], T. HIRATA[2], Y. SAWAKI[3], K. AOKI[1], A. ISHIKAWA[1], Y. OKADA[4], K.D. COLLERSON[5], AND T. KOMIYA[1]

[1]Department of Earth Science and Astronomy, The University of Tokyo, Komaba, Meguro, Tokyo, 153-8902, Japan (*correspondence: shimojo@ea.c.u-tokyo.ac.jp)
[2]Laboratory for Planetary Sciences, Kyoto University, Kyoto, Japan
[3]Japan Agency for Marine-Earth Science and Technology (JAMSTEC), Kanagawa, Japan
[4]Department of Earth and Planetary Sciences, Tokyo Institute of Technology, Tokyo, Japan
[5]School of Earth Sciences, The University of Queensland, Brisbane, Qld. Australia

Early Archean crustal records are rare, but contiguous units are best preserved in N. Labrador and the NWT (Canada) and in SW Greenland. The Saglek-Hebron area (N. Labrador), located at the W. extension of the North Atlantic Craton (NAC), contains well-preserved Eo-Paleoarchean suites including pre-3.8 Ga Nanok Fe-rich monzodioritic gneiss, the Nulliak supracrustal assemblage (*ca.* 3.8 Ga), 3.7-3.6 Ga Uivak I TTG gneisses, 3.5-3.4 Ga Uivak II augen gneisses and Mesoarchean 3.2 Ga Lister gneiss [1-3]. Saglek dykes are present in the Eo and Paleoarchean gneisses, but not in the younger Lister gneisses. Despite confirmation of the antiquity of the area [3,4] a comprehensive zircon U-Pb dating with LA-ICPMS employing cathodluminescence (CL) imaging has not been undertaken for orthogneisses and supracrustal suites. CL images are essential to discuss inherited grains, pristine core and overgrowth.

We conducted LA-ICPMS U-Pb geochronological study of zircons from TTG Uivak I gneiss from the Saglek-Hebron area. The CL images of zircon grains display internal structures of oscillatory zoning and homogeneous core with overgrowth rim. Results show that samples collected as Uivak I TTG gneisses can be classified into three groups based on the distribution of zircon ages. The first group of TTGs is characterized by both presence of older zircons than 3.8 Ga, with the maximum age of 3914 ± 40 Ma in $^{207}Pb/^{206}Pb$ age, and apparent lack of 3.6 to 3.8 Ga zircons. These are obviously members of the Nanok gneiss. Based on intrusive relationships observed in the field, the Nanok gneiss is pre-date emplacement of the protoliths of the Uivak I gneisses. The second and third groups have clear peaks at 3.7-3.6 Ga and *ca.* 3.3 Ga in their age distribution of zircon cores, indicating that TTGs of the second and third groups correspond to Uivak I gneiss and the Lister gneiss, respectively. Importantly, overgrowth rims of zircons we analyzed here show *ca.* 2.7 Ga, which reflect zircon growth during late Archean thermal event in the NAC, possibly associated with assembly of different terranes within the gneiss complex. We show that the combination of *in-situ* U-Pb dating and CL imaging can reveal the tectonothermal history of early Archean from the gneisses in N. Labrador.

[1] Collerson (1983) *Lunar planet. Inst. Tech. Rep.* **83-03**, 28-33. [2] Schiøtte *et al.* (1989) *Can. J. Earth Sci.* **26**, 1533-1556. [3] Collerson *et al.* (1991) *Nature* **349**, 209-214. [4] Schoenberg *et al.* (2002) *Nature* **418**, 403-405.

Volatile inventory of excess degassing

HIROSHI SHINOHARA[1*]

[1]Geological Survey of Japan, AIST, Tsukuba, Japan.
shinohara-h@aist.go.jp (* presenting author)

Overview

Excess degassing is heterogeneous emission of volatiles and magma caused by gas-magma decoupling in the upper crust. There are two types of excess degassing caused by different mechanisms. Excess degassing by eruption is considered as the result of eruption of bubble accumulated magma [1] whereas excess degassing by non-erupting persistant degassing is driven by conduit magma convection [2]. Sulfur budgets of eruptions, in particular of silicic magmas at subduction zones, suggest that one to two orders of magnitude larger amount of sulfur than in the erupted magma was accumulated prior to the eruption. Composition of the accumulated gas phase can be estimated based on melt inclusion and solubility studies [1, 3], however, bulk volatile composition of the magma supplied to the shallow crust is hard to constrain based on those studies.

Persistent degassing emits about ten times larger amount of SO_2 than degassing by erutpion at subduction zone and is the major source of crustal degassing [2]. Conduit magma convection continuously transports magams stored at a deep chamber to a shallow vent and causes low-pressure degassing, resulting in almost complete magma degassing of volatiles species with low solubility, such as H_2O, CO_2 and S. Therefore, compositions of the persistent degassing would be a good approximate of bulk volatile composition of original magmas and provied important constraints to volcatile budget of the shallow crust.

Composition of Persistent Degassing

Quantitative estimates of Composition of persistent degassing became possible by application of FT-IR and Multi-GAS techniques to volcanic plume observation. Accumulation of such data for Japanese volcanoes suggests that magmas with a similar volatile comosition are supplied to different volcanoes. One of the most intensively degassed volcano in this century, is Miyakejima volcano, Japan, which emitted about 24 Mt of SO_2. The intensive degassing of started in 2000 and the SO_2 flux decreased by almost 100 times during ten years but gas compositions remained similar; H_2O/CO_2 (mol ratio) =50, CO_2/SO_2 = 0.7. Based on H_2O content of basalt melt inclusions, volatile contents in the original basaltic magma are estimated as H_2O=3.0, CO_2=0.15 and S=0.17 (wt.%) [4]. Other persistently degassing volcanoes in Japan have similar CO_2/SO_2 ratio of 0.5-2, indicating that subduction zone magmas are not always CO_2-rich. In contrast, there are some other subduction volcanoes, such as Stromboli, Masaya and Sourfiere Hills, which persistently discharge gases with larger CO_2/SO_2 ratios of 6-10. If the CO_2-rich magma is necessary to cause bubble accumilation at a deep chamber resulting in the excess degassing by erutpion, occurrece of the excess degassing might be coincident with the CO_2-rich persistent degassing. Further accumulation of the composition data of persistent degassing might reveal such coincidence, if any, and constrain the volatile budget in the upper crust.

[1] Wallace (2001) *J Volcanol Geotherm Res* **108**, pp. 85-pp. 106. [2] Shinohara (2008) *Rev Geophys* **45**, 2007RG0244. [3] Keppler (2010) *Geochim Cosmochim Acta* **74**, 646-600. [4] Saito *et al* (2010) J Geophys Res 115, doi:10.1029/2010JB007433. [5] Blundy *et al* (2010) *Earth Planet Sci Lett* **290**, 289-301.

Characteristic of the long-term accumulation of lanthanides on *Saccharomyces cerevisiae*

H. SHIOTSU[1], M. JIANG[1], Y. NAKAMATSU[1], T. OHNUKI[2] AND S. UTSUNOMIYA[1]

[1]Department of Chemistry, Kyushu University, Fukuoka 812-8581, Japan (utu@chem.rc.kyushu-u.ac.jp)
[2]Advanced Science Research Center, Japan Atomic Energy Agency, Tokai, Ibaraki 319-1195, Japan (ohnuki.toshihiko@jaea.go.jp)

Interaction between actinides and fissiogenic rare earth elements (REEs) and microorganisms have attracted increasing attention due to the ubiquitous occurrence of microorganisms in the subsurface environment and to implication to the safety assessment of nuclear waste disposal. Although the post-adsorption nanomineralization process of individual REE was proposed by a recent study [1], the contaminating fluid may contain a series of actinides and fission products. Hence, the present study has investigated the post-adsorption process on microorganisms in the system containing a series of lanthanides (Ln) to understand the effect of coexisting Ln on the adsorption and post-adsorption process.

S. cerevisiae (yeast) was harvested in a YPD (P-rich) media prior to the experiment. The yeast was then contacted with a P-free solution containing 14 lanthanide elements (La-Lu) upto 72 h, in which the concentration of individual Ln was 0.0063 mM with the total Ln concentration of 0.085 mM. The experiment was conducted at three pHs, 3, 4, and 5, and at two different temperatures, 25 and 4 ^{o}C (no metabolism). The analytical techniques include ICP-MS -AES, FESEM-EDX, and TEM.

During exposure in the solution at 25 ^{o}C, all Ln were eliminated from the solution by 24 h at pH 4 and 5, while 50 % of the initial amount remained in the solution at pH 3 after 24 h. Particle at the size of ~100 nm precipitated on the cell surfaces at pH 3, while ~30 nm-sized nanoparticles were observed at pH 4 and 5. These nanoparticles are phosphate containing a series of Ln. The nanoparticles at pH 3 had monazite strucure, while the particles formining at pH 4 and 5 were amorphous, indicating that crystallization took place only at pH 3. Deprotonation merely occurs at the funcional group at pH 3 as evidenced by the other experiments at 4 ^{o}C, and the nanocrystallites possibly nucleated from the locally saturated solution adjacent to the cell surfaces. In contrast, Ln electrostatically adsorbed to the functional group was bound to P released from inside cell at pH 4 and 5. Most likely the geometry of Ln complex formation prevented the crystallization.

As for the Ln pattern, the greater amount of light REEs was removed from the solution than that of heavy REEs. The difference between the distribution coefficient, K_d(ml/g), of LREE and of HREE increased with time increasing. At 24 h, the K_d rate Nd to Tm ($K_{d,\,Nd}/K_{d,\,Tm}$) is 1.72, 4.61, and 6.86 at pH 3, 4, and 5, respectively. The K_d ratios greater than 1 indicate the preferential uptake of LREE by the microorganisms, which may be attributed to the lower solubility products of REE phosphate [2]. The present study demonstrated that the cell surfaces play a key role on kinetics and crystal formation in the post-adsorption biomineralization.

[1] M. Jiang *et al.* (2010) Chemical Geology, 277, 61-69
[2] Z. S. Cetiner *et al*. (2005) Chemical Geology, 217, 147-169

Microbial Coenocline Associated with Geochemical Gradients at a Groundwater Discharge Zone

V.L. SHIROKOVA[1]* AND F.G. FERRIS[2]

[1] University of Toronto, Toronto, Canada, vshi@geology.utoronto.ca
[2] University of Toronto, Toronto, Canada, grant.ferris@utoronto.ca

Abstract

A combined metagenomic, geochemical, and statistical investigation was used to characterize a groundwater spring with a dramatic electrochemical gradient. Eh, pH, precipitated iron, and sulfate concentration increased downstream of the source. The ferrihydrite saturation index, as well as ferrous iron, ferric iron, sulfide, ammonium, and nitrite concentration decreased downstream. A total of 672 clones were compiled into a cDNA library, with taxonomic identities across 9 phyla, including *Acidobacteria, Actinobacteria, Bacteroidetes, Chlorobi, Chloroflexi, Firmicutes, Nitrospirae, Planctomycetes,* and *Proteobacteria*. The variation in the relative abundance of the OTU phyla in response to geochemical parameters was modeled using coenoclines. *Alpha-proteobacteria* were the most sensitive to geochemical change, while *Acidobacteria* were least sensitive. Spearman's rank correlation coefficients were used to evaluate the relationship between geochemical variables and relative abundance of microbial OTU. Reduction-oxidation potential appears to be an overarching parameter in the stream, controlling the distribution of redox species and leading to strong segregation of microbial functional groups. Our study of Ogilvie Creek represents one of the first to combine geochemical, metagenomic, and statistical analysis in an effort to gain insight on the interrelationships between biogeochemical processes in natural systems.

Determining reactive thiol concentration in naturally occuring organic molecules

ELIZABETH M. SHOENFELT[1], CLARESTA M. JOE-WONG[2*], NYSSA M. CROMPTON[3], EMILY A. JAYNE[3], SATISH C. B. MYNENI[3]

[1] Department of Geosciences, Princeton University, Princeton, USA, eshoenfe@princeton.edu
[2]Departments of Geosciences & Chemistry, Princeton University, Princeton, USA, cmjoe@princeton.edu (*presenting author)
[3]Departments of Geosciences & Chemistry, Princeton University, Princeton, USA

Thiols, components of soil and aquatic organic molecules, exhibit high affinity for soft Lewis acids such as Cd^{2+} and Hg^{2+} and play an important role in metal speciation in natural waters. However, thiols' low abundance, high reactivity, and structural similarity to other reduced-S ligands such as methionine make their detection difficult. We propose a novel method to measure thiol concentrations in natural systems using the water soluble, charged, thiol-sensitive fluorophore monobromo(trimethylammonio)bimane (qBBr), which fluoresces upon binding to a thiol. Once the sample's natural fluorescence is subtracted out, a solution's fluorescence intensity is proportional to the concentration of thiol-bound fluorophore. By measuring the fluorescence intensities of a series of solutions with fixed sample concentration and increasing fluorophore concentrations, the saturation point can be calculated, giving the sample's thiol concentration. This method accurately estimates thiol concentrations in pure thiol-containing solutions, dissolved organic matter (DOM), and microbial cell membranes. Moreover, the presence of other chemical species often found in natural systems does not influence this method's sensitivity.

When pure glutathione or cysteine solutions were examined, this method produced an estimated thiol concentration within 1.85% of the expected value at micromolar concentrations, and within 7.40% at nanomolar concentrations. Although species such as dissolved salts, carboxylic acids, and other organo-sulfide groups might affect the absolute fluorescence intensity of the thiol-bound fluorophore, we found that these species do not interfere with determining the thiol concentration. Testing glutathione solutions with dissolved magnesium chloride in 500-fold excess resulted in calculated saturation values accurate to 6.40%. Likewise, adding up to 15-fold excess malate, a surrogate for carboxylic acids common in DOM, does not affect accuracy. Similar tests show that qBBr does not react with other sulfur groups such as disulfides and thioesters.

Using the technique developed for model systems, thiol concentrations in the DOM pool and microbial biopolymers can be calculated. The cell membrane thiol concentrations of three model microorganisms common to natural systems—*Bacillus subtilis*, *Shewanella oneidensis*, and *Geobacter sulfurreducens*—were estimated. *G. sulfurreducens* exhibited the highest thiol concentration, and *B. subtilis* the lowest. The calculated thiol: dissolved organic carbon ratio in surface water DOM from the Pine Barrens in New Jersey is approximately 10^{-3}-10^{-4}. Estimation of thiol concentration is necessary to understand the role of thiols in contaminant and nutrient speciation and transformation, and this method offers a simple way to measure thiol concentrations in natural systems.

Compositional trends of Icelandic basalts: Implications for short-length scale lithological heterogeneity in mantle plumes

OLIVER SHORTTLE* AND JOHN MACLENNAN

University of Cambridge, Department of Earth Sciences, Cambridge, UK, os258@cam.ac.uk (* presenting author), jcm1004@cam.ac.uk

Lithological variations in the mantle source beneath mid-ocean ridges and ocean islands have been proposed to play a key role in controlling melt generation and basalt composition. Iceland, as an extremum of oceanic crustal thickness and positioned at the centre of a long wavelength geochemical enrichment in Mid-Atlantic Ridge basalt chemistry, is an excellent place to study the relative importance of source lithology, mantle potential temperature and mantle flow field in generating melting and compositional anomalies on the Earth.

We begin by looking specifically at the major element composition of the end-member Icelandic melts, to constrain the lithologies contributing to melting. End-member melt compositions are identified using a plot of whole rock Nb/Zr against MgO, and coloring the points by a second major element. With a large dataset, as exists for Iceland, a plot such as this allows the effect of concurrent mixing and crystallisation on basalt major element chemistry to be separated from the geochemical variability which is mantle in origin. Applying this technique we identify the enriched end-member melt on Iceland to have higher FeO (11.3 wt%) and lower CaO (11.2 wt%) than the depleted melts (9.2 wt% FeO and 12.9 wt% CaO). To relate these end-member melt characteristics to source lithology we compare their compositions to a dataset of experimental partial melt compositions from the literature, produced from melting at a range of pressures, melt fractions and of peridotitic and pyroxenitic starting lithologies. Traditionally, experimental partial melts and natural melts have been compared graphically. In contrast, we quantify the difference between the basalt compositions across the major oxides (CaO-FeO-MgO-Al_2O_3-SiO_2) and, accounting for uncertainties, identify those experimental melts most like the end-member Icelandic basalts. The key result of this analysis is that no single source lithology available in the literature can account for the major element variability observed on Iceland, with the enriched Icelandic melt compositions requiring their source to have been refertilized by addition of up to 40% mid-ocean ridge basalt.

Significant refertilization of the enriched source beneath Iceland means that it will be more fusible than a KLB1-like peridotite, and as such will be over-represented in accumulated melts compared with its abundance in the source. The likely abundance of enriched material in the Icelandic source was estimated to be ~10%, by taking this bias into account and weighting observed compositions by erupted volume. To investigate whether this fraction of enriched material can account for the high crustal thickness at Iceland (up to 35 km) we develop a bi-lithologic peridotite-pyroxenite melting model in which the latent heat of melting of both the enriched and depleted material are considered - allowing for the effect of significant amounts of fusible source material on melt production to be assessed. This modelling demonstrates that with 10% pyroxenite in the source, significant temperature anomalies (+200K) and a plume driven mantle flow field are required to generate crustal thickness as high as observed in central Iceland.

A dedicated “clean lab” sampling facility for studying the natural filtration of trace metals by soils: the artesian springs of the Elmvale Groundwater Observatory

WILLIAM SHOTYK, BOCOCK CHAIR FOR AGRICULTURE AND THE ENVIRONMENT

Department of Renewable Resources, University of Alberta, 839 General Services Building, Edmonton, Alberta T6G 2H1 shotyk@ualberta.ca

Increasing, elevated concentrations of trace metals in the surface layers of soils may result from a diverse array of anthropogenic, atmospheric sources, in addition to chemical weathering of parent material and other natural sources. There is considerable, ongoing concern about the fate and transformations of these elements, and their eventual release to surface waters and groundwaters. The first step in this process is their release to the soil solution, and the first step in beginning to understand these processes is to obtain representative water samples for testing and analysis. The Elmvale Groundwater Observatory (Springwater Township, Ontario) consists of two dedicated groundwater sampling systems designed exclusively for the analysis of trace metals. One well was constructed entirely of surgical stainless steel, the other made using acid-washed high density polyethylene (HDPE). Both wells are artesian flow systems. Using ICP-SMS and the clean lab methods developed for polar snow and ice, it is possible to measure all of the trace metals of contemporary environmental interest. Sampling the water within a laminar flow clean air cabinet helps to eliminate variability by protecting the samples from anthropogenic aerosols in ambient air. Many trace metals such as Cr and Pb are found at concentrations (1 ng/L) significantly lower than the Arctic ice from the mid-Holocene (ca. 4 K to 8 K yr BP). Groundwater quality monitoring programs undertaken in the same region typically show “concentrations” for the same trace metals which are three orders of magnitude greater (1 µg/L) because of the introduction of colloids during sampling. The purpose of our studies is analytical and academic whereas the monitoring studies are intended to ensure that metal concentrations in groundwaters do not exceed the relevant water quality guidelines. Illustrative results of the two approaches are presented and their implications compared, with a view to better understanding the mechanisms of natural filtration of water by soils as well as analytical procedures to better characterize soil water quality.

Reconstructing anthropogenic, atmospheric emissions of trace metals using environmental archives: comparison of polar snow and ice, ombrotrophic peat bogs, *Sphagnum* moss from herbaria, and lake sediments

WILLIAM SHOTYK, BOCOCK CHAIR FOR AGRICULTURE AND THE ENVIRONMENT

Department of Renewable Resources, University of Alberta, Edmonton, Alberta, Canada T6G 2H1

shotyk@ualberta.ca

Given the long history of mining and metallurgy, many trace elements of contemporary environmental interest have been released to the environment since Antiquity. Reconstructing anthropogenic emissions requires suitable archives to provide records extending sufficiently far back in time to allow the natural fluxes and sources to be determined, for comparison with modern values. A number of archives have been employed to reconstruct historical records of atmospheric trace elements, each with its inherent advantages and disadvantages.

Ice cores from the Arctic and peat cores from ombrotrophic bogs both receive inputs of Pb exclusively from the atmosphere. Using examples from Devon Island, Nunavut, Canada and Etang de la Gruére, Jura Mountains, Switzerland, it was found that

1) the natural ratio of Pb to Sc was effectively constant for thousands of years and comparable values were found in both archives; this supports the hypothesis that natural atmospheric Pb was effectively dominated by soil dust particles supplied by weathering of crustal rocks.

2) anthropogenic Pb inputs to the Arctic are clearly seen in ice layers ca. 3,000 years old, with pronounced Pb enrichments and declines in $^{206}Pb/^{207}Pb$ ratios in samples from the Roman and Medieval periods, supporting the hypothesis that human activities have dominated atmospheric Pb inputs for three millenia.

3) although Pb enrichments have declined during recent decades, even in the most recent snow samples, the Pb/Sc and Pb isotope data show that 90 to 95% of the Pb is still anthropogenic.

Although *Sphagnum* moss from herbaria do not extend back in time further than ca. 200 years, they received trace metals exclusively from the atmosphere, the date of sample collection is known exactly, and they are not affected by chemical diagenesis in acidic, anoxic bog waters. The isotopic composition of atmospheric Pb obtained using peat cores from Europe (dated for the past ca. 150 years using ^{210}Pb) are in excellent agreement with the records for the same interval preserved in *Sphagnum* moss from herbaria.

Comparing the isotopic composition of Pb in recent layers of lake sediments from the Kawagama Lake watershed in central Ontario with a peat core from a local bog shows that the sediments are a much less sensitive indicator of atmospheric change, largely failing to record the declines in $^{206}Pb/^{207}Pb$ ratios since the elimination of leaded gasoline, and the growing relative importance of Pb from smelters in northern Ontario and Quebec.

The *in situ* occurrence of bacteria on gold grain surfaces: Implications for bacterial contributions to gold nugget structure and chemistry

JEREMIAH SHUSTER[1*], CHAD JOHNSTON[2], NATHAN MAGARVEY[2] , ROBERT GORDON[3] NEIL BANERJEE[1] AND GORDON SOUTHAM[1]

[1]Department of Earth Sciences, The University of Western Ontario, London, Canada, jshuster@uwo.ca (*presenting author)

[2]Department of Biochemistry & Biomedical Sciences/Chemistry and Chemical Biology, McMaster University, Hamilton, Canada

[3]Advanced Photon Source, Argonne National Laboratory, Lemont, USA

16a. Microbe-mineral interactions in time and space

Natural gold grains often possess secondary gold as colloidal particles, crystalline gold and bacteriomorphic structures. The latter form known as 'biogenic' gold that was first reported as structures resembling gold-encrusted microfossils on placer gold specimens [1]. Recent research suggest that Bacteria and Archaea are involved in the biogeochemical cycling of gold [2, 3, 4]. In this study gold grains from sediment sampled from Rio Saldana, Colombia were analyzed for the purpose of better understanding the formation of secondary gold in a tropical placer environment. Morphological analysis, using scanning electron microscopy, demonstrated that gold grains appeared as elongated disk shapes with articulated surfaces occurring predominantly on the perimeter. Bacteria were directly and indirectly attached as biofilms on the articulated surfaces of all gold grains. Iron oxide occurred on some grains as globular and patina coatings possessing casts of bacteria. The grains also possessed micron size secondary gold textures occuring on the outer periphery of the grains. Compositional analysis, inferred from energy dispersive spectroscopy and x-ray absorption fine structure, indicated that trace silver, mercury and copper was associated with gold. Unlike silver, mercury and copper appeared to have localized regions of heterogenous distributions throughout the gold grain. A pure bacterial culture, isolated from a single gold grain, was identified as *Nitrobacter* sp. 263 based on 16S sequencing. This *Nitrobacter* sp. removed gold from a gold (III) chloride solution within an hour. Transmission electron microscopy and scanning electron microscopy demonstrated that gold immobilization occurred as abundanct colloids and octahedral platelets less than 100 nm in diameter concentrated within the cell envelope. The occurrence of secondary gold on the surface of these grains and the ability of *Nitrobacter* to form crystalline gold suggests that this organism may contribute to the growth of gold grains in this placer environment. Gold biomineralization would be continuous if concentrations of aqueous gold input are low and bacterial metabolic growth is maintained by reproducing biomass lost to biomineralization.

[1] Watterson (1992) *Geology* **20**, 315-318. [2] Reith and McPhail (2009) *Chem. Geol.* **258**, 315-326. [3] Reith *et al.* (2011) *Geochim. Cosmochim. Acta.* **75**, 1942-1956. [4] Reith *et al.* (2010) *Geology.* **38, 843-846.**

Did I lose some LA-ICP-MS data somewhere?

STEPHEN SHUTTLEWORTH[1*], STUART GEORGITIS[2]

[1]Photon Machines, Redsmond, WA, USA, Shutts@photon-machines.com (* presenting author)
[2]Spectro Analytical Instruments, Mahwah, NJ, USA, Stuart.Georgitis@ametek.com

The combination of Laser Ablation (LA) and Inductively Coupled Plasma Mass Spectrometry (ICP-MS) provides an analytical tool capable of both high sensitivity elemental analysis and high precision isotopic analysis in a wide variety of matrices. Since its introduction in the mid 1980's LA-ICP-MS has been applied to a very broad range of applications across science in order to provide high spatially resolved chemical and isotopic information at the micron scale in the solid. The technique is now commonly used by researchers across the geochemical sciences.

As a destructive technique, data not captured as a consequence of detection duty cycle and dead time will be forever lost. Only now has a truly simultaneous ICP-MS been coupled to a laser thus eliminating the prior limitations that single spot analysis can only best be done with a restricted number of isotopes or a restricted section of the mass range. This paper will discuss the merits of laser ablation coupled with a truly simultaneous ICP-MS capable of analysing the entire periodic table for each indivudual laser shot. The use of a simultaneous dual detection range ICP-MS for laser ablation is investigated as a means to capture the whole ICP-MS spectrum of a single laser transient signal. The technique will be applied for both elemental mapping and isotopic analysis of mineral phases.

The Early Paleozoic of the Argentine Precordillera: C-isotope Excursions

A. N. SIAL[1*], S. PERALTA[2], C. GAUCHER[3], A.J. TOSELLI[4], V.P. FERREIRA[1], R. FREI[5], M. M. PIMENTEL[6]

[1]NEG-LABISE, Dept. Geol. UFPE, Recife, Brazil, sial@ufpe.br (* presenting author)
[2] Inst. Geología, Univ. Nac. San Juan-CONICET, Argentina
[3] Dept. Paleont., Fac. de Ciencias, 11400 Montevideo, Uruguay
[4] INSUGEO, San Miguel de Tucuman, Argentina, 4000
[5] Inst. Geogr. Geol., Geol. Section, Univ. Copenhagen, Denmark
[6] Inst. Geosc., Fed. Univ. Rio Grande do Sul, Porto Alegre, Brazil

Introduction. We have searched for the register of C-isotope excursions in the Upper Cambrian and Ordovician of the Argentine Precordillera. We report the register of the SPICE and SNICE in one same section in the Precordillera. The Darriwilian positive excursion (MDICE) and a Late Sandbian positive C-isotope excursion (GICE) have been registered in two sections. A pre-GICE positive C-isotope excursion (Sandbian S1, *N. gracilis* biozone) with $\delta^{13}C$ peak of ~ +3‰ is, perhaps, equivalent to the positive Spechts Ferry excursion of N. America. A positive $\delta^{13}C$ excursion registered at the base of the Upper Hirnantian La Chilca Fm. probably corresponds to HICE. **Causes**. These C-isotope excursions are probably related to oceanographic events: (a) sea-level rise and vigorous fluctuations in the Steptoean (SPICE), (b) sea-level fall in the Sunwaptan (SNICE), (c) important transgression in the Sandbian (pre-GICE and GICE), and (d) sea-level fall in the Late Hirnantian (HICE). In the Darriwilian and Sandbian stages, organic burial has led to a large ^{12}C sequestration in deep-ocean anoxia with saline bottom water, recorded by the graptoliferous black shales in the Gualcamayo and Los Azules formations, helped the building of the MDICE, one pre-GICE and GICE anomalies. O-isotope values for the Upper Cambrian are likely near-primary signals that point to progressive cooling from the SPICE to the SNICE, whereas for Sandbian carbonates they indicate strong T fluctuations. The $\delta^{13}C$ peaks of the GICE coincide with cooler periods with T progressively cooler towards Late Hirnantian. In the Zonda Fm., $^{87}Sr/^{86}Sr$ ratios vary from 0.7090 to 0.7109 while in Los Azules and Las Aguaditas Fms., they are ~ 0.7090. εNd values plot along the Nd isotopic evolution trend of the Iapetus Ocean.

Conclusions. The register of these excursions in the Precordillera is valuable proxy for the Early Paleozoic stratigraphy, regional/global high-resolution correlations, and sea-level change history.

Kinetics of phosphorus adsorption on iron oxyhydroxide residuals

PHILIP L. SIBRELL[1*]

[1]U.S. Geological Survey, Leetown Science Center, Kearneysville, West Virginia, USA, psibrell@usgs.gov (* presenting author)

Experimental Research and Findings

We have investigated the use of iron oxide media generated from mine drainage residuals for the removal of oxyanions from waste water, with a special emphasis on phosphorus (P) [1]. The use of packed column or fixed bed sorption systems allows treatment of waste water without requiring subsequent solid-liquid separation, and has been the focus of our research. In these trials we used 2.5 cm diameter glass columns packed with air-dried iron oxyhydroxides for treatment of wastewater with a variety of influent P concentrations, flow rates and media particle sizes. We then used Adsorption Design Software from the Michigan Technological University [2] to model results, estimate test parameters and to predict future outcomes. Results of several fixed bed trials are shown in Figure 1, where the effluent P concentration (normalized by the influent concentration C_i) has been plotted as a function of treatment time. It is clear that early breakthrough of the P was experienced in many of the column tests. In the most successful test (Run 7), we removed over 96% of the P from the influent waste stream over a period of 46 days of continuous operation. We have also observed that performance was strongly related to the value of the surface diffusion modulus *Ed*, enabling prediction of column performance based on test conditions.

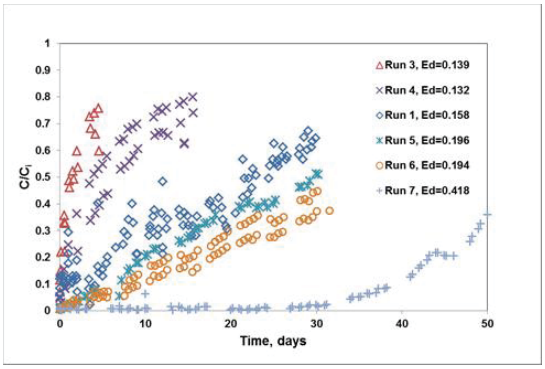

Figure 1: Fixed bed performance based on treatment time

Summary and Conclusions

Test results show that very good removal of P is possible using fixed bed columns packed with iron oxyhydroxide media. Conversion of test parameters into dimensionless forms enables prediction of the shape of the breakthrough curve based on the value of the surface diffusion modulus *Ed*. Preliminary batch tests with arsenic suggest that similar results may be possible for other metalloids as well, including arsenic and selenium.

[1] Sibrell *et al.* (2009) *Water Research*, **43(8)**, 2240-2250. [2] Mertz, K. A., *et al.* (1999) *Manual: Adsorption Design Software for Windows*, available at http://cpas.mtu.edu/etdot/

Zircon U–Pb, O and Hf isotope characteristics of granites emplaced during Cretaceous wrench to transtension in West Antarctica

CHRISTINE S. SIDDOWAY[1*], C. YAKYMCHUK[2], C. MARK FANNING[3], AND MICHAEL BROWN[2]

[1] Geology Dept., Colorado College, Colorado Springs, CO 80903, USA, csiddoway@coloradocollege.edu (*presenting author)

[2]Laboratory for Crustal Petrology, Department of Geology, University of Maryland, College Park, MD 20742, USA

[3]Research School of Earth Sciences, The Australian National University, Mills Road, Canberra, ACT 0200, Australia

The Fosdick Mountains in West Antarctica expose a migmatitic gneiss dome emplaced within a wrench setting during the Cretaceous dextral oblique convergence along the East Gondwana margin that affected both West Antarctica and once-contiguous New Zealand. Kilometer-scale, three-dimensional outcrop offers expansive views of a region of formerly melt-rich middle crust that responded to changes in strain during sequential wrench, transtension and oblique detachment [1]. Consistent with temperatures >800°C attained during metamorphism [2, 3], there is pervasive evidence for the prior presence of melt across a range of scales, including granite within foliation-parallel sheets and interboudin partitions, magmatic folds, and conjugate magmatic shear bands. Microstructures include euhedral to subhedral phases bordered by thin, delicate residual melt pseudomorph structures in interstices and on grain boundaries.

Based on SHRIMP U-Pb zircon and monazite geochronology for anatectic granites and residual migmatites, crustal melting, and melt transfer and accumulation occurred from c. 130 to 96 Ma, with the possibility that these processes were underway as early as c. 140 Ma [1, 3]. This previous work has revealed three phases of anatectic granite that occupy distinct structural settings. To evaluate whether there are distinctions in source for these three generations of granite, a Lu–Hf and O isotope study of previously dated zircon grains from 8 granite samples was undertaken. Taken together, zircons from Cretaceous granites show a comparatively large spread in εHf(t), with values from -14 to +5, and a wide range of $\delta^{18}O$ values between 6‰ and 14‰. In zircon of c. 120–99 Ma age, there is a trend toward higher $\delta^{18}O$ with greater homogeneity of zircon populations. An exception is one of the youngest granites, which has lower $\delta^{18}O$ values of 6.4 to 7.8. The isotopic characteristics of zircon from the three granite phases change with time. Zircon in c. 117–114 Ma granites, emplaced in steep foliation-parallel panels during *wrench* tectonics, has a wide range of $\delta^{18}O$ values from 6.2 to 11.6, reflecting a low degree of homogeneity of the zircon populations. Zircon in leucogranites that occur in subhorizontal sheets emplaced during *transtension* at c. 107–102 Ma, have elevated $\delta^{18}O$ values and more enriched εHf(t), attributed to a greater contribution of metasedimentary rocks in the source. Finally, zircon of c. 102 Ma age from a *detachment*-hosted granite records input from a source with more juvenile εHf(t) and $\delta^{18}O$, which may mark the availability of a less-evolved, mantle-like source due to lithosphere thinning.

[1] McFadden et al. (2010) Tectonics, 29, TC4022.
[2] Yakymchuk (2012) this volume.
[3] Korhonen et al. (2012) J Metamorphic Geology, Early View.

Stable isotope geochemistry of the Varuträsk rare-element pegmatite (northern Sweden)

KARIN SIEGEL[1*], THOMAS WAGNER[2], ROBERT TRUMBULL[3], ERIK JONSSON[4], CHRISTOPH A. HEINRICH[2]

[1]McGill University, Earth and Planetary Sciences, Montreal, Canada, karin.siegel@mail.mcgill.ca (* presenting author)
[2]ETH Zurich, Institute of Geochemistry and Petrology, Zurich, Switzerland, thomas.wagner@erdw.ethz.ch, heinrich@erdw.ethz.ch
[3]GFZ Potsdam, Inorganic and Isotope Geochemistry, Potsdam, Germany, bobby@gfz-potsdam.de
[4]Swedish Geological Survey, Mineral Resources, Uppsala, Sweden, erik.jonsson@sgu.se

The Varuträsk pegmatite, located in the Skellefte district in northern Sweden, is a classical representative of highly fractionated LCT-type rare-element pegmatites [1,2]. The Varuträsk pegmatite shows a typical primary zonation pattern, composed of well-developed border, wall and intermediate zones and a quartz core [3]. Major rare-element enrichment is mainly related to late-stage assemblages such as albite-lepidolite and pollucite units. Previous work [4] has focused on the major and trace element characteristics of key minerals (feldspars, micas, tourmaline, columbite-tantalite), demonstrating progressive magmatic fractionation trends in the primary pegmatite zones. Significant compositional changes observed in the late-stage mineral assemblages (reversals of magmatic fractionation trends, depletion in elements typically enriched in aqueous fluids) indicate that a magmatic fluid exsolved after the development of the primary pegmatite zonation.

The results of the present stable isotope (B, H, O) study further constrain the role of a magmatic fluid phase in formation of rare-element enrichment. Stable isotope analysis (O, H, B) has been performed on quartz, mica and tourmaline from all principal mineral assemblages in the pegmatite body. Boron isotope data of tourmalines using SIMS microanalysis are in the range between –14.6 and –6.2 ‰. The $\delta^{11}B$ data of different tourmaline types conforming to the primary pegmatite zonation show a clear magmatic fractionation trend. By contrast, tourmalines related to late-stage assemblages show a reversed fractionation that is correlated with the behavior shown by several major and minor elements in the tourmaline (Na, Fe, Mn, F). The B isotope evolution cannot be modeled by purely magmatic melt-tourmaline fractionation, but requires fluid-tourmaline partitioning to be operative for the late-stage assemblages. Hydrogen isotope data of micas indicate a substantial increase in δD from –76 to –53 ‰ from the wall to the innermost zones, requiring closed-system fractionation processes that involved melt and fluid. Taken together, the stable isotope data demonstrate that rare-element enrichment in the most fractionated assemblages is related to the transition from purely magmatic crystallization to conditions where a magmatic fluid phase was important.

[1] Cerny, P. 1991: Rare-element Granitic Pegmatites. Part I: Anatomy and internal evolution of pegmatite deposits. Geosci. Canada, 18, 49-67 [2] Cerny, P., Ercit, T.S. 2005: The classification of granitic pegmatites revisited. Can. Mineral., 43, 2005-2026 [3] Quensel, P. 1952: The Paragenesis of the Varuträsk Pegmatite. Geol. Mag., 89, 49-60 [4] Matalin, G., Wagner, T., Jonsson, E., Wälle, M., Heinrich, C.A., 2012. Evolution of the Varuträsk LCT-type rare-element pegmatite (N Sweden): mineral chemistry constraints. Contrib. Mineral. Petrol. (submitted)

Deep ocean mixing, the bipolar seesaw, and polar ocean biogeochemical change

D.M. SIGMAN [1*], A.S. STUDER[2], M. TREMBLAY[3], M. STRAUB[2], M.P. HAIN[1], G.H. HAUG[2]

[1]Department of Geosciences, Princeton University, Princeton, USA (*sigman@princeton.edu, mhain@princeton.edu)
[2]Department of Earth Sciences, ETH Zurich, Zurich, Switzerland (anja.studer@erdw.ethz.ch, marietta.straub@erdw.ethz.ch, gerald.haug@erdw.ethz.ch)
[3]Barnard College, New York, USA (mmt2130@barnard.edu)

At the scale of the global ocean, deep water formation is coupled to processes – most notably, vertical mixing and wind-driven upwelling – that reduce the density of deep water or otherwise remove dense water from the deep ocean. This formation/removal coupling may play a critical role in glacial/interglacial changes in polar ocean circulation and in atmospheric carbon dioxide. Considering the two regions of modern deep water formation, the North Atlantic and the Antarctic, if deep water formation ceases in one region but the loss of dense deep water does not decrease equivalently, then the other polar region must increase its deep water formation rate. This is one proposed physical mechanism behind the observed "bipolar seesaw" in high latitude temperatures on millennial time scales. Since deep water formation in the North Atlantic and the Antarctic have opposite effects on the efficiency of the global biological pump, any tendency for anti-correlation in their rates has a major effect on atmospheric CO_2. Accordingly, there is intense focus on an ocean seesaw mechanism for the CO_2 rises at the end of ice ages. However, there are divergent views as to the importance of deep ocean mixing *versus* the winds in driving such a North Atlantic/Antarctic seesaw. If the biogeochemical conditions of the polar ocean surface can be reconstructed back through time, we will have greater insight into how the polar regions have changed in their ventilation of the ocean interior and their impact on deep ocean carbon storage. In this talk, in addition to drawing upon numerical model experiments to lay out the arguments above, we will describe new diatom- and foraminifera-bound nitrogen isotope data from the Antarctic and the North Atlantic that support the view of seesaw-like behaviour between the two regions over major glacial/interglacial transitions and on millennial time scales. In this context, we will revisit the question of deep mixing *versus* the winds as driving this pattern.

Characterizing vadose zone hydrocarbon biodegradation using CO_2 effluxes, isotopes, and reactive transport modeling

NATASHA J. SIHOTA[1] AND K. ULRICH MAYER[1]*

[1]University of British Columbia, Department of Earth and Ocean Sciences, Vancouver, Canada, nsihota@eos.ubc.ca , umayer@eos.ubc.ca (* presenting author)

Introduction

Biodegradation in the vadose zone may result in substantial mass removal at hydrocarbon spill sites. At these sites, estimates of contaminant loss rates are needed to evaluate source zone longevity and long-term impact on the environment. Recently, Sihota et al. [1] showed that the measurement of CO_2 effluxes at the ground surface is a suitable method to derive depth-integrated rates of contaminant degradation. However, the accuracy of loss rate estimates obtained from CO_2 effluxes is limited by the ability to quantitatively separate CO_2 effluxes from contaminant destruction and naturally occuring soil respiration. To address this gap, measured CO_2 effluxes were complemented with detailed analysis of vadose zone gas composition, including stable and radioisotope analysis in CO_2. Results of field measurements were integrated using the reactive transport code MIN3P-DUSTY [2], which accounts for advective and multicomponent diffusive gas transport.

Results and Conclusions

Comparison of measured pore gas distributions to previous observations at the Bemijdi site [3] show biodegradation has approached a quasi steady state within the vadose zone. Radiocarbon results prove that, in the source zone, the majority of CO_2 is produced from contaminant destruction and indicate that the CO_2 efflux method provides an adequate estimate of contaminant mass loss rates.

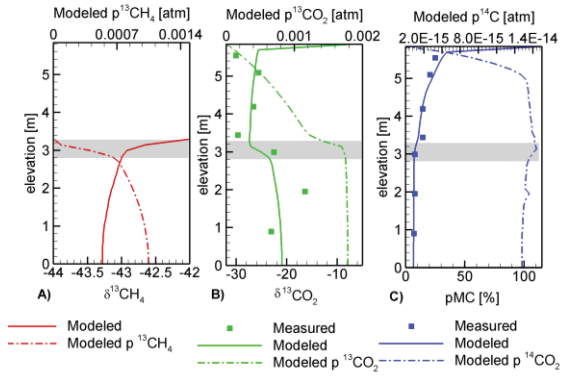

Figure 1: Comparison of measured and simulated isotopic values for a 1D vertical profile in the vadose zone at the Bemidji site.

Highly constrained simulations for a 1D vertical profile in the source zone are able to closely reproduce historical saturations, field observed fluxes, concentration profiles, and isotopic signatures. Simulation results also showcase that gas transport is diffusion-dominated and strongly affects measured isotopic signatures, in addition to effects caused by biogeochemical reactions.

[1] Sihota, Singurindy & Mayer (2011) *Environ. Sci. Tech.* **45**, 482-488. [2] Molins & Mayer (2007) *Water Resour. Res.* **43**, W05435. [6] Molins *et al.* (2010) *J. Contam. Hydrol.* **112**, 15-29.

Hand-held XRF in exploration for REE–bearing phosphate deposits.

GEORGE J. SIMANDL[1]*; SUZANNE PARADIS[2], ROBERT FAJBER[3], AND KEITH GRATTAN[4]

[1]British Columbia Geological Survey, Victoria, Canada, george.simandl@gov.bc.ca (*presenting author)
[2]Natural Resources Canada, Sidney, BC, Canada
[3]University of Victoria, Victoria, Canada
[4]Elemental Controls Limited, Mississauga, Canada

Sedimentary phosphate deposits consist of francolite [$(Ca_5(PO_4)_3(OH,F,Cl)$] and gangue minerals. They supply most of the phosphate raw materials used by the phosphate fertilizer industry and they are also considered as potential sources of F, REE, and/or U. Samples of phosphate rocks from the Fernie Formation (British Columbia) were analysed using a hand-held XRF analyser (HhXRF) and by lithium metaborate fusion–inductively coupled plasma (LMB-ICPMS) method. The results from both methods were compared; and correction factors for the HhXRF analyser were developed. HhXRFs can be used in exploration for phosphate deposits by analyzing samples directly for phosphorus (P) and if correction factors are applied for vectoring towards REE-rich zones, and/or delineating zones with high levels of deleterious elements such as U, Th, Cr, As, Hg, Cd and Se. Figures 1 illustrates two examples of relationships between hhXRF and LMB-ICPMS methods. Following a successful orientation survey, HhXRF does become fast and reliable vectoring tool that is easily incorporated into integrated exploration programs.

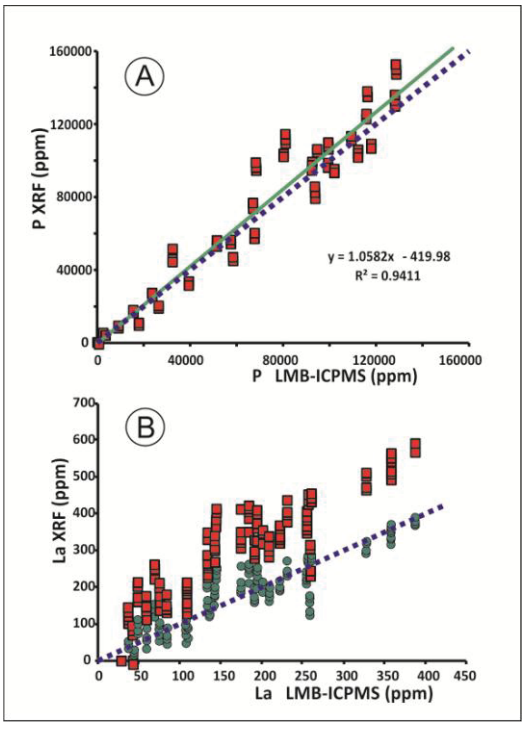

Figures 1: Comparison of the HhXRF and LMB-ICPMS for P (A) and La (B). Raw data as red squares. Corrected values as green circles. No correction was required for P.

Using Melt Inclusions to Constrain Magma Evolution and Pre-eruptive Plumbing System Architecture of Mutnovsky Volcano, Russia

SIMON, A. [1*], ROBERTSON, K. [1], PETTKE, T. [2], SMITH, E. [1], KIRYUKHIN, A. [3], SELYANGIN, O. [3], MULCAHY, S. [4], WALKER, J. [5]

[1]University of Nevada Las Vegas (UNLV), Las Vegas, NV, U.S.A., adam.simon@unlv.edu
[2]University of Bern, Bern Switzerland
[3]Institute of Volcanology and Seismology, Petropavlovsk-Kamchatsky, Russian Federation
[4]University of California Berkeley, Berkeley, California, U.S.A.,
[5]Universityof Kansas, Lawrence, Kansas, U.S.A.

Melt inclusions provide much more detailed samples of melt compositions than can be accessed with whole rock analyses alone. As such, melt inclusions have become an increasingly powerful tool for improving our understanding of magmatic processes owing to their ability to record discrete time steps during the polybaric and polythermal evolution of a particular magmatic system. In this study, we report and discuss melt inclusion data for samples from Mutnovsky Volcano, located on the Kamchatka island arc, that elucidate the causes for compositional diversity, and the iterative assembly of the pre-eruptive subvolcanic magma chamber.

Mutnovsky has formed a series of four stratocones over its ~100 ka history. Erupted rocks are dominantly basalt and basaltic andesite, and also include andesite, dacite and rhyodacite. We analyzed melt inclusions from all erupted compositions and eruptive centers to investigate the causes of the compositional heterogeneity, melt evolution, and pre-eruptive magma storage system. Melt inclusion compositions range from low silica (44 wt. %), hosted in olivine and clinopyroxene and plagioclase, to high silica (78 wt. %), hosted mainly in plagioclase and orthopyroxene. The melt inclusion compositions span a wider range than whole rocks. Geochemical modeling of the melt inclusion data, combined with field evidence and plagioclase phenocryst zoning, indicate that fractional crystallization and magma mixing operated in tandem to produce compositional diversity of the rocks erupted at Mutnovsky. The data are consistent with a model wherein fractional crystallization of individual aliquots of magma in an evolved subvolcanic magma chamber drove the melt(s) toward more felsic bulk compositions. Textural and compositional evidence also indicate that the subvolcanic magma chamber was effected by periodic injection and admixture of new olivine- ± clinopyroxene-saturated basaltic magma. This finding is consistent with observations from other volcanic systems.

The new twist that we employed was to calculate apparent pressures and temperatures of entrapment of orthopyroxene- and clinopyroxene-hosted melt inclusions by using the chemistry of melt inclusions and host mineral with the mineral-liquid thermobarometry equations from [1,2]. The results suggest that orthopyroxene and clinopyroxene crystallized at distinctly different levels in the magma plumbing system, which allows us to assess the variation in melt compositions as a function of vertical position in the evolving magma plumbing system. We will discuss these results, and the role that post-entrapment modification of melt inclusions may have on the model thermobarometry results, in the context of the iterative assembly and evolution of crustal magma chambers.

[1] Putirka et al. (2003) *American Mineralogist* **88**, 1542-1554. [2] Putirka (2008) *Reviews in Mineralogy and Geochemistry* **69**, 61-120.

Magnetic, mineralogical and geochemical (μXRF) properties of a central Baffin Bay sedimentary sequence spanning the last 100 ka

QUENTIN SIMON[1,*], GUILLAUME ST-ONGE[1,2], CLAUDE HILLAIRE-MARCEL[1], PIERRE FRANCUS[1,3]

[1]GEOTOP-UQAM, Montréal, Qc, Canada,
[2]Canada Research Chair in Marine Geology, ISMER-UQAR, Rimouski, Qc, Canada,
[3]INRS-ETE, Québec, Qc, Canada,
*quentin.simon@gmx.com

A terrigenous sedimentary sequence from central Baffin Bay (core HU2008-029-016PC – 70°46.14'N/-64°65.77W – 2063 m) was analyzed for its magnetic, mineralogical and geochemical (μXRF - Itrax) properties in order to 1) link the sedimentary history to ice-margin dynamics along the surrounding coastlines (W. Greenland, E. Baffin Island and N.E. Ellesmere Island), and 2) eventually associate the continental ice dynamics to specific climate events of the last glacial cycle. A chronology based on relative paleointensity (RPI) and paleomagnetic secular variation (PSV) has been set. It provides an age model for a site where current chronological approaches (^{14}C and isotope stratigraphy) failed for various reasons. This age-model indicates a mean sedimentation rate of ~6.5 cm/ka, but also illustrates increases (> 15 cm/ka) linked to major sedimentological events of local origin. The timing and properties of these sedimentological events are discussed with special emphasis on their source and mode of deposition, as well as their linkage with specific ice margin responses to climate changes along surrounding islands. On one hand, coarse-grained and rapidly-deposited detrital carbonate-rich layers seem broadly coeval with major interstadials of the GISP2 ice core record. This suggests fast retreat episodes along related ice-stream routes during major interstadials. Rock magnetic data point to coarser magnetic grain size in these layers. This is especially the case during the 11– 12 ka (~YD) and 14.8–16 ka (H1) intervals. On the other hand, feldspar-rich layers also depicting high clay and silt size material contents are characterized by a finer magnetic grain size in the pseudo single domain to single domain ranges. Magnetic grain size ratios such as k_{ARM}/k_{LF} and Fe/k_{LF} show finer magnetic grains during the locally extendedLast Glacial Maximum interval (16 – 24 cal ka BP). This suggests that, during glacial maxima, mechanical grinding of the bedrock by surrounding ice sheets (in particular along the continental shelves of Greenland and Baffin Island) released large amounts of "glacial flour" characterized by feldspar-rich and finer magnetic supplies.

An account of the Chernobyl Pilot Site studies: 25 years later

CAROLINE SIMONUCCI[1*], ARNAUD MARTIN-GARIN[2], NATHALIE VAN MEIR[1,3], PIERRE DICK[1], OLIVIER DIEZ[4], CELINE ROUX[1,5], DMITRI BUGAI[6] AND VALERIY KASHPAROV[7]

[1]IRSN, SRTG/LETIS, caroline.simonucci@irsn.fr (* presenting author), pierre.dick@irsn.fr
[2]IRSN, SERIS/L2BT, arnaud.martin-garin@irsn.fr
[3]IG-BAS, Geosciences, nathalie.vanmeir@irsn.fr
[4]IRSN, SRTG/LAME, olivier.diez@irsn.fr
[5]UMR 7330, Geosciences, celine.roux.1@etu.univ-cezanne.fr
[6]IGS, Geosciences, dmitri.bugay@gmail.com
[7]UIAR/NUBiP, Geosciences, vak@uiar.org.ua

Introduction

25 years have passed since the accident at the Chernobyl NPP, but up to now scientists are still working on answering the question "what are the consequences of the accident?", and in particular, can we define radionuclide (RN) migration processes today and for the future in soils, vegetation and possibly air re-suspension?. Following the Chernobyl accident (26/04/1986), the contaminated topsoil layers containing fuel particles and contaminated organic matter, coming from the Red forest, were buried in trenches only a few meters deep in the Chernobyl exclusion zone in order to prevent RN dispersion and especially to diminish the exposure dose to workers (liquidators) on site in 1987. Since 1999, the French Institute of Radioprotection and Nuclear Safety (IRSN), in collaboration with the Ukrainian Institute of Agricultural Radiology (UIAR/NUBiP) and the Ukrainian Institute of GeoSciences (IGS), has been studying the impact of the contaminated waste trench T-22, located 2.5 km South-West from Chernobyl NPP, on the aquifers below. The Chernobyl Pilot Site (CPS), which includes the trench T-22, was equipped to carry out in situ radioecological and hydrogeological investigations. The objectives of the research are devoted to the characterization of RN migration both upward into the vegetation and downward to the aquifer, in order to validate RN's transfer models in the environment.

Results and Conclusion

To this end, flow and transport mechanisms were first decoupled. Water flow only studies are still carried out in the different soil layers and in the aquifer. Soil –RN interactions are still studied first in the laboratory (especially for Cs-137 and Sr-90) and analogues were/are also studied on the field. In a second step, these processes were re-coupled by calculating, the reactive transport of RN both at the laboratory scale, under well controlled conditions, and in the CPS where the Sr-90 migration's plume is surveyed for 20 years. In connection to the dynamic of RN migration, our studies also addressed: (i) the nature of the waste material in order to better estimate the amount of the RN stock and its release properties over time; (ii) the possible evidence of enhanced transport down to the aquifer and in the saturated zone due to specific and stable aqueous species of RN and/or to the presence of colloidal substances, and (iii) the upward migration of RN due to the root system of the plants that grow mainly over the trench as such export fluxes from the trench probably constitute one of the main hazards for the near future. The future investigation at CPS and extended to the larger Chernobyl Exclusion Zone include a better understanding of the joint biogeochemical, radioecological and hydrological processes.

Local structure and crystallization pathways of amorphous calcium carbonate

JARED WESLEY SINGER[1]*, A. ÖZGÜR YAZAYDIN[2,3], GEOFFREY M. BOWERS[1,4], AND R. JAMES KIRKPATRICK[5]

[1] Department of Material Science and Engineering, New York State College of Ceramics at Alfred University, Alfred, New York, USA, jws4@alfred.edu (* presenting author)
[2] Department of Chemical Engineering, University of Surrey, Guildford, UK, a.yazaydin@surrey.ac.uk
[3]Department of Chemistry, Michigan State University, East Lansing, Michigan, USA, yazaydin@msu.edu
[4]Division of Chemistry, College of Liberal Arts & Sciences, Alfred University, Alfred, New York, USA, Bowers@alfred.edu
[5]College of Natural Science, Michigan State University, East Lansing, Michigan, USA, rjkirk@cns.msu.edu

We compare local structures of synthetic amorphous calcium carbonate (ACC) by ^{43}Ca- and ^{25}Mg-nuclear magnetic resonance (NMR) to long-range order by low-angle and conventional x-ray diffraction and to characterization by thermal gravimetric analysis, scanning electron microscopy, and energy dispersive spectroscopy. The range of parent solution compositions, temperatures, and $Na_2CO_{3(s)}$ induced precipitation yields ACC compositions of 10-40 weight percent water and 0-50% Mg. Subsequent crystallization can yield all anhydrous and hydrous polymorphs of $CaCO_3$, mixed assemblages, and dolomite. In spite of this variability, the ^{43}Ca NMR spectra of ACC collected immediately after synthesis consist of broad, featureless resonances with Gaussian line shapes (mean chemical shift = -0.4±0.5ppm, FWHH = 27.6±1ppm) that do not depend on Mg^{2+} or H_2O content. We derive indistinguishable maximum mean Ca-O bond distances of 2.45 Å for all samples and our analysis suggest that spectral widths are dominated by chemical shift dispersion that arises from local disorder. Preliminary ^{25}Mg-NMR suggests the presence of rigid and mobile ^{25}Mg populations. [Mg] of the parent solution correlates with ACC stability, though our data suggest Mg^{2+} incorporation in the solid phase is not responsible for the observed stabilization. Within experimental ranges we also observe ACC mesocrystallization, ikaite ($CaCO_3 \bullet 6H_2O$) decomposition to monohydrocalcite ($CaCO_3 \bullet H_2O$), and low-temperature proto-dolomite.

Extracellular *c*-Type Cytochromes from *Geobacter bemidjiensis*

CINDY J. CASTELLE[1], KELLY C. WRIGHTON[2], MICHAEL J. WILKINS[3], MARY S. LIPTON[3], JILLIAN F. BANFIELD[2], STEVEN W. SINGER[1*]

[1]Lawrence Berkeley National Laboratory, Berkeley, CA, USA; SWSinger@lbl.gov
[2]University of California-Berkeley, Berkeley, CA, USA
[3]Pacific Northwest National Laboratory, Richland, WA, USA

The subsurface clade 1 of the *Geobacteraceae* often predominates during acetate-stimulated bioremediation of uranium-contaminated sites. The metabolic activity of this clade has been linked to solid phase U(VI) and Fe(III) reduction in the subsurface. Despite its importance for subsurface metal reduction, the complement of electron transfer proteins expressed by members of this clade have not been identified. *Geobacter bemidjiensis* is a cultured representative of subsurface clade 1 and is an excellent model system to begin to understand electron transfer in the subsurface *Geobacteracae* clade 1. Inspection of the genome of *G. bemidjiensis* identified 84 proteins predicted to encode for *c*-type cytochromes. To identify the dominant *c*-type cytochromes expressed by *G. bemidjiensis*, proteomics was performed on cultures grown with fumarate as an electron acceptor. A substantial fraction of *c*-type cytochromes were localized in the extracellular medium or were easily sheared from the outer-membrane. The most abundant of these *c*-type cytochromes was a flavocytochrome that clustered with fumarate reductases from *Shewanella* species. Other abundant *c*-type cytochromes included a homolog of OmcB, a cytochrome required for optimal reduction of Fe(III) oxides in *G. sulfurreducens*, and a nonaheme cytochrome whose only homologs were found in *Geobacter* species from subsurface clade 1. Seven expressed *c*-type cytochromes were predicted to have >25 heme prosethetic groups. Peptides from the abundant *G. bemidjiensis* cytochromes were also found in proteomic measurements of groundwater from a uranium-contaminated site at Rifle, CO undergoing acetate stimulation. The extracellular *c*-type cytochromes are distinct from those cytochromes identifed for *G. sulfurreducens* and suggest that the *Geobacteraceae* from subsurface clade 1 may possess novel pathways for electron transfer.

Dissolution of uranyl precipitates in contaminated vadose zone sediments

ABHAS SINGH[1*], JOHN M. ZACHARA[1], JAMES P. MCKINLEY[1], CHONGXUAN LIU[1], MAXIM I. BOYANOV[2], KENNETH M. KEMNER[2], DEAN A. MOORE[1]

[1]Pacific Northwest National Laboratory, Richland, WA 99354 USA; abhas.singh@pnnl.gov (* presenting author), john.zachara@pnnl.gov, james.mckinley@pnnl.gov, chongxuan.liu@pnnl.gov, damoore@pnnl.gov
[2]Argonne National Laboratory, Argonne, IL 60439 USA; mboyanov@anl.gov, kemner@anl.gov

Metatorbernite, $Cu(UO_2PO_4)_2 \cdot 8H_2O_{(s)}$, was idenified as the dominant form of uranium in contaminated sediments below former nuclear waste disposal ponds in the Hanford 300-Area (Washington State) in past microscopic and synchrotron-based spectroscopic and diffraction studies [1-3]. Uranium(VI) release from these sediments to groundwater, however, could not be explained by metatorbernite solubility determined from pure mineral studies at acidic conditions [4]. This work aims to reconcile these differences between known solid-phase speciation and the aqueous phase composition generated. Carbonate and synthetic groundwater extractions on metatorbernite and variable sediment:solution ratios and sediment sizes were peformed in different experimental settings (e.g., batch, stir-flow) to quantify uranium(VI) release. Solid phase speciation before and after these extractions was investigated using scanning and transmission electron microscopy, micro X-ray diffraction and X-ray absorption techniques.

Preliminary results indicate that metatorbernite dissolution in synthetic groundwater is slow and is facilitated by secondary precipitation of an unidentified copper phase that limits the dissolved copper concentration (Figure 1). Metatorbernite in sediments may be gradually tranforming to a uranyl carbonate phase as indicated by X-ray absorption spectroscopy. These results will be combined with other solid-phase characterization results and interpreted within a reaction-based modeling framework including dissolution-precipitation and aqueous speciation reactions.

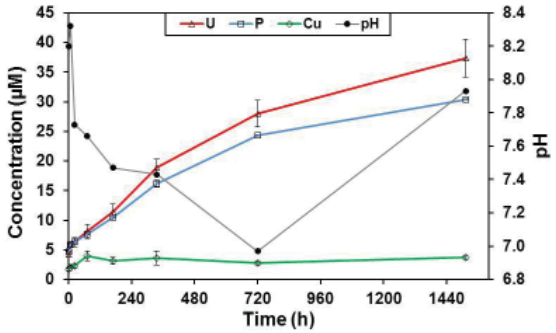

Figure 1: Measured dissolved concentrations and pH from metatorbernite dissolution in synthetic groundwater.

[1] Catalano et al. (2006) *Environmental Science & Technology* **40**, 2517-2524. [2] Arai et al. (2007) *Environmental Science & Technology* **41**, 4633-4639. [3] Stubbs et al. (2009) *Geochimica Et Cosmochimica Acta* **73**, 1563-1576. [4] Ilton et al. (2010) *Environmental Science & Technology* **44**, 7521-7526.

Distribution of dissolved neodymium and ε_{Nd} in the Bay of Bengal

SATINDER PAL SINGH[1] AND SUNIL KUMAR SINGH[2*]

[1]Physical Research Laboartory, Ahmedabad, India, satinder@prl.res.in
[2]Physical Research Laboartory, Ahmedabad, India, sunil@prl.res.in (* presenting author)

The concentrations and isotope composition of dissolved Nd have been measured in the water column along 87°E transect in the Bay of Bengal to investigate the impact of water mass mixing and desorption of Nd from particulates in determining their distribution in the Bay. The concentration of Nd in surface waters of the BoB shows a North-South decreasing trend (~ 46 to ~ 22 pmol/kg) with increasing salinity, whereas its depth profiles typically show a high value in surface waters, a minimum (~ 15 to ~ 23 pmol/kg) in shallow subsurface (~ 50-200 m) followed by a gradual increase with depth. The Nd concentration of the BoB waters is generally higher than that at corresponding depth in nearby oceanic basins. The ε_{Nd} of the northern BoB waters ~ -15 ± 1 overlaps with that of dissolved and particulate phases of the Ganga-Brahmaputra (G-B) Rivers, but less radiogenic than those reported for other regions of global oceans, except the Baffin Bay and the North Atlantic Subpolar Gyre. The abundance and distribution of dissolved Nd and its unradiogenic isotope composition suggests that the dominant source of Nd in the BoB is the dissolved and/or particulate phase of the G-B river system.

The ε_{Nd} values in the BoB show greater variation in the upper water column with more radiogenic values ~ -8 in surface waters of the southernmost profile (~ 6°N), which decreases to -15 in the northernmost profile (~ 20°N). This latitudinal trend is most likely a result of the variation in mixing proportion between the Indonesian Throughflow surface waters (IW) and the G-B river water. Inverse model calculations suggest that excess Nd of the order of ~1 to 65 % of measured Nd concentration is required from other source(s) in addition to various water masses. The calculations also show that ε_{Nd} of the additional source(s) has to be in the range of ~ -16 ± 2, typical of G-B river sediments. These observations coupled with the North-South distribution of dissolved Nd and ε_{Nd} indicate that this additional source is release from particulate phases supplied by the G-B river system and the continental margin sediments. This study underscores the significant role of dissolved/particulate Nd from the Ganga-Brhamputra river system in contributing to the dissolved Nd budget of the global ocean.

LA-MC-ICPMS iron isotopic measurements of zoned olivine

C.K. SIO [1*], N. DAUPHAS[1], F.Z. TENG[2], M. CHAUSSIDON[3], R.T. HELZ[4], M. ROSKOSZ[5], Y. XIAO[6], AND T. IRELAND[1]

[1] Origins Lab, Dept. of the Geophysical Sciences, the University of Chicago, USA, ksio@uchicago.edu (* presenting author)
[2]Dept. of Geosciences, the University of Arkansas, USA
[3]CRPG-CNRS, Vandoeuvre lès Nancy, France
[4]United States Geological Survey, Reston, VA, USA
[5]UMET, Université de Lille 1, France
[6]Institute of Geology and Geophysics, Chinese Academy of Sciences

Previous studies have revealed that iron and magnesium isotopes may be used to identify diffusion-driven zoning in olivine crystals [1-3]. In magmatic systems, Mg-rich olivine is an early crystallizing phase. As the melt evolves, it becomes more Fe-rich, so that in reaching equilibrium, Fe diffuses into and Mg diffuses out of the initial olivine crystal. Because light isotopes diffuse faster than heavy isotopes [4-5], such diffusion-driven mechanism is accompanied with 1) a negative correlation of Fe and Mg isotopes, and 2) a negative correlation of Fe isotopes and a postive correlation of Mg isotopes with Fo#. Teng et al. [1] showed these correlations in olivine fragments from Kilauea Iki lava lake. Sio et al. [3] used microdrilling techniques to spatially resolve the same correlations in a single olivine crystal.

Many zoned olivine crystals are smaller than or comparable to the size of a drill bit (300 μm used in [3]). Hence, it is imperative to develop *in-situ* techniques that provide better spatial resolution. Using a UP193HE laser, we conducted LA-MC-ICPMS iron isotopic measurements on the same sample analyzed in [3]. The spot sizes used in the sessions were 40-55 μm, an improvement of lateral and depth spatial resolution by approximately an order of magnitude relative to microdrilling. Smaller spot sizes may be used if ^{57}Fe is not analyzed.

Numerous tests were conducted to evaluate sample mount orientation and matrix effects. These tests suggest that the orientation effect must be carefully evaluated in order to obtain accurate data and true errors, which can be three times greater than the error taken only from measured isotopic variations on a single crystal. The typical precision is 0.2 ‰ (1 SD) based on repeat analyses of the same profile. The final iron isotopic profile agrees with the microdrilling results, with the rim at δ^{56}Fe -0.2 ‰ and the core at -1.2 ‰. A plot of δ^{56}Fe versus Fo# is also in perfect agreement with microdrilling data.

LA-MC-ICPMS provides the means to measure iron isotopic compositions with high spatial resolution in olivines. Such techniques can be employed on zoned crystals to better understand their crystallization and cooling histories. Our work establishes LA-ICPMS Fe isotopic analyses as a powerful tool of petrology in the study of igneous zoned minerals.

[1] Teng *et al.* (2011) *EPSL* **308**, 317-324. [2] Dauphas *et al.* (2010) *Geochim. Cosmochim. Acta* **74**, 3274-3291. [3] Sio *et al.* (2011) Goldschmidt Abstract 1884. [4] Richter *et al.* (2009) Geochim. Cosmochim. Acta **73**, 4250-4263. [5] Roskosz *et al.* (2010) Goldschmidt Abstract A882.

Effects of water on the nucleation of Li-rich granitic melts

MONA-LIZA C. SIRBESCU[1*], MAX WILKE[2], ILYA VEKSLER[2], AND ALAN G. WHITTINGTON[3]

[1]Central Michigan University, Earth and Atmospheric Sciences, Mt. Pleasant, MI, USA, sirbe1mc@cmich.edu (* presenting author)
[2]Deutsches GeoForschungsZentrum, Potsdam, Germany
[3] University of Missouri, Geological Sciences, Columbia, MO, USA

The amount of dissolved water controls the nucleation and crystallization of granitic melts by lowering their liquidus and glass transition temperature, their free energy relative to crystals, and viscosity. Although pegmatites and rhyolites are similarly affected by undercooling and cooling rate, they are at the opposite ends of the spectrum of igneous texture because pegmatite melts have incorporated and retained H_2O whereas rhyolites have lost H_2O [1].

Sixty nucleation-crystallization experiments on Li-B-haplogranite-H_2O compositions confirm that igneous texture is strongly controlled by the concentration of water. Time-series, isothermal runs (from 1 to 30 days) were performed at temperatures ranging from 400 to 700°C at 300 MPa, coresponding to variable degrees of undercooling between liquidus and glass transition. H_2O contents ranged from 2.6 to 8.3%, and kept below fluid saturation. Although metastable, mineral assemblages are reproducible. Viscosity data collected via the parallel-plate method indicate that the glass transition of both melts containing 6.5 % H_2O is just under 300°C, indicating that nucleation and crystallization took place in a liquid not in glass.

Clearly, H_2O concentration influences the time of incubation, nucleation densities, and crystal growth rates, but the effects are a nonlinear function of dissolved H_2O. For example, at 600°, nucleation delays are >5 days for a concentration of 8.3 % H_2O, decrease to a minimum of only one day for 6.5 % H_2O, and increase again to 2.5 days at 3.0 % H_2O. Growth and nucleation rates follow a similar parabolic behavior, as a consequence of the double role played by H_2O. On one hand, H_2O stimulates development of large crystals because of increased diffusion rate. On the other hand, H_2O decreases the liquidus temperature of the melt, therefore reducing the value of effective undercooling, which has the opposite effect of slowing down crystal growth. A "Goldilocks" behavior rules the development of pegmatite texture including large, skeletal crystals, graphic intergrowth, and low nucleation density. Ultimately, the value of effective undercooling has to be "just right".

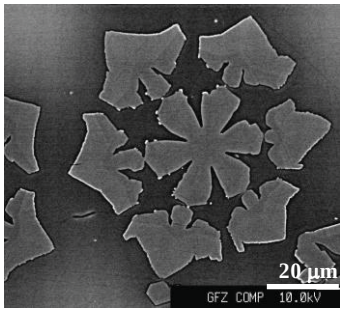

Figure 1: Skeletal "stuffed" beta-quartz produced in 30-day long run, at 500°C, in a haplogranitic melt with 3.0% (g/g) H_2O, 1% Li_2O, and 2.3 % B_2O_3

[1] Nabelek et al. (2010) *Contrib. Min. Pet.* **160**, 313-325.

Feedback effects of clay minerals formation on the kinetics and mechanisms of olivine carbonation within tholeiitic basalt

OLIVIER SISSMANN[1,2*], DAMIEN DAVAL[3], ISABELLE MARTINEZ[1], FABRICE BRUNET [4], ANNE VERLAGUET [5] , YVES PINQUIER [2], FRANÇOIS GUYOT [1,6]

[1]IPGP - CNRS UMR 7154, Université Paris Diderot, Paris, France
*sissmann@ipgp.fr
[2] Laboratoire de Geologie - CNRS UMR 8538, ENS, Paris, France
[3] LHyGeS - CNRS UMR 7517, Strasbourg, France
[4] ISTerre - CNRS UMR 5275, Univ. J. Fourier, Grenoble, France
[5] ISTeP - CNRS UMR 7193, UPMC, Paris, France
[6] IMPMC - CNRS UMR 7590, UPMC, Paris, France

Geological storage of CO_2 in basic rocks relies on the dissolution of its silicate components, followed by the precipitation of carbonates. However, the slow dissolution kinetics of Mg-rich silicates has proven a critical issue. Previous batch carbonation studies on separated olivine grains[1] ($(Mg,Fe)_2SiO_4$), have emphasized the deleterious role of secondary phases, such as amorphous silica layers (SiO_2(am)) in controlling the dissolution rate of the parent mineral and the transport of reactants from and to the reactive surface.

We show here that carbonation processes and kinetics are strongly different for olivine within a tholeiitic basalt than for separated olivine. Batch experiments were conducted (at 150°C and P_{CO2} = 280 bars) on an Mg-rich (9.3 wt.% MgO and 12.2 wt.% CaO) tholeiitic basalt from Iceland, composed of olivine, Ti-magnetite, plagioclase and clinopyroxene. After 45 days of reaction, carbonation rates were quantified by CO_2 extraction with phosphoric acid, yielding up to 60 wt.% carbonation of Mg-rich phases as $MgCO_3$, but less than 0.5 wt.% of Ca-rich phases as $CaCO_3$.

Such observations diverge noticeably from those previously reported in lower T carbonation studies on Ca-rich, Mg-poor basalts[2]. In addition, X-ray diffraction analysis on the reaction products reveals a substantial decrease in olivine content, supporting the idea that magnesite formation mainly follows from olivine dissolution. Therefore, these results suggest that in our experiments, no passivating silica layer was formed on the surface of olivine. Instead, investigations by transmission electron microscopy reveal that a thin layer (~100 nm) of porous, iron-bearing, aluminous phyllosilicate has formed on the surface of the remaining primary silicates. Taken together, these observations suggest that, in an Al rich-medium, the formation of clay minerals may consume the silicon of potential silica-rich surface layers, or directly inhibit their formation. Those phyllosilicates would therefore represent the ultimate sink for Si, with lesser impact on the transport of reactants than SiO_2(am). By providing a constant driving force for Si removal, we eventually propose that such phases allow olivine to dissolve as rapidly as it is known to occur in open natural systems, and therefore to reach higher carbonation rates[3].

[1] Daval et al (2011), Chemical Geology, v.284, p.193-209
[2] Schaef et al (2010), IJGGC, v.4, p.249-261
[3] Matter and Kelemen (2010), Nature Geoscience, v.2, p.837-841

Nanoparticle remediation through porous media

R.L. SKUCE[1*], D.J. TOBLER[1], M.R. LEE[1] AND V.R. PHOENIX

[1]School of Geographical and Earth Sciences, University of Glasgow, Glasgow, G12 8QQ, UK (*correspondence: r.skuce.1@research.gla.ac.uk)

The use of engineered nanoparticles continues to expand rapidly. As this intensifies, so does the environmental risk posed if they are released into the environment. This is of particular concern due to the potential toxicity of some nanoparticles. As it stands, we are poorly prepared to deal with nanoparticle pollution and thus remediation strategies must be developed Here, ureolysis-driven calcium carbonate precipitation by the urease positive bacterium *Sporosarcina pasteurii* is investigated as a means of removing nanoparticles from aquatic systems. This technology has been investigated for the solid phase capture of radionuclide and trace element contaminants in groundwater systems [1]. However its potential to capture nanoparticles has yet to be examined.

Batch experiments show the successful removal of highly stable organo-metallic nanoparticles at concentrations up to 10mg/l (the highest concentration tested thus far). Over 90% of nanoparticles where captured within 24 hours and capture efficiency appeared to be inversely proportional to calcite precipitation rate. As calcite precipitates, the nanoparticles become trapped within the growing calcite crystal. As the calcite-nanoparticle composite continues to grow, it adheres to surfaces (such as the edge of the reaction flask, or the edge of a pore space), immobilizing the nanoparticles from solution.

Following this an experiment was devised to determine the capture efficiency of nanoparticles through saturated porous media. It has been demonstrated that nanoparticles act as nucleation sites to the precipitating calcite, it is now imperative to determine whether nanoparticles are preferentially incorporated into the precipitating calcite when multiple nucleation sites are available, that is the sand grains. Breakthrough curves obtained determine the capture efficiency of nanoparticles in saturated porous media.

This technology has the potential for application in contaminated groundwater and soil as an in-situ remediation technique for nanoparticle pollutants.

[1] Warren, L.A Maurice, P.A. Ferris, N, P, F, G. (2011) *Geomicrobiology Journal* **18**, 93-115.

Bottom water redox conditions and sea level changes during Zn-Pb and phosphate mineralization, Howards Pass district, Yukon Territory

JOHN F. SLACK[1]*, HENDRIK FALCK[2], KAREN D. KELLEY[3], GABRIEL G. XUE[4]

[1]U.S. Geological Survey, MS 954, Reston, VA 20192, USA, jfslack@usgs.gov (*presenting author)
[2]NWT Geoscience Office, P.O. Box 1500, Yellowknife, NWT X1A 2R3, Canada
[3]U.S. Geological Survey, MS 973, Denver, CO 80225 USA
[4]Selwyn Resources Ltd., 509 Richards St., Vancouver, BC V6B 2Z6, Canada

Stratabound Zn-Pb sulphide deposits of the Howards Pass district occur in the Middle Ordovician-Early Silurian Duo Lake Formation (DLF). From base to top, the DLF in the district comprises four principal members: pyritic mudstone, calcareous mudstone, active (Zn-Pb), and upper siliceous mudstone. Sulphide lenses in the active member consist of layered, laminated, and massive sphalerite ± galena. Pyrite forms thin laminae of fine-grained framboids. The upper calcareous mudstone and the base of the active member locally contain apatite-rich units; the upper siliceous member has abundant apatite laminae 0.1-1.5 cm thick.

Whole-rock analyses for Zn- and Pb-poor DLF mudstones (n = 58) from three drill cores in relatively undeformed parts of the XYC and HCW deposits contain variable silica (to 90 wt % SiO_2), phosphate (to 24.7 wt % P_2O_5), and carbonaceous material (to 16.5 wt % Corg). V concentrations are highest in the calcareous mudstone member (to 3000 ppm), implying sedimentation near the suboxic-anoxic boundary; large variations in marine V/Mo ratios (0.74-209) reflect fluctuating bottom-water redox over time [1]. Re/Mo ratios [2], considered the best paleoredox proxy, record sulphidic or anoxic conditions (Re/Mo <0.001) in bottom waters during deposition of the pyritic mudstone, most of the calcareous mudstone, and active members; these conditions predominated in the basin prior to and during Zn-Pb mineralization, aiding accumulation and preservation of sulphides. In the upper siliceous member, Re/Mo ratios are mostly higher (0.004-0.013), indicating suboxic (<5 μM O_2) bottom waters. Suboxic conditions within the upper part of the calcareous mudstone and the base of the active member, and especially in the upper siliceous member, promoted deposition of abundant phosphate and correlate temporally with two periods of global sea level rise [3]; falling sea level may have facilitated the development of crucial anoxic to sulphidic bottom waters during Zn-Pb mineralization. Lithologic similarity to part of the Monterey Formation (Miocene) of coastal California suggests that the DLF and its contained Zn-Pb deposits formed in a restricted basin near a continental margin, accompanied by high productivity required for the accumulation of abundant phosphate, biogenic silica, and organic matter.

[1] Piper, D.Z., Calvert, S.E. (2009) *Earth-Sci. Reviews* **95**, 63-96.
[2] Ross, D.J.K., Bustin, R.M. (2009) *Chem. Geol.* **260**, 1-19.
[3] Munnecke, A., et al. (2010) *Palaeogeogr. Palaeoclimatol. Palaeoecol.* **296**, 389-413.

Exploring Water Quality and Flow Paths Using Boron Isotope Data

A.T. SLADE[1]*, N.R. WARNER[2], A. VENGOSH[2] AND B. WHITEHEAD[1]

[1] School of Environment, The University of Auckland, 23 Symonds Street, Auckland 1142, New Zealand, a.slade@auckland.ac.nz (* presenting author)

[2] Division of Earth and Ocean Sciences Nicholas School of the Environment, Duke University, Durham, NC 27708

Boron isotope data is rarely used by water quality (WQ) authorities to elucidate processes occurring in hydrologic systems in order to improve WQ management protocols. In concert with a suite of chemicals this study explores the use of boron as a tracer in a WQ study that also helps reveal potential flow paths for water in a pulp and paper waste site. The results not only provide the local WQ authorities with a tool for improving the management of their waterways, they come at a critical stage in the history of the site as the parties legally responsible for the waste and management of the site will change in December of 2012.

Study Site

A pulp and paper waste site, located on top of active geothermal features, in the Bay of Plenty region of New Zealand is at risk of having a sustained and detrimental impact on the environment given the following historical and contemporary issues: 1) the waste site floods periodically causing temporary ponding, which in the past has resulted in the banks of the adjacent Tarawera River (TR) to breach; 2) the natural underlying geologic units and waste material generated by the pulp and paper mill are highly permeable; and 3) the two shallow unconfined aquifers in and under the waste are thought to house substantial volumes of water that are connected to the TR. As such, it is important to identify the source, provenance, and chemical profile of the water as it migrates through the geologic units and waste material in an effort to assist in mitigating any future environmental impacts.

Results of Study

This study involves a comprehensive chemical evaluation of water samples collected between 2009 and 2011, from the pulp and paper waste site, with an emphasis placed on boron isotope data. The types of water sampled and their associated $\delta^{11}B$ values collected from the 1 km^2 area that encompasses the waste site were: surface water (10.1-15.4‰); groundwater (-5.0-0.0‰); leachate (-1.5-6.7‰); geothermal water (-1.2‰); natural spring water (11.9‰); and rain water (25.9-28.9‰). The collation of the data provides a final assessment of the waste site's hydrologic system through the lens of boron isotope chemistry and showcases the ability to use it to improve WQ management protocols.

Timing and carbon sources for microbial processses in the deep terrestrial carbon cycle

SLATER, G.F.*[1], MAILLOUX, B[2]., SILVERN, R.[2], LI, L[3], SHERWOOD LOLLAR B[3]., ONSTOTT T.C.[4],

[1]McMaster University, Hamilton, Canada, gslater@mcmaster.ca,
[2]Bernard College, New York, USA
[3]University of Toronto, Toronto, Canada
[4]Princeton University, USA

The presence of microbial communities living in ancient, fractured rock in deep (2-3+ km) subsurface terrestrial environments suggests that the metabolic activities of these organisms may play a role in fluxes of carbon moving into, or out of, these deep Earth environments. This study investigated the carbon source and metabolic activities in fracture water feeding an artesian borehole located 1.3 deep in the Beatrix mine, South Africa. Isotopic analysis of the ^{18}O and ^{2}H of the waters lie along the GMWL but offset from modern precipitation indicating a paleometeoric origin confirmed by noble gas derived residence times on the order of a few Ma (1).

Multiple isotope analysis of carbon isotopes (^{13}C, ^{14}C) was applied to microbial cellular components (PLFA, DNA) and potential carbon sources and/or metabolites including dissolved inorganic carbon (DIC) and CH_4. $\Delta^{14}C$ of DIC was observed to be -980 ‰, slightly enriched above expectation for geologically old carbon ($\Delta^{14}C$ = -1000 ‰). Concurrently, PLFA and DNA $\Delta^{14}C$ were -940 ‰ demonstrating microbial utilization of highly ^{14}C depleted carbon sources. This is the first study we are aware of to compare two such distinct cellular components. The close agreement of these independent measurements supports the accuracy of both approaches. The fact that these microbial cellular components were slightly isotopically enriched related to the DIC suggests inputs from a ^{14}C enriched carbon source. The potential role of methane ($\delta^{13}C$ =-52 ‰ at this site) as a C source in this ecosystem is suggested by the $\delta^{13}C$ of PLFA from these communities (-50 to -65 ‰). This hypothesis will be investigated by on-going isotopic analysis of the ^{14}C methane and ^{13}C DIC pools.

[1] Lippman et al, (2003) GCA 67: 4597-4619

Subduction-driven growth and modification of cratons: examples from Canada and Greenland

K. A.SMART[1, 2*], S.TAPPE[1, 2], A.SIMONETTI[1,3] AND S.KLEMME[2]

[1]University of Alberta, Edmonton, Canada

[2]WWU, Münster, Germany kasmart@uni-muenster.de (*presenting author) sebastian.tappe@uni-muenster.de, stephan.klemme@uni-muenster.de

[3]Univ. of Notre Dame, Notre Dame, USA simonetti.tony@gmail.com

Cratonic crust and underlying mantle roots are thought to have a shared history of growth and modification since the Archean. However, debate continues on whether their coupled growth was due to mantle plumes or early forms of subduction. Cratonic mantle eclogites are central to this debate and here we present evidence from two such xenolith suites from Canada and Greenland for subduction-driven growth and modification of cratonic lithosphere.

We have determined the Pb isotope compositions of clinopyroxenes from eclogite xenoliths from the northern Slave and the West Greenland North Atlantic craton (NAC). Clinopyroxenes from NAC eclogites define a secondary isochron with an age of 2.7±0.3 Ga, which intersects a terrestrial Pb isotope evolution curve at ca. 2.62 Ga. This suggests Late Archean eclogite formation via melt extraction during subduction of oceanic crust [1]. Pb isotope compositions of the Slave clinopyroxenes do not define a statistically meaningful isochron. Instead, they appear to form a mixing array extending from clinopyroxene with unradiogenic Pb ($^{206}Pb/^{204}Pb$ ~ 14.3) to the host Jurassic kimberlite ($^{206}Pb/^{204}Pb$ ~ 19.2). We believe this array was produced by mixing between kimberlitic- and eclogitic derived Pb. Hence, the least radiogenic Pb isotope composition that intersects the Stacey-Kramers evolution curve at ca. 2.2 Ga has age significance. Importantly, this model age falls within the age range of 2.3-1.8 Ga shown by other eclogites from the Slave craton [2].

Both the Slave and NAC eclogite xenoliths have geochemical signatures that indicate oceanic crust protoliths, including $\delta^{18}O$ values that range above the mantle average (5.2-6.4‰). Moreover, the eclogite ages coincide with putative subduction events in each craton. NAC eclogite formation coincides with 2.9-2.7 Ga crustal growth marked by the intrusion of TTG granitoids in West Greenland. These TTGs are interpreted as melts of subducted oceanic basalts from their complementary relationship with the refractory NAC eclogites. The Slave eclogites coincide in age with the ca. 1.9 Ga subduction event that affected the western craton margin. Unlike Greenland, this subduction event did not add significantly to the Slave cratonic crust, and instead introduced eclogitic material to the craton root [2]. Furthermore, ca. 1.9 Ga eclogitic diamonds from the Slave craton [3] suggest that this subduction event introduced appreciable amounts of carbon into the mantle lithosphere. Thus, while both eclogite suites record craton evolution events, major crustal growth was only associated with the Archean Greenland eclogites, whereas late-stage cratonic root modifcation including metasomatism and diamond growth are marked by the Paleoproterozoic Slave eclogites.

[1] Tappe *et al.* (2011) *Geology* **39** 1103-1106. [2] Schmidberger *et al.* (2005) *EPSL* **240**, 621-633.

Formation of eclogites and pyroxenites below Attawapiskat, Superior Craton (Canada)

KAREN V. SMIT*[1], THOMAS STACHEL[1], ROBERT A. CREASER[1], S. ANDREW DUFRANE[1], RYAN B. ICKERT[2], RICHARD A. STERN[2] AND MICHAEL SELLER[3]

[1] Department of Earth and Atmospheric Sciences, University of Alberta, Edmonton, Canada, kvsmit@ualberta.ca*

[2] Canadian Centre for Isotopic Microanalysis, Department of Earth and Atmospheric Sciences, University of Alberta, Edmonton, Canada

[2] De Beers Canada, Toronto, Canada

Seventeen eclogite and 16 pyroxenite xenoliths from the Victor kimberlite at Attawapiskat will be used to assess whether they show evidence for a shallow origin as oceanic crust, emplaced into the Superior SCLM by tectonic stacking. Eclogites contain omphacite + garnet, whereas the pyroxenites contain diopside + garnet ± enstatite; three broad groups (Ca, Fe or Mg-rich) are recognised through their reconstructed whole rock major and rare earth element chemistry.

The sole high-Ca kyanite-bearing eclogite is the only sample with a positive Eu anomaly and has a subchondritic REE_N pattern consistent with an oceanic crust precursor undergoing dehydration/low degree partial melting during subduction. Fe-rich eclogites have flat $MREE_N$ to $HREE_N$ –indicative of a low-pressure origin – and depleted $LREE_N$. The high Mg eclogites and pyroxenites have similar flat $MREE_N$ to $HREE_N$, but enriched $LREE_N$ indicating a shallow origin and a subsequent stage of fluid metasomatic enrichment. Reconstructed whole rock compositions for these high Mg eclogites and pyroxenites rocks overlap with orogenic pyroxenites [1], suggesting a possible primary origin as basaltic intrusives in the shallow lithosphere.

Cpx from all the compositional groups have depleted Sr isotopic compositions (0.7019-0.7039) relative to present day bulk earth (0.7045). The majority of the samples have $\delta^{18}O$ overlapping, within uncertainty, to the mantle value. Mantle-like $\delta^{18}O$ values do not rule out oceanic crust as protoliths [2,3], and therefore these data cannot be used to distinguish between a low versus a high pressure origin. Evidence for involvement of crustal components in the genesis of the Superior's lithospheric mantle are flat $MREE_N$ to $HREE_N$ patterns and a positive Eu anomaly in the kyanite-bearing eclogite. Re-Os analyses and in-situ cpx Pb-Pb dating of these eclogites and pyroxenites are currently underway.

[1] Pearson et al. (1993) *Journal of Petrology* **34,**1,125-172 [2] Hart et al. (1999) *Geochimica et Cosmochimica Acta* **63**,4059-4080 [3] Schmickler et al. (2004) *Lithos* **75**,173-207

Iron isotope fractionation in stromatolitic oncoidal iron formation, Mesoarchean Witwatersrand-Mozaan Basin, South Africa

ALBERTUS J.B. SMITH[1*], NICOLAS J. BEUKES[1], JENS GUTZMER[1,2], CLARK M. JOHNSON [3], AND ANREW D. CZAJA[3]

[1]PPM, Department of Geology, University of Johannesburg, Johannesburg, South Africa, bertuss@uj.ac.za (* presenting author), nbeukes@uj.ac.za

[2]Department of Mineralogy, Techische Universität Bergakademie Freiberg, Freiberg, Germany, jens.gutzmer@mineral.tu-freiberg.de

[3]Deparment of Geoscience, University of Wisconsin-Madison, Madison, Wisconsin, USA, clarkj@geology.wisc.edu, aczaja@geology.wisc.edu

Iron isotope fractionation in an Archean marine basin through biological and abiological processes is well illustrated in an iron rich unit in the Mesoarchean (2.96-2.92 Ga) Witwatersrand-Mozaan Succession [1] of South Africa and Swaziland. The unit comprises the oldest known shallow water oncoidal granular iron formation interbedded with magnetite- and stilpnomelane-rich mudstone and mixed mineralogical facies banded iron formation. The banded iron formation marks the most distal and the oncoidal iron formation the most proximal depositional settings. The oncoidal iron formation shows domal and columnar micro-stromatolite rims composed of magnetite around chert and calcite grains in a matrix of chert and minor iron-rich silicate. The more distal banded iron formations and iron-rich mudstones have δ^{56}Fe values ranging from slightly positive to strongly negative depending on the dominant iron-rich phase. The stromatolitic oncoidal iron formation has δ^{56}Fe values from zero to strongly positive. Moreover, the δ^{13}C values of the calcite in the latter are strongly negative, suggesting the carbonates formed through the oxidation of organic carbon.

The geochemical evidence along with the depositional facies reconstrution show that the mode of iron deposition varied from the distal to proximal depositional settings, and is the most dominant control on iron isotope fractionation. The limited iron source that reached the proximal setting of the stromatolitic oncoidal iron formation had zero to positive δ^{56}Fe values. Textural and geochemical evidence suggest that iron oxidizing microbes [2] living on the rims of reworked chert grains used the limited ferrous iron in the shallower part of the basin in their metabolism to precipitate ferrihydrite, which would concentrate heavy iron isotopes [3]. The ferrihydrite underwent a redox reaction with organic carbon during diagenesis to form magnetite that retains the heavy iron isotopic signature and isotopically light calcite. The lighter iron isotopes remaining in solution were incorporated into iron-rich silicates in the matrix.

[1] Beukes & Cairncross (1991) *Trans. Geol. Soc. S. Afr.* **45**, 44-69. [2] Konhauser *et al.* (2002) *Geology* **30**, 1079-1082. [3] Croal *et al.* (2004) *Geochim Cosmochim Ac* **68**, 1227-1242.

The pyroxene sponge: amphibole signatures and controls on water in arc magmas

D. J. SMITH[1*]

[1]University of Leicester, Leicester, UK, djs40@le.ac.uk (* presenting author)

Many arc magmas show evidence of amphibole fractionation, in the form of characteristic REE profiles and exhumed amphibole cumulates. However, amphibole is not always a major modal phase in the erupted suites: thus, fractionation is cryptic [1]. In water-rich (>4 wt% H_2O) magmas where amphibole fractionation is most pronounced, high Sr/Y signatures develop [2]. Elevated Sr/Y magmas have an association with porphyry mineralisation (e.g. [3]) – most likely an indicator that water-rich, amphibole stable melts are fertile for porphyry formation [4].

Clinopyroxene is an early and abundant fractionating phase in most arc magmas, and unlike amphibole is common in the erupted rocks. New data from the Solomon Islands suggest that the early-formed clinopyroxene cumulates can react with evolving magmas, forming amphibole as a secondary metasomatic phase. The "cryptic" fractionation of amphibole may in fact be clinopyroxene cumulate−melt reactions, generating REE profiles characteristic of amphibole removal without it being a major modal phase in the crystallising magma.

Furthermore, the Solomon Islands data show that these metasomatic amphibole cumulates can be contrasted with true amphibole cumulates (i.e. directly crystallised and fractionated amphibole), with only the true amphiboles generating strong Y depletion (and by extension, high Sr/Y) in the daughter magmas.

The clinopyroxene cumulates are potentially acting as a sponge, modifying the daughter magma's REE signature, and locking up water as they react to form amphibole. More hydrous magmas, able to directly crystallise amphibole and generate high Sr/Y, may only form where the sponge has been entirely metasomatised, and is no longer capable of locking up water. The clinopyroxene sponge possibly limits water content and magma fertility under normal arc-fractionation conditions. Fertile magmas are either more hydrous at source (able to directly crystallise amphibole), or only develop after repeated cycles of intrusion and cumulate−melt reaction.

References

[1] Davidson *et al.* (2007) *Geology* **35**, 787–790.
[2] Smith *et al.* (2009) *Contributions to Mineralogy & Petrology*, **158**, 785–801.
[3] Oyarzun et al. (2001) *Mineralium Deposita*, **36**, 794–798.
[4] Richards (2011) *Economic Geology* **106**, 1075-1081.

Enhanced multicollector ICP-MS coupled with a desolvating nebulizer system for geochronology

FRED G. SMITH[1*], VICTOR POLYAK[2]

[1]CETAC Technologies, Omaha NE USA, fsmith@cetac.com(* presenting author)

[2]University of New Mexico, Earth and Planetary Sciences, Albuquerque NM, USA, polyak@unm.edu

Abstract

Multicollector ICP-MS instruments are very specialized devices for high precision isotope ratio measurements. For accurate measurement of low abundance isotopes, signal enhancement is often required. In addition, sample preparation and/or sample aerosol desolvation may be necessary to reduce or eliminate mass spectral interferences such as oxides and hydrides.

This paper will examine the coupling of an enhanced multicollector ICP-MS instrument with a dedsolvating nebulizer system for geochronology. The hardware specification of the ICP-MS will be detailed, including a revised vacuum system and special sampler and skimmer interface cones. Important operating conditions of the desolvating nebulizer system include argon sweep gas and nitrogen addition gas flows.

Application of this coupled system to U-series dating will be described.

Mineralogy and porewater geochemistry of processed kimberlite: implications for acid rock drainage and metal releases

LIANNA J.D. SMITH[1*], MICHAEL C. MONCUR[2], DOGAN PAKTUNC[3], AND YVES THIBAULT[3]

[1]Rio Tinto - Diavik Diamond Mines, Yellowknife, YK, Canada, Lianna.smith@riotinto.com (*presenting author)

[2]Alberta Innovates-Technology Futures, Calgary, AB, Canada, michael.moncur@albertainnovates.ca

[3]CANMET Mining and Mineral Sciences Laboratory, Ottawa, ON, Canada, dpaktunc@NRCan.gc.ca, ythibaul@nrcan.gc.ca

The development of diamond mines in Canada's North emphasizes the need to assess the environmental implications of storing processed kimberlite tailings (PK) in regions with continuous permafrost. The Diavik Diamond Mine (Diavik) is located in the barren lands on an island in Lac de Gras, 300 km northeast of Yellowknife, NT, Canada. During the life of the mine, up to 42 million tonnes of PK will be produced and disposed on site for permanent storage. In 2009, a study was initiated to understand the mineralogy and evolution of porewater geochemistry in the PK tailings impoundment. Porewater was collected and analyzed from a number of core and drive-point piezometers located across an exposed PK beach and in the central pond. The core samples were analyzed and characterized in detail. The samples collected from the tailings pond are composed of Ni-bearing olivine, calcite, quartz, garnet, lizardite, biotite, albite, saponite and both framboidal and massive pyrite. Olivine and its alteration products made of lizardite, iron oxides and magnesian aluminosilicates are the dominant minerals. Neutralization potentials of the samples are between 39 to 85 kg $CaCO_3$ eq/t, far exceeding the acid generating potentials in the 5 to 12 kg $CaCO_3$ eq/t range due to the presence of pyrite. Porewater samples from the unsaturated zone of the impoundment have the lowest pH values and highest concentrations of dissolved SO_4 and metals. With depth, pH values increase and dissolved SO_4 and metals concentrations decrease towards the water table. In the saturated zone, average dissolved concentrations decrease by almost an order of magnitude compared to the unsaturated zone for SO_4, major cations and most metals (e.g SO_4: 3500 to 350 mg/L; Mg: 730 to 80 mg /L, Ni: 0.82 mg/L to 0.038 mg/L). Sulfur isotope ratios measured from the porewater are strongly depleted averaging -17.9 ‰ and show minimal fractionation from the unprocessed kimberlite, suggesting dissolved sulfate concentrations are resulting from sulfide oxidation; however, there are no apparent mineralogical features on pyrite grains indicative of oxidative dissolution. Except for a single grain of $BaSO_4$, no other sulfate minerals were identified in the PK. Porewaters from the underlying frost zone show further increases in pH and decreases in dissolved SO_4 and metal concentrations. Groundwaters collected from piezometers installed in PK stored below a water cover revealed dissolved concentrations of major ions and metals which are comparable to those measured from the frost zone. Results from this study show that subaqueous disposal and freezing of the PK material would restrict oxidation and dissolution processes and limit the release of dissolved concentrations of metals and SO_4.

Solubilities of arsenic oxy- and thio–compounds in calcium rich waters

MATT SMITH[1*] AND DIRK WALLSCHLÄGER[2]

[1]Trent University ENLS Graduate Program, Peterborough, Canada, mattsmith@trentu.ca (* presenting author)

[2]Trent University Department of Chemistry, Peterborough, Canada, DWallsch@trentu.ca

16l. Biogeochemistry of Oxyanion-Forming Trace Elements in the Environment

The mobilisation of arsenic by thiolation is a significant driver of As solubility in sulphidic, reducing systems and alkaline environments [1, 2]. The determination of the chemistry of arsenic thioanions requires specific analytical methods to for detection. The complex chemistries of environments containing thioarsenicals create problems with regard to preservation of *in situ* arsenic speciation. Co-precipitation of arsenic with iron[3] or other minerals salts has been shown to occur during the lag time between *in situ* sampling and laboratory analyses. Calcium (Ca) is a ubiquitous element in alkaline natural systems containing As. The insolubility of Ca-arsenate salts has been documented[4] thus quantitative losses of As from *in situ* samples containing Ca is a probable mechanism.

Interactions between Ca and arsenic oxy- and thioanions were studied under anoxic, alkaline conditions. We have studied the precipitation of Ca-thioarsenate salts, and have been able to experimentally determine the K_{SP}, $\Delta G°_f$, $\Delta H°_f$, and $\Delta S°$, for Ca-monothioarsenate, Ca-arsenite, and Ca-arsenate. Trithioarsenite, trithioarsenate and tetrathioarsenate do not form Ca-arsenic salts or absorb to Ca carbonate ($CaCO_3$), Ca hydroxide or Ca sulphate, indicating that these species are the most soluble anionic arsenic species. Dithioarsenate is more soluble than monothioarsenate and arsenate, and arsenite is the least soluble As species. The solubilities of Ca sulphate and $CaCO_3$ are less than those of the Ca-arsenic salts, thus adsorption of arsenite and arsenate to Ca sulphate and $CaCO_3$ can be a significant mechanism of removal of As oxyanions in the environment. Increasing thiolation enhances the solubility of As anions such that no chemical interaction exists between As and Ca in the environment for tri- and tetra-thiolated species.

[1] Fisher (2008) *Environ. Sci. Technol,* **42(1),** 81–85.

[2] Wallschläger (2007) *Anal. Chem,* **79,** 3873–3880.

[3] Suess (2011) *Chemosphere* **83(11),** 1524–1531.

[4] Bothe (1999) *J. Haz. Mater. B* **69,** 197–207.

Ionic force fields for electrolytes and molecular simulation of chemical potentials and aqueous solubility

WILLIAM R. SMITH[1*] AND FILIP MOUČKA,[1,2]

[1]University of Ontrio Institute of Technology, Oshawa, Canada, william.smith@uoit.ca*

[2]J.E. Purkinje University, Ústí n. Labem, Czech Republic, fmoucka@seznam.cz

We have recently [1,2] developed the Osmotic Ensemble Monte Carlo (OEMC) method for calculating the chemical potentials and solubility of aqueous electrolytes and their mixtures by molecular simulation. OEMC is a computationally efficient algorithm that uses a type of semi grand canonical ensemble, with a fixed number of water molecules at temperature *T* and pressure *P*, and electrolyte chemical potentials specified by the inter-phase equilibrium reaction involving the ions and their crystalline solid. To calculate solubility, we use accurate chemical potential data for the solid from thermochemical tables[3]. By appropriately setting the solid's chemical potential to other values, the entire chemical potential vs concentration curve of the ions in solution can be mapped out.

Although our results show good qualitative and reasonable quantitative accuracy, improvements depend on the use of more accurate ionic force fields. In this talk, we describe calculation strategies and show results for new force-field models for Na^+ and Cl^- compatible with SPC/E water. Our new force fields demonstrate good accuracy for the combined ion pair chemical potentials, the solution density, the predicted solubility and the solid chemical potential and density. Preliminary results are shown in the figure.

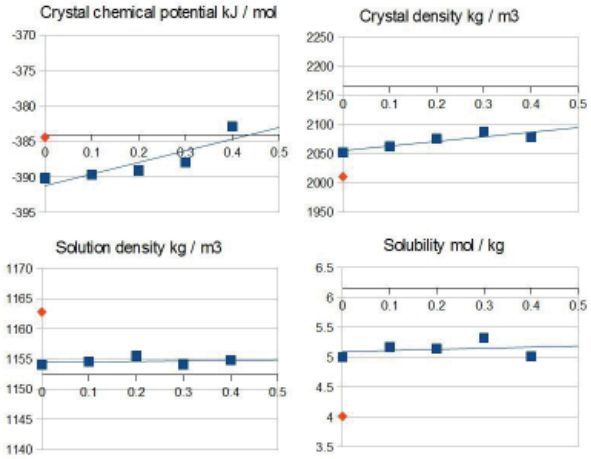

Figure: NaCl crystal and solution properties as functions of a model parameter after one iteration of the force-field adjustment strategy. Blue: our results; Orange:results using the force field of Joung and Cheatham[4]; Horizontal lines: experiment.

[1] Moučka, Lísal, Škvor, Jirsák, Nezbeda & Smith (2011) *J. Phys. Chem. B* **115**, 7849–7861.

[2] Moučka, Lísal, Smith (2012) *J. Phys. Chem. B*, submitted.

[3] Chase (1998) *J. Phys. and Chem. Reference Data Monograph No.9, Am. Chem. Society, Am. Inst Physics*.

[4] Joung, & Cheatham (2008) *J. Phys. Chem. B* **112**, 9020-9041.

Insights into the 2300Ma magmatic shutdown

R.G. SMITS[1*], M.HAND[1], W.J. COLLINS[2]

[1]Centre for Tectonics, Resources and Exploration, University of Adelaide, S.A. 5005, Australia, russell.smits@adelaide.edu.au (* presenting author)

[2]School of Environmental and Life Sciences, University of Newcastle, NSW 2308, Australia,

Zircon geochronology and isotope geochemistry allows insights into the temporal and geodynamic controls on tectonic events. The global record of magmatic events reflected from zircon spectra is episodic, with large widespread events in zircon geochronology occurring periodically and related to supercontinent amalgamation. Conversely large troughs in the zircon spectra have been inferred to tectonic shutdown and magmatic hiatus. A large trough in the global zircon record around 2300Ma is interpreted to reflect this phenomenon, with widespread reduction in magmatic activity beginning at 2.45Ga to 2.2Ga (Condie *et al*. 2009). Whilst no direct outcrop of 2.3Ga magmatic lithologies has been sampled, a number of detrital samples record distinct populations at 2.3Ga allowing for interrogation of this geodynamically distinct time in the Earths evolution. The detrital zircon spectra in the Warumpi Province sediment samples display peaks at 1.8Ga, 2.5Ga with minor 2.3Ga comparable to the North China Craton and to a lesser extent Antarctica. Coupled U-Pb geochronology and Hf isotopic data from detrital samples in the central Australian Warumpi Province reveals distinct populations of 2300Ma zircons and the source mantle composition. The similarities in the age distributions raise the possibilities of co-evolution between these cratons and the links to the Nuna Supercontinent formation in the Paleoproterozoic. The coupled Hf isotope and U-Pb age analysis for zircons between 2.45-2.2Ga display variable arrays and large distribution between juvenile mantle to evolved sources, with distinct clusters observed. The variable spread of the Hf isotopic data indicates there are varied geodynamic systems at large during a period of proposed tectonic quiescence.

CONDIE K. C., O'NEILL C. & ASTER R. C. 2009. Evidence and implications for a widespread magmatic shutdown for 250 My on Earth. *Earth and Planetary Science Letters* **282**, 294-298.

The U-Th-Pb allanite petrochronometer: a combined ID-TIMS and LA-ICP-MS study

A.J. SMYE [1*], N.M.W. ROBERTS[1], D.J. CONDON[1], M.S.A. HORSTWOOD[1], R.R. PARRISH[1,2]

[1]NERC Isotope Geosciences Laboratory, British Geological Survey, Keyworth, Nottingham, NG12 5GG, U.K.

[2]Department of Geology, University of Leicester, University Road, Leicester, LE1 7RH, U.K.

Abstract

Allanite ($(Ce,Ca,Y,La)_2(Al,Fe^{+3})_3(SiO^4)_3(OH)$) is important as a U-Th-Pb petrochronometer of metamorphic and igneous crustal processes. Largely, this is because of its extended *P—T—X* stability field over other U-Th-Pb mineral chronometers [1], its ubiquity in felsic to aluminous melts [2] and its ability to retain radiogenic Pb at temperatures > 650ºC [3]. Furthermore, allanite plays a key role in the transport of LREE, U, Sr and Th in subducted crust [4].

Weight % concentrations of U and Th mean that both U-Pb and Th-Pb systems can potentially be used to constrain the age of radiogenic Pb in-growth. Th/U values up to 1000 mean that the Th-Pb system is preferentially targeted. However, successful U-Th-Pb allanite geochornology is hampered by: (**i**) the propensity of allanite to sequester high levels of non-radiogenic Pb (up to 95%); (**ii**) the presence of excess-^{206}Pb arising from incorporation of ^{230}Th; (**iii**) its common lack of crystallographic integrity, and (**iv**) compositional solid-solution with the epidote group minerals. Therefore, as the use of allanite U-Th-Pb data becomes more widespread, it is vitally important to understand the limitations and strengths of allanite as a petrochronometer.

Available allanite reference materials are poorly characterised; notably, there is a dearth of accurate U-Pb, and particularly, Th-Pb ID-TIMS data. Given that allanite is most commonly dated by LA-ICP-MS and SIMS, this means that many published datasets likely conceal considerable uncertainty in the accuracy of calculated age estimates.

This contribution presents the results of a combined ID-TIMS and LA-ICP-MS U-Th-Pb study on a suite of allanite reference materials, including two of the most commonly used allanite standards: the SISS and Tara allanites [5], in addition to a new potential allanite reference material. Both ID-TIMS and LA-ICP-MS analyses have been performed on the same allanite grain fractions so as to minimise normalisation-induced uncertainty. The high spatial resolution of the LA-ICP-MS technique, together with WDS-SEM imaging and powder XRD shows that allanite retains closed-system U-Th-Pb isotope systematics despite its pervasively metamict state. Open-system behaviour is restricted to clearly-identifiable zones of fluid-mediated alteration.

[1] Spear (2010) *Chem. Geol*. **279**, 55-62.
[2] Giere *et al*. (2004) *Rev.Min. Geochem.* **56**, 431-493.
[3] Heaman *et al*. (1991) *Min. Assoc. Can*. **19**, 59-102.
[4] Hermann (2002) *Chem. Geol*. **192**, 289-306.
[5] Gregory *et al*. (2007) *Chem. Geol*. **245**, 162-182.

Redox conditions of Hadean magmas: Insight from Ce-in-zircon oxygen barometry

DUANE J. SMYTHE[1*] AND JAMES M. BRENAN[1]

[1]University of Toronto, Department of Geology, Toronto, Canada, smythe@geology.utoronto.ca (* presenting author), j.brenan@utoronto.ca

Positive Ce anomalies on chondrite normalized REE abundance diagrams are a nearly ubiquitous feature of zircon. This is the result of the presence of trace amounts of Ce^{4+} in natural systems and the higher compatibility of Ce^{4+} over Ce^{3+} in zircon. Using experimental determinations of the Ce^{4+}/Ce^{3+} in the melt as a function of fO_2 and melt composition, we have calibrated a Ce-in-zircon oxygen barometer independent from that of Trail et al. [1]. Our method takes the approach of Ballard et al. [2], applying the lattice strain model to measured D(zircon/melt) trace element distribution coefficients for both the REEs and a suite of 4+ cations (Zr, Hf, Th, U) which allows the estimation of the end-member D values for Ce^{3+} and Ce^{4+}. Measured "bulk" D_{Ce} values, which plot on a mixing curve between these end members, can then be related to the fraction of Ce as 4+ in the melt. Our calibration then allows for this to be linked directly to fO_2.

Evaluation of this technique has been carried out on zircons from three different lithologies whose fO_2 (expressed as Δ FMQ) has been estimated independently: rhyolite from the Bishop tuff, California (FMQ +1.1 ± 0.6), dacite from the Toba tuff, Indonesia (FMQ +0.9 ± 0.6), and monzodiorite from the Umiakovik pluton, Nain plutonic suit, Labrador (FMQ -2.4 ± 1.4). Trace element concentrations of zircon and host glass were measured by LA-ICP-MS. Values of Δ FMQ calculated by our method are +1.6 ± 0.4 (Bishop tuff), +0.8 ± 0.7 (Toba tuff) and -3.9 ± 0.5 (Umiakovik pluton), which are within error of the independent estimates.

Using D(zircon/melt) values for the REEs from Sano et al. [3] and empirical estimates for the 4+ cations, we have applied our oxygen barometer to Hadean zircons from the Jack Hills, Australia. Calculated values of Δ FMQ for zircons whose $\delta^{18}O$ is in the mantle range yield a bimodal distribution with peaks at –2.4 (n = 4) and +2.0 (n = 7). This appears to be connected to the crystal chemistry as light REE enriched samples consistently give lower estimations of fO_2. In addition to fO_2 we have also observed considerable dependence in Ce^{4+}/Ce^{3+} on melt composition. For the likely range in composition of zircon crystallizing melts this would affect the calculated fO_2 by at most 1 Δ FMQ unit. Therefore, the range in fO_2 observed is beyond that which can be explained by melt composition alone. This suggests that heterogeneities in fO_2 persisted in the source region for the zircon-producing magmas during the Hadean.

[1] Trail et al. (2011) *Nature* **480**, 79-82. [2] Ballard et al. (2002) *Contrib. Mineral. Petrol.* **144**, 347-364. [3] Sano et al. (2002) *Chem. Geol.* **184**, 217-230.

Atomic scale imaging of U, Th and radiogenic Pb in zircon

DAVID R. SNOEYENBOS[1*], DAVID REINHARD[1], AND DAVID P. OLSON[1]

[1]Cameca Instruments Inc., Madison, WI, USA
David.Snoeyenbos@ametek.com (* presenting author)

Radiometric dating of a mineral depends on the assumption that the parent radionuclides and daughter radiogenic Pb have remained together within the analyzed volume. Isotopic dating techniques continue to evolve from bulk methods towards *in situ* techniques with ever smaller analyzed volumes such as afforded by LA-ICPMS and SIMS. The use of small sample volumes in zircon minimizes common Pb from microinclusions, but increases the importance of knowing if there has been any spatial redistribution of the radiogenic Pb relative to its parents.

In Atom Probe Tomography (APT) a specimen with dimensions of a few hundreds of nanometers is evaporated atomic layer by atomic layer. The original position of each atom is identified, along with its atomic species, and in most cases its isotope. The result is a reconstruction allowing quantitative three-dimensional study of the specimen at the atomic scale, with very low detection limits and high mass resolution.

A zircon specimen in garnet from recently identified possible UHP rocks from the Taconian of Western Massachusetts, USA [1] was selected for study by APT. WDS mapping and quantitative analysis by FE-EPMA had revealed high concentrations of Th and U in a submicron envelope between a resorbed zircon core, and a subsequent metamorphic overgrowth.

Guided by FE-EPMA trace-element mapping, a sample of this envelope was extracted by FIB and milled into 200nmX100nm conical tips appropriate for APT. A dataset of ~11 million atoms was obtained, revealing a 25nm wide band of zircon between core and overgrowth containing >0.25 at% each of U and Th.

Sufficient radiogenic Pb had accumulated within the specimen to be detectable by APT, consistent with the high concentrations of radionuclides and the expected 4-500my age of the specimen,. Strong spatial covariance was observed between U and 206Pb, without apparent migration or agglomeration of the radiogenic Pb atoms.

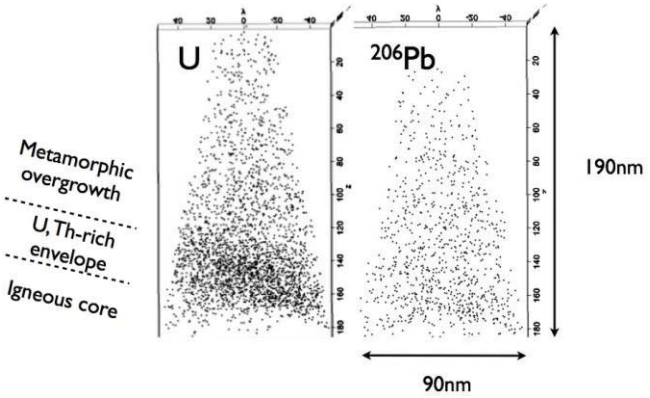

Figure 1: Ion image of U(total) and 206Pb atoms detected by APT.

[1] Snoeyenbos, Koziol, Russell, Ebel and Valley (2011) *EOS Trans. Fall meeting Suppl.* **Vol 92**, Abstract V21G-04

Sr, Nd, Pb and Hf isotopic constraints on mantle sources in the Payenia backarc basalts (Mendoza, Argentina)

NINA SØAGER[1*], PAUL MARTIN HOLM[1], MATTHEW F. THIRLWALL[2]

[1]University of Copenhagen, Copenhagen, Denmark, ns@geo.ku.dk (*presenting author)

[2]Royal Holloway University of London, London, UK, M.Thirlwall@rhul.ac.uk

The mainly alkaline basalts and trachybasalts from the Payenia volcanic province of southern Mendoza show a great variation in geochemistry ranging from intraplate to arc-backarc compositions. In Pb-Sr-Nd-isotopic space the retroarc and Nevado volcanic field samples form a common trend from the isotopic composition of the Andes transitional southern volcanic zone arc (TSVZ) towards a component with higher Sr and lower Nd-isotopes. This is interpreted as contamination by lithospheric mantle melts due to a sharp decrease in La/Sm, Tb/Yb and incompatible element contents (except Ti) along this trend, making upper crustal contamination unlikely.

The intraplate basalts from the Río Colorado area have lower Pb and Sr and slightly higher Nd-isotopic composition than the Nevado samples and apparently reveal the composition of an astenospheric mantle end-member. The very low Th/Nb, high U/Pb and Ce/Pb of the Río Colorado basalts precludes any significant input from the subduction zone. In Nd-Hf isotopic space they plot at negative $\Delta\varepsilon Hf$ along with FOZO and HIMU-type basalts but the Sr-isotopic values are slightly higher (~0.70355) than these. The Pb-isotopes and trace element patterns are comparable to EM1-type ocean island basalts (OIB) which could suggest that the Río Colorado mantle source is a mixture of FOZO and EM1 material. Even though the trace element patterns are very similar to some Somuncura basalts (another Patagonian hotspot [1, 2]), the Somuncura EM1 end-member is dissimilar in Pb-isotopic space [2]. The presence of recycled crust in the mantle source is supported by the indication that some of the Río Colorado and Payún Matrú basalts are pyroxenite melts as judged by their low Ca, Sc, Mn and MgO and high FeO_T, Ni and SiO_2 compared to peridotite melts.

The high $^{143}Nd/^{144}Nd$ Nevado and retroarc samples have similar εNd to Río Colorado samples but higher εHf and possibly trend towards South Atlantic N-MORB compositions. Furthermore, the major element composition of these lavas is akin to peridotite melts. This suggests that there are two asthenospheric mantle sources beneath the Payenia province: a South Atlantic normal upper mantle and an OIB-type mantle which dominates in the Río Colorado and Payún Matrú regions. The normal upper mantle peridotite is apparently only melted when fluids are added from the subduction zone whereas the OIB mantle melts due to a higher mantle temperature or/and a lower solidus temperature of the pyroxenite components.

[1] Remesal et al. (2002) *Rev. Asoc.Geol. Arg.* **57 (3)**, 260-270. [2] Kay et al. (2007) *Journal of Petrology* **48 (1)**, 43-77.

Melt inclusions as a source of principal geochemical information

ALEXANDER V. SOBOLEV[1,2,3]

[1] University J. Fourier, ISTerre, Grenoble, France. alexander.sobolev@ujf-grenoble.fr

[2] Max Planck Institute for Chemistry, Mainz, Germany.

[3] Vernadsky Institute of Geochemistry, RAS, Moscow, Russia.

Recent papers [1-5] on the in-situ radiogenic isotope composition of melt inclusions report controversial conclusions on the scale and origin of isotope heterogeneities. In this paper I will review these results focusing mostly on the question: whether melt inclusions can provide the new geochemical information on the origin, composition and scale of mantle heterogeneity?

The study of some 140 olivine hosted melt inclusions from a single lava of Mauna Loa volcano (Hawaii) reveals incredible Sr isotope source heterogeneity: at least 87Sr/86Sr=0.7027-0.7074 (Fig 1) [5]. Based on the 2-sigma criterion we found that 21% of inclusions fall out of the isotopic range of Mauna Loa lavas and 8% fall out of the isotopic range of all Hawaiian Lavas (Fig 1). Most compositionally distinct melts were trapped in high Mg olivine (Fo>86). We show that melt fractions with different compositions were mixed up during olivine crystallization producing typical Mauna Loa lavas. This result indicates unprecedented Sr isotope anomaly in Hawaiian mantle source caused by entrainment of Phanerozoic oceanic crust altered by seawater [5]. It also shows that bulk rocks could easily mask original source heterogeneity, which can be often deciphered ONLY by melt inclusions study.

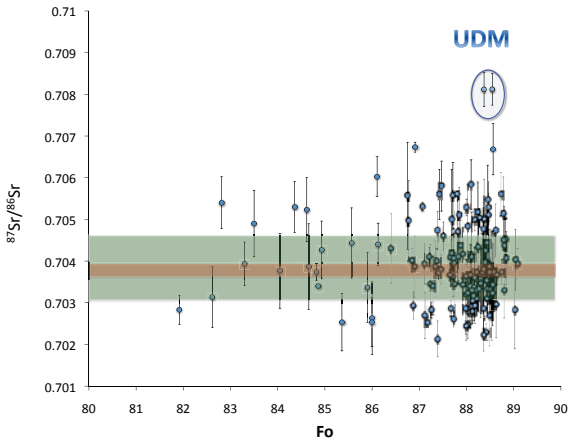

Figure 1: Isotope compositions of melt inclusions in olivine phenocrysts from a single lava sample of Mauna Loa volcano, Hawaii versus composition of host olivine [5]. Narrow (brown) and wider (green) fields manifest composition of all Mauna Loa lavas and all Hawaiian lavas respectively. Error bars: one standard error. Outlined are ultra-depleted melt inclusions (UDM).

[1] E. Saal *et al.*, (2005) *EPSL* **240**, 605-620. [2]. M. G. Jackson, S. R. Hart, (2006) *EPSL* **245**, 260-277. [3] J. Maclennan, (2008) *GCA* **72**, 4159-4176. [4] B. Paul *et al.*, (2011) *Chemical Geology* **289**, 210-223. [5] A. V. Sobolev, et al (2011), *Nature* **476**, 434-437.

The way to destroy thick cratonic lithosphere

STEPHAN V. SOBOLEV [1]* AND ALEXANDER V. SOBOLEV[2,3]

[1]GFZ, Geodynamic Modelling, Potsdam, Germany, stephan@gfz-potsdam.de (* presenting author)
[2]University J. Fourier, ISTerre, Grenoble, France, alexander.sobolev@ugf-grenoble.fr
[3] Vernadsky Inst. of Geochemistry, RAS, Moscow, Russia

Thick and chemically distinct cratonic lithosphere is known to be tectonically stable. However there are natural examples when large areas of such lithosphere are flooded by huge volumes of basalts comprising Large Igneous Provinces (LIPs). The examples of LIPs that were at least partially extruded at Archean or Proterozoic lithosphere since 250 Ma are numerous, i.e. Siberian Traps, Central Atlantic Province, Karoo, Parana, North-Atlantic Province etc. The outstanding example of the older (2 Ga) LIP is Bushveld Complex located at Archean craton. Thinning of lithosphere is required by any model of origin of such LIPs because only when the source ascends to shallow level can normal mantle peridotite produce a large amount of melt.

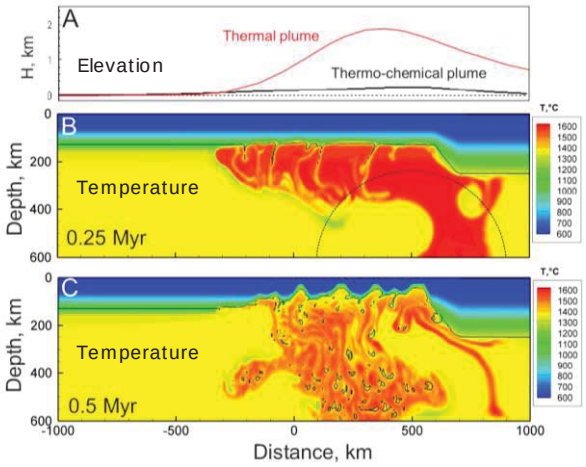

Figure 1: Model of rapid destruction of thick cratonic lithosphere by thermochemical plume without pre-magmatic surface uplift [1].

Recently, a numeric model of LIPs formation focused at Siberian LIP [1] explained rapid destruction of the cratonic lithosphere by the thermo-chemical mantle plume having potential temperature of 1600°C and containing large amount (15 Wt%) of recycled oceanic crust. The huge amount of melt generated from this plume intruded into the lithosphere and caused its delamination/foundering in less than 1 mln years (Figure 1).

In this study we explore limitations of this process. We demonstrate that realistic mantle plume with potential temperature up to 1650 °C, carrying as much recycled oceanic crust as it can remaining positively buoyant in the mantle, can significantly damage lithospheric root up to 200km thick.

[1] S.V. Sobolev et al. (2011) *Nature* **477**, 312-316.

Integrated geochemical and mineralogical investigation of lake deposits at Da Langtan (China) - implications for surface processes on Mars.

SOBRON, P.[1*], WANG, A.[2], MAYER, D.P.[3], SOBRON, F.[4], KONG, F.J.[5], ZHENG, M.P.[5]

[1]Canadian Space Agency, St. Hubert, Canada, pablo.sobron@asc-csa.gc.ca (* presenting author)
[2]Dept. of Earth and Planetary Sciences and the McDonnell Center for the Space Sciences, Washington University in St. Louis, St. Louis, USA, alianw@levee.wustl.edu
[3]Clark University, Worcester, USA, dmayer@clarku.edu
[4]Unidad Asociada UVa-CSIC, Centro de Astrobiologia (CAB-INTA), Valladolid, Spain, sobron@iq.uva.es
[5]R&D Center of Saline Lakes and Epithermal Deposits, Chinese Academy of Geological Sciences, Beijing, China, kongjie69@hotmail.com, zmp@public.bta.net.cn

The Qaidam Basin (QB)(32°-35°N/90°-100°E), located in the northern edge of the Qinghai-Tibet Plateau (China), is a high-altitude desert (aridity index ~0.04). Located at ~3000 m above sea-level, the basin features numerous dissicated evaporative lakes. Fig. 1 displays a partially eroded anticlinal structure (Xiao Liangshan (XL)) within the remains of a former lake in the Da Langtan (DL) playa region of the QB. The evaporation of the lake occurred in parallel with the rise of the anticline, thus producing the spectacular sequence of light and dark-toned rings shown in Fig. 1. This sequence depicts the multiple stages in the evolution of the lake. In-situ IR reflectance spectra were recorded along a traverse across XL, and samples were collected for subsequent laboratory analysis using Vis-NIR reflectance spectroscopy, Raman spectroscopy, and laser-induced breakdown spectroscopy (LIBS). XL was also imaged by Hyperion onboard NASA's EO-1 satellite to extract spectral endmembers from the scene and generate a mineral facies classification map. The surface mineralogy includes carbonates, gypsum, halides, hydrated Mg- and Na-sulfates, and chlorites. This mineral sequence resembles that observed at various locations on Mars, particularly at Gale crater. We have built a lake evaporation model that constrains the physico-chemistry of the DL lake's water (T, pH ...), and can help understand the occurrence of water-related mineral deposits and elucidate the geochemistry of putative former aqueous systems on Mars that resemble those we are investigating at Da Langtan.

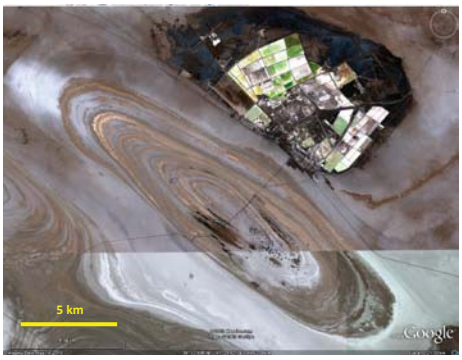

Figure 1: Xiao Liangshan image. Note the ring structure of the deposits across the anticline. Older deposits are on top.

Soil water vapor isotopes as a tool for understanding ecohydrological processes

K. SODERBERG*[1], S. P. GOOD[1], L. WANG[2], AND K. K. CAYLOR[1]

[1]Department of Civil and Environmental Engineering, Princeton University, Princeton, NJ, USA, soderbrg@princeton.edu (* presenting author)

[2]School of Civil and Environmental Engineering, University of New South Wales, Australia

Abstract

Soil evaporation can represent a significant loss of moisture from an ecosystem. As part of our research into evapotranspiration (ET) dynamics [1], we utilize continuous (1 Hz) measurements of water vapor isotopes to help partition ET into transpiration (T) from plants and evaporation (E) from the soil. This type of measurement is made possible through the recent development of portable, laser-based water vapor isotope analyzers. Defining the necessary isotopic endmembers is relatively straightforward in the case of δ_T using a chamber attached to leaves [2]. The δ_E isotopic signal is more difficult to characterize given that it involves both equilibrium and kinetic isotope fractionation. The liquid soil water isotope composition that gives rise to the δ_E signal can also be very heterogeneous in time and space. We have utilized both a modified Craig-Gordon (CG) modelling approach [3,4] as well as *in situ* measurement of soil water vapor isotopic composition. The CG model was designed to describe the evolution of isotopic composition during evaporation from open water, but is commonly applied to soil evaporation. We propose that soil water potential be used to adjust the normalized humidity parameter in this model, just as the activity of water is used to model evaporating brines. We present results from field measurements at our eddy covariance flux tower in central Kenya, as well as some laboratory data. The effect of this modification is variable, but appears to become significant with soil water potentials drier than around -10 MPa. The *in situ* measurements indicate that even shallow (5-10 cm) soil water vapor appears to be in isotopic equilibrium with adjacent liquid soil water. However, we are currently looking into the effects that soil matric forces can have on equilibrium isotope fractionation factors.

[1] Wang et al. (2010) *Geophysical Research Letters*. **37**, L09401
[2] Wang et al. (2012) *Agricultural and Forest Meteorology*. **154-155**, 127-135.
[3] Craig and Gordon (1965) *Stable isotopes in oceanographic studies and paleotemperatures,* pp. 9-130.
[4] Horita (2008) *Isotopes in Environmental and Health Studies*, 44, 23-49.

Stoichiometry of dissolved bioactive trace metals in the Indian Ocean

HUONG THI DIEU VU[1] AND YOSHIKI SOHRIN[2]*

[1]Institute for Chemical Research, Kyoto University, Uji, Japan, huong@inter3.kuicr.kyoto-u.ac.jp

[2] Institute for Chemical Research, Kyoto University, Uji, Japan, sohrin@scl.kyoto-u.ac.jp (* presenting author)

Introduction

GEOTRACES JAPAN has conducted a section study in the Indian Ocean during the KH-09-5 cruise of R/V Hakuho Maru from November 2009 to January 2010 (Fig. 1). Here we report the results on dissolved bioacitive trace metals (Al, Mn, Fe, Co, Ni, Cu, Zn, Cd and Pb) in seawater. This is the first simultaneous distribution of the nine metals in the Indian Ocean.

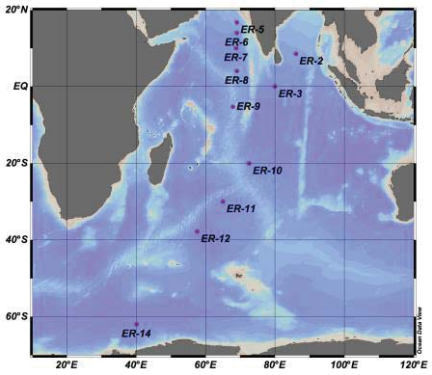

Figure 1: Sampling locations in the Indian Ocean

Methods

Seawater samples were collected using clean technique in accordance with the GEOTRACES protocol. The bioactive trace metals were preconcentrated by solid extraction using the NOBIAS CHELATE-PA1chelating resin [1] and determined by HR-ICP-MS.

Results and Conclusion

The dissolved bioactive trace metals are divided into 3 groups: (1) scavenged-type for Al, Mn, Co and Pb, (2) nutrient-type for Ni, Cu, Zn and Cd, and (3) recycled and scavenged-type for Fe. The atmospheric dust deposition and horizontal advection cause elevated concentrations of DAl, DMn, DCo, DCu and DPb in the upper water column in the Arabian Sea and the Bay of Bengal. Manganese reduction and iron reduction occur in the Oxygen Minimum Zone resulting the increase of DMn, DCo and DFe. Mid-depth enrichment of DMn and DFe above the Central Indian Ridge is influenced by hydrothermal plumes. The distribution of DNi, DCu, DZn and DCd is controlled by the biogeochemical cycle. Although DFe does not show a linear correlation with macronutrients and nutrient-type DMs, iron will be a co-limiting factor for phytoplankton production in most of the study area. The stoichiometry of DMs is generally comparable between deep waters in the northern Indian Ocean and the North Pacific Ocean, suggesting consistence of the mechanism controlling the behaviors of DMs between the Indian and Pacific Oceans.

[1] Sohrin, *et al.* (2008) *Anal. Chem.* **80**, 6267-6273.

Iberian paleogeography traced by U-Pb zircon ages of Ediacaran-Cambrian rocks

RITA SOLÁ[1*], FRANCISCO PEREIRA[2, 5], MARTIM CHICHORRO[3], LUÍS LOPES[2], AXEL GERDES[4] AND J.BRANDÃO SILVA[5]

[1] Laboratório Nacional de Energia e Geologia and Centro de Geociências, Portugal, rita.sola@lneg.pt (* presenting author)
[2] Dep. de Geociências, Universidade de Évora, Portugal
[3] Dep. de Ciências da Terra, Universidade Nova de Lisboa, Portugal
[4] Institut für Geowissenschaften, Frankfurt am Main, Germany
[5] Instituto Dom Luiz, Universidade de Lisboa, Portugal

The stratigraphic sequence of the Estremoz Anticline in the Ossa-Morena Zone (SW Iberia) includes: 1) an Neoproterozoic basement in the core - Série Negra Succession with greywackes, pelites and black cherts - unconformably overlain by 2) a lower Cambrian Dolomitic Formation, with arkosic sandstones and dolomitic limestones followed by 3) a Volcanic-Sedimentary Complex (VSC) with rhyolites and basalts interbedded with pelites and marbles.

The age of the VSC of the Estremoz Anticline has been a matter of debate, either due to the scarcity of fossils or to the complexity of the regional Variscan deformation. It was firstly attributed to the lower Cambrian, latter reported to the Ordovician or even to the Silurian [1]. Recently, a new interpretation attributed an upper Silurian to Devonian age to the VSC based on a lithological correlation with fossiliferous detritic carbonate rocks that outcrop in the vicinity of the Estremoz Anticline [2].

In this study we present new U-Pb ages of zircons from the Estremoz Anticline stratigraphic sequence.

The spectra of detrital zircon ages of the Ediacaran greywackes (Série Negra Succession) and lower Cambrian arkosic sandstones (Dolomitic Formation) indicates a predominance of Neoproterozoic ages (69-86%) and few Paleoproterozoic (10-16%) and Archean (2-12%) ages. The spectra of Proterozoic detrital zircon ages (with a typical gap in Mesoproterozoic ages) are similar to other peri-Gondwana correlatives with West African Craton provenance [3]. The source area is characterized by an important population of zircon ages in the range c. 850-545Ma. These Cryogenian and Ediacaran ages correspond to zircon crystallization events related to North Gondwana assembly during Pan-African/Cadomian orogenic processes.

The metarhyolites that are interbedded in the marbles of the VSC yielded a magmatic zircon crystallization age of 499.4 ± 3.3 Ma (MSWD=1.16; n=15/16; upper Cambrian). The result obtained indicates that carbonate production was episodic and occurred during lower and upper Cambrian in SW Iberia, related to North-Gondwana break-up. This new evidence should be taken into account in the reshaping of paleogeographic reconstruction models that have erroneously insisted on placing Iberia at southerly cold water higher latitudes (>60ºS) during the Furongian [4].

[1] Piçarra & Le Menn (1994) *Comunicações do Instituto Geológico e Mineiro* **80**, 15-25. [2] LNEG-LGM (2010) *Geological Map of Portugal, scale* 1:1000 000. [3] Pereira *et al* (2008) *GSL-Special Publication* **297**, 385-408. [4] Pereira *et al* (accepted) *Gondwana Research.*

The importance of a conceptual framework for interpreting tracer data

D. K. SOLOMON[1*], S. D. SMITH[1], B. J. STOLP[1], A. MASSOUDIEH[2]

[1]University of Utah, SLC, USA, kip.solomon@utah.edu (* presenting author)
[2]The Catholic University of America, Washington D.C., USA

Introduction

The interpretation of tracer data are highly dependent on the conceptual framework of the system being investigated. We describe several of our field and laboratory investigations in which the time scale of the tracer was poorly matched to the equilibration time of the system being invesitaged. Numerical modeling has been used to evaluate the extent to which a suite of tracer data can be used to uniquely characterize groundwater flow systems.

Results and Conclusions

A stream tracer test was performed by injecting NaBr for a period of about three times the the in-stream transit time, but steady was still not obtained due to long hyporheic flow paths. This led to estimates of groundwater discharge into the stream that were inflated by a factor of five. A combination of groundwater age data and major ion chemistry in both the stream and groundwater were required to develop a conceptual model that is more consistent with the injected tracer data.

At a geologic time scale we have evaluated the equilibration of helium in pore fluids with quartz grains in an attempt to use the helium content of quartz as a proxy for pore fluids [1]. While pore fluid and quartz helium values agree to within an order of magnitude, we have found differences that are best explained by transients in the groundwater flow systems that are less than the quartz equilibration time (0.01 to 2 MA). A realization of the non-steady effects resulted by applying multiple methods, each with their own time scale.

We have employed multiple tracers/techniques in an attempt to help define the conceptual framework of systems including the residence time distributions with some limited success; however, the introduction of transients as additional unknowns severly complicates obtaining a unique model from even a large suite of tracer data. Such complexities are likely to require large amounts of distributed data within a system, as well as tracer data at discharge points, to even narrow the possible range of conceptual models.

[1] Lehmann, B.W., Waber, H.N.m Tolstikhin, I, Kamensky, I., Gannibal, M., and Kalashnikov, E. (2003) *JGR* **30,** no. 3 p. 4

Investigations of Fe(II) sorption onto montmorillonite. A wet chemistry and XAS study

D. SOLTERMANN[1*], M. MARQUES FERNANDES[1], R. DÄHN[1], B. BAEYENS[1], AND M.H. BRADBURY[1]

[1]Laboratory for Waste Management, Paul Scherrer Institut, Villigen PSI, Switzerland, (*daniela.soltermann@psi.ch)

For some important radionuclides (RN) redox processes in high-level waste repositories play an important role in their retention. Virtually all deep underground repository concepts contain large amounts of iron, and reducing conditions will prevail in the long-term. The presence of high ferrous iron (Fe(II)) concentrations in the interstitial porewaters in the near- and far-fields could have a significant influence on the sorption behaviour of certain RNs through sorption competition effects. The best suited approach to investigate the sorption of Fe(II) on clay minerals and the influence of high aqueous Fe(II) concentrations on the RN retention is a multi-disciplinary one, consisting of macroscopic sorption experiments and advanced microscopic techniques, such as X-ray absorption spectroscopy (XAS).

Fe(II) sorption isotherms were measured on native iron containing montmorillonites (SWy with 3.4 wt.% structural Fe and STx with 0.7 wt.% Fe [1]), on a partially reduced SWy (structural Fe(III) reduced by sodium dithionite [2]) and on a synthetic iron-free montmorillonite (IFM) at pH 6.2 in 0.1 M $NaClO_4$ under anoxic conditions (O_2 < 0.1 ppm). The iron sorption on a reduced SWy and on IFM is significantly lower than that measured on native SWy and STx montmorillonites and agrees well with a calculated Fe(II) isotherm using the 2 Site Protolysis Non Electrostatic Surface Complexation and Cation Exchange (2SPNE SC/CE) sorption model [3]. The high sorption values on native iron bearing montmorillonites suggest that the sorbed Fe(II) is oxidised at the clay mineral surface to Fe(III).

XAS was employed to determine the oxidation state and the local structural environment of Fe sorbed on IFM. The results indicate that iron is predominantly present as Fe(II). Furthermore, the XAS analysis showed that Fe(II) is forming inner-sphere complexes at the IFM surface.

These findings support the hypothesis that oxidation of sorbed ferrous iron on the clay mineral surface might occur through an electron transfer to the structural ferric iron. The results of this study will help to better understand the role of Fe(II) in retention processes in radioactive waste repositories and contribute to an improved molecular interpretation of the Fe(II)-clay interaction at the solid-liquid interface under anoxic conditions.

Reference:

1. Van Olphen, H. and J.J. Fripiat, Data Handbook for Clay Materials and Other Non-metallic Minerals. 1979, New York: Pergamon.
2. Stucki, J.W., D.C. Golden, and C.B. Roth, Preparation and handling of dithionite-reduced smectite suspensions. Clays Clay Miner., 1984. **32**(3): p. 191-197.
3. Bradbury, M.H. and B. Baeyens, A mechanistic description of Ni and Zn sorption on Na-montmorillonite. 2. Modelling. J. Contam. Hydrol., 1997. **27**(3-4): p. 223-248.

Identification of Cu-Mo anomalous zones using the Thermo Scientific Niton portable XRF analyzer in the Eaglehead Cu-Mo porphyry deposit, British Columbia, Canada

ALIREZA SOMARIN[1*], AND DAVID CLIFFORD[1]

[1]Thermo Fisher Scientific, Billerica, MA 01824
alireza.somarin@thermofisher.com (* presenting author)

Introduction

The Eaglehead Cu-Mo deposit is a classic porphyry style mineralization hosted by a granite-granodiorite intrusion and felsic volcanic wall rocks in northern British Columbia, Canada. The mineralization varies from disseminated to sporadic veins and veinlets of quartz±chalcopyrite±bornite±molybdenite. To identify Cu-Mo anomalous zones and compare assay data from the Thermo Scientific Niton portable XRF analyzer with the lab data, three sets of analyses were carried out on samples from drill hole DDH-106. These assays include direct shot on the core with the analyzer, and analyses of powder samples obtained from portable mill and grinder.

Results and Conclusion

The comparative studies show that Cu correlation (R^2) increases from 0.81 in direct shot assays to 0.84 and 0.86 in powder samples from mill and grinder, respectively (Table 1). Mo correlation increases from 0.87 in direct shot analyses to 0.95 in samples obtained by grinder. Zn correlation also increases by using powder samples from mill and grinder.

Thermo Scientific Niton XRF Analyzer Method	Lab (ICP-MS)		
	Cu	Mo	Zn
Direct Shot	0.81	0.87	0.66
Grinder	0.86	0.95	0.82
Mill	0.84	NA*	0.88
* Mill material contains Mo.			

Table 1: Correlation (R^2) between Thermo Scientific Niton XRF analyzer and lab assays.

In addition, depth-metal diagrams (Figure 1) show that Cu and Mo anomalous zones can be identified by using the Thermo Scientific Niton analyzer in the field.

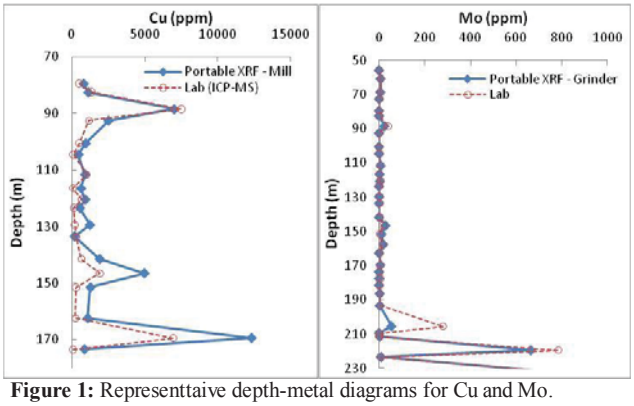

Figure 1: Representtaive depth-metal diagrams for Cu and Mo.

Characterization of re-suspended ash from the Eyjafjallajökull

FRANK SOMMER[1*], VOLKER DIETZE[2], BERNARD GROBÉTY[3], AND RETO GIERÉ[1]

[1] Universität Freiburg, Geowissenschaften, 79104 Freiburg, Germany (FrankSommer@t-online.de) (* presenting author)
[2] Deutscher Wetterdienst, Research Centre Human Biometeorology, Air Quality Department, 79104 Freiburg, Germany
[3] Université de Fribourg, Geosciences, 1700 Fribourg, Switzerland

The 2010 eruption of the Eyjafjalla volcano had a great impact on international air traffic as well as on the local population and illustrated the potential risks of active volcanism. The explosive reaction between magma and glacier ice produced an ash plume of up to 20 km in height in the atmosphere. The present study is focussed on re-suspended ash in ambient air samples collected near the volcano and aims to develop automated analysis techniques for airborne particles in volcanic environments.

Ambient air samples of airborne re-suspended ash were collected in winter 2010/11 with a passive sampler (Sigma-2, Deutscher Wetterdienst), positioned 12 km south of the eruption zone. In a first step, approximately 200 particles were characterized individually using an optical microscope under transmitted, polarized and cross-polarized light and an electron microprobe with BSE and EDX analysis. Subsequently, the light optical images from the same sample were processed with an automated image analysis program, which allowed for classification of the individual particles as glass, mineral, composite or agglutinated particles. Chemical compositions of individual particles were determined from EDX spectra. To gain a statistically relevant dataset for the sample and to maximize the efficiency of the analytic work, a larger area of the same sample, including the area studied manually, was examined using automatic single-particle SEM analysis (EDAX Genesis program), which resulted in characterisation of approximately 1600 particles. The results of both methods were compared against each other to evaluate the advantages and disadvantages of the different approaches and to advance this combined analytical approach. Additionally, one sample of re-suspended ash was examined using X-ray diffraction supplemented by Rietveld-refinement to determine its mineral content.

The examined particles range from 2.5-80 µm in size (equivalent diameters), and their size distribution is typical of ambient aerosol, particles, i.e., decreasing number of particles with increasing diameter. Only ~10% (surface area) of the particles consist of glassy material, i.e. most particles are crystalline. With a surface-area fraction of 63%, feldspar is the predominant mineral (plagioclase 43%, K-feldspar 20%), followed by pyroxene (18%), and quartz (12%). Minor quantities (≤1%) of olivine, ilmenite and titanite are found as well. The sample is also contaminated with salt of oceanic and/or volcanic origin. These results are consistent with the data obtained from the Rietveld-refinement.

Our study shows that a combination of automated and manual analysis is required to obtain best results. Only an automated method allows for examination of a large number of particles, but the manual control is necessary to collect more detailed information about the composition and the crystallinity of the individual particles.

Geochemical evaluation of the karstified Bangestan reservoirs in the Dezful Embayment, SW Iran

HOSSEIN RAHIMPOUR-BONAB[1], AMIN NAVIDTALAB[1], HAMZEH MEHRABI[1], ROSHANAK SONEI[1,2*]

[1]Department of Geology, College of Science, University of Tehran, Iran rahimpor@khayam.ut.ac.ir
[2]Department of Earth Sciences, University of Ottawa, Canada rsone092@uottawa.ca (* presenting author)

Geochemical composition of carbonate sediments are in equilibrium with the contemporaneous sea-water composition in absence of considerable biotic fractionation. However, in carbonate sediments, diagenetic imprints may have considerable effects on primary sediments textures, mineralogy, reservoir quality and finally geochemical characters. Depending on some factors including primary (depositional) sediments characteristics, governing climate and diagenetic history, geochemical composition of carbonates has been altered by post-depositional overprints. Stable isotopes and trace elements analyses can be used as a good tool to measure the extent of these alterations[1,2]. Coupled imprints of tropical climate and recurring emersions had considerable effects on Middle-Upper Cretaceous carbonate reservoirs of the SW Iran (Dezful Embayment) and Middle East region[3]. Petrographic studies (from core to thin section scales) and geochemical analyses (stable isotopes and trace elements) were carried out on 478 samples from five giant and supergiant oilfields in these embayment to reveal the main diagenetic alterations of these karstified carbonate sequences (Fig. 1). Variations in $\delta^{18}O$ and $\delta^{13}C$ compositions and trace elements (Mn, Fe and Sr) concentrations are useful diagenetic indicators that resulted in classification of studied intervals into four diagenetic classes according to their meteoric diagenetic features, intensities and developments.

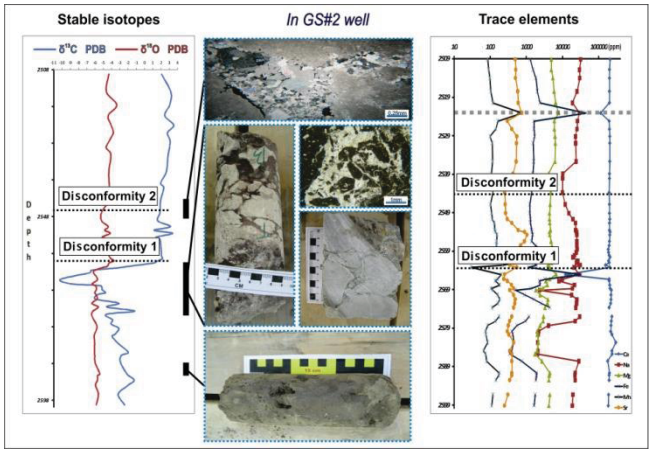

Figure 1: Plot of stable isotopes and trace elements versus depth including the petrographic evidences of karstified intervals of the Bangestan reservoir in GS-2 well.

[1] Brand, U. and Veizer, J., 1980. Chemical diagenesis of a multicomponent carbonate system-I: Trace elements. J. Sediment. Petrology 50: 1219–1236.
[2] Brand, U. and Veizer, J., 1981. Chemical diagenesis of a multicomponent carbonate system-II: stable isotopes: J. Sediment. Petrology, v. 51, p. 987-997.
[3] Hollis, C. 2011. Diagenetic controls on reservoir properties of carbonate successions within the Albian–Turonian of the Arabian Plate. Petroleum Geoscience vol. 17, 3: 223-241.

Silicate polymerization on crystalline and amorphous TiO_2: an ATR-IR and synchrotron XPS investigation

YANTAO SONG[1*], PETER JAMES SWEDLUND[1], JAMES METSON[1], GEOFFREY I.N. WATERHOUSE[1] AND BRUCE COWIE[2]

[1]School of Chemical Sciences, the University of Auckland, y.song@auckland.ac.nz (* presenting author)
[2]Australian Synchrotron, SoftXRay@synchrotron.org.au

Introduction

The presence of silicate at metal oxide-aqueous interfaces influences many oxide properties. Understanding the chemistry of silicate at these interfaces is important to describe the geochemistry of these metal oxides and elements associated with the oxides [1-2]. This work compares silicate sorption and polymerization on the disordered surface of an amorphous TiO_2 ($TiO_{2(am)}$) with silicate chemistry on the well defined faces of rutile TiO_2. The work used *in situ* attenuated total reflectance-infrared spectroscopy (ATR-IR) and *ex situ* synchrotron based X-ray photoelectron spectroscopy (XPS).

Results and Conclusion

The ATR-IR results show that a monomeric silicate species with a Si-O stretching mode at ≈ 950 cm^{-1} formed on all TiO_2 surfaces at low surface coverage. Linear oligomeric silicates with a Si-O IR adsorbance at ≈ 1020 cm^{-1} form when the surface coverage reaches a threshold value (Figure 1). The process of silicate oligomerization was favoured on the crystalline rutile surface compared to the amorphous TiO_2. This agrees with the XPS results and the proposed model of heterogeneous silicate polymerization which would be favoured by the arrangement of TiO_2 octahedra on the rutile (110) face (Figure 2).

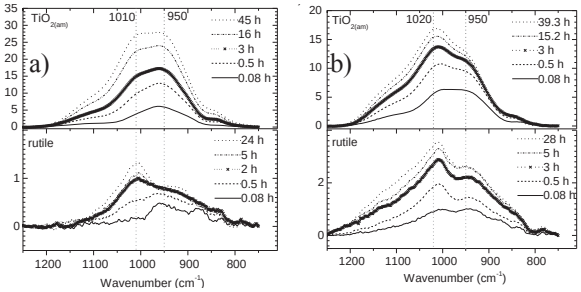

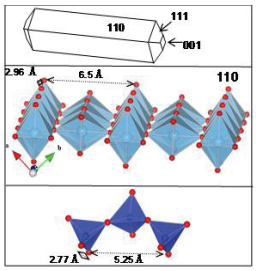

Figure 1 (above): ATR-IR spectra of H_4SiO_4 adsorbed on the surface of $TiO_{2(am)}$ and rutile at pH 9 and 0.1 M NaCl measured over time. Final concentrations of H_4SiO_4 are (a) 0.2 mM and (b) 1.5 mM.

Figure 2 (left): Rutile morphology and enclosing faces. Bottom panel shows a section of ferrosilite, a linear silicate.

[1] Swedlund *et al.* (2011) *Chem. Geol.* **285**, 62-69.
[2] Dol Hamid *et al.* (2011) *Langmuir*. **27**, 12930-12937.

Cr(VI) Reduction and Isotopic Fractionation In Bacteria: Cytoplasmic/Extracellular Reduction Rate and Diffusion Controls

ERIC SONNENTHAL[1*], JOHN N. CHRISTENSEN[1], AND RUYANG HAN[1]

[1]Earth Sciences Division, Lawrence Berkeley National Lab, Berkeley, CA, USA, elsonnenthal@lbl.gov (* presenting author)

Reduction of Cr(VI) to Cr(III) by bacteria is well documented and leads to significant Cr isotopic fractionation ($^{53}Cr/^{52}Cr$), with experimental values in abiotic systems of ~3.4‰[1] to 5‰[2], and theoretical equilibrium values of 6-7‰[3]. Biologically-mediated Cr isotopic fractionation of ~4.2‰[4] has been attributed to kinetic fractionation, with possible controls by metabolic pathways, transport, or reduction sites. In lactate-amended cell suspension experiments with *Pseudomonas stutzeri* strain RCH2, Cr isotopic fractionation was less under denitrifying vs. aerobic conditions[5], and attributed to Cr(VI) transport limitation. In this work, a reactive-transport model was developed to evaluate effects of cytoplasmic/extracellular reduction rates and transport in bacteria on Cr isotopic fractionation with comparison to experimental data.

The multicontinuum reactive-transport model is based on a simplified structure of bacterium *Pseudomonas stutzeri*, of average dimension of 2 x 0.5μm, a cell membrane thickness of 15nm, and an average bacterium spacing derived from the suspension cell density. Cr reduction in the cytoplasm is dependent on chromate diffusive transport through the outer membrane (via sulfate channels), the periplasmic space, and to reduction sites. Cell wall diffusivities were estimated from published cell wall permeabilities. Cr reduction was assumed to be thermodynamically and kinetically-controlled by $Cr(OH)_3$ precipitation using a solid solution model of $^{53}Cr(OH)_3$ and $^{52}Cr(OH)_3$. Simulations considered an aerobic case with lactate oxidation to pyruvate, and a denitrifying case forming pyruvate, as well as conditions of the experiments described in [4].

Simulations with differing cell densities using Toughreact [7] showed that it is necessary to limit diffusive transport through the cell wall by ~4 orders of magnitude to match the change in Cr isotopic fractionation from ~2‰ (aerobic) to ~0.4‰ (denitrifying). By severely limiting diffusive transport, Cr reduction rates decrease significantly, inconsistent with experimental data. In contrast, by increasing the Cr reduction rate in the cytoplasm, a large decrease in the fractionation factor is observed, without inhibiting the Cr reduction rate, capturing the observed $^{53}Cr/^{52}Cr$ and Cr reduction rates over a range of cell densities. Although it is not known where Cr reduction was localized in the cell suspension experiments[5], simulations show that Cr reduction in the extracellular medium also leads to higher Cr reduction rates and Cr isotopic ratios close to the maximum value for the reduction reaction.

[1] Ellis, Johnson & Bullen (2002) *Science* **295**, 2060–2062. [2] Zink, Schoenberg & Staubwasser (2010) *GCA* **74**, 5729–5745. [3] Schauble, Rossman & Taylor (2004) *Chem Geol* **205**, 99-114. [4] Sikora, Johnson & Bullen (2008) *GCA* **72**, 3631-3641. [5] Han *et al.* (in press) *AEM*. [6] Han *et al.* (2010) *ES&T* **44**, 7491-7497. [7] Xu *et al.* (2011) *Comp Geosc* **37**, 763-774.

Structural modifications in densified soda alumino silicate glasses

CAMILLE SONNEVILLE[1*], DOMINIQUE DE LIGNY[1], DANIEL R. NEUVILLE[2], PIERRE FLORIAN[3], SYLVIE LE FLOCH[4], CHARLES LE LOSQ[2] AND GRANT S. HENDERSON[5]

[1]Université de Lyon, Université Lyon 1, Laboratoire de Physico-Chimie des Matériaux Luminescents, CNRS, UMR5620, Villeurbanne, France. camille.sonneville@univ-lyon1.fr (*presenting author)

[2]CNRS-IPGP, Sorbonne Paris Cité, Paris, France

[3]CEMHTI-CNRS, Orléans, France

[4] Université de Lyon, Université Lyon 1, Laboratoire PMCN; CNRS, UMR 5586, Villeurbanne Cedex, France

[5]Dept of Geology, University of Toronto, Toronto, Canada

Summary:

The behaviour of soda aluminosilicate glasses and melts under pressure and temperature is of interest in both the materials and Earth Sciences, especially for understanding magmatic processes. Although these systems have been well studied at room pressure by several workers, their structural modifications at high pressure (HP) are less well known. Several studies have been carried out on glasses quenched from HP using both NMR and XANES. The latter have also been performed on glasses and melts at HP. All these studies revealed structural changes occurring in the glasses and/or melts with increasing pressure.

We synthesized glasses along the NS3/Albite glass join extended into the peralumimous domain. The glasses were permanently densified in a Belt press at the Lyon Plateform of High Pressure Experimentation (PLECE) (5GPa, 600°C) and in a Multi Anvil press at the University of Toronto (7GPa, 600°C). The densified samples were studied with various methods in order to follow the pressure induced structural modifications. Short range order (SRO) was investigated using ^{23}Na, ^{27}Al NMR and Si L-edge XANES. The intermediate range order (IRO) was studied by Raman spectroscopy and long range order (LRO) with Brillouin spectroscopy.

^{27}Al NMR spectra show, with increasing pressure, an increase in the Al coordination, with large amounts of ^{V}Al and ^{VI}Al appearing in glasses with low Al_2O_3 contents. Contrary to this, ^{V}Al and ^{VI}Al increase more slowly for albite and peraluminous glasses. ^{23}Na NMR spectra exhibit a decrease in the Na-O bond length with pressure.

For glasses between NS3 and albite composition, Raman experiments show an increase in Q^2 and Q^4 species with pressure and a symmetrical decrease of the Q^3 species. A strong shift of the vibrational band around 500 cm^{-1} toward higher wavenumbers is observed for albite and peraluminus glass.

The pressure induced structural modifications noted in these glasses are dependent upon composition. For compositions characteristic of depolymerized glasses Al coordination increases and further depolymerization are primarily responsible of the densification process. For compositions indicative of fully polymerized glasses densification mainly occurs as a decrease in the intertetrahedral angle T-O-T. Al *L*- edge XANES and O, Na, Al, and Si *K*-edge XANES along with *in situ* (DAC) experiments will be performed soon to complete this preliminary study.

Heterogeneous hydrous mantle in arc settings: Constraints on the genesis of silica-undersaturated arc magmas

F. SORBADERE[1,2*], E. MEDARD[1,2], D. LAPORTE[1,2], P. SCHIANO[1,2]

[1] Laboratoire Magmas et Volcans, Clermont Université, Université Blaise Pascal, BP 10448, 63000 Clermont-Ferrand, France.

[2] CNRS, UMR 6524, IRD, R 163, 5 rue Kessler, F-63038 Clermont-Ferrand Cedex.

(*F.Sorbadere@opgc.univ-bpclermont.fr)

Partial melting of a hydrous lherzolite mixed with variable amounts of amphibole-bearing clinopyroxenite (OCA2) [1] has been experimentally investigated at 1 GPa between 1150 and 1300°C (piston-cylinder, $Au_{80}Pd_{20}$ capsules) under oxidized condition (FMQ+2). Our new capsule configuration [2] allows efficient melt extraction, with melt layers more than 50 μm wide in the capsule traps.

Peridotite derived melts are hypersthene-normative while amphibole-clinopyroxenite melts are strongly Si-undersaturated (~7 % normative nepheline). Melts derived from lherzolite-clinopyroxenite mixtures containing less than 50% clinopyroxenite have identical major element compositions than melts derived from pure peridotite. Above 50% pyroxenite, the CaO content in melt increases and the SiO_2 content decreases with increasing fraction of pyroxenite in the starting mixture. The transition between Hy-normative and Ne-normative melts occurs for mixtures containing between 50 and 75 % clinopyroxenite, when orthopyroxene disappears from the residue. In contrast, minor elements (K_2O, Na_2O, TiO_2 and H_2O) show a more linear behaviour with continuous mixing trends between the two lithologies, thus highlighting the source heterogeneity. Thus the signature of mantle heterogeneities is preserved in the minor/trace elements composition of the magmas, whereas the major elements are buffered by the dominant peridotitic lithology. Forsterite content of olivines in equilibrium with the melts reaches 91.3 for peridotite and 91.8 for clinopyroxenite and/or mixed lithologies at 1300°C. High-Mg olivines can thus crystallize from non-peridotitic magmas under relatively oxidized conditions at high temperatures.

Most primitive magmas found in arc environments and preserved as melt inclusions in high-Mg olivine (Fo ≥ 88) show Si-undersaturated compositions. The involvement of a heterogeneous source containing amphibole-bearing clinopyroxenites in addition to peridotites is often mentioned to account for the Si-undersaturated character of these melt inclusions [1; 3-5]. Our experiments give further support for this hypothesis, but indicate that either the source is almost exclusively made of amphibole-bearing clinopyroxenites, or the Si-undersaturated melts issued from the clinopyroxenites do not reequilibrate with the peridotites.

[1] Médard *et al.* (2006) *J. Petrol.* **47**, 481-504. [2] Hoffer (2008) PhD thesis, Clermont-Ferrand [3] Métrich *et al.* (1999) *EPSL* **167**, 1-14. [4] Schiano *et al.* (2000) *G3* **1**, n°5, 1018. [5] Elburg *et al.* (2007) *Chem. Geol.* **240**, 260-279.

Transition metal stable isotopes in komatiites

PAOLO A. SOSSI[1], OLIVER NEBEL[1], HUGH ST. C. O'NEILL[1], STEPHEN M. EGGINS[1], MARTIN VAN KRANENDONK[2]

[1] Research School of Earth Sciences, Australian National University, Canberra, 0200, Australia
[2] Geological Survey of Western Australia, 100 Plain St, East Perth, WA 6004, Australia

Komatiites represent large degree partial melts of the mantle (30-50%), which segregated from their sources at high temperatures (>1500°C) and pressures (>5GPa), and are thus largely restricted to the Archaean. As the magnitude of stable isotope fractionation decays according to $1/T^2$, the difference in the stable isotope composition between komatiites and their mantle source is negligible (Dauphas et al., 2009). This permits the characterisation of the stable isotopic composition of the mantle source, provided the effects of alteration and fractional crystallisation can be accounted for.

We present high precision Cu, Zn and Fe isotope analyses for a suite of Early Archaean komatiites (3.5-3.2Ga) from the Pilbara craton, separated from a single dissolution. Fe isotopes bracket a range of compositions from δ^{57}Fe (vs. IRMM-014) of -0.17‰ to +0.17‰. Zn isotopes show a more restricted range of compositions, with δ^{66}Zn varying from -0.1‰ to -0.16‰ (vs. IRMM-3702), consistent with the smaller range hitherto observed in igneous rocks (Albarède, 2004). A well defined increase in both δ^{57}Fe and δ^{66}Zn with decreasing Cr and MgO is attributed to a strong olivine control on their stable isotope composition. Cu isotopes scatter around 0‰ (vs. SRM-976), lacking any systematic trend with indices of differentiation. Nevertheless, confirmation of δ^{65}Cu values near 0‰ in other igneous rocks (Li et al., 2009) indicates no discernible change in the Cu isotope composition of the Earth over time.

While δ^{66}Zn and δ^{65}Cu values are representative of current-day mantle, the komatiite array has δ^{57}Fe that extends to ≈-0.15‰ lighter than the contemporary mantle value. At a given stage in their differentiation, the Pilbara komatiites are also 0.1‰ lighter than komatiites from Alexo (Dauphas et al., 2010).

Compared to carbonaceous chondrites, the Zn composition of the Earth lies at the volatile-poor end of a volatile-depletion trend, where δ^{66}Zn becomes lighter with decreasing Zn/Mg. This is the opposite trend to that expected if Zn were being lost by vaporisation.

[1] Dauphas et al., (2009) *EPSL* **288**, 255-267. [2] Albarède (2004) *RiMG* **55**, 409-427 [3] Li et al., (2009) *Chem. Geol.* **258**, 38-49 [4] Dauphas et al., (2010) *GCA* **74**, 3274-3291

Use of MC-ICPMS for laser ablation U/Pb geochronology of baddeleyite

SOUDERS A.K[1*] AND SYLVESTER P.J.[1]

[1]Department of Earth Sciences, Memorial University of Newfoundland, St. John's, NL, Canada (*kate.souders@mun.ca, psylvester@mun.ca)

Microbeam analyses by laser ablation inductively coupled plasma mass spectrometry (LA-ICPMS) are increasingly used for U-Pb geochronology of zircon. LA-ICPMS is a powerful method for U-Pb geochronology because grains can be dated directly in thin section, avoiding time-consuming laboratory procedures involving heavy liquid separations and ion exchange chromatography. In many silica-poor terrestrial rocks such as mafic dikes, anorthosites, gabbros and carbonatites as well as lunar rocks and Martian meteorites, baddeleyite (ZrO_2) rather than zircon is present. Unlike zircon, the baddeleyite tends to form very small elongate grains, typically no more than 30-50 μm in the longest dimension and less than 20 μm in the smallest dimension. This makes U-Pb analyses of baddeleyite by LA-ICPMS more challenging than for zircon because smaller laser spot sizes (<20 μm) and shorter ablation times (<30 sec) are required, reducing analytical precision significantly compared to zircon analyses.

High-precision thermal ionization mass spectrometry (TIMS) is commonly used for U-Pb baddeleyite geochronology of Large Igneous Provinces (LIPs), particularly where mafic magmatic events need to be determined with a precision better than 5 Ma. In cases where ages with uncertainties of approximately 20 Ma provide useful data for LIPs, however, it would be desirable however to apply LA-ICPMS to U-Pb baddeleyite geochronology.

We report a U-Pb dating method for baddeleyite by LA-multi-collector-ICPMS using a Thermo Scientific NEPTUNE MC-ICPMS. The collector array consists of six Channeltron ion counters allowing for the simultaneous collection of ^{202}Hg, ^{204}Pb, ^{206}Pb, ^{207}Pb, ^{208}Pb and ^{235}U isotopes. The use of a collector array consisting only of ion counters eliminates the need of cross-calibration between ion counters and Faraday detectors. Standard – sample – standard bracketing is employed to correct for instrumental mass bias using Forest Center baddeleyite (FC-4b; TIMS age = 1095.42 ± 0.16 Ma) as a standard. A slow line scan ablation is used where a 4μm laser beam with an energy density of 9 J/cm^2 and a repetition rate of 5 Hz scans across the sample surface at a rate of 1 μm/sec. Using the method described, after 30 sec (150 pulses) of ablation, the ^{207}Pb/^{206}Pb age determined for the ca. 2060 Ma Phalaborwa baddeleyite is 2058.9 ± 18 Ma (2σ, n = 6) with an external precision of 0.9 % (2RSD). While this result is comparable to U-Pb zircon and analyses by single-collector LA-ICPMS, the smaller volume of material consumed and the shorter ablation time required to achieve such precision during multi-collector analyses is more suitable for, typically smaller, baddeleyites. The described method can be used as a reconnaissance tool to screen baddeleyite grains prior to physical separation for further high precision TIMS analyses, in order to identify critical samples that can be used for paleocontinental reconstruction in LIPs.

AMS studies in "Foz do Douro metamorphic complex" (N Portugal): preliminary insight

MÓNICA SOUSA[1*], HELENA SANT'OVAIA[1] AND FERNANDO NORONHA[1]

[1]Porto University, DGAOT, CGUP, Porto, Portugal, monica.sousa@fc.up.pt (* presenting author) hsantov@fc.up.pt fmnoronh@fc.up.pt

Introduction

The "Foz do Douro Metamorphic Complex" (FDMC) is situated on the shoreline of Porto extending along a series of small beaches between the Douro river mouth and the "S. Francisco Xavier" Fort. The geology of this zone is marked by the presence of Porto-Tomar-Fereira do Alentjo, NNW-SSE dextral, shear zone and by magnificent outcrops of a thin band of Precambrian metamorphic rocks intruded by Variscan granites [1,2]. The metamorphic band is represented by outcrops of metasedimentary rocks, spatially associated to orthogneisses of different types and ages (606±17 to 567± 6 Ma) and amphibolites that constitute the FDMC [3]. The granites belong to a late-Variscan granite group (298±11Ma) [4].

A Anisotropy of magnetic susceptibility (AMS) study is being carried out in these several types of orthogneisses. In this work we present the first data obtained with 49 samples of leucocratic gneisses, some with garnet, and augen gneisses (Group 1) and with 15 samples of biotite-rich orthogneisses (Group 2).

Results and Discussion

Magnetic susceptibility (K) ranges between 20.0 and 72.3 x 10^{-6} SI in Group 1 orthogneisses which indicates a paramagnetic behaviour of this lithology, due to ferromagnesian minerals, such as biotite. However in Group 2 orthogneisses, K presents values > 10^{-3} SI (0.12 x 10-3 SI, in average) which enhance the presence of magnetite. These two distinct behaviours indicate two different types of Precambrian magmatism: a oxidized type (magnetite type) (Group 2) and a reduced type (Group 1).

Magnetic anisotropy, expressed by the ratio Kmax/Kmin, ranges from 1.052 to 1.144 in Group 1 orthogneiss and is higher (1.204) in the Group 2 gneisses. These values are typical of deformed rocks but the high anisotropy of the Group 2 orthogneisses also reflects the presence of magnetite. In both lithologies, magnetic fabric is characterised by subvertical magnetic lineations associated to subvertical E-W to ESE-WNW and NW-SE trending magnetic foliations, related to a shear deformation.

[1] Chaminé *et al*. (2003) *Cadernos Lab. Xeolóxicos de Laxe* **28**, 37-78. [2] Ribeiro *et al*. (2009) *C. R. Geoscience* **341**, 127-139. [3] Noronha & Leterrier (2000) *Revista Real Academia Galega de Ciências* **XIX,** 21-42. [4] Martins *et al*. (2011) *C. R. Geoscience* **343**, 387-396.

Acknowledgements

Research carried out at the "Centro de Geologia UP" an R & D unit from "Fundação para a Ciência e Tecnologia" (FCT) and first author is being funded by a doctoral scholarship from FCT (SFRH/BD/47891/2008).

The Role of Metal Redox Coupling Processes in Carbon Cycling and Stabilization

DONALD L. SPARKS[*1], CHUNMEI CHEN[1], OLESYA LAZAREVA[1], JOSHUA LEMONTE[1], JAMES J. DYNES[2], JIAN WANG[2], AND TOM REGIER[2]

[1] Delaware Environmental Institute (DENIN), Newark, USA dlsparks@udel.edu* (*presenting author), cmchen@udel.edu, olazarev@udel.edu, lemonte@udel.edu

[2]Canadian Light Source, Saskatoon, Canada James.Dynes@lightsource.ca , Jian.Wang@lightsource.ca, Tom.Regier@lightsource.ca

The association of carbon with mineral phases has been increasingly recognized as a major stabilizing mechanism for protecting organic matter against microbial degradation in soils. Iron (Fe) and manganese (Mn) oxides are of particular importance because of their abundance in soils and high reactive surface area. Both Fe and Mn are susceptible to redox variability along landscape gradients. Reductive dissolution and transformation of Fe and Mn minerals governs the amount, form and transport of sequestered C. We have investigated Fe speciation as well as the composition of organic matter and its molecular interaction with soil minerals across hillslope transects within the Christina River Basin Critical Zone Observatory (CRB-CZO) to link iron-redox coupling processes with soil C cycling. Selective chemical extractions, X-ray absorption spectroscopy (XAS), micro-XAS techniques, and Mossbauer spectroscopy were employed to characterize soil Fe speciation. Applying scanning transmission X-ray microscopy (STXM) and carbon near edge X-ray absorption fine structure (CNEXAFS) spectroscopy, we mapped the spatial distribution of carbon and carbon forms, and imaged the association of organic functional groups with specific minerals in the soils. Ferrihydrite, because of its ubiquitous occurrence in the environment and its high surface area, contributes significantly to the sorption of organic matter and protects it against microbial degradation in soils and sediments. In addition, ferrihydrite often forms in the presence of dissolved organic matter in the natural environment, which leads to coprecipitation of organic matter with ferrihydrite. However, the extent and mechanisms of organic matter adsorption to or coprecipitation with ferrihydrite, and the consequences of such reactions for the properties of sorbed versus coprecipitated organic matter remain largely unknown. In this presentation, we compare adsorption and coprecipitation with dissolved organic matter from a forest litter layer. To examine the chemical fractionation of the organic matter and the mechanisms of organo-ferrihydrite complex formation associated with these two processes CNEXAFS and Fourier transform infrared (FTIR) spectroscopic techniques were employed. To study spatial distribution, macromolecular structure, and chemical composition of sorbed and coprecipitated OM at the nanometer-scale we used STXM. Data on the role of Mn in C cycling will also be presented. Such studies will enhance our understanding of OM stabilization mechanisms on soil mineral surfaces and will provide new insights on the metal-redox coupling processes affecting carbon cycling at soil/sediment-water interfaces.

Tectonic implications of short metamorphic episodes

FRANK S. SPEAR[1]*, KYLE T. ASHLEY[2], LAURA E. WEBB[3], AND J. B. THOMAS[1]

[1]Renssaelaer Polytechnic Institute, Troy, USA, spearf@rpi.edu (*presenting author), thomaj2@rpi.edu
[2]Virginia Tech, Blacksburg, USA, ktashley@vt.edu
[3]University of Vermont, Burlington, USA, lewebb@uvm.edu

Quartz inclusions in garnet undergo exchange of Ti with the host garnet resulting in diffusion of Ti into the quartz. Modeling of this diffusion in samples from the Barrovian terrane of eastern Vermont reveals that the entire metamorphic episode (heating from 450 C to metamorphic peak and cooling back to 450 C) has occurred in less than 1 m.y. and perhaps in as little as a few hundred thousand years, depending on the presumed peak metamorphic temperature. This terrane does not contain volumetrically significant plutons, so the only possible cause must be tectonic.

Two-dimensional thermal modeling has been used to constrain the rates of thrusting required to achieve such short-lived metamorphic episodes. Rocks heat rapidly when overthrust by hot rocks and cool rapidly when they are thrust onto cooler rocks, a process that has been modeled as a simple, mid-crustal duplex structure. A typical model involves the first thrust sheet moving up a 20 degree ramp at a rate of 10 cm/year (0.1 m/year) for 0.1-0.5 m.y. then the fault stepping out (in sequence) and a second thrust sheet moving up a similar ramp for a similar time interval. The rocks of interest are those in the horse between the two thrusts which are initially loaded quickly and subsequently heated by thermal conduction from the overlying hotter rock mass. The second thrust places these hot rocks onto cooler substrate which initiates cooling of the mass but not necessarily a change in pressure. Exhumation was likely to have been rapid following the metamorphic peak, consistent with the rapid post-peak cooling history inferred from the diffusion studies. The near isothermal loading exhibited by P-T paths of rocks from eastern Vermont also supports the hypothesis of crustal loading at rates of 5-10 cm/year.

The rate of heating and cooling depends on the thermal difference between the overthrust sheet and the rocks of interest, and the proximity of the rocks to the thrust. Models with different thrust sheet dimensions reveal that it is impossible to rapidly heat and cool the same rock if the sheet is thicker than ca 5 km. This fact raises the interesting possibility that metamorphic terranes that have experienced such rapid heating and cooling are comprised of thin thrust sheets bounded by ductile shear zones stacked together in duplex-like geometries with significant internal deformation. Such geometries might be very difficult to decipher with the limited outcrop exposure in Vermont. It is also interesting to speculate that the two major “deformations” that produce the two dominant fabrics in these rocks were caused by the initial loading and subsequent ramping of the thrust sheet, respectively. Thrust ramps also produce ramp anticlines that, in ductile terranes, will have the geometries of domes as are seen in eastern Vermont.

Such rapid tectonic juxtaposition is unresolvable by current geochronologic techniques, and is only revealed through diffusion modeling of systems with diffusivities appropriate for the metamorphic conditions.

Timing and mechanism for intratest Mg/Ca variability in living planktic foraminifera

HOWARD J. SPERO[1*], STEPHEN M. EGGINS[2], ANN D. RUSSELL[1], LAEL VETTER[1], BÄRBEL HÖNISCH[3]

[1]University of California Davis, Dept. Geology, Davis CA., USA; hjspero@ucdavis.edu (* presenting author)
[2]The Australian National University, Research School of Earth Sciences, Canberra, Australia; Stephen.Eggins@anu.edu.au
[3] Columbia University, Lamont-Doherty Earth Observatory, Palisades, NY, USA, hoenisch@ldeo.columbia.edu

Problem and Results

Recent microscale data indicate that Mg/Ca in foraminifera tests is distributed heterogeneously, thereby challenging its use as a robust tool for paleotemperature reconstructions. We present Mg/Ca and Ba/Ca data collected by laser ablation (LA) ICPMS from living *Orbulina universa*, that were grown in controlled laboratory experiments. Test calcite was labeled with Ba-spiked seawater for 12h periods during either day or night calcification, to quantify the timing of intratest Mg-banding across diurnal cycles. Results demonstrate high Mg bands are precipitated during the night, whereas low Mg bands are precipitated during the day. Similarly, the amplitude of the Mg/Ca ratios in Mg-rich bands decreases in experiments with elevated pH (and $[CO_3^{2-}]$). These results suggest that symbiont photosynthesis influences but does not fully control Mg/Ca banding. We hypothesize that mitochondrial uptake of Mg^{2+} may explain Mg-depleted calcite layers. Symbiont photosynthesis and foraminifera respiration may exert a secondary influence on shell Mg/Ca via their effect on $[H^+]$ in the microenvironment around the calcifying shell. Data obtained from specimens growing at 20º and 25ºC show that intrashell Mg/Ca ratios increase with temperature in both high and low Mg bands, such that average test Mg/Ca ratios are in excellent agreement with temperature calibrations based on bulk solution ICPMS analyses.

Conclusion

Results presented here demonstrate that Mg banding is an inherent component of the biomineralization process. However, despite intratest Mg/Ca variability, the Mg/Ca paleothermometer as measured on whole tests remains a robust tool for reconstructing past ocean temperatures from the fossil foraminifera record.

Ab initio vibrational properties of silica species in aqueous fluids

G. SPIEKERMANN[1*], M. STEELE-MACINNIS[2], C. SCHMIDT[1], P. M. KOWALSKI[1] AND S. JAHN[1]

[1]GFZ German Research Centre for Geosciences, Section 3.3, Telegrafenberg, 14473 Potsdam, Germany, spiek@gfz-potsdam.de (* presenting author)

[2]Department of Geosciences, Virginia Tech, Blacksburg VA 24061, USA, mjmaci@vt.edu

The solubility of minerals in aqueous fluids is an important property to understand the chemical transport of elements. On the atomic-scale the solubility is related to the solute speciation in the fluid. Vibrational spectroscopy is especially useful for probing solute speciation in aqueous fluids because vibrational frequencies depend on molecular structure. Assignment of spectroscopic features to specific structural units can be challenging, but atomic-scale modeling may provide support [1, 2].

We investigate the vibrational properties of silica species in aqueous solution at high pressures and temperatures. The investigated species include H_4SiO_4 and $H_3SiO_4^-$ monomers, $H_6Si_2O_7$ and $H_5Si_2O_7^-$ dimers, three and fourfold silica rings and higher polymers [3]. Simulations are performed at the level of density-functional theory with the PBE exchange-correlation functional. We use periodic boundary conditions and a system of 25-27 H_2O molecules at 300 K and 1000 K, at a fluid density around 1 g/cm^3.

In our approach to analyze the vibrational properties, we exploit the two facts that (1) observed Raman frequencies are equal to the real vibrational frequencies, and (2) the spectroscopically important silica vibrations are quasi-localized normal-mode-like vibrations. The concept of mode-projected velocity autocorrelation (VACF) and its Fourier transform [4] is applied to yield normal-mode-like vibrational subspectra of the vibrational density of states, e.g. from tetrahedral subunits (T_d), Si-O-Si units of bridging oxygens (C_{2v}), the dimer (C_{3d}/C_{3h}), the SiOH bending, and "breathing" of silica rings.

Our results give a comprehensive picture of the vibrational behaviour of small silica species such as monomers and dimers. New insight is given into the polymerization-driven frequency shift. Our studies help to clarify vibrational contributions of Q^1 tetrahedra, the silica dimer, Q^2 tetrahedra, and the SiOH bending motions. We demonstrate that the mode-projection technique is a powerful tool for investigation of vibrational properties of isolated and network-forming species in their environment at elevated temperatures and pressures.

[1] Zotov & Keppler (2000), *American Mineralogist*, **85**, 600-604
[2] Tossell (2005), *Geochimica et Cosmochimica Acta*, **69**, 283-291
[3] Spiekermann, Steele-MacInnis, Kowalski, Schmidt & Jahn (2012), submitted to *Journal of Chemical Physics*
[4] Pavlatou, Madden & Wilson (1997), *Journal of Chemical Physics*, **107**, 10446-10457

Lunar Lu-Hf and Sm-Nd systematics – effects of neutron capture reactions

P. SPRUNG[1*], T. KLEINE[2], AND E.E. SCHERER[3]

[1]Institute for Geochemistry and Petrology, ETH Zürich, Switzerland, sprung@erdw.ethz.ch (* presenting author)

[2]Institut für Planetologie, Westfälische Wilhelms-Universität Münster, Germany, thorsten.kleine@uni-muenster.de

[3]Institut für Mineralogie, Westfälische Wilhelms-Universität Münster, Germany, escherer@uni-muenster.de

The silicate differentiation history of planetary objects including the Moon can be constrained by combined Lu-Hf and Sm-Nd studies [1]. Previous Lu-Hf studies on lunar basalts [2-6] yielded results broadly consistent with a magma ocean history for the Moon as constrained by Sm-Nd systematics, but some inconsistencies persist: Most KREEP-rich bulk rocks have initial $^{176}Hf/^{177}Hf$ that are too radiogenic, overlapping the composition of chondrites at the same time, and are inconsistent with the unradiogenic initial $^{143}Nd/^{144}Nd$ of KREEP. This disparity in the Lu-Hf and Sm-Nd systems may reflect a non-chondritic composition of the Moon [7] but could also be due to capture of (epi)thermal neutrons (NC) during cosmic-ray exposure of the lunar surface [8]. NC reactions can induce positive shifts in measured $^{176}Hf/^{177}Hf$ [8] and negative shifts in measured $^{143}Nd/^{144}Nd$ [9]. However, none of the previous Lu-Hf studies of lunar samples accounted for NC effects. To assess the significance of NC effects on the lunar Lu-Hf and Sm-Nd systematics we obtained Lu-Hf, Sm-Nd, and Hf and Sm isotope data for a suite of lunar samples (KREEP-rich rocks and mare basalts).

The KREEP-rich samples display no NC-induced Hf or Sm anomalies and yield the lowest initial $^{176}Hf/^{177}Hf$ yet reported for any KREEP-rich rock. In contrast, most mare basalts exhibit well-resolved, NC-induced anomalies in Hf and Sm. Low-Ti mare basalts show the strongest NC effects, with $^{180}Hf/^{177}Hf$ and $^{149}Sm/^{152}Sm$ as low as ≈820 ppm and ≈72 ε-units below those of terrestrial samples, respectively. NC-induced ^{180}Hf and ^{149}Sm anomalies are well correlated, yielding distinct slopes for low- and high-Ti mare basalts. The errors in measured $^{176}Hf/^{177}Hf$ and $^{143}Nd/^{144}Nd$ induced by NC reactions are up to +12 and -0.7 ε-units, respectively.

The well-defined, distinct correlations between ^{149}Sm and ^{180}Hf anomalies in low- and high-Ti mare basalts imply almost constant neutron energy spectra for chemically similar samples. Using the respective neutron energy spectra and published ^{149}Sm data [e.g., 9], we estimate that the $^{176}Hf/^{177}Hf_{now}$ previously reported for low- and high-Ti mare basalts are too high by up to 7 and 1.7 ε-units, respectively. Published ^{149}Sm data suggest that previously reported data for KREEP-rich rocks are biased by NC reactions too, thus yielding more radiogenic initial $^{176}Hf/^{177}Hf$ values than expected for KREEP. Interpreting lunar Lu-Hf and Sm-Nd systematics without accounting for NC effects may thus yield erroneous conclusions.

[1] Patchett (1983) *GCA* **47**, 81-91. [2] Unruh et al. (1984) *J Geophys Res* **89 suppl.**, B459-B477. [3] Unruh and Tatsumoto (1984) *LPS XV*, 876-877. [4] Beard et al. (1998) *GCA* **62**, 525-544. [5] Patchett and Tatsumoto (1998) *LPS XII* , 819-821. [6] Brandon et al. (2009) *GCA* **73**, 6421-6445. [7] Caro and Bourdon (2010) *GCA* **74**, 3333-3349. [8] Sprung et al. (2010) *EPSL* **295**, 1-11. [9] Nyquist et al. (1995) *GCA* **59**, 2817-2837.

Integrating geochemical, reactive transport, and facies-based modeling approaches at the contaminated Savannah River F-Area

NICOLAS SPYCHER[1*], SERGIO BEA[1], HARUKO WAINWRIGHT[1], SUMIT MUKHOPADHYAY[1], JOHN N. CHRISTENSEN[1], WENMING DONG[1], SUSAN S. HUBBARD[1], JIM A. DAVIS[1], AND MILES DENHAM[2]

[1]Lawrence Berkeley National Lab., Berkeley, CA 94720, USA, nspycher@lbl.gov (* presenting author)

[2]Savannah River National Laboratory, Aiken, SC 29808, USA

Objective

This study aims at understanding key hydrogeochemical processes dictating pH behavior and U transport at the Savannah River F-Area in South Carolina, USA. A nearly 1 km long acidic plume has developed under this site from the disposal of low-level acidic radioactive waste solutions into seepage basins overlying relatively permeable, mostly sandy sediments. The impact of chemical and physical heterogeneities on contaminant mobility is of particular interest.

Approach and Results

Various geochemical, horizontal 1D, and vertical 2D reactive transport simulations are conducted, that include the effects of mineral dissolution and precipitation, as well as H+ and U(VI) sorption using surface complexation models. Simulations consider the historical 35-year discharge of U-bearing nitric acid solutions, followed by a post-discharge period of 65 years. The concept of "reactive facies", integrating sediment chemical and hydrophysical properties with geophysical signatures, is explored to spatially distribute linked physical and chemical heterogeneities at local and field scales. Results of isotopic studies are also used to constrain the modeling effort. Simulations are conducted in a step-wise manner, first considering only the saturated zone then increasing complexity by including the vadose zone and a free water table.

Simulations indicate that H^+ sorption reactions on goethite and kaolinite (the main minerals at the site besides quartz), and the precipitation of Al minerals could delay the pH rebound for decades. Such slow rebound is likely to be exacerbated by residual saturation of the plume below the discharge basins. U concentrations potentially could decrease faster than pH from dilution with clean recharge water.

Two reactive facies are identified in the main formation at the site, each with distinct effects on predicted plume migration. Heterogeneous reactive properties (i.e., surface areas) within each facies, however, do not appear to affect the simulated historical pattern of the plume, because sorption sites become quickly saturated by the massive H^+ and U influx during the discharge period. Consequently, intra-facies heterogeneities mostly affect the predicted pH and U transport at early times and at the plume edges, and are expected to become relevant over the long term only once contaminant concentrations have decreased below sorption saturation levels. Rigorous uncertainty quantification studies are underway to further evaluate the effect of key model input parameters on model predictions.

Calcite Growth from the Molecular Scale.

ANDREW G. STACK[1*], JACQUELYN N. BRACCO[2], PAOLO RAITERI[3], JULIAN D. GALE[3], MEG C. GRANTHAM[2]

[1] Chemical Sciences Division, Oak Ridge National Laboratory, Oak Ridge, TN, U.S.A., stackag@ornl.gov * presenting author

[2] School of Earth and Atmospheric Sciences, Georgia Institute of Technology, Atlanta, GA, U.S.A.

[3] Nanochemistry Research Institute, Dept. of Chemistry, Curtin University, Perth, WA, Australia

Calcite ($CaCO_3$) growth and dissolution play important roles in determining ocean and subsurface geochemistry, such as buffering pH and serving as a biomineral for a large number of organisms. An understanding of the molecular-level mechanisms by which calcite grows and dissolves may enhance our ability to understand and predict the response of calcite to changes in these environments.

While abundant measures of calcite growth and dissolution rates exist, these are often made by measuring the solution composition over time, a method which convolutes the multiple reactions that occur on the mineral surface itself and these studies therefore have limited value in understanding reaction mechanisms. Historically, most surface sensitive techniques applied to this problem have probed calcite reactivity under stoichiometric solution compositions, which also cannot distinguish between the independent reactivities of calcium and carbonate. Using *in situ* atomic force microscopy, Stack and Grantham[1] and others[2] have recently shown that the ratio of calcium-to-carbonate plays an important role in determining overall reaction rate.

Here, we will evaluate the efficacy of analytical crystal growth models applied to the advance of monomolecular steps on the calcite surface. In particular we will focus on how well they capture the response of step velocity under varying saturation index as well as aqueous calcium-to-carbonate ratio. We will use strontium and its inhibitio of growth as an indicator of how well these models are capturing the salient aspects of reactions such as the nucleation and propagation of kinks on steps. At the time of writing, no single model yet derived captures the entirety of the richness of reactivity observed.

As an alternative to pre-defined analytical models fit to experimental data, we also will show the results of rare event theory molecular dynamics simulations applied to the same kink site reactions on the calcite surface. This method was recently successfully applied to the barite ($BaSO_4$) {120} steps[3]. These have the potential to give accurate reaction rates and mechanisms independent of a crystal growth model.

This research was sponsored by the Division of Chemical Sciences, Geosciences, and Biosciences, Office of Basic Energy Sciences, U.S. Department of Energy.

[1] Stack, A. G.; Grantham, M. C. (2010) *Cryst. Growth Des.*, **44**, 1602.
[2] Perdikouri, C. et al. (2009) *Cryst. Growth Des.*, **9**, 4344.
[3] Stack, A. G.; Raiteri, P.; Gale, J. D. (2012) *J. Am. Chem. Soc.* **134**, 11.

Arsenic transport from former mine sites: an empirical modeling approach

DAVID H. STACK[1*], CHRISTOPHER S. KIM[2], JAMES J. RYTUBA[3]

[1]Chapman University, School of Earth and Environmental Sciences, Orange, USA, stack104@mail.chapman.edu (* presenting author)
[2]Chapman University, School of Earth and Environmental Sciences, Orange, USA, cskim@chapman.edu
[3]U.S. Geological Survey, Menlo Park, USA, jrytuba@usgs.gov

As a result of extensive gold and silver mining in California, elevated levels of naturally-occurring arsenic and other trace metals are exposed in mine wastes located in semi-arid regions (e.g. the western Mojave Desert). With extended periods of weathering and erosion, these potentially toxic elements can become mobilized and contaminate surrounding communities. Concerns over the health of individuals living in and visiting these communities have increased due to the greater awareness of this issue [1, 2]. In the past, other studies on this topic have focused on the chemical characteristics of wash sediments [3], the spatial distribution around mine sites [4], and the sources of the heavy metals [5]. While there has been some work in other semi-arid environments examining wash sediments [6], an empirical model used to reconstruct the concentration patterns observed in mining regions has not been developed.

This study sought to examine the role infrequent rain events have on the transport of mine tailings down washes and conduct a quantitative analysis of the empirical observations at multiple mine sites. Soil and sediment samples were collected from multiple mine sites in the Mojave Desert and analyzed for a suite of 49 elements. Distances between points were calculated and plotted against arsenic concentration. An empirical model was then developed and fitted to the data to explain the fluvial migration of mine wastes down washes.

The field data indicated that arsenic concentrations are highest closest to the main waste pile. Generally, as the distance from the pile increases, the arsenic concentration decreases. However, due to the complex patterns of each wash resulting from multiple source inputs and episodic movements of mine wastes, multiple power law trends were used to model the variations, and apparent pulses, of arsenic concentration. These pulses can be representative of infrequent, but intense, rainfall events occurring in the past that are characteristic to semi-arid environments. This has implications for future modeling efforts in similar environments as a potentially predictive tool for the nature of mine waste fate and transport.

[1] Eisler (2004) *Elements* **180**, 133-165. [2] Hudson-Edwards (2011) *Elements* **7**, 375-379. [3] Gonzalez-Fernandez (2011) *Environmental Earth Sciences* **63**, 1227-1237. [4] Chopin (2007) *Water Air and Soil Pollution* **182**, 245-261. [5] Wu (2011) *Environmental Earth Sciences* **64**, 1585-1592. [6] Razo (2004) *Water Air and Soil Pollution* **152**, 129-152.

Strontium-, Magnesium- , Sulfur- and Bromine-isotopes as indicators for brine origin and migration

SUSANNE STADLER[1]*, FRIEDHELM HENJES-KUNST[1], ORFAN SHOUKAR-STASH[2], DIETER BUHL[3]

[1]BGR-Federal Institute for Geosciences and Natural Resources, susanne.stadler@bgr.de (* presenting author)
[2]University of Waterloo, Canada
[3]Ruhr-University Bochum, Germany

Introduction

Causes and extents of subrosion processes following potash mining activities are still under debate for the city of Stassfurt, Germany. In our study, we investigate the role of groundwater in this context, and examined a set of environmental tracers to identify the water's origin from different aquifers (Quaternary, Triassic, caprock and the saline Zechstein formation (including flooded former mining shafts). Groundwater flow in strata covering the salt dome is well constrained: Stadler et al. [1] showed that the sampled groundwater could be related to multi-component mixing processes having occurred under three time scales: young groundwater ages were locally found (0-50 a), an old (< 40 ka) component was identified by radiocarbon data, and contact between meteoric water and Zechstein salts (naturally or anthropogenically induced) could be identified by the presence or absence of Permian crystallization water from the dissolution of e.g. Carnallite and/or Kieserite. Interactions between these components could be idenfied for the studied site. However, the origin and fate of highly saline water sampled from both the salt dome and the mining shalts remained unclear. A non-traditional isotope ($^{87}Sr/^{86}Sr$, $\delta^{26}Mg$, $\delta^{81}Br$, $\delta^{34}S\text{-}SO_4$ and $\delta^{18}O\text{-}SO_4$) study was initiated to gain insight into the brine history.

Results and Conclusion

$^{87}Sr/^{86}Sr$ of saline water samples range 0.70713 to 0.71014 with Sr concentrations varying between 0.2 and 52.3 mg/L. $\delta^{81}Br_{SMOB}$ values were found to range between 0.16‰ and 1.01‰ with Br concentrations of 6 to 3336 mg/L. $\delta^{34}S_{VCDT}$ and $\delta^{18}O_{VSMOW}$ (of SO_4) range from 0.5‰ to 15.4‰ and from 4.5‰ to 11.7‰, respectively, with SO_4 concentrations varying between 0.2 and 33 g/L. $\delta^{26}Mg_{DSM3}$ values range from -0.794‰ to 0.291‰ with Mg concentrations up to 84 g/L. Rocks from the various aquifers were also examined. Combining the isotopic results with geochemical data indicate that saline water samples from the Zechstein formation are largely unmodified residual brines formed during evaporation. The brines could be identified according to their origin (potash salt z(K2) or anhydrite z(A3) (and in few cases Leine salt residuals z(Na3)). For instance, potash salts and related brines could be linked by in part highly radiogenic $^{87}Sr/^{86}Sr$. $\delta^{26}Mg$ could not differentiate betweeen z(K2) and z(A3). Both sets of isotopes can however, clearly identify evaporitic components in fluids of cover layers.

[1] Stadler, S., Sültenfuß, J., Holländer, H., Bohn, C. Jahnke, C., Suckow, A. (2012): Isotopic and geochemical indicators for groundwater flow and multi-component mixing near disturbed salt anticlines. Chemical Geology 294-295: 226-242.

The stability of carbon and carbonate within eclogites

V. STAGNO[1]*, Y. FEI[1], C.A. MCCAMMON[2] AND D. J. FROST[2]

[1] Geophysical Laboratory, Carnegie Institution of Washington, Washington, DC, USA. (* presenting author)
vstagno@ciw.edu
[2] Bayerisches Geoinstitut, Universität Bayreuth, D-95440, Germany

The redox conditions at which carbon and carbonate are stable in eclogitic settings are still relatively uncertain with respect to temperature and pressure of stability for these rocks. A comparison between the oxygen fugacity defined by carbon/carbonate equilibria in peridotite [1] and eclogite assemblages [2] indicates that diamond-bearing eclogites might be stable at conditions where only carbonates would be stable in peridotite rocks. However, these conclusions are suggested by thermodynamic predictions involving possible equilibria in eclogitic rocks, while an experimentally calibrated oxybarometer is still not available.

We conducted experiments to determine the oxygen fugacity at which elemental carbon coexists with carbonate minerals and melts in synthetic eclogites representative of natural assemblages. We performed experiments at both above and below the solidus of a carbonated eclogite in the Na-Ca-Mg-Al-Si-Fe-O-C system at pressures between 3 and 25 GPa and temperature of 800-1600 °C. Iridium powder was added to the starting mixture to act as redox sensor. Experiments were run in piston cylinder and multi anvil devices. Further, we were able to measure the ferric iron of omphacite and garnet equilibrated with graphite (or diamond) and carbonate (solid or melt) in the eclogitic assemblages using Mössbauer spectroscopy. Experimental results of the oxygen fugacity at which graphite/diamond and carbonate are equilibrated within an eclogitic assemblage, were parameterized as a function of pressure and temperature.

Results from this study improve our knowledge regarding the origin of diamonds in eclogitic rocks as well as the fate of carbon when subducted back into the mantle. Further, the results allow us to determine the ferric iron contents of eclogitic minerals, such as garnet and omphacite, as a function of pressure and temperature in presence of carbon-bearing phases, and they are used to develop an oxygen thermo barometer for eclogitic rocks.

[1] Stagno, V., and D. J. Frost (2010) *Earth Planet. Sci. Lett.* **30**, 72-84. [2] Luth, R.W. (1993) *Science,* **261**, 66-68.

Carbon cycling in oil sands tailings ponds mature fine tailings under sulphate - reducing and methanogenic conditions: A microcosm study

SEBASTIAN STASIK[1]* AND KATRIN WENDT-POTTHOFF[1],

[1]UFZ Helmholtz Centre for Environmental Research,Magdeburg, Germany, sebastian.stasik@ufz.de (* presenting author)

Oil sands tailings ponds are considered as a permanent storage and remediation approach for the extraction waste of the oil sands industry in the Athabasca Basin in northeastern Alberta (Canada). The anaerobic biodegradation of organic contaminants as well as the microbially mediated methane production, which can enhance the densification of the fine tailings, have been studied for many years. Thereby the anaerobic degradation of hydrocarbons is proposed to be accomplished by a complex microbial consortium, including syntrophic and methanogenic microorganisms as well as microbes of the iron,- nitrogen- and sulphur cycle.

Using selective cultivation, we detected heterotrophic and autotrophic sulphate reducers, thiosulphate oxidisers, and iron reducers in frequencies similar to those of natural lakes. To understand the interactions of indigenous methanogenic and sulphate-reducing communities, we conducted a 6 month microcosm experiment with mature fine tailings (MFT) supplemented with different carbon sources as well as molybdate and/or BES as specific inhibitors for the processes of sulphate reduction and methanogenesis. The carbon sources comprised low molecular weight electron donors (e.g. acetate, lactate, ethanol) that are and typically generated during hydrocarbon degradation and serve as easily available carbon sources[1].

We found that sulphate reduction was more limited by the presence of sulphate than by the availability of extra carbon sources, since considerable sulphate reduction occurred in microcosms without additional organic carbon, when sulphate was available. Methanogenesis increased when microcosms were supplemented with extra carbon sources, but was completely inhibited by the addition of BES. Molybdate not only inhibited sulphate reduction, but also methanogenesis, indicating a positive relation between the two processes. The turnover of the extra carbon sources differed between microcosms treated with molybdate and BES. Acetate and propionic acid were not consumed in microcosms amended with molybdate, indicating that sulphate–reducing communities were most responsible for the metabolization of these carbon sources, and that methane was rather produced by hydrogenotrophic instead of acetoclastic methanogens. In microcosms without molybdate, concentrations of lactate, ethanol and propionic acid decreased, while acetate accumulated during the first weeks and was consumed afterwards, indicating the occurrence of both, incomplete and complete oxidizing sulphate reducers. Ethanol and lactate were consumed in microcosms even when treated with BES and molybdate together, demonstrating that other processes than methanogenesis and sulphate reduction are involved in carbon cycling in the MFT.

[1] Hulecki JC, Foght JM, Gray MR, Fedorak PM (2009) *J. Ind. Microbiol. Biotechnol.* **36**, 1499-1511.

Interactions between network cation coordination and oxygen speciation in oxide glasses

JONATHAN F. STEBBINS[1*], LINDA M. THOMPSON[1], JINGSHI WU[1]

[1]Dept. of Geological and Environmental Sciences, Stanford University, Stanford CA 94305 USA, stebbins@stanford.edu (* presenting author)

Recent experimental studies of aluminosilicate glasses and melts have greatly enhanced our information on the details of network structure that supersede conventional approximations, notably the presence of non-bridging oxygens (NBO) in metaluminous and even peraluminous compositions, and the widespread presence of significant concentrations of five-coordinated Al even in highly peralkaline (and peralkaline-earth) regions. Especially as Al, Si, (and B) coordination increase at high pressures, the interactions of these species become important for melt properties (e.g. density, viscosity, configurational entropy) and component activities. This interplay can sometimes be more apparent in borosilicate and germanate analog systems, even at ambient pressure, as composition and temperature have now well-known, large effects on structure. For example, the sizes and charges of the network modifier cations can have strong effects, as smaller and/or higher-charged cations often favor the formation of NBO and/or BO such as Al-O-Al linkages, both of which serve as relatively concentrated negative charge that can more effectively coordinate the modifier cations. We will compare results on such speciation reactions for a variety of oxide melt systems, note similarities and differences, and suggest important areas for future investigation.

Diffusion versus surface reaction control of mineral precipitation and dissolution kinetics at the pore scale

CARL I. STEEFEL*, DAVID TREBOTICH, SERGI MOLINS, LI YANG, CHAOPENG SHEN

Lawrence Berkeley National Laboratory, Berkeley, USA, CISteefel@lbl.gov (* presenting author)

Introduction

The rates of mineral precipitation are important as a subsurface carbon sequestration mechanism in the case of carbonates, while mineral dissolution is important as a source of both metal cations and alkalinity for precipitation. Pore scale flow and transport processes within the complex pore structure of the subsurface can lead in some cases to a complete or partial control of reaction rates by molecular diffusion. The extent to which a diffusion control develops depends on the rates of local surface reaction, but also on the pore geometry and the rate of flow, since these effects influence the width of diffusion boundary layers that develop adjacent to reactive mineral surfaces.

Approach and Results

In this study, we use Direct Numerical Simulation of pore scale reactive transport processes to investigate the effect of a complete or partial limitation of rates by molecular diffusion through a hydrodynamic boundary layer (Figure 1). We focus here on the dissolution and precipitation of carbonate phases, with rates at the mineral surface taken from experimental studies in which a complete surface reaction control can be demonstrated. The partial control of rates by molecular diffusion, which is particularly pronounced for larger grain sizes within porous subsurface materials, is investigated as a function of the saturation state of the bulk solution with respect to the carbonates, as well as temperature and pH, since these can influence both the rate of surface reaction and multicomponent diffusion. The simulations are combined with selected microfluidic reactor experiments in which hydrodynamic boundary layers and surface reaction can be rigorously quantified. The simulations demonstrate that a partial diffusion control of reaction rates in medium to coarse grained materials is much more prevalent than is commonly thought.

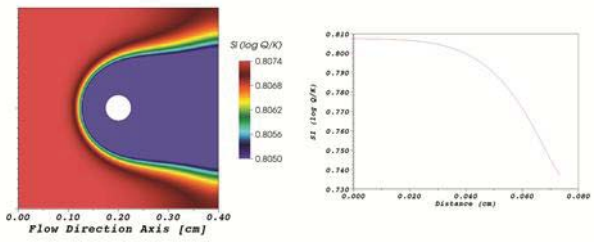

Figure 1: Left: Contour plot of calcite supersaturation surrounding a spherical calcite grain. Right: Profile of supersaturation with respect to calcite across a diffusion boundary layer, with mineral grain on the right, bulk solution on the left.

Quartz precipitation and fluid-inclusion characteristics in submarine hydrothermal systems

M. STEELE-MACINNIS[1*], L. HAN[1], R.P. LOWELL[1], J.D. RIMSTIDT[1] AND R.J. BODNAR[1]

[1]Department of Geosciences, Virginia Tech, Blacksburg VA 24061 USA, mjmaci@vt.edu (* presenting author)

Numerical modeling of quartz dissolution and precipitation in a sub-seafloor hydrothermal system was used to predict where in the system quartz could deposit and trap fluid inclusions. The spatial distribution of zones of quartz dissolution and precipitation is complex, owing to the many inter-related factors controlling quartz solubility, including temperature, fluid salinity and fluid immiscibility, and quartz may exhibit either prograde or retrograde solubility, depending on the *PTX* conditions [1]. Using the *PVTX* properties of H_2O-NaCl, the petrographic and microthermometric properties of fluid inclusions trapped at various locations within the hydrothermal system are predicted. Vapor-rich inclusions are trapped as a result of the retrograde temperature-dependence of quartz solubility as deep convecting fluid is heated in the vicinity of the magmatic heat source. Coexisting liquid-rich and vapor-rich inclusions are also trapped in this deep region when quartz precipitates as the convecting fluid enters the region of fluid immiscibility. Vapor generated as a result of fluid immiscibility migrates upward, entraining variable amounts of brine and/or heated seawater. During ascent, vapor condenses and mixes with seawater entrained in the upwelling plume. Fluid inclusions trapped along the upflow path in the shallower subsurface near the seafloor vents and in the underlying stockwork are liquid-rich and homogenize at 200-400 °C. Salinities of these inclusions are similar (but generally not equal) to that of seawater. Volcanogenic massive sulfide (VMS) deposits represent fossil submarine hydrothermal systems, in which mineralization commonly forms a stockwork zone beneath seafloor vents. Because the spatial variation of fluid-inclusion properties in this portion of the submarine hydrothermal system can be predicted, relationships between fluid-inclusion properties and location within the hydrothermal system can be inferred. Fluid inclusion properties can thus be used as an exploration tool for VMS deposits. Importantly, fluid inclusions can define vectors to infer the direction towards potential massive sulfide ore within fossil submarine hydrothermal systems, and can be used to determine the "up" direction within a deformed or tilted volcanic pile.

[1] Akinfiev, Diamond (2009) *Geochim. Cosmochim. Acta* **73**, 1597-1608.

Climate forcing of ice sheet dynamics in West Antarctica

ERIC J. STEIG[1]*

[1]University of Washington, Seattle, WA, USA, steig@uw.edu (* presenting author)

Recent West Antarctic Climate and Ice Sheet Change

Ice shelves and glaciers along the margin of the Antarctic ice sheet are thinning rapidly. The greatest thinning rates are in West Antarctica, where warm Circumpolar Deep Water (CDW) floods the continental shelf and melts the ice shelves from below. This region has also experienced significant climate changes in the last 30 years or more, including rising temperatures over most of continental West Antarctica and the Antarctic Peninsula, and declines in sea ice in the Amundsen-Bellingshausen Seas [1].

Climate and glaciological changes in West Antarctica are linked by changes in the regional atmospheric circulation which have caused increased poleward warm-air advection, sea ice convergence, and wind-driven inflow of CDW onto the shelf. These changes in regional atmospheric circulation are largely a response to forcing from the tropical Pacific (Figure 1). Particularly in the 1990s, strong sea surface temperature anomalies and anomalous deep convection in the central tropical Pacific caused enhanced Rossby wave activity, resulting in anomalous westerlies along the Amundsen Sea coast of West Antarctica [2].

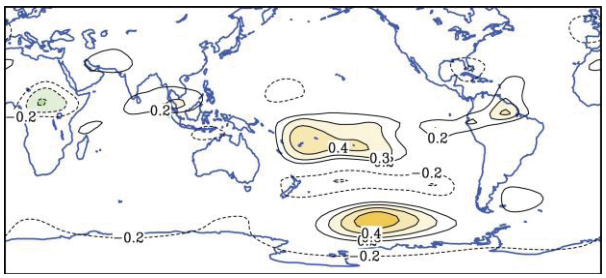

Figure 1: Correlation between the global 200 hPa stream function and the westerly wind stress over the West Antarctic shelf edge [2].

Attribution

These results imply that recent glaciological changes in West Antarctica can be attributed to anthropogenic forcing only to the extent that recent changes in the tropical Pacific can be so attributed. Paleoclimate record from corals shows that the anomalous conditions in the tropics in the last ~30 years are very likely exceptional in the last millennium. Similarly, the ice core record from West Antarctica shows that the 1990s are the most anomalous decade in at least the last 300 years. Nevertheless, attribution of tropical Pacific climate changes to anthropogenic forcing remains equivocal, largely because there is significant uncertainty in the response of the El Niño-Southern Oscillation. Uncertainty in projections of the future behavior of the West Antarctic ice sheet is further complicated by uncertainty in projections of tropical climate.

[1] Ding *et al*. (2011), *Nature Geosci.* **4,** 398-403.
[2] Steig *et al.* (2012) *Annal. Glaciol.* **62**, in press.

What is source rock?

H.J. STEIN[1,2] AND J.L. HANNAH[1,2]

[1] AIRIE Program, Colorado State University, Fort Collins, CO, USA
[2] Physics of Geological Processes, University of Oslo, Norway

From the perspective of a commodities expert, the likely answer will be organic-rich shales with hydrocarbon potential, or metal-bearing magmatic or sedimentary systems. You're either a petroleum geologist or an ore geologist, and the two professions typically stay on their own side of the fence. Has anyone seen a petroleum geologist regularly gobbling-up science at ore geology meetings or, even more unheard of, the reverse? And up the middle, are those studying "fluids in the crust", knowing the economic potential of their efforts but feeling uncertain how to access it – how to break into the terminology and be embraced as an outsider in resource-driven clubs. These are the statements that give us pause and discomfort.

The futures of research in both resource fields, hydrocarbons and metals, are co-dependent. The big leaps in commodity-driven science will be made by those who move unabashed between these two fields. Too many ore geologists fall back on the same tired models, never stepping outside their own sandbox to explore different ways to play. Ore deposits are formed by "deep-seated mantle-derived fluids" or by "granite-derived fluids", we are told. Who stops to consider the importance of organic complexes, or the chemical and physical consequences of hydrocarbon maturation? Similarly, how many petroleum geologists ponder the metal porphyrins that populate hydrocarbon systems, and what becomes of those metals as the organic molecules are cracked?

Modeling the mobility and concentration of both metals and hydrocarbons requires a keen understanding of fluids and volatiles in all kinds of rocks. Source rock is any rock that experiences breakdown of kerogen or undergoes oxidation thereby liberating metal from sulfide, silicate, or organic-rich material. Neither process is very interesting in the absence of water and CO_2, a pressure gradient, and space to move.

It is the fluid and volatile phases in rocks that move natural resources into place. The processes involved may be incremental to catastropic. The time scales may be instantaneous to hundreds of millions of years depending on one's perspective. But the notion that an ore deposit in the crust had a direct pipeline to the mantle should be put to rest. Rather, large scale mantle events stimulate processes in the crust over long time-scales. Source rock can be any rock implicated in the process with volatile, fluid, metal, or hydrocarbon to contribute.

Field-based examples that capture these processes are explored in this contribution. Processes that "upgrade metals" and "downgrade kerogen" are constrained in absolute time through precise Re-Os dating of sulfides and hydrocarbon.

Mantle plume chemical asymmetry - implications from geodynamic models

BERNHARD STEINBERGER[1,2*], RENÉ GASSMÖLLER[1] AND ELVIRA MULYUKOVA[1]

[1]GeoForschungsZentrum Potsdam, Potsdam, Germany, bstein@gfz-potsdam.de (* presenting author)
[2]Physics of Geological Processes, Univ. of Oslo, Oslo, Norway

Introduction

Recent results indicate that mantle plume composition systematically varies with position relative to the plume center, and that this heterogeneity could correspond to different regions where the plume material came from before rising through the plume conduit [1,2]. Here we present results of a numerical model regarding the relation of source region and location in the plume.

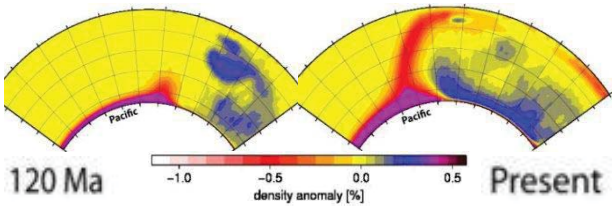

Figure 1: Cross sections for a mantle model [3]. Subducted slabs (blue) sink to the base of the mantle, and push hot material from the thermal boundary layer (red) towards the edges of thermo-chemical piles (violet) where it rises in the form of mantle plumes.

Observations and Models

Almost all Large Igneous Provinces, when reconstructed to their eruption locations, fall above the margins of either of the two Large Low Shear Velocity Provinces beneath the Pacific and Africa [4], often viewed as chemically distinct. Based on plate reconstructions since 250-300 Ma, we model a pattern of several plumes each at the edges of two thermo-chemical piles in the lowermost mantle, both with a numerical code based on spherical harmonics [5] and the finite element code CitcomS [6,7]. We develop a 2-D finite element code that allows us to accurately model entrainment of chemically distinct material in plumes.

Results and Conclusions

Model plumes often occur at locations similar to observed hotspots with conduit shapes similar to [8] where flow is based on tomography-based density models. By tracking along flow lines, both for subduction- and tomography-based flow superposed with plume influx, we map source regions onto predicted location in the plume. The mapping allows insights into the element distribution in the source region by comparing the properties of plume-related magmas. Furthermore, comparing the created models allows us to constrain under which conditions plumes entrain chemically distinct material in their source region and whether these are likely to occur on earth. Based on high-resolution 2-D results we assess entrainment and where inside the conduit chemically distinct material is expected to occur.

[1] Weis *et al.* (2011) *Nat. Geosci.* **4**, 831-838. [2] Huang, Hall & Jackson (2011) *ibid.*, 874-878. [3] Steinberger & Torsvik [2012] *G-Cubed* **13,** Q01W09. [4] Torsvik et al. [2006] *GJI* **167**, 1447-1460. [5] Hager & O'Connell [1981] *JGR* **86**, 4843-4867. [6] Zhong et al. [2000] *JGR* **105**, 11063-11082. [7] Tan et al. [2006] *G-Cubed* **7**, Q06001. [8] Steinberger & O'Connell [1998] *GJI* **132**, 412-434.

Compositional heterogeneity within the Yellowstone magma reservoir: Insight from zircon age, trace-element, and Hf-isotopic analyses

MARK E. STELTEN[1*], KARI M. COOPER[1], JORGE A. VAZQUEZ[2], JOSH WIMPENNY[1], GRY H. BARFOD[1], QING-ZHU YIN[1]

[1]University of California – Davis, Davis, CA, USA, mestelten@ucdavis.edu (* presenting author)

[2]U.S. Geological Survey, Menlo Park, CA, USA

Introduction

The Yellowstone Plateau (USA) hosts one of the largest Quaternary magmatic systems in the world, with caldera forming eruptions at 2.059 ± 0.004 Ma, 1.285 ± 0.004 Ma, and 0.639 ± 0.002 Ma, as well as numerous intracaldera and extracaldera eruptions between caldera-forming events [1]. The most recent eruptive episode at Yellowstone caldera produced the Central Plateau Member (CPM) of the Plateau Rhyolite, which erupted intermittently between ~170-70ka with a cumulative volume ≥600km^3, thereby approaching the ≥1000km^3 (dense rock equivalent) of rhyolite erupted during the preceding caldera forming eruption of the Lava Creek Tuff [1]. Thus, the CPM rhyolites provide snapshots of an evolving large silicic magma reservoir though time.

In this study we examine the degree of compositional heterogeneity ca. 100ka in the Yellowstone magma reservoir by comparing sub-crystal-scale SIMS age, SIMS trace-element, and LA-MC-ICPMS Hf-isotopic data from zircons hosted in three CPM rhyolites erupted at different locations within the caldera during the 100-120ka time period, as well as an ~118ka extracaldera rhyolite. Linking the age, trace-element, and Hf-isotopic compositions of zones within individual zircons provides a robust method for recognizing distinct crystal populations and magma compositions within the CPM reservoir, and monitoring the evolution of the magma reservoir over time using crystal zoning patterns. Comparing crystal populations in coeval rhyolites erupted from different parts of the caldera furthermore allows for assessment of whether the rhyolites have similar crystal populations and provides insight into the degree of compositional heterogeneity within the magma reservoir at ~100ka.

Results and Conclusions

Age, trace-element, and Hf-isotopic data for zircons from the intracaldera West Yellowstone flow, Solfatara Plateau flow, and Hayden Valley flow as well as from the extracaldera Gibbon River flow document the presence of multiple zircon populations within the CPM magma reservoir. Hf-isotopic compositions of zircons in the CPM rhyolites vary from -8.5 εHf to 1.2 εHf, with individual grains displaying large (>4 εHf) Hf-isotopic variations. These data document that the CPM reservoir experienced mixing and crystal exchange with multiple magmas prior to eruption, and place constraints on the degree of compositional heterogeneity in the Yellowstone magma reservoir ca. 100ka.

[1] Christiansen *et al.* (2007) *Geol. Sur. Open File Rep*, **1071**, 1-98.

Temporal variation of sulfur and iron metabolisms within composite tailings and overlying sand cap at Syncrude's Mildred Lake property

KATE STEPHENSON[1*], KATHRYN KENDRA[1], TARA COLENBRANDER-NELSON[1], RODERICK AMORES[1], STEVEN HOLLAND[1], TARA PENNER[2], AND LESLEY WARREN[1]

[1]McMaster University, School of Geography and Earth Sciences, Hamilton, Canada, stephk2@mcmaster.ca (* presenting author)

[2]Syncrude Environmental Research, Edmonton, Canada, penner.tara@syncrude.com

In accordance with provincial regulations, the Alberta oil sand companies must reclaim mined areas and composite tailings (CT) deposits produced as a by-product of bitumen extraction. Syncrude, the largest operator in the Alberta oil sands is currently building the first pilot fen reclamation project overtop of CT. Dewatering of CT associated with reclamation activities at Syncrude's Mildred Lake property (Fort McMurray, AB), has resulted in unexpected incidents of H_2S gas release from CT dewatering wells, identifying the need for in depth biogeochemical characterization of these materials and identification of the potential roles of microbial activity in H_2S generation. The objectives of this field and experimental research are to establish the existence of Fe- and S- respiring bacteria within CT porewaters and their potential linkages to H_2S release over seasonal and spatial scales within the CT deposit. An operationally defined sequential extraction procedure was used to quantify biologically accessible pools of amorphous Fe and S substrates within the sand cap overlying the CT, an important interface between the CT pore-water brine and the developing fen. Results show high concentrations of bioavailable Fe (124 μmol/g) and S (48 μmol/g) in the reducible ("amorphous and crystalline oxyhydroxides") and the oxidizable ("organic/sulfide") sediment fractions respectively. Porewater wells within CT and the overlying 10 m sandcap on which the fen is currently being constructed were sampled 4 times from June 2010 to October 2011. H_2S was detected in all wells and at all sampling dates, the highest concentration detected was for a well within the sandcap of 183 μmol/L. Enrichments for S and Fe oxidizing and reducing bacteria from samples collected in June and September 2010 and July 2011, have shown positive growth for S- and Fe- oxidizing and reducing bacteria in well water from the location of reported H_2S_g release, consistent with the involvement of these microbes in S- cycling and H_2S production in CT. Experimental mesocosms with targeted Fe and S metabolisms are currently being assessed for H_2S generation to identify key metabolic pathways involved. Select field and laboratory results, including 16S rRNA sequencing of environmental enrichments and the bulk well water community, along with the results of experimental mesocosms will be discussed.

The role of subduction erosion in the recycling of continental crust

CHARLES R STERN[1]

[1]University of Colorado, Department of Geological Sciences, Boulder, CO 80309-0399 USA, Charles.Stern@colorado.edu

Subduction erosion occurs at all convergent plate boundaries, even if they are also accretionary margins. Frontal subduction erosion results from a combination of erosion and structural collapse of the forearc wedge into the trench, and basal subduction erosion by abrasion and hydrofracturing above the subduction channel. High rates of subduction erosion are associated with relatively high convergence rates (>60 mm/yr) and low rates of sediment supply to the trench (<40 km^2/yr), implying a narrow and topographically rough subduction channel which is neither smoothed out nor lubricated by fine-grained water-rich turbidites such as are transported into the mantle below accreting plate boundaries. Rates of subduction erosion, which range up to >440 km^3/km/my, vary temporally as a function of these same factors, as well as the subduction of buoyant features such as seamount chains, submarine volcanic plateaus, island arcs and oceanic spreading ridge, due to weakening of the forearc wedge. Globally, subduction erosion is responsible for >1.7 Armstrong Units (1 AU = 1 km^3/yr) of crustal loss [1], a significant proportion of the yearly total crustal loss caused by sediment subduction, continental lower crustal delamination, crustal subduction during continental collision, and/or subduction of rock-weathering generated chemical solute that is dissolved in oceanic crust. The paucity of pre-Neoproterozoic blueschists suggests that global rates of subduction erosion were probably greater in the remote past, perhaps due to higher plate convergence rates. Subducted sediments and crust removed from the over-riding forearc wedge by subduction erosion may remain in the crust by being underplated below the wedge, or these crustal debris may be carried deeper into the source region of arc magmatism and incorporated into arc magmas by either dehydration of the subducted slab and the transport of their soluble components into the overlying mantle wedge source of arc basalts, and/or bulk melting of the subducted crust to produce adakites. In selected locations such as in Chile [2,3], Costa Rica, Japan and SW USA, strong cases can be made for the temporal and spatial correlation of distinctive crustal isotopic characteristics of arc magmas and episodes or areas of enhanced subduction erosion. Nevertheless, overall most subducted crust and sediment, >90% (>3.0 AU), is transported deeper into the mantle and neither underplated below the forearc wedge nor incorporated in arc magmas. The total current rate of return of continental crust into the deeper mantle is equal to or greater than the estimates of the rate at which the crust is being replaced by arc and plume magmatic activity, indicating that currently the continental crust is probably slowly shrinking [4,5]. However, rates of crustal growth may have been episodically more rapid in the past, most likely at times of supercontinent breakup, and conversely, rates of crustal destruction may have also been higher during times of supercontinent amalgamation. Thus the supercontinent cycle controls the relative rates of growth and/or destruction of the continental crust. Subduction erosion plays an important role in producing and maintaining this cycle by transporting radioactive elements from the crust into the mantle, perhaps as deep as the core-mantle boundary.

[1] Stern (2011) *Gondwana Research* **20,** 284-308.
[2] Stern (1991) *Geology* **19**, 78-81.
[3] Stern et al. (2011) *Andean Geology* **38**, 1-22.
[4] Stern & Scholl (2010) *International Geology Review* **52**, 1-31.
[5] Clift et al. (2009). *Earth Science Reviews* **97**, 80-104.

Stable strontium isotope behaviour in Himalayan river catchments

EMILY I. STEVENSON[1]*, KEVIN W. BURTON[2], IAN J. PARKINSON[3], CHRISTOPHER R. PEARCE[3] FATIMA. MOKADEM[1], AND RACHAEL JAMES[4]

[1]Department of Earth Sciences, Oxford University, South Parks Road, Oxford, OX1 3AN, UK. emilys@earth.ox.ac.uk (* presenting author)
[2]Department of Earth Sciences, Durham University, Durham, DH1 3LE, UK
[3]Department of Environment, Earth and Ecosystems, The Open University, Milton Keynes, MK7 6AA, UK
[4]National Oceanography Centre, European Way, Southampton, SO14 3ZH, UK

The radiogenic strontium ratio ($^{87}Sr/^{86}Sr$) is commonly used as a weathering tracer of continental sources in seawater, with carbonate and silicate based lithologies having different $^{87}Sr/^{86}Sr$ ratios. However, $^{87}Sr/^{86}Sr$ interpretations can be hindered by the difficulty of distinguishing changes in riverine flux from changes in composition. This is a particular problem for Himalayan rivers as those draining both silicate and carbonate catchments have elevated $^{87}Sr/^{86}Sr$ ratios, and there is debate as to how much of the ^{87}Sr flux is actually derived from silicate weathering [1].

Recent stable strontium isotope data suggested that carbonate weathering yields a $\delta^{88/86}Sr$ value distinct from those of both silicate weathering and seawater [2]. This difference in isotopic ratio could resolve whether inputs into rivers, and eventually the oceans, are truly dominated by either silicate or carbonate lithologies and may also be used to distinguish between flux and source.

This study presents high-precision $\delta^{88/86}Sr$ data and $^{87}Sr/^{86}Sr$ data obtained from river waters draining both silicate and carbonate dominated terrains in the Himayala. Rivers draining carbonate based terrains have an average $\delta^{88/86}Sr$ value of 0.28±0.08‰ and increase to heavier values downstream (heading towards those of the Ganges, 0.38±0.01‰ [3]), possibly because of continued carbonate precipitation through the catchment. The $\delta^{88/86}Sr$ of carbonate rivers also correlates with [Si], and other major divalent cations as well as sulphate concentration. [4] Silicate rivers are generally heavier (0.34±0.07‰), but show little systematic behaviour with other elements. These results indicate that the carbonate rivers are generally lighter than those draining silicate terrains, and also suggest that continued secondary mineral precipitation (primarily carbonates) is occuring with within those catchments.

[1] Bickle et al. (2005) *GCA* **69**, 2221-2240. [2] Krabbenhöft et al., (2010) *GCA* **74** 4097-4109. [3] Pearce et al., (2011) *AGU, Fall Meet. Abs*. B21D-0342. [4] Kisakürek et al., (2005) *EPSL* **237** 387-401.

Uranium association and interaction with redox boundary in Rifle surface seep sediments

BRANDY D. STEWART [1*], PETER S. NICO[2], AND BRENT M. PEYTON[1]

[1]Montana State Universiy, Bozeman, MT, USA
(* presenting author)
[2]Lawrence Berkeley National Laboratory, Berkeley, CA, USA
Brandy.stewart@erc.montana.edu
psnico@lbl..gov
bpeyton@coe.montana.edu

Owing to ecosystem and human health consequences, understanding uranium's potential for mobility in environmental settings is important. In anaerobic soils and sediments, oxidized U(VI) may be reduced through biological or chemical pathways to U(IV), forming sparingly soluble solids. However, formation of uranyl-calcium-carbonato complexes may limit reduction and authogenic UO_2 is susceptible to reoxidation. Determining reaction pathways of uranium that promote solids stable under aerobic and anaerobic conditions is critical for limiting dissolved concentrations and migration of uranium. This is of particular concern in settings near or at redox boundaries where surface and subsurface environments may be subjected to fluctuating redox conditions. We examined the nature and association of solid-phase uranium in both oxidized and reduced sediments from a hillside surface seep in Rifle, Colorado where uranium appears to be naturally attenuated in the solid phase. Visibly reduced sediments occur at the surface of the seep adjacent to (< 100cm from) pockets of freshly precipitated iron (III) phases, indicative of a redox boundary. Uranium release and solid-phase association were measured in systems containing sediment and 3 mM Fe(II) that were maintained under reducing conditions for 15 d followed by 5d of oxidation to simulate a redox cycle. Aqueous and solid-phase results show that >75% of uranium present in the sediments remains associated with the solid phase throughout the oxidation portion of the experiments.

Predicting the speciation and transport behaviour of contaminants in a wet discard dam

GIDEON STEYL[1]*, IZAK L. MARAIS[2], LORE-MARI CRUYWAGEN[2]

[1]University of the Free State, Chemistry Department, Bloemfontein, South Africa, steylg@ufs.ac.za (* presenting author)
[2]University of the Free State, Institute for Groundwater Studies, Bloemfontein, South Africa, CruywagenLM@ufs.ac.za

The burning of pulverised coal in coal-fired boilers to generate heat causes the production of fly ash. In addition water used in the process of cooling and turbine propulsion results in the production of high saline effluents. The high saline streams (ca. 20% ash) are used for the hydraulic transport of ash to the dumping sites, which results in ash dams that can act as salt sinks. The slurry that is pumped onto the wet dump area is allowed to settle. The water that has separated from the ash is skimmed off and re-circulated to transport more fly ash to the site. However a certain fraction of the water infiltrates the dam resulting in geochemical transformations.

Due to the presence of high saline water during the operational phase an extensive salt loading is observed onto the ash particles. During the decommisioning phase of the ash dam certain physical and chemical processes need to be considered to manage the produced water from the system. In particular the mechanism of leachate production needs to be considered in conjunction with the temporal and spatial extent.

The results presented will focus on the effect that disposal methods of the fly ash has on the transport of chemical species within the ash dam (Figure 1). In addition the rate of release of chemical species will also be presented as this influences the measures required to manage these facilities over an extended time period.

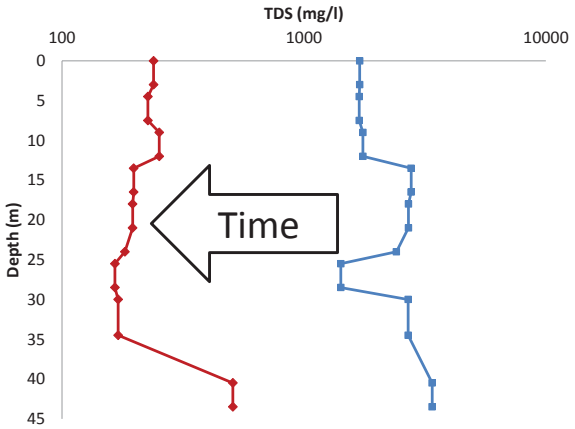

Figure 1: Diagram depicting the change in TDS values over time from a leachate analysis. The build-up of initially higher TDS values can be observed in two distinct areas (15 – 24 and 30 – 45 m).

When the surface is not what you think it is

STIPP S.L.S.[1], HASSENKAM T.[1], YANG M.[1], SKOVBJERG L. L.[1], SAND K.K.[1], PASARÍN I.[1], BOHR J.[2]

[1]Nano-Science Center, Department of Chemistry, University of Copenhagen, stipp@nano.ku.dk
[2]DTU Nanotech, Danish Technical University, Denmark.

More than a century ago, chemists began to explore the thermodynamic and kinetic relationships between solids and fluids in nature. Goldschmidt attempted to classsify them and Garrels, Christ, Krauskopf, Stumm, Schindler, Helgeson, Sposito and many others taught us to use thermodynamic relationships to predict natural system behaviour. When it has failed, we have often blamed kinetics.

About two decades ago, surface sensitive techniques first demonstrated that a calcite surface is not simply a termination of the bulk atomic structure. Surface atoms shift position, water delocalises charge on dangling bonds, adventitious carbon is ubiquitous and even on surfaces that appear dry, an adsorbed water film promotes recrystallisation[1]. New instruments allow us to see ever closer, giving new insights into the properties and behaviour of nano-particles and mineral-fluid interfaces so there is now little doubt. Surfaces are not simply where the bulk terminates.

Still, however, there are many cases where natural surfaces do not behave as we assume they ought to[2]. Molecular modelling, atomic force microscopy (AFM) and X-ray reflectivity show that water, structured at calcite surfaces, is displaced by ethanol and the alcohol orders itself, almost like a lipid layer. Adhesion properties change in response to ionic strength but reproducibility is elusive on ideal surfaces, whereas mineral grains plucked from sandstone, with their natural adventitious carbon, behave consistently. It is this organic "contamination" on these mineral surfaces that determines their hydrophillic properties, not the mineral beneath. Recent AFM studies have also revealed that sediment grain surfaces are frequently covered by nanocrystals of clay. These are far too thin for detection by X-ray diffraction so they have previously gone unnoticed but in some cases they cover significant portions mineral surfaces, meaning they can control water-rock properties. Finally, sea creatures produce aragonite and calcite in crystal forms tailored to their needs but these biogenic materials behave differently than inorganically produced minerals, even when organic components that remain associated with the biominerals are present only in the parts per billion range.

Materials adsorbed on mineral surfaces change properties in unexpected ways. By understanding surfaces better, we are likely to discover why large scale geological systems do not always behave as thermodynamics leads us to expect. We can hope that our new insight brings us to a point where we might have less need of the excuse "kinetically hindered".

[1] Stipp and Hochella (1991) *GCA* **55**, 1723-1736; Stipp et al. (1994) *Amer. Min.* **81**, 1-8; Stipp (1999) *GCA* **63**, 3121-3131. [2] Bohr et al. (2010) *GCA* **74**, 5985-5999; Cooke et al. (2010) *Langmuir* **26**, 14520-14529; Sand et al. (2010) *Langmuir* **26**, 15239-15247; ; Hassenkam et al. (2011) *PNAS*, 7307-7312; Hassenkam et al. (2011) *Coll. Surf. A* **390**, 179-188; Skovbjerg et al. (2012) *GCA in review*; Pasarín I.S. et al. (2012) *Langmuir in press*.

Mechanisms controlling $^{238}U/^{235}U$ isotopic fractionation in low- and high-temperature environments

C.H. STIRLING[1*], A. KALTENBACH[1] AND Y. AMELIN[2]

[1]Department of Chemistry, University of Otago, Dunedin, New Zealand, cstirling@chemistry.otago.ac.nz (* presenting author), akaltenbach@chemistry.otago.ac.nz
[2]Research School of Earth Sciences, Australian National University, Canberra ACT, Australia, yuri.amelin@anu.edu.au

Recent studies have documented sizeable, permil-level isotopic fractionation between ^{238}U and ^{235}U in low-temperature environments, facilitated by analytical advancements in multiple-collector ICP-MS (MC-ICPMS) [1,2]. Variability in $^{238}U/^{235}U$ has a direct impact on the accuracy of the U decay series chronometers, requiring the $^{238}U/^{235}U$ of every sample to be characterized, and the revision of important cosmo- and geo-chronological models. Further efforts have focussed on investigating the processes controlling $^{238}U/^{235}U$ isotope fractionation, especially during U reduction. To this end, the ^{238}U-^{235}U isotope system offers significant potential as a monitor of redox conditions in U bioremediation studies [3], and as a paleo-redox tracer of the extent of anoxia in the historic oceans [4] to complement the growing inventory of other redox-sensitive metal isotope tracers (e.g. Mo and Fe) which each have differing redox potentials and respond to anoxia at different rates. However, additional studies are required to gain an improved understanding of the mechanisms controlling ^{238}U-^{235}U isotope fractionation before these applications can be fully explored, as the available datasets show some contrasting U isotopic behaviour during U reduction.

Using MC-ICPMS, we report $^{238}U/^{235}U$ observations for samples collected from a range of low- and high-temperature environments. A ^{233}U-^{236}U double spike was employed to monitor instrumental mass fractionation, allowing variations in $^{238}U/^{235}U$ to be resolved at the 0.005 % level (2σ) on 50 ng U sample sizes, and at the 0.003 % level (2σ) on larger sample sizes by pooling the data of replicate analyses. In all of the low-temperature environments we have investigated, the magnitude and direction of the $^{238}U/^{235}U$ isotopic fractionation is consistent with the 'nuclear field shift effect' [5] as the dominant fractionation mechanism, favouring enriched $^{238}U/^{235}U$ compositions in the reduced reaction product where the electron density near the nucleus is lower. Our results for a wide range of meteorites [6,7] and volcanic terrestrial samples reveal small (0.01 % level) but resolvable variations in $^{238}U/^{235}U$ in high-temperature environments. Further efforts should focus on identifying U fractionation mechanisms in high-temperature systems by linking $^{238}U/^{235}U$ to U concentration and oxidation state. Bulk samples and mineral aggregate sub-samples spanning the primitive to differentiated meteorite classes should also be be investigated to determine the extent to which $^{238}U/^{235}U$ variations are controlled by U isotope heterogeneity or extant ^{247}Cm effects in the early solar system versus U 'stable' isotope fractionation during subsequent chemical and thermal processing.

[1] Stirling et al. (2007). *EPSL* **264**, 208-25; [2] Weyer et al. (2008). *GCA* **72**, 345-59; [3] Bopp et al. (2010). *Env. Sci. Tech.* **44**, 5927-33; [4] Montoya-Pino (2010). *Geol.* **38**, 315-18; [5] Bigeleisen (1996). *J. Am. Chem. Soc.* **118**, 3676-80; [6] Amelin et al. (2010). *EPSL.* **300**, 343-350; [7] Kaltenbach et al. (2012). *LPSC* #1691.

Deep water in the Upper Rhine Rift Valley, central Europe

INGRID STOBER

Institute of Geosciences. University of Freiburg. Albertstr. 23b. D-79102 Freiburg. Germany. ingrid.stober@minpet.uni-freiburg.de

Section 9f: Innovative geochemical approaches to understanding geothermal systems

Hydrochemical data from deep wells in the Upper Rhine Graben area in France and Germany were collected und examined. Primary targets were the potential geothermal reservoirs: Hauptrogenstein (Dogger). Upper Muschelkalk (middle Triassic) and Buntsandstein (lower Triasic). The data (table) were used to characterize the fluids found in the hydrogeothermal reservoirs [1. 2]. Waters at < 500 m depth are weakly mineralized. Water composition is controled by the rock. With increasing depth also TDS increases and the distinct waters of the three different aquifers all evolve to Na-Cl brines independent of the reservoir rock. Water from 3000 m depth is of very similar composition. All waters are saturated with respect to calcite and some other minerals. When thermal water is pumped to the surface and cooled, they become oversaturated with respect to a series of predictable solids including calcite, barite, celestite and others.

Table: Selected hydrochemical analyses (mg/kg):

Well	depth (m)	Na	Ca	Cl	HCO_3	SO_4
Buntsandstein						
GB1 Bruchsal	2537.	35840.	7415.	82220.	520.	384.
TB Zähringen II	843.	1115.	621.	330.	680.	3114.
Eschau 1	1619.	28307.	400.	44375.	180.	125.
GB Cronenbourg	3220.	32560.	4680.	61550.	305.	220.
Meistratzheim 2	1437.	8500.	600.	12800.	671.	2240.
Mutzenheim 1	1857.	23500.	912.	35720.	1415.	4640.
Muschelkalk						
Langenbrücken	607.	12240.	1660.	21130.	500.	1850.
Bad Schönborn	636.	9760.	1367.	16770.	571.	1942.
Bad Krozingen	591.	554.	707.	348.	1519.	1960.
TB Freiburg 1	858.	390.	632.	113.	918.	2240.
Bad Bellingen III	1194.	308.	2525.	3454.	2227.	1585.
GB 1 Riehen	1547.	4900.	805.	7270.	1012.	2550.
Eschau 1	1407.	28307.	400.	44375.	180.	125.
Staffelfelden 9	2529.	19710.	800.	30530.	950.	1900.
GB Helios	1146.	6712.	1979.	13783.	326.	960.
Hauptrogenstein						
TB 3 Freiburg	483.	59.	67.	31.	386.	98.
Georg-Quelle	487.	928.	462.	1758.	961.	291.
Blodelsheim I	1891.	7431.	1200.	13490.	1870.	1300.

Within the underlain Variscan crystalline basement the fracture porosity is filled with saline thermal water[3]. Its composition forms a continuum with the waters from the deep sedimentary aquifers. The crystalline basement in the Upper Rhine Graben is used for enhanced geothermal systems (EGS). TDS at 5000 m depth is about 100 g/kg.

[1] HE. K. & STOBER. I. & BUCHER. K. (1999): Chemical Evolution of Thermal Waters from Limestone Aquifers of the Southern Upper Rhine Valley. - Applied Geochemistry. 14. 223 – 235. Exeter/UK.
[2] STOBER. I. & JODOCY. M. (2011): Hydrochemie der Tiefenwässer im Oberrheingraben - eine Basisinformation für geothermische Nutzungssysteme. – Z. geol. Wiss.. 39. 1. S. 39 - 57.
[3] STOBER. I. & RICHTER. A. & BROST. E. & BUCHER. K. (1999): The Ohlsbach Plume: Natural release of Deep Saline Water from the Crystalline Basement of the Black Forest.- Hydrogeology Journal. vol 7 (3). pp. 273-283. Springer. Berlin/Heidelberg.

Magnetite (U-Th)/He dating– Attractive Dates in Mafic and Ultramafic Rocks

DANIEL F. STOCKLI[1], JORDAN L. TAYLOR[2*], EUGENE SZYMANSKI[2], RICHARD A. KETCHAM[1]

[1]University of Texas, Austin, USA, stockli@jsg.utexas.edu (*presenting author), ketcham@jsg.utexas.edu
[2]University of Kansas, Lawrence, USA, jordanleightaylor@gmail.com, eugene.szymanski@gmail.com

Magnetite is a common mineral phase in felsic, mafic, hydrated ultramafic igneous and metamorphic rocks. Magnetite (U-Th)/He (MHe) dating has been shown to be a reliable and powerful alternative method for obtaining absolute age constraints from mafic volcanic rocks in light of inherent difficulties in $^{40}Ar/^{39}Ar$ dating due to excess ^{40}Ar and/or recoil, susceptibility to alteration, or lack of datable mineral phases [1]. More recently, we have explored MHe as a novel and exciting geo- and thermochronometric technique for constraining the formation and thermal processes related to serpentinization and exhumation of sub-lithospheric mantle during continental break-up. While ultramafic rocks (e.g., sub-lithospheric mantle) do not commonly contain mineral phases that are datable by traditionally for geo- and thermochronometric, magnetite occurs ubiquitously as an alteration phase in serpentinized peridotites as a result of olivine breakdown. MHe Tc of ~250°C [1] can be exploited to elucidate the thermal history of exhumed mantle and formation of serpentinites. Application of MHe ages should provide critical temporal insights into continental rifting and serpentinization during break-up along magma-poor continental margins. As attractive and powerful as MHe dating is, not all magnetite samples are suitable for MHe dating due to its texture, grain size, and [U] making it prone to matrix He implantation. Detailed petrographic characterization of basaltic and ultramafic magnetite is required to determine the suitability of magnetite size and textures for MHe dating. The biggest hurdles in reliable magnetite dating, however, are grain morphology and He implantation, as matrix [U] commonly is one order of magnitude greater than magnetite (~100 ppb). While air-abrasion tends to alleviate this in large magnetite [1], irregular and complexly intergrown magnetite require careful pre-analysis screening. We have the developed the routine use of non-destructive microCT scanning for imaging of magnetite, identification of suitable magnetite, and monitoring of air-abrasion progress and high-U matrix removal. Understanding petrologic context and screening prior and during analysis are critical for deriving reliable and meaningful MHe dates.

[1] Blackburn et al. (2007) EPSL, vol. 259, p. 360–371.

Calcite nucleation and growth on basaltic glass and silicate minerals

GABRIELLE J. STOCKMANN[1,2*], ERIC H. OELKERS[2,3], DOMENIK WOLFF-BOENISCH[3], NICOLAS BOVET[4] AND SIGURDUR R. GISLASON[3]

[1]Nordic Volcanological Center, University of Iceland, Iceland, gjs3@hi.is (* presenting author)
[2]GET-Université de Toulouse-CNRS-IRD-OMP, France, eric.oelkers@lmtg.obs-mip.fr
[3]Institute of Earth Sciences, University of Iceland, Iceland, sigrg@raunvis.hi.is
[4]Nano-Science Center, University of Copenhagen, Denmark, bovet@nano.ku.dk

Mineral substrates and their effect on calcite nucleation and growth

Calcite was precipitated in flow-through experiments at 25 °C from supersaturated aqueous solutions in the presence of seeds of calcite and six different silicates: augite, basaltic glass, enstatite, labradorite, olivine, and peridotite. The aim of the experiments was to determine how calcite nucleation and growth depends on the identity and structure of the growth substrate. Calcite saturation was achieved mixing a $CaCl_2$-rich solution with a $NaHCO_3$-Na_2CO_3 buffer in a mixed-flow reactor containing 0.5-2 grams of mineral grains. This led to a calcite saturation index of 0.6 and pH 9.1 for the reactive solution inside the reactor.

Although chemical conditions, flow rate and temperature were identical for all experiments, the onset of calcite nucleation and the amount of calcite being precipitated depended on the identity of the mineral substrate. With calcite as the growth substrate, new calcite crystals formed instantaneously. Calcite nucleated relatively rapidly on olivine, enstatite, and peridotite (mainly composed of Mg-olivine). Scanning Electron Microscope images showed silicate crystals to be almost completed covered with calcite coatings at the end of the experiments. Less calcite growth was found on labradorite and augite, and least on basaltic glass. In all cases, calcite precipitation occurs on the mineral substrate and not adjacent to them.

Results and Conclusion

These findings indicate that calcite nucleation and its subsequent growth depends on the crystal structure of the silicate substrate. Orthorhombic silicate minerals (olivine and enstatite) are the easiest for trigonal calcite to nucleate on. Monoclinic augite and triclinic labradorite show intermediate behavior, whereas basaltic glass with its non-ordered crystal structure is the least favorable platform for calcite growth. The results have implications for CO_2 mineralization in ultramafic and basaltic rocks [1,2] indicating that trigonal carbonates easier precipitate on crystalline rather than glassy rocks, but even glass surfaces can serve as a substrate for calcite nucleation.

[1] Oelkers *et al.* (2008) *Elements* **4**, 333-337. [2] Gislason *et al.* (2010) *Int. J. Greenhouse Gas Control* **4**, 537–545.

Smart K_d-concept based on Surface Complexation Modeling

M. STOCKMANN[1]*, V. BRENDLER[1], J. SCHIKORA[1], S. BRITZ[2], J. FLÜGGE[2], AND U. NOSECK[2]

[1]Helmholtz-Zentrum Dresden-Rossendorf, D-01328 Dresden, Germany, m.stockmann@hzdr.de (*presenting author)
[2]GRS Braunschweig, D-38122 Braunschweig, Germany

Methodology

Sorption on mineral surfaces of sediments is one important retardation process for radionuclides to be considered in long-term safety assessments for radioactive waste repositories. Previously, the K_d-concept with temporally constant values was applied to describe the radionuclide retardation in the far field of a repository.

In this study, pre-calculated distribution coefficients (K_ds) based on surface complexation models (SCM) are implemented in the existing 3D transport program r^{3}t [1]. The so-called smart K_d-values are calculated as a function of important environmental parameters to reflect changing geochemical conditions. Respective multi-dimensional K_d-matrices are generated and stored a-priori to any r^{3}t run. The calculations follow a bottom-up approach, i.e. the sorption of an element on each single mineral phase contributes to the distribution coefficient for a sediment.

Results

As an exemplary proof-of-concept, the Gorleben site (a potential repository site in Germany) was selected. Figure 1 shows the 3D plot for the logK_d-matrix of UO_2^{2+} in the upper aquifer (UAF) at the Gorleben site as a function of pH, [Ca], and [DIC] (logarithmic scale).

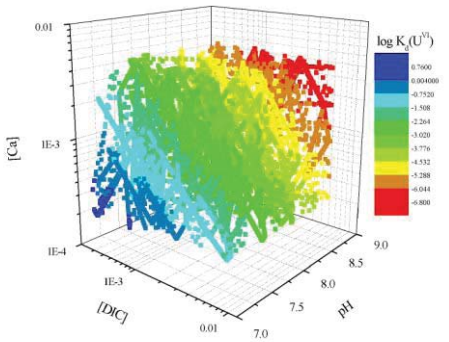

Figure 1: Multidimensional K_d-matrix for UO_2^{2+} in UAF as a function of pH, [Ca], and [DIC] (K_d in m^3/kg, logarithmic scale).

These pre-calculated logK_d-values vary between -6.8 and 0.75. Comparing to the temporally constant conservative logK_d of -2.7 from [2], which was previously used in r^{3}t for the retention of UO_2^{2+} in fresh water in the upper aquifer at the Gorleben site, the resulting mean logK_d of -2.74 shows a good general agreement, but account now for geochemical variations.

[1] Fein (2004) *Report GRS-192*, *BMWi-FKZ 02E9148/2*. [2] Suter *et al.* (1998). *Proceedings DisTec 98*.

Measurement of intact methane isotopologues, including $^{13}CH_3D$

DANIEL A STOLPER[1], ALEX L SESSIONS[1], JOHN M EILER[1]

[1]California Institute of Technology, dstolper@caltech.edu

Methane (CH_4) is both a significant greenhouse gas and resource. Its present and past cycling can be studied through measurements of concentration and/or bulk isotopic ratios ($^{13}C/^{12}C$, D/H, and $^{14}C/^{12}C$). Currently, isotope ratios are measured by mass spectrometric analysis of H_2 and CO_2 produced from CH_4, or by spectroscopy of CH_4. However, the interpretation of bulk isotopic variations of CH_4 are often equivocal, necessitating additional tracers.

We have developed a technique for mass spectrometric analysis of several isotopologues of intact CH_4, including $^{12}CH_4$, $^{13}CH_4$, $^{12}CH_3D$, and $^{13}CH_3D$ (and the method can be extended to others). Our most novel capability is the analysis of the multiply substituted isotopologue $^{13}CH_3D$, which is expected to differ relative to a random isotopic distribution due to kinetic isotope effects, mixing processes, and as a function of temperature at equilibrium. Measurements of $^{13}CH_3D$ concentrations (along with the singly substituted species) could elucidate the formation temperatures of thermally generated CH_4, discriminate between sources of CH_4 to the atmosphere (e.g., microbial vs thermogenic gas), and help to characterize CH_4 chemistry in the atmosphere where potentially large enrichments are expected (e.g., [1], [2], [3]).

Measurement of intact CH_4 requires a mass spectrometer capable of separating CH_4 species both from water and from internal isobars (CH_4 adducts, fragments, and isotopologues). We show here the initial results and capabilities of such measurements using the MAT 253 Ultra prototype high-resolution gas-source mass spectrometer. We reproduced δD values of known samples to within 0.2 ‰ (1 s.e. = 0.1‰). In addition to demonstrating accuracy, this result reveals that the method may result in improved precision for δD measurements of CH_4 relative to conventional techniques. We have measured ratios of $^{13}CH_3D$ to mass 17 species ($^{13}CH_4$, $^{12}CDH_4$, and $^{12}CH_5$) to better than ±0.4 ‰ (1 s.e.); this value reflects counting statstics and should be improved with longer counting times. The critical enabling feature of our mass spectrometer is the ability to cleanly separate a portion of the $^{13}CH_3D^+$ peak from that of $^{13}CH_5^+$ (shown in Figure 1.)

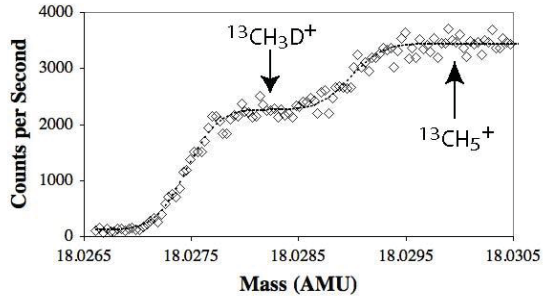

Figure 1: Peak scan of mass 18 CH_4 with a model fit through the data. Water is sufficiently resolved as to not appear at this scale.

[1]Ma et al., (2008) *GCA* **72** 5446-56. [2] Mroz et al., (1989) *GRL* **16**, 677-678. [3] Kaye and Jackman (1990) *GRL* **17**, 659-60.

The Unsaturated (Vadose) Zone—the Where of Weathering

DAVID A. STONESTROM[1*], MARJORIE S. SCHULZ[2], AND ARTHUR F. WHITE[3]

[1]US Geological Survey, Menlo Park, CA, USA, dastones@usgs.gov (*presenting author)

[2]US Geological Survey, Menlo Park, CA, USA, mschulz@usgs.gov

[3]US Geological Survey, Menlo Park, CA, USA, afwhite@usgs.gov (emeritus)

The unsaturated zone (UZ), that portion of the Earth's crust between land surface and the regional water table—the latter being defined as the surface below which pore-water pressure is persistently above atmospheric—is the vital bio-geochemical reactor that sustains the planetary critical zone. Weathering reactions in the UZ sustain life by releasing bioessential elements such as potassium, calcium, and magnesium that are mostly locked up in solid mineral phases during the bioaccessible parts of the rock cycle. The UZ sits at the intersection of the lithosphere, atmosphere, and terrestrial biosphere, acting as a highly non-linear regulator of water, carbon, and nutrient dynamics. It is the key interface controlling hydrospheric influences on land based life. UZ water is the mobile solvent that delivers aqueous reactants and removes aqueous products from the sites of weathering reactions. It also partitions the pore space within the evolving geometry of soil structure, thereby controlling crucial pore-geometric relations including proximal and long-range connectedness (topology) of gas and liquid phases. The resulting dynamics mediate residence times, redox states, complexation, and chemical activity, along with fluid permeabilities and solute dispersivities. Hysteresis in the relations between water content θ and matric pressure ψ acts to partially constrain fluxes of water (and heat) to the uppermost UZ. This provides plant-root microcosms more opportunity for water and nutrient extraction and moderates weathering reactions by controlling equilibrium versus kinetic control of chemical processes. UZs may be classified according to water-table depth, water balance, and water-flux variability in time and space. These determine whether UZs act as (1) rapid, disequilibrium pass-through conduits with little opportunity for weathering reactions, (2) equilibrium controlled static reservoirs of water and solutes where not much is happening, or (3) totally happening places essential for oxygen-intensive life.

The ideas herein stem from many fruitful discussions and collaborations with Art White, Jorie Schulz, Alex Blum, Jennifer Harden, Sue Brantley, Kate Maher, Michelle Walvood, Bridget Scanlon, Jim Constantz, John Nimmo, Dave Prudic, Amanda Garcia, Brian Andraski, Jacob Rubin, Laurie Flint, Alan Flint, and others.

Vive la Weathering. Vive l'UZ Science. Vive l'Art!

The Fingerprint of Geologic Carbon on Glacial/Interglacial Marine Carbonate Chemistry and Atmospheric CO_2

LOWELL STOTT[1*]

[1] University of Southern California, Earth Sciences, stott@usc.edu (* presenting author)

The rise in atmospheric pCO_2 during the last glacial termination was accompanied by a 190‰ decrease in surface ocean $\Delta^{14}C$ between 17 to 10 kyB.P., which cannot be explained without calling upon an input of ^{14}C-depleted carbon from either a formally isolated deep ocean reservoir or input of geologic carbon. There are now enough marine $\Delta^{14}C$ records spanning the deglaciation to make clear that Pacific deep water $\Delta^{14}C$ did not track the atmosphere whereas the $\Delta^{14}C$ of intermediate waters did, except in the eastern equatorial Pacific (EEP) where there were large negative excursions in $\Delta^{14}C$. To explain the contrasting deep and upper ocean deglacial $\Delta^{14}C$ histories a new hypothesis calls upon a release of ^{14}C-depleted CO_2-rich hydrothermal fluids at intermediate water depths as the ocean warmed during the deglaciation. Here we use an Earth System model of intermediate complexity (cGENIE) with new geochemical records from the tropical Pacific to test this hypothesis. We show that a total release of 1400Gt of ^{14}C-dead DIC into intermediate waters of the EEP (700Gt) and Arabian Sea (700Gt) causes $\Delta^{14}C$ changes throughout the ocean that agree with observations. The injection also causes a ~40µmol/kg drop in $[CO_3^{=}]$ of tropical surface waters. Trace metal proxies of $[CO_3^{=}]$ and carbonate preservation data are presented for the EEP that document a transient decrease in $[CO_3^{=}]$ in association with the deglacial $\Delta^{14}C$ excursions. This carbonate preservation event is associated with elevated V/Ca, Zn/Ca and Cu/Ca in planktonic foraminifera from the EEP.

Taken together, the model and geochemical data provide strong support for the hypothesis that there was a release of geologic carbon during the deglaciation that contributed as much as 60ppm to the rise in atmospheric pCO_2. If the geochemical signatures documented across glacial Termination 1 are found to occur at earlier glacial terminations as well, these findings will have profound implications for our understanding of glacial/interglacial CO_2 variability. Hydrothermal systems in the oceans may act as a CO_2 capacitor, regulating storage and release of carbon, and in doing so, affect the radiative balance that determines Earth's climate on orbital time scales.

Inter-mineral Mg isotope fractionation in mantle xenoliths

ANDREAS STRACKE[1,2*], EDWARD T. TIPPER[3,2], MICHAEL BIZIMIS[4]

[1]Westfälische Wilhelms Universität, Münster, Germany, stracke.andreas@uni-muenster.de (* presenting author)
[2]ETH Zürich, Zürich, Switzerland
[3]University of St. Andrews, St Andrews, U.K., ett@st-andrews.ac.uk
[4]University of South Carolina, Columbia, SC, U.S., mbizimis@geol.sc.edu

The bulk Mg isotope composition of the silicate Earth is homogeneous and identical within analytical error to that of chondritic meteorites [1-7]. Systematic fractionations among minerals in mantle peridotites [1,2,4,8-10] are resolvable, however, and are broadly consistent with theoretical predictions for high-T equilibrium Mg isotope fractionation [10]. Theory predicts that tetrahedral crystallographic sites have higher $^{26}Mg/^{24}Mg$ than octahedral sites; up to 0.5 – 0.8‰ for spinel – silicate pairs at 1000K [10], which is in agreement with recent data from two spinel peridotites [9].

Here we investigate the inter-mineral Mg isotope fractionation in 5 spinel peridotite and 5 garnet pyroxenite xenoliths from Salt Lake Crater, Hawaii. Calculated whole rock $\delta^{26}Mg$ compositions of both rock types are within error of those of bulk silicate Earth, suggesting that inter-mineral differences are due to equilibrium isotope fractionation. In the spinel peridotites, the $\delta^{26}Mg$ of olivine (ol), orthopyroxene (opx) and clinopyroxene (cpx) are indistinguishable. In the three measured olivine-spinel pairs, the spinels (sp) have consistently higher $\delta^{26}Mg$ values than the olivines, by 0.21 - 0.28‰. The sp-ol difference in $\delta^{26}Mg$ suggests an equilibration temperature of ca. 1700°C, considerably higher than the calculated opx-cpx mineral equilibration temperature of ca. 1100°C. The $\delta^{26}Mg$ of garnet in the garnet pyroxenites is consistently lower by 0.38 - 0.45‰ than in the coexisting cpx. Hence, the $\delta^{26}Mg$ values increase from garnet with a Mg coordination number of 8, to the octahedrally coordinated silicates ($ol \leq opx \leq cpx$) and the tetrahedrally coordinated spinels, consistent with coordination number exerting a first-order control on inter-mineral high-T equilibrium Mg isotope fractionation [10].

However, a strong positive correlation of $\delta^{26}Mg_{spinel}$ with the spinel Cr (Al) content or spinel Cr# shows that composition also influences the $\delta^{26}Mg$ values of individual minerals. The latter observation may explain the discrepancy between calculated equilibration temperatures based on mineral equilibria (opx-cpx) and Mg isotope fractionation ($\delta^{26}Mg_{ol-sp}$), and may hamper the use of spinel-silicate Mg isotope fractionation as a reliable geothermometer in magmatic rocks.

[1] Yang et al. (2009), *Earth Planet. Sci. Lett.* **288**, 475-482. [2] Handler et al. (2009) *Earth Planet. Sci. Lett.* **282**, 306-313. [3] Bourdon et al. (2010) *Geochim. Cosmochim. Acta* **74**, 5069-5083. [4] Chakrabarti & Jacobsen (2010) *Earth Planet. Sci. Lett.* **293**, 349-358. [5] Schiller et al. (2010) *Earth Planet. Sci. Lett.* **297**, 165-173. [6] Teng et al. (2010) *Geochim. Cosmochim. Acta* **74**, 4150-4166. [7] Pogge van Strandmann et al. (2011) *Geochim. Cosmochim. Acta* **75**, 5247-5268. [8] Wiechert & Halliday (2007) *Earth Planet. Sci. Lett.* **256**, 360-371. [9] Young et al. (2009) *Earth Planet. Sci. Lett.* **288**, 524-533. [10] Schauble (2011) *Geochim. Cosmochim. Acta* **75**, 844-869.

Tracing subduction erosion through arc chemistry in the central Mexican Volcanic Belt

SUSANNE M. STRAUB[1*], GEORG F. ZELLMER[2], ARTURO GÓMEZ-TUENA[3], YUE CAI[1], FINLAY M. STUART[4], CHARLES H. LANGMUIR[5]

[1]LDEO, Columbia University, Palisades, NY USA, smstraub@ldeo.columbia.edu (* presenting author), cai@ldeo.columbia.edu

[2]Institute for Earth Sciences, Academia Sinica, Taipei, Taiwan, gzellmer@earth.sinica.edu.tw

[3] Centro de Geociencias, UNAM, Querétaro, México, tuena@dragon.geociencias.unam.mx

[4] Isotope Geosciences Unit, SUERC, East Kilbride, UK, fin.stuart@glasgow.ac.uk

[5]EPS, Harvard University, Cambridge, MA USA, langmuir@eps.harvard.edu

Continental crust recycled via subduction erosion has been suggested to be a quantitatively important component that may overshadow the crustal contributions from subducted trench sediment to arc magmas at erosional convergent margins [1]. However, unlike the trench sediment that can be measured directly and linked to arc chemistry [2], the composition of eroded lower continental crust is essentially unknown. Hence, its identification in arc magmas poses a real challenge as signals of the eroded crust must be distinguished from those of the trench sediment and also from contamination by the overlying crust.

Here we present results of a comprehensive geochemical study from two Holocene high-Nb monogenetic arc volcanoes (Texcal Flow and V. Chichinautzin) that were erupted within ~1100 year and within only 6 km from each other. Major and trace element and Sr-Nd-Hf-Pb-He isotope systematics demonstrate that the basaltic and basaltic-andesitic magmas are mixtures of mantle and crustal materials. High $^{3}He/^{4}He$ of 6-7 R_a in equilibrium olivines, however, and high and increasing melt Nb (from 17 to 36 ppm) and Nb/Ta (from 16 to 19) with increasing melt SiO_2 preclude substantial assimiliation of the overlying crust. Combined Sr-Nd-Hf isotope data and trace elements argue against the trench sediment as an isotopic end member as this would require an unreasonably large loss of Nd (~50%) relative to Hf in the trench sediment. Alternatively, we propose that Sr-Nd-Hf-Pb isotope and trace element systematics may best be explained through melting of a subarc mantle that was infiltrated with crustal components recycled via subduction erosion from the lower Mexican forearc crust. The data suggest for this region a model in which the recycled eroded crust may dominate arc chemistry together with fluids released from the subducted igenous oceanic crust while the signals of the subducted trench sediment are largely eclipsed. This may be explained by the low volumeric flux of sediment in this region owing to the young age of the subducting plate.

[1] Clift & Vannucci (2004) *Reviews of Geophysics* **42(2)**, 1-31. [2] Plank & Langmuir (1993) *Nature* **362,** 739-743.

The diagenetic history of marine sediments as revealed by C-S-Fe systematics

HARALD STRAUSS

Westfälische Wilhelms-Universität, Münster, Germany, hstrauss@uni-muenster.de

Marine sediments archive the products of primary productivity, subsequent mineralization of the sedimentary organic matter through microbial and/or inorganic processes, the input of detrital components, and the authigenic mineral formation within the sedimentary column. The C-S-Fe system constrains respective depositional as well as diagenetic aspects within marine sediments, frequently occurring under changing redox conditions. A diverse set of petrographic, geochemical, and isotopic proxy signals has evolved during the past fifty years with an ever increasing specificity. These proxy signals allow distinguishing between local/regional phenomena and perturbations of global geochemical cycles, both in modern sediments as well as for sedimentary rocks in the geologic record. Hartmann and Nielsen [1] were among the very early researchers applying some of these proxy signals in their study of marine coastal sediments from the Kiel Bight, Baltic Sea, northern Germany.

Abundances of carbon, sulfur, and iron, organic and inorganic carbon isotopes, multiple sulfur isotopes of sulfides and sulfates, and oxygen isotopes for sulfate were measured in pore waters and sediments collected during a revisit of these Baltic Sea sediments some 45 years after the original study. Respective proxy signals reveal a complex diagenetic evolution that is largely governed by bacterial sulfate reduction. Key features include a sizeable sulfur isotopic fractionation of up to 64‰ between sulfate and sulfide. The downcore evolution towards ^{34}S-enriched sulfur isotope values for both sulfur species in the pore waters suggest the development of sulfate limiting conditions. Disproportionation of sulfur intermediates cannot be excluded and would be consistent with the observed large fractionations in $\delta^{34}S$ as well as from a combination of $\delta^{34}S$ and $\Delta^{33}S$. Conclusions derived here overall confirm interpretations made by [1]. At the same time, an expanded analytical approach allows for more detailed information about microbially driven processes in the pore water realm and the sediments.

[1] Hartmann & Nielsen (1965) *Geologische Rundschau* **58**, 621-655.

Microbial characterization of groundwater from boreholes at CRL

SIMCHA STROES-GASCOYNE[1*], DANIELLE BEATON[2], MARILYNE AUDETTE-STUART[2], KAREN KING-SHARP[2], AMY FESTARINI[2], CONNIE HAMON[1], STEVE ROSE[2] AND LEE BELLAN[2]

[1]Atomic Energy of Canada Limited, Whiteshell Laboratories (WL), Pinawa, MB, Canada, stroesgs@aecl.ca (* presenting author)

[2]Atomic Energy of Canada Limited, Chalk River Laboratories (CRL), Chalk River , ON, Canada

Purpose of study and methods

A microbiological characterization study was carried out on groundwater samples from various depths in older (CR9, CR18) and recently drilled boreholes (CRG-1, CRG-2, CRG-4A) at Chalk River Laboratories (CRL). This work was carried out as part of a technical feasibility study assessing the suitability of the CRL site to host a proposed Geologic Waste Management Facility for CRL's radioactive non-fuel waste.

A multi-analysis approach was used to characterize the water samples for microbial content. Analyses included: (1) Geochemical analysis for major cations, anions, pH, Eh and DOC. (2) Total (live + dead) and viable (live) cell counts using a number of different dyes and probes. (3) Phospholipid fatty acid (PLFA) analysis for viable cells and community structure. (4) Classic culturing for heterotrophic aerobic and anaerobic bacteria, nitrate-utilizing and -reducing bacteria and sulphate-reducing bacteria. (5) Identification of isolates using BIOLOG GEN III. (6) Identification of microbes using DNA extraction and (pyro-) sequencing.

Result and Conclusions

The water samples contained a total population of 10^4 to 10^5 cells/mL of which generally only < 1% could be cultured. However, a large percentage of the total population was viable and showed some signs of metabolic activity. Identification results for isolates showed a dominance of *Pseudomonas*, *Sphingomonas* and *Acidovorax* species. Identification based on DNA sequencing showed a dominance of different species. The combined microbial and geochemical results suggest an oligotrophic biogeochemical system in the CRL groundwater. The presence of a population of viable but not culturable cells implies that, given an increased source of electron donors (e.g., DOC) and electron acceptors (e.g., metals) leached from the waste, microbial activity could increase significantly in a potential GWMF. This could have both positive effects (e.g., lower Eh and radionuclide (RN) solubility) and negative effects (e.g., increased RN mobility, ^{14}C-containing gas production). Ultimately the biogeochemical system is expected to return to its original oligotrophic conditions but the rate at which this would occur is uncertain because waste leach rates and *in situ* microbial metabolic activity rates are unknown. This study illustrates that microbial effects need to be considered in the safety assessment of a deep geologic nuclear waste repository.

Biogeochemical Characterization of a Late Archean Sub-Seafloor Hydrothermal System, Dome Mine, Timmins, Ontario, Canada

JESSICA STROMBERG[1]*, NEIL BANERJEE[1], GORD SOUTHAM[1], ED CLOUTIS[2], GREG SLATER[3], ERIK BARR[4]

[1]University of Western Ontario, Earth Science, London, Canada, jstromb@uwo.ca*

[2]Univeristy of Winnipeg, Geography, Winnipeg, Canada, e.cloutis@uwinnipeg.ca

[3]McMaster University, Geography and Environmental Science, Hamilton, Canada, gslater@mcmaster.ca

[4]Goldcorp Porcupine Mine, South Porcupine, Canada, Erik.Barr@goldcorp.com

Much of our understanding of early life on Earth is dependant on the characterization of habitable environments preserved in Archean terrains. One such example can be found in the Tisdale mafic volcanics and hydrothermally altered metasediments of the Abitibi greenstone belt in Northern Ontario [1]. These late Archean volcanics host greenstone quartz-carbonate vein gold desposits, which are characterized by iron-carbonate alteration from low-salinity, CO_2-rich hydrothermal fluids, resulting in the precipitation of carbonates such as dolomite and ankerite.

Previous work has identified endogenous molecular fossils within the 2,770-2,685 Ma Tisdale assemblage, suggesting the presence of a subsurface hydrothermal biosphere [1]. This study is focused on a unique set of 2,690-2679 Ma crustiform banded ankerite veins within the Tisdale mafic volcanics at the Dome mine, in Timmins. This ankerite horizon provides an opportunity for the characterization of an ancient sub-seafloor hydrothermal system and its potential biosphere. We are using multiple biogeochemical techniques to characterize the system, to elucidate its environmental conditions, genesis and evolution, as well as biomarkers, and any associations with gold mineralization.

XRD and IR-spectroscopy have identified compositional variations in the carbonate speciation and minerology of the ankerite horizon. These datasets in combination with SEM and stable C- and O- isotope analysis are being used to determine the degree of hydrothermal alteration, the fluid composition and genesis, and provide environmental constraints for the system. Extracted biosignatures are being characterized by GC-MS, stable C-isotope, and ToF-SIMS analysis.

An understanding of early earth habitable environments, the developement of methods for their characterization, and the identification of biosignatures is a key aspect in furthering the search for evidence of habitable environments and extant life on Mars [2]. In particular, given the detection of Fe-Mg carbonates on the Martian surface [3,4]. As well, this research has potential implications for the development of paleobiological vectors for mineral exploration.

[1] Ventura et al. (2007) *PNAS* **104**, 14260-14265. [2] Summons et al. (2011) *Astrobiology* **11**, 157-181. [3] Ehlmann et al. (2008) *Science* **322**, 3671-1832. [4] Morris et al. (2010) *Science* **23**, 421-424.

Photochemistry of arsenite on ferrihydrite and goethite

NARAYAN BHANDARI[1], RICHARD J. REEDER[2], AND DANIEL R. STRONGIN[1,*]

[1]Department of Chemistry, Temple University, Philadelphia, PA 19122, USA (dstrongi@temple.edu)

[2]Department of Geosciences, Stony Brook University, Stony Brook, NY 11794, USA

The photochemistry of arsenite (As(III)) in the presence of the iron oxyhydroxides, ferrihydrite and goethite, has been investigated. Attenuated total reflection Fourier transform infrared spectroscopy (ATR-FTIR), X-ray absorption near edge structure (XANES), and solution phase analysis have been used to characterize the surface bound and aqueous phase species. Both ATR-FTIR and XANES show that the exposure of ferrihydrite or goethite to As(III) for up to 24 h in the dark leads to no change in the oxidation state of the adsorbed or aqeuous phase As species. Exposure of either the As(III)/ferrihydrite or As(III)/goethite system to simulated solar radiation results in the majority of the surface bound As(III) becoming oxidized to arsenate (As(V)). At a solution pH of 5, this conversion of As(III) to As(V) on ferrihydrite results in the partitioning of a stoichiometric amount of Fe(II) into the aqueous phase. The majority of the As(V) product remains bound to the ferrihdyrite surface. This chemistry on ferrihydrite is relatively similar in the absence or presence of dissolved oxygen. Also, in the ferrihydrite circumstance, the As(III) to As(V) conversion shows the characteristics of a self-terminating reaction in that there is a significant suppression of this redox chemistry before 10% of the total iron making up the ferrihydrite partitions into solution as ferrous iron. The self-terminating behavior exhibited by this photochemical As(III)/ferrihydrite system is likely due to the passivation of the ferrihydrite surface by the strongly bound As(V) product. In contrast, the As(III)/goethite system shows a different photochemical behavior in the absence or presence of dissolved oxygen. In the presence of dissolved oxygen at a solution pH of 5, results suggest that in contrast to ferrihydrite the majority of the As(V) product is in the aqueous phase and the relative amount of aqueous Fe(II) is significantly less than in the ferrihydrite circumstance. A possible reason for this experimental observation is that in the oxic environment Fe(II) on the goethite, which forms via the photoinduced oxidation of As(III), is oxidized to Fe(III) by dissolved oxygen resulting in the formation of reactive oxygen species that can lead to the further oxidation of As(III) in solution. Additional experiments suggest that this behavior is not observed on ferrihydrite at pH 5, due to the lower affinity of the surface for Fe(II), compared to goethite. Overall, the research has brought forward how differences in the surface properties of iron oxyhydroxides can result in changes in redox chemistry.

Characterisation of arsenic and trace metals in acid sulfate environments

JACQUELINE L. STROUD[1]* AND RICHARD N. COLLINS[1]

[1]School of Civil and Environmental Engineering, UNSW, Sydney, Australia, j.stroud@unsw.edu.au (* presenting author)

Contaminant mobilisation in acid sulfate environments

Disturbed acid sulfate environments pose a serious threat to water quality, ecosystem health and commercial activities. The interaction between hydro-biogeochemical factors leads to the discharge of sulfuric acid and toxic concentrations of dissolved contaminants including iron and aluminium to adjacent water bodies. Comparatively little is known about trace metals and arsenic mobilisation in these environments.

We evaluated the mobilisation of trace metals and arsenic in groundwater and adjacent drain waters during a 10-day rainfall event at our Tweed Valley field site, NSW, Australia. This site has previously been identified as a metal mobilisation hotspot. We used multi-piesometers, drain water autosamplers and Diffusive Gradients in Thin films (DGT) devices to monitor the temporal changes in contaminant mobilisation. Metal and metalloid concentrations were determined using ICP-MS, and arsenic speciation (As(III), As(V), DMA and MMA) was analysed using HPLC-ICP-MS. Changes in contaminant concentrations were compared to concomitant changes in redox potential, pH, anions and dissolved organic carbon concentrations in order to characterise mobilisation processes. Elevated concentrations of cadmium, zinc and arsenic (arsenate and arsenite) were detected, suggesting that trace metals and arsenic also contribute to the poor water quality in these environments. DGT devices were effective in metal and metalloid assessments, and we were able to measure the fluctuations in contaminant concentrations downstream from the metal mobilisation hotspot.

Outcomes

These results will help us to understand the mobilisation and transport processes of trace metals and metalloids in these environments and better predict their risk to water quality.

Oxidative corrosion of the uraninite (111) surface

JOANNE E. STUBBS[1]*, PETER J.ENG[1], CRAIG A. BIWER[1], ANNE M. CHAKA[2], GLENN A. WAYCHUNAS[3], AND JOHN R. BARGAR[4]

[1]Center for Advanced Radiation Sources, University of Chicago, Chicago, IL, USA, stubbs@cars.uchicago.edu (* presenting author)

[2] Physical Measurement Laboratory, National Institute of Standards and Technology, Gaithersburg, MD, USA

[3] Lawrence Berkeley National Laboratory, Berkeley, CA, USA

[4] Stanford Synchrotron Radiation Lightsource, Menlo Park, CA, USA

Uraninite (UO_2) is the most abundant uranium ore mineral, the product of proposed bioremediation strategies for uranium-contaminated soils and aquifers, and its synthetic analog is the primary constituent of most nuclear fuels (1-3). This material is known to incorporate interstitial oxygen up to a stoichiometry of $UO_{2.25}$ without disruption of the uranium lattice, but the structural details of the process are the subject of ongoing study and debate (e.g., 4-5). Because the solubility and dissolution kinetics of uraninite depend heavily on the oxidation state of uranium, understanding the mechanims of UO_2 surface oxidation and corrosion is essential to predicting its stability in the environment throughout the nuclear fuel cycle. To date, however, no study has addressed this process at the molecular scale at atmospheric pressure and room temperature.

We present results of a crystal truncation rod (CTR) x-ray diffraction study of the UO_2 (111) surface. This hard x-ray technique is ideally suited to such studies, because it can probe the structures of interfaces at atmospheric conditions and buried below liquids and solids. The single-crystal surface was prepared under anoxic conditions, measured under dry helium, then exposed to dry O_2 gas and measured at several time points over the course of two weeks. The pristine surface is characterized by minimal contraction of the uppermost atomic layers and the addition of an oxygen layer above the vacuum-terminated surface. Following exposure to dry O_2, an oxidation front proceeds into the crystal, intersitial oxygen atoms penetrate to depths of 30 Å or more, U-U layer distances contract (consistent with bulk uraninite oxidation), and an ordered superlattice, which is commensurate with the underlying bulk, forms. These results demonstrate that the solid state diffusion of oxygen into UO_2 and UO_{2+x} surfaces is facile and that ordering kinetics are relatively rapid, even at room temperature.

Ab initio thermodynamics, which combines density-functional theory calculations with macroscopic thermodynamics, provides insight into the energetics, bonding, and oxidation processes that occur as oxygen reacts with the surface and diffuses into the solid. Surface oxidation results in formation of a U^{+6} cation triply bonded to single oxygen adatoms. Subsurface oxidation is predicted to contract U-U layers consistent with experimental observations.

[1] Finch & Murakami (1999) *Rev. Mineral. Geochem.* **38**, 91-180.
[2] Bargar et al. (2008) *Elements* **4,** 407-412.
[3] Janeczek et al. (1996) *J. Nucl. Mat.* **238**, 121-130.
[4] Willis (1987) *J. Chem. Soc., Faraday Trans.* **83**, 1073-1081.
[5] Conradson et al. (2004) *Inorg. Chem.* **43**, 6922-6935.

A COMPARISON OF GLASS AND MINERAL INCLUSIONS IN QUARTZ AND ZIRCONS FROM KEWEENAWAN RHYOLITE FLOWS

JAMES STUDENT[1*] AND ALEXANDRA MASSAD[2]

[1] Central Michigan University, Mount Pleasant, MI 48859, USA stude1jj@cmich.edu (* presenting author)

[2]Department of Geological Sciences, University of Texas at El Paso, El Paso, TX 79968, USA

Melt inclusions (MI) and a wide-variety of mineral inclusions are well preserved in quartz phenocrysts and zircons from porphyritic rhyolite flows of the Midcontinent Rift System. The inclusions and their host minerals have been examined using EPMA, cathodoluminescence microscopy (CL), SEM/EDS, and LA-ICP-MS. Rhyolite from the North Shore Volcanic Group, the Porcupine Mountains, the Portage Lake Volcanics, and the Michipicoten Island Formation were utilized in this study. Inclusions hosted by quartz and zircons were studied in thin sections and grain mounts, respectively.

The MI were categorized based on their phase assemblages and preservation style [1]. CL images of the host quartz phenocrysts reveal multiple stages of growth and dissolution. Ti contents (measured by EPMA and LA-ICP-MS) in the quartz vary widely and range from <15 to 280 ppm. Using a modified TitaniQ method [2], this corresponds to a temperature change of more than 250 °C in individual samples (using $aTiO_2$=1 and isobaric conditions). Presently there are still too many variables to constrain the absolute crystallization temperatures. The MI were analysed by LA-ICP-MS for major oxides and trace elements including Zr and Ti. The ranges in zircon saturation temperatures calculated using the model described by [3] agree with the TitaniQ temperature ranges. Unfortunately, it has been difficult to confidently constrain the Ti content (for TiO_2 activity calculations) in the MI using LA-ICP-MS analyses. This is due to the complex nature of the Ti distribution in the surrounding host quartz. The occurrence and distribution of zircon as inclusions in the quartz does suggest coeval crystallization of both phases.

An examination of SEM/EDS spectra of inclusions in zircon revealed at least 18 different minerals. They include K-spar, plagioclase, pyroxene, quartz, Fe-Ti oxides, apatite, monazite, and several different sulphides. Mineral inclusion assemblages in the zircons are distinct in each of the rhyolite samples that were studied. The mineral inclusions occur as isolated grains within zircon and inside glass bearing MI in zircon. While the majority of the inclusions appear to be primary and pristine, some of mineral and MI show evidence of modification by secondary processes. Utilization of the trace element chemistry of the mineral and MI trapped in zircon can potentially be used to better constrain the activity of TiO_2 in the melt during crystallization. This approach can lead to a more accurate estimate of quartz crystallization temperatures for Keweenawan rhyolite.

[1] Student *et al.* (2006): *Eos Trans. AGU,* **87**(52), Abstract V23C-0619. [2] Thomas *et al.* (2010) *Contrib. Mineral. Petrol.* **160**, 743-759. [3] Watson & Harrison (1983) *Earth and Planet. Sci Lett.* **64**, 295-304.

Enhanced nutrient consumption in the glacial Antarctic

A.S. STUDER[1*], A. MARTINEZ-GARCIA[1], M. STRAUB[1], D.M. SIGMAN[2], R. GERSONDE[3], G.H. HAUG[1]

[1]Department of Earth Sciences, ETH Zurich, Zurich, Switzerland ([*]anja.studer@erdw.ethz.ch, alfredo.martinez-garcia@erdw.ethz.ch, marietta.straub@erdw.ethz.ch, gerald.haug@erdw.ethz.ch) ([*] presenting author)
[2]Department of Geosciences, Princeton University, Princeton, NJ, USA (sigman@princeton.edu)
[3]Alfred Wegener Institute, Bremerhaven, Germany (Rainer.Gersonde@awi.de)

Productivity in surface waters leads to the sequestration of carbon dioxide (CO_2) in the deep ocean, a process known as the ocean's "biological pump." The Antarctic Zone of the Southern Ocean represents the major "leak" in this pump. Nutrient- and CO_2-rich waters are brought to the surface, allowing CO_2 to outgas. The scarcity of iron and/or light reduces phytoplankton productivity, leaving some of the major nutrients (nitrate, phosphate) unused. Those "preformed" nutrients are subducted into the subsurface without re-sequestering CO_2 into the deep ocean, introducing a degree of inefficiency to the global biological pump. To explain lower glacial atmospheric CO_2, it has been suggested that there was a decrease in the exchange between polar surface water and ocean interior, described as "polar ocean stratification." This physical change would have, in itself, reduced the outgassing of CO_2, and it may have increased the fraction of nutrients utilized in Antarctic surface ocean, rendering the region a more efficient part of the global biological pump. The first efforts to reconstruct nitrate utilization in the Antarctic measured nitrogen (N) isotopes on bulk sediment, but this can be biased by diagenesis and/or allochthonous N input. Subsequent studies measured the N isotopes encapsulated in diatom frustules ($\delta^{15}N_{db}$), which carry the pristine signal, but results have varied. Here, we report a consistent increase in $\delta^{15}N_{db}$ into the last two glacial periods, with abrupt decreases during the subsequent deglaciations. In contrast, the descent from interglacial to glacial conditions was more gradual/stepwise, reminiscent of the general atmospheric CO_2 pattern. The first major $\delta^{15}N_{db}$ increase into the last ice age occurred at the MIS 5e/5d transition, coincident with the major decline in Antarctic temperature and the first 40 ppm step in ice age CO_2 decline. In addition to our analysis of the total biogenic opal <100 µm, we analyzed the $\delta^{15}N_{db}$ of two distinct diatom species assemblages. Their $\delta^{15}N_{db}$ values are offset by roughly 1‰ but show the same trends through time. This rules out the possibility that the glacial-interglacial $\delta^{15}N_{db}$ changes measured on the total diatom community are caused by changing diatom species composition, a concern that had been raised previously.

Noble gas radionuclides in Yellowstone geothermal gases

N. C. STURCHIO[1*], R. YOKOCHI[2], R. PURTSCHERT[3], W. JIANG[4], G.M. YANG[4], P. MUELLER[4], Z.T. LU[2,4], B.M. KENNEDY[5], AND Y. KHARAKA[6]

[1]University of Illinois at Chicago, Chicago, IL, USA, sturchio@uic.edu, (* presenting author)
[2]University of Chicago, Chicago, USA, yokochi@uchicago.edu
[3]University of Bern, Switzerland, purtschert@climate.unibe.ch
[4]Argonne National Laboratory, Argonne, IL, USA, wjiang@anl.gov, pmueller@anl.gov, lu@anl.gov
[5]Lawrence Berkeley National Lab., Berkeley, CA, USA, bmkennedy@lbl.gov
[6]U. S. Geol. Survey, Menlo Park, CA, USA, ykharaka@usgs.gov

We collected and analyzed noble gas radionuclides (^{39}Ar, half-life = 269 yr; ^{81}Kr, half-life = 229,000 yr; ^{85}Kr, half-life = 10.8 yr) in gases from four geothermal features at Yellowstone National Park (Beryl Spring, Frying Pan Spring, Ojo Caliente Spring, and Mud Volcano). In the field, condensation of water vapor and chemical stripping of CO_2 were done to reduce the samples to manageable volumes which were compressed into gas cylinders. Separations of Kr and Ar from gas samples were performed by existing methods [1,2]. Kr radionuclides were measured by atom-trap trace analysis at Argonne using ATTA-3 [3], and ^{39}Ar was measured by low-level counting at Bern [2].

Isotopic abundances of ^{39}Ar in all four samples were 4 to 6 times higher than atmospheric, indicating substantial contributions from subsurface nucleogenic production, as reported earlier [4]. ^{81}Kr isotopic abundances were not significantly different from atmospheric. ^{85}Kr isotopic abundances were 0.55 to 0.96 times atmospheric, possibly indicating contributions from recent groundwater recharge (≤ 10 yr) and/or contributions of both ^{39}Ar and ^{85}Kr from subsurface production at a ratio typical of that in granitic rock (see Figure).

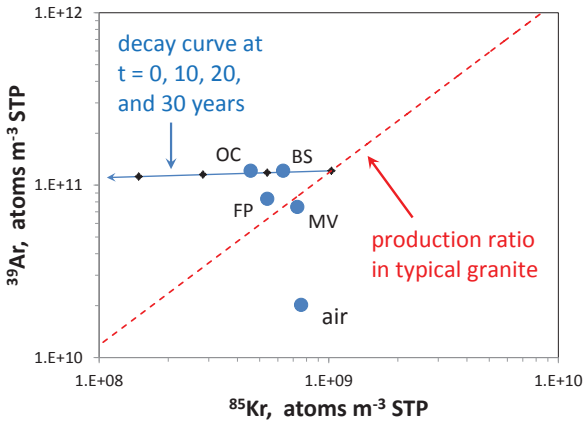

[1] Yokochi et al (2008) *Anal. Chem.* **80**, 8688-8693.
[2] Forster & Loosli (1989) In: *Isotopes of Noble Gases as Tracers in Environmental Studies*, IAEA, Vienna.
[3] Jiang et al. (2012) manuscript in review.
[4] Purtschert et al. (2009) Goldschmidt abstract, Davos.

Residence times of the upper low-arsenic aquifers in Bangladesh at the onset of increased abstraction

M. STUTE[1,2*]. I. MIHAJLOV[1], P. SCHLOSSER[1], K.M. AHMED[3] AND A. VAN GEEN[1]

[1]Lamont-Doherty Earth Observatory of Columbia University, Palisades, NY, USA, martins@ldeo.columbia.edu (*presenting author)

[2]Barnard College, New York, NY, USA

[3]Dhaka University, Dhaka, Bangladesh

Elevated levels of dissolved arsenic in shallow aquifers in the Bengal basin will result in increased use of deeper, currently low-arsenic aquifers. Compared to the shallow aquifers, relatively little is known about the flow dynamics of the deeper systems (>100 m depth).

Radiocarbon, ^3H, stable isotope, and noble gas data were obtained from both aquifer systems in our field area in Araihazar, 25 km east of Dhaka, Bangladesh. Noble gas temperatures of shallow groundwater generally reflect current water temperature at the water table despite elevated CO_2 (up to 12%) and depleted O_2 concentrations in the unsaturated zone. ^3H and $^3H/^3He$ data are consistent with recharge during the past 50 years. Most of the deeper groundwater (>100m depth) underlying the high-arsenic zone is ^3H free; and radiocarbon, stable isotope, and noble gas data indicate that recharge likely occurred at the transition between the late glacial period and the Holocene, a time of major changes in sea level, vegetation, and climate.

The relatively high residence time of water in the aquifer suggests a low recharge rate (cm's/year) until large-scale groundwater pumping for municipal supplies began in Dhaka in the 1960s.

Increased usage of this resource will result in higher recharge rates and might cause leakage from shallow high-arsenic aquifers and needs to be considered in management of water resources in Bangladesh.

Modulation of the product of U(VI) reduction by phosphate and calcium

MALGORZATA STYLO[1]*, DANIEL S. ALESSI[1], JUAN S. LEZAMA-PACHECO[2], JOHN R. BARGAR[2] AND RIZLAN BERNIER-LATMANI[1]

[1]Environmental Microbiology Laboratory, Ecole Polytechnique Federale de Lausanne, EPFL, Lausanne CH 1015, Switzerland, malgorzata.stylo@epfl.ch (*presenting author)

[2]Stanford Synchrotron Radiation Lightsource, Menlo Park, CA 94025, USA, bargar@slac.stanford.edu

One bioremediation strategy for uranium-contaminated aquifers involves the enzymatic reduction of soluble U(VI) to less mobile U(IV) species. The mineral uraninite, $UO_{2(s)}$, is considered to be the most desirable product of bioremediation due to its relative stability under reducing conditions. However, it has been shown repeatedly that uraninite is not the sole product of U(VI) reduction. Among these other U(IV) products are monomeric U(IV) species, believed to coordinate to bacterial biomass via phosphate and/or carboxylate groups and likely to be less stable than uraninite. For bioreduction to be a viable remediation strategy, it is crucial to pinpoint the factors promoting the formation of uraninite versus monomeric U(IV). Investigations to date have suggested that certain solutes, including PO_4^{3-} and Ca^{2+}, lead to preferential formation of monomeric U(IV). However, the mechanism of this process remains unknown.

In this study, we examine (1) the influence of PO_4^{3-} and Ca^{2+} on the product of U(VI) bioreduction and (2) the fate and behavior of those solutes during U(VI) reduction. Uranium L_{III} edge X-ray absorption spectroscopy and a wet chemical extraction technique were used to quantify the relative contribution of these two U(IV) species in systems in which the solute concentrations were systematically varied. We initially hypothesized that Ca^{2+} shields PO_4^{3-} from negatively charged groups and thus allows the binding of phosphate to the cell wall and the complexation of U(IV) by phosphate, leading to preferential monomeric U(IV) formation. To test this hypothesis, we measured the concentration of the two solutes during U(VI) reduction.

The results confirm that the U(IV) product of bioreduction is a mixture of uraninite and monomeric U(IV). The presence of calcium enhances the fraction of monomeric U(IV) produced. Moreover, even a low concentration of phosphate (1.9 mg/l) promotes greater formation of monomeric U(IV). However, the contribution of monomeric U(IV) does not change with increasing concentrations of this solute. The combination of calcium and phosphate results in a close to pure monomeric U(IV) product. Surprisingly, the aqueous concentrations of PO_4^{3-} or Ca^{2+} during U(VI) bioreduction are constant, suggesting little binding of these solutes to biomass. Hence, the direct association of these solutes with biomass cannot account for the observed effect. This suggests an indirect influence of phosphate and calcium on biological controls over the product of U(VI) reduction. For example, the production of bacterial extracellular polymeric substances could be limited by these solutes, restricting the number of nucleation sites for uraninite precipitation and promoting the formation of monomeric U(IV).

Our work provides a first glimpse into the complexity of the influence of geochemical factors on the biological controls of U(IV) product formation.

Solubility of Palladium (Pd) in Hydrocarbons: Application to Ore Genesis

ICHIKO SUGIYAMA[1]* and ANTHONY WILLIAMS-JONES[1]

[1]Department of Earth and Planetary Sciences, McGill University, Montreal, Quebec, ichiko.sugiyama@mail.mcgill.ca (*presenting author)

In natural systems, the platinum group elements (PGE) are commonly associated spatially with hydrocarbons. For example, pyrobitumen in the Kupferschiefer, Poland, has been shown to have high concentrations of Pd and Pt [1]. Black shales in South China likewise have been shown to contain elevated Pd and Pt (0.4 ppm Pd and 0.3 ppm Pt in the Zunyi deposit) [2]. These observations and preliminary experiments showing that crude oils can dissolve metals to potentially exploitable concentrations, suggest that liquid hydrocarbons could constitute important ore fluids [3]. The objective of this research is to experimentally determine the solubility of Pd in selected organic compounds known to be important constituents of natural liquid hydrocarbons, and thereby contribute to the body of knowledge on ore forming processes involving hydrocarbons. Approximately 40 to 50% of crude oil is composed of paraffins, including straight chain alkanes. In view of this and the fact that Pd is known to have a strong affinity for sulphur (some crude oils contain appreciable sulphur), we have investigated the solubility of Pd in dodecane and dodecanethiol.

Our experiments were performed in light-weight titanium autoclaves treated with nitric acid to produce an inert internal surface coated with TiO_2, and involved measuring the solubility of palladium metal in dodecane and dodecanethiol at 150 °C. The durations of the experiments ranged from 15 to 60 days. After completion of an experiment, the autoclave was quenched, and samples of the quenched solutions, and solutions used to wash the autoclaves (Pd commonly precipitated on the surface of the autoclave), were analyzed for Pd using NAA.

The concentration of Pd in dodecane was 0.33 ppm ± 0.18 ppm and in dodecanethiol was 0.90 ppm ± 0.45 ppm. These data show that that Pd is very soluble in these simple analogues of natural liquid hydrocarbons at temperatures commonly encountered in oil reservoirs, and that its solubility may be increased by complexation with thiol groups. We therefore conclude that liquid hydrocarbons could be very effective agents of Pd transport. This and the observed close spatial association of Pd with hydrocarbons in some PGE deposits suggest that liquid hydrocarbons could be important ore fluids for these deposits.

[1] Kucha, H. and Przybylowicz, W. (1999) Noble metals in organic matter and clay-organic matrices, Kupferschiefer, Poland. Economic Geology, 94,1137-1162. [2] Coveney, R.M., Nansheng, C. 1991. Ni-Mo-PGE-Au-rich ores in Chinese black shales and speculations on possible analogues in the United States. Mineralium Deposita, 26, 83-88. [3] Williams-Jones AE, Bowell RJ, Migdisov AA (2009) Gold in solution. Elements 5: 281-287.

Exploration and enhancement of Sm/Nd carbonate geochronology

N.C. SULLIVAN[1], E.F. BAXTER[1], AND K. MAHER[2]

[1]Boston University, Boston, MA, norasull@bu.edu, efb@bu.edu
[2]Stanford University, Palo Alto, CA, kmaher@stanford.edu

Carbonate mineralization occurs across a broad spectrum of Earth's environment. Direct dating of carbonate minerals has become an important goal. Prior work has used the ^{14}C, U-series, and U/Pb isotope systems, but all have limtations. The Sm-Nd system has rarely been attmepted because most carbonate has very low $^{147}Sm/^{144}Nd$ ratios (<0.2), indicating limited geochronologic potential. A handful of published studies [e.g. 1,2,3] suggest that some high (0.2 to >1.0) $^{147}Sm/^{144}Nd$ carbonates do exist and that meaningful age information can potentially be extracted. These studies use mild acids to extract multiple carbonate separates from a single vein or deposit.

Our preliminary work has focused on three samples: a metamorphic calcite vein from Vermont, a hydrothermal dolomite from an ultramafic hosted talc deposit, also from Vermont, and a siderite from the Copper Chief Mine in Arizona. All three samples were put through an 8-step sequential extraction procedure (5.0, 4.2, 3.9, 3.5pH acetic, glacial acetic, 1.5N HCl, conc. HNO_3, HF) to isolate a high $^{147}Sm/^{144}Nd$ reservoir within the carbonates. All leachates were analyzed for Sm/Nd isotopes and major and trace element concentrations. Differences in Ca, Mg, Mn, Fe, and Sr between each leachate show that they represent different reservoirs. Electron microprobe data confirms there is subtle compositional zoning within the carbonate, at the micron scale, in all three samples.

As with previous studies, there is scatter in our "isochron" data. A 9-point isochron for the Vermont calcite vein shows a $^{147}Sm/^{144}Nd$ range of 0.09884-0.21180 yielding an age of 386 ± 34 Ma (MSWD 4.7). The high MSWD implies that some leached material did not form in isotopic equilibrium with the concordant carbonate fractions and therefore does not belong on the isochron. Assuming most of the carbonate is dissolved in the pH-controlled acetic leachates, and discarding the stronger acid extractions, we calculate a 4-point isochron age of 353 ± 27 Ma (MSWD 1.17). This age agrees with a published monazite age of 352.9 ± 8.9 Ma from the same outcrop [4]. The same effect is seen with the Vermont dolomite sample: when all leachates are considered the isochron yields an age of 508 ± 93 Ma (MSWD 41), but if we eliminate the stronger acid leachates the age becomes 657 ± 62 Ma (MSWD 1.05). The low MSWD implies this is a reliable "isochron", however the age is clearly older than Taconic or Acadian metamorphism expected for this sample. The siderite sample from Arizona shows a $^{147}Sm/^{144}Nd$ range of 0.21105-0.44711 and gives a reasonable Proterozoic age.

Our data shows that there are multiple chemical and isotopic domains present within each sample and our leaching procedure has begun to successfully isolate them. To refine sample selection and improve the reliability and precision of the carbonate ages, we are combining major and trace element data with electron microprobe images to identify the origin of the compositional variations and determine which acid extractions should be included in the isochron.

[1] Henjes-Kunst *et al.* (2008) *GCA* A368. [2] Nie *et al.* (1999) *Resource Geology* **49**, 13-25. [3] Peng *et al.* (2003) *Chemical Geology* **200**, 129-136. [4] Wing *et al.* (2003) *Contrib. Mineral Petrol* **145**, 228-250.

Halogens and noble gases subducted into the mantle: constraints from mantle wedge peridotites and olivines in arc lavas

HIROCHIKA SUMINO[1*], LISA ABBOTT[2], AYA SHIMIZU[3], RAY BURGESS[2] AND CHRIS J. BALLENTINE[2]

[1]GCRC, University of Tokyo, Tokyo, Japan, sumino@eqchem.s.u-tokyo.ac.jp

[2]SEAES, University of Manchester, Manchester, UK, lisa.abbott@postgrad.manchester.ac.uk, ray.burgess@manchester.ac.uk, Chris.Ballentine@manchester.ac.uk

[3]Tokyo Metropolitan Industrial Technology Research Institute, Tokyo, Japan, shimizu.aya@iri-tokyo.jp

Findings of subducted halogens and noble gases with seawater and sedimentary pore-fluid signatures in exhumed mantle wedge peridotites and eclogites from the Sanbagawa-metamorphic belt, southwest Japan [1, 2], as well as that of seawater-derived heavy noble gases (Ar, Kr, Xe) in the convecting mantle [3], challenge a popular concept that the water flux into the mantle wedge is controlled only by hydrous minerals in altered oceanic crust and sediment resulting in that subduction volcanism acts as a 'subduction barrier' which efficiently recycles volatile components contained in subducted slabs back to the Earth's surface. To verify whether and how such subduction fluids modify the composition of the mantle beneath subduction zones, we determined noble gas and halogen compositions of mantle wedge peridotites and olivines in arc lavas.

MORB-like $^{3}He/^{4}He$ and halogen ratios of olivines in lavas from the northern Izu-Ogasawara arc and a peridotite from the Horoman alpine-type peridotite complex in northern Japan indicate insignificant contribution to the mantle wedge of radiogenic ^{4}He and porefluid-like halogens both observed in the subduction fluids in the Sanbagawa samples to a depth ranging from 40 to 100 km [1, 2]. A hotter mantle wedge than those of mature subduction zones is proposed for the Sanbagawa subduction system [4], in contrast the Izu subducting slab is relatively cold and would therefore lose relatively little water at equivalent depths to other slabs [5]. This implies a relatively small amount of the pore water subduction fluids would be released from the Izu slab at a sub-arc depth (150-200 km) resulting in further subduction to great depths in the mantle.

The mechanism by which the seawater-like noble gases are delivered to the convecting mantle remains to be elucidated. Serpentinized lithosphere of subducting slab is probably the best candidate, because if the hydration of the lithosphere by pore fluids is operating in a closed system, subduction of the serpentinized lithosphere can transport pore-fluid derived noble gases and halogens into the deep mantle [1, 2]. This is supported by a recent observation of noble gases and halogens in exhumed serpentinites similar to that of seawater and sedimentary pore fluids [6].

[1] Sumino *et al.* (2010) *Earth Planet. Sci. Lett.* **294**, 163-172. [2] Sumino *et al.* (2011) *Mineral. Mag.* **75**, 1963. [3] Holland & Ballentine (2006) *Nature* **441**, 186-191. [4] Mizukami & Wallis (2005) *Tectonics* **24**, TC6012. [5] van Keken *et al.* (2011) *J. Geophys. Res.* **116**, B01401. [6] Kendrick *et al.* (2011) *Nature Geosci.* **4**, 807-812.

Gold complexation within a halophilic cyanobacterium

KELLY L. SUMMERS*, JEREMIAH SHUSTER, MARTIN J. STILLMAN AND GORDON SOUTHAM

The University of Western Ontario, London, Canada
ksummer4@uwo.ca (* presenting author)

Introduction

Understanding the biogeochemical processes that transform gold are important in improving our ability to identify anomalies within dispersion halo environments, and potentially to recover trace amounts of gold [1]. Cyanobacteria have been implicated as potential gold nanofactories [2], and may contribute to gold nanoparticle formation in placer environments [3].

Octahedral platelet and nanoparticle gold precipitation has been observed after exposure of bacteria, e.g., *Plectonema boryanum* 485 [4], to $HAuCl_4$. The mechanism by which gold nanoparticles form within these cells is not well understood; however, adsorption of Au(I) to sulfur was reported following the addition of $HAuCl_4$.

Results and Discussion

X-ray analysis of near edge spectra (XANES), a synchrotron method, showed that the reaction of a halophilic *Plectonema sp*., with 0.5 mM $HAuCl_4$ reduced Au(III) to Au(I), which then formed complexes with sulfur. At higher gold concentrations (5 mM) Au(III) was reduced to elemental Au.

To investigate Au binding to known sulfur-containing proteins we probed glutathione (GSH), using Electrospray Ionization Mass Spectrometry (ESI-MS). GSH reduced Au(III) chloride to Au(I) and coordinated the Au through its cysteine residue (Figure 1). GSH binds Au as a monomer and as a dimer.

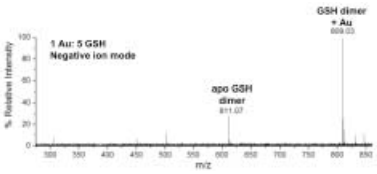

Figure 1. ESI-MS of a glutathione (GSH) complex with Au(I). $HAuCl_4$ added to 40 μM GSH for a final ratio of 1 Au: 5 GSH.

Cells reacted with 0.5 mM $HAuCl_4$ were lysed by liquid homogenization. Visualization of disrupted cells using phase contrast light microscopy revealed cell debris, and examination of whole mounts using TEM showed some cell envelope fragments. We recovered a soluble- and a cell envelope-fraction that bound Au. AAS and ESI-MS of the soluble fraction demonstrated the presence of low molecular weight Au-binding peptides. Occurrences of low molecular weight cysteine-rich metallothionein proteins in some species of marine cyanobacteria [5, 6] are targeted as possible gold-complexing organic compounds [7].

[1] Lengke et al. (2006) *Geomicrobiol. J.* **23**, 591–597.
[2] Chakraborty et al. (2009) *J. Appl. Phycol.* **21**, 145–152.
[3] Reith et al. (2010) *Geology* **38**, 843–846.
[4] Lengke et al. (2006) *Environ. Sci. Technol.* **40**, 6304–6309.
[5] Blindauer (2008) *Chem. Biodiv.* **5**, 1990–2013.
[6] Blindauer (2011) *J. Biol. Inorg. Chem.* **16**, 1011–1024.
[7] Stillman et al. (1994) *Met. Based Drugs.* **1**, 375-394.

Microbial siderophore effects on Pb sorption and mineral nucleation

SARA SUMMERS[1]*, GELIANG SONG[2], BRUCE BUNKER[2], AND PATRICIA MAURICE[1]

[1]University of Notre Dame, Civil Engineering & Geological Sciences, Notre Dame, IN 46556, USA ssummer1@nd.edu (* presenting author), pmaurice@nd.edu

[2]University of Notre Dame, Physics, Notre Dame, IN 46556, USA gsong@nd.edu, bunker@nd.edu

Siderophores are low molecular weight organic ligands released by many aerobic microorganisms and plants to acquire Fe. These ligands may also bind other metals such as Pb, thus affecting Pb sorption and nucleation and growth of Pb-bearing minerals. In this study, a combination of batch experiments and XAS analysis was used to determine the effects of the trihydroxamate siderophore desferrioxamine B (DFOB) on Pb sorption to montmorillonite (mmt) clay. In the absence of DFOB, Pb sorption increased with increasing pH and decreased at higher background electrolyte ($NaClO_4$) concentrations. In some instances, Pb carbonates were detected in the sorption experiments, with nucleation perhaps enhanced by the presence of the clay. DFOB was observed to have complex pH- and ionic-strength dependent effects on Pb sorption to mmt. Ternary surface complexes were observed when both Pb and DFOB were present, under pH conditions at which Pb-DFOB complexes form in solution.

In order to explore more thoroughly Pb carbonate formation, experiments were conducted in which cerussite ($PbCO_3$) and/or hydrocerussite ($Pb_3(CO_3)_2(OH)_2$) were grown in the presence and absence of DFOB. DFOB was found to strongly affect the crystal size and habit of the Pb(hydroxy)carbonate precipitates. XAS analysis of structure is ongoing.

Bacterial Necromass as a driver of bacterial weathering

STEPHEN SUMMERS*[1,2], CHARLES S. COCKELL[3] AND ANDREW S. WHITELEY[2]

[1]Department of Planetary Science, The Open University, UK, stemme@ceh.ac.uk (* presenting author)

[2]Molecular Microbial Ecology Laboratory, Centre for Ecology & Hydrology, UK, aswhi@ceh.ac.uk

[3]School of Physics and Astronomy, University of Edinburgh, UK, c.s.cockell@ed.ac.uk

Background

The rock – soil interface (critical zone) is where many crucial geochemical processes occur. This region of the Earth's crust is an important source of nutrients that are required for life; however these are locked away in minerals unavailable to most biota. Recent studies have shown that bacteria can play a pivotal role in the release of these elements in a biologically available form [1, 2]. Many bacteria that show the ability to weather minerals are known to be heterotrophic [3], yet the environments that are most significant when discussing weathering are limited in organics. We have investigated the question: can heterotrophic bacteria in the critical zone use isotopically labelled bacterial necromass as a source of carbon? Plants have been shown to actively select for bacterial communities in rhizosphere by manipulating the environment and providing nutrients [4, 5], yet where does organics originate in areas known to have significant weathering but lacking in plants.

A lake site in Skorradalur, Iceland that has been shown to have significant rates of weathering at locations in some cases devoid of plants was investigated. We show that necrotic bacterial matter is a source of carbon for the organisms in the critical zone. Some of this necromass may be accounted for by fresh bacterial input during spring snowmelt.

Results and Conclusions

Stable isotope probing was used to show that most bacteria in the critical zone are heterotrophic and able to utilize bacterial necromass to drive metabolic activity. Exceptions to this were of Nitrospirales, some of which are lithoautotrophic [6] and Rhizobiales some of which are methanotrophic and are capable of using methyl alcohol and methane as a sole carbon source.

Using flow cytometry observed cell concentrations within snow packs covering sample site were measured to be up to 4.4 $x10^5$ cells per millilitre. This is a substantial influx of fresh organic matter each spring as snow melts.

[1] Cockell, C.S., et al (2009) Geomicrobiology Journal **26**(7) p. 491-507.

[2] Cockell, C.S., et al (2009) Geobiology **7**(1) p. 50-65.

[3] Uroz, S., et al (2007) Applied and Environmental Microbiology **73**(9) p. 3019-3027.

[4] Bashan, Y., G. Holguin, and R. Lifshitz (1993) Methods in plant molecular biology and biotechnology. CRC Press, Boca Raton, Fla, p. 331-345.

[5] Calvaruso, C., M.P. Turpault, and P. Frey-Klett (2006) Applied and Environmental Microbiology **72**(2) p. 1258-1266.

[6] Lebedeva, E., et al (2008) International journal of systematic and evolutionary microbiology **58**(1) p. 242-250.

U-Pb ages and Sr–Nd isotopic compositions of perovskite from the Yakutian kimberlites, Siberian Craton

JING SUN[1*], FU-YUAN WU[1], CHUAN-ZHOU LIU[1]

[1]Institute of Geology and Geophysics, Chinese Academy of Sciences, sunjing@mail.iggcas.ac.cn (* Presenting author)

Perovskite in kimberlites commonly contain high contents of U, Sr and Nd, and thus could provide effective constraints on the emplacement age and Sr-Nd isotopes of kimberlitic magmas [1, 2]. In this study, perovskite have been selected from 38 kimberlites from 10 fields in the Yakutian area, Siberian Craton, and analysed in-situ by LA-MC-ICPMS method. The obtained perovskite U-Pb ages suggest that kimberlites in the Yakutian field were emplaced in four episodes, ~420 Ma, ~360 Ma, ~220 Ma and ~160 Ma. Different kimberlite pipes in the same field were emplaced at the same time. Furthermore, all the diamondiferous kimberlites in Yakutian field were erupted around 360 Ma. The perovskites display $^{87}Sr/^{86}Sr$ ratios ranging from 0.70282 to 0.70375 and $^{143}Nd/^{147}Nd$ ratios from 0.51229 to 0.51271. The Sr-Nd isotope range displayed by perovskites is much narrower than that given by the whole-rock Sr-Nd isotopic compositions, i.e., 0.70318~0.70641 and 0.51048~0.51270, respectively [3]. On one hand, this suggests that whole-rock Sr-Nd isotope compositions of kimberlites have been contaminated during erupted route to surface. On the other hand, the relatively depleted Sr-Nd isotopic compositions shown by the perovskites also indicate that the Yakutian kimberlites belong to the Group-I kimberlite, and were derived from a similarly depleted mantle source.

[1] Yang *et al*. (2009) *Chemical Geology* **264**, 24-42. [2] Wu *et al.* (2010) *Lithos* **115**, 205-222. [3] Kostrovitsky *et al.* (2007) *Russian Geology and Geophysics* **48**, 272-290.

The formation of the giant Bayan Obo REE deposit: Constraints from Mg isotopes

WEIDONG SUN[1*], MING-XING LING[2], YU-LONG LIU[1], XIAOYONG YANG[3], FANG-ZHEN TENG[4]

[1]Key Lab of Mineralogy and Metallogeny, Guangzhou Institute of Geochemistry, The Chinese Academy of Sciences, Guangzhou China, weidongsun@gig.ac.cn (* presenting author)

[2]State Key lab of Isotope Geochemistry, Guangzhou Institute of Geochemistry, The Chinese Academy of Sciences, Guangzhou China, mxling@gig.ac.cn

[3]School of Earth and Space Sciences, University of Science and Technology of China, Hefei, China, xyyang@ustc.edu.cn

[4] Isotope Laboratory, Department of Geosciences, University of Arkansas, Fayetteville, AR 72701, USA, fteng@uark.edu

The Bayan Obo REE-Nb-Th-Fe deposit, located in Inner Mongolia, North China, is the largest REE deposit and the second largest Nb deposit in the world. Its genesis is highly debated, ranging from carbonatite magmatism, alteration of sedimentary carbonate rocks, through deposition of carbonates on the sea floor accompanied by simultaneous metasomatism, to formation due to Caledonian subduction. None of the models so far proposed can fully explain all the major facts[1, 2]. The key problem is the relationship between carbonatite dykes, sedimentary dolomite, REE ore body and iron ore body. The REE ore bodies have trace element patterns and initial Nd isotope values identical to those of carbonatite dykes nearby, implying genetic links. Carbon isotopic composition of the carbonatite dyke is similar to the normal mantle $\delta^{13}C$ value of -5±2‰, but their O isotope compositions range from 13.9 to 16.4‰ for calcite, which are much higher than the mantle $\delta^{18}O$ value of 5.7±1.0‰. Consistently, the Mg isotopes of calcite carbonatite dykes range from mantle value to sedimentary values. All these indicate that the calcite carbonatite dykes have major sedimentary components, through recycling or assimilation, or a combination of both. By contrast, Mg isotopic compositions of ore bodies and dolomite carbonatite dykes are all close to mantle value, indicating major components from the mantle. The age of ore-forming monazite (330 to 760 Ma) is scattered with a main peak at about 400 Ma, roughly coincident with the evolution of the Central Asian orogenic belt nearby, but is much younger than carbonatite dykes (1300 Ma). Such large age dispersal indicates protracted mineralization driven by a persistent heat source for about 400 Ma. Considering that the host dolomite has high SiO_2 contents and carbon and oxygen isotopes distinctively different from those of carbonatite dykes, all these observations point to protracted steam-cooking of carbonatite by subduction released high-Si fluids, which leached Fe from the mantle wedge and, REE, Nb and Th from carbonatite, forming the Bayan Obo deposit in overlying sedimentary carbonate.

[1] Yang X Y, Sun W D, Zhang Y X, et al. Geochimica et Cosmochimica Acta, 2009, 73: 1417-1435

[2] Liu Y L, Williams I S, Chen J F, et al. American Journal of Science, 2008, 308: 379-397

Si isotope signatures preserved in BSi hold temperature information

XIAOLE SUN[1*], PER ANDERSSON[2], CHRISTOPH HUMBORG[3,4], BO GUSTAFSSON[4], DANIEL CONLEY[5], PATRICK CRILL[1], AND CARL-MAGNUS MÖRTH[1,4]

[1]Stockholm University, Geological Sciences, Stockholm, Sweden, xiaole.sun@geo.su.se (* presenting author)
[2]Swedish Museum of Natural History, Labrotary for Isotope Geology, Stockholm, Sweden
[3]Stockholm University, Applied Environmental Science, Stockholm, Sweden
[4]Stockholm Resilience Center, Baltic Nest Insititute, Stockholm, Sweden
[5]Lund University, Earth and Ecosystem Sciences, Lund, Sweden

High-latitude aquatic ecosystems of the subarctic and arctic region have been shown to be influenced by climate fluctuations on short growing seasons for diatoms[1]. In our study[2], we reconstructed diatom production in Bothnian Bay, the subarctic northern tip of the Baltic Sea, by analysing Si isotopes in biogenic silica (BSi) perserved in sediments using MC-ICP-MS. The sediment core dated by ^{210}Pb gamma-ray spectrometer covered the period of 1820 to 2000, consisting of an unperturbed period from 1820 to 1950 and a second period affected by human activities from 1950 to 2000. The Si isotope values ranging between δ^{30}Si −0.18‰ and +0.58‰ in BSi were used to infer diatom production by using the Rayleigh model for fractionation patterns (Fig. 1). This exhibited that the production was correlated with air and water temperature, which in turn were correlated with the mixed layer depth. Especially after cold winters and deep water mixing, diatom production was limited. We also observed a shift of Si isotope values in the sediments after 1950, which is most likely caused by large scale damming of rivers which was heavily carried out between 1940 and 1960. Our findings offers a new way to estimate diatom production over much longer periods of time in diatom dominated aquatic systems, i.e. a large part of the world's ocean and coastal seas.

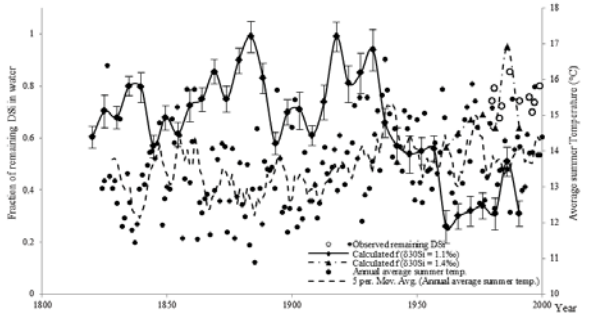

Figure 1: Fraction of the remaining DSi (f) in the water column reconstructed by the Rayleigh model, plotted with average summer air temperature through years. The inferior and superior error bars on f -values are the first quartile and third quartile for each f -value[2].

[1] Douglas & Smol (2010), The diatoms: applications for the environmental and earth sciences, *Smol J.P. & Stoermer E. F. eds, 12,* 231-248. [2] Sun et al. (2011) *Biogeosciences* **8**, 3491-3499.

EXAFS studies of Fe speciation in natural stream waters

ANNELI SUNDMAN*, TORBJÖRN KARLSSON, PER PERSSON

Umeå University, Umeå, Sweden
anneli.sundman@chem.umu.se (* presenting author)
torbjorn.karlsson@chem.umu.se
per.persson@chem.umu.se

Introduction

Fe speciation in organic rich soils and aquatic environments depends on the interactions between Fe and natural organic matter (NOM)[1]. These interactions also have a large influence on the availability of nutrients such as phosphorus and thus on biological productivity in natural environments. Accordingly, the Fe-NOM interactions are of fundamental importance but the generally low Fe concentrations in natural stream waters prevent direct spectroscopic studies. In this work we have developed a gentle and non-invasive method for concentrating stream water samples using adsorption via electrostatic forces onto permanently charged particles. The Fe speciation in these samples was subsequently analyzed by means of EXAFS spectroscopy. Stream waters were collected at the well-studied Krycklan Catchment[2], 64°, 16'N, 19°, 46E, in northern Sweden, with Fe concentrations in the range of 8-40μM.

Results

EXAFS investigations of negatively charged metal model complexes concentrated by our method showed that no significant distortions were induced as compared to the solution structures, which is in accordance with previous results[3,4]. The local structures of Fe(III) complexes in stream water samples from a forested site were investigated by applying the same technique. The EXAFS results indicated that the Fe(III) speciation was dominated by mononuclear organic chelate complexes and hydrolyzed Fe with ferrihydrite-like structures. We have also performed EXAFS studies of Fe speciation in soil solutions and groundwater, and these results will also be discussed. Finally, the method is not limited to EXAFS and we will show how it can be applied to P-NMR studies of natural waters, facilitating differentiation between inorganic and organic phosphorus species.

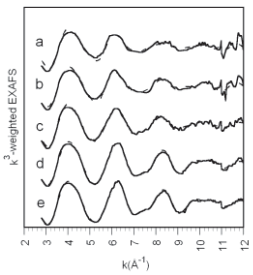

Figure 1. k^3-weighted EXAFS data from stream waters collected at the Krycklan Catchment[2], in February 2010, for a gradient series with a) 100%, b) 84%, c) 77%, d) 42% and e) 28% adsorption of Fe from the stream water. Solid lines represent experimental data and broken lines are fitted data.

[1] Rose et al. (1998) *Colloids and Surfaces A: Physicochemical and Engineering Aspects* **136**, 11-19. [2] Laudon et al. (2011) *Ecosystems* **14**, 880-893. [3] Bargar et al. (1999) *Geochimica et Cosmochimica Acta* **63**, 2957-2969 [4] Kaplun et al. (2008) *Langmuir* **24**, 483-489

Strontium stable isotope variations in lunar basalts

CHELSEA N. SUTCLIFFE[1*], KEVIN W. BURTON[2], IAN J. PARKINSON[3], DAVID COOK[1], BRUCE L. A. CHARLIER[3], DON PORCELLI[1], FATIMA MOKADEM[1], ALEX N. HALLIDAY[1]

[1]Department of Earth Sciences, University of Oxford, Oxford , UK chelsea.sutcliffe@st-annes.ox.ac.uk (* presenting author)
[2]Department of Earth Sciences, Durham University, Durham, UK
[3]Department of Earth and Environmental Sciences, The Open University, Milton Keynes, UK

In the terrestrial environment strontium stable isotopes may experience significant fractionation, both at low- and high-temperatures (e.g. [1,2]). Recent data for lunar basalts suggests that these rocks may possess light Sr stable isotope compositions (δ^{88}Sr = +0.16±0.07) [2] relative to mantle derived terrestrial basalts (δ^{88}Sr = +0.30±0.07) [2,3]. However, few samples have been analysed thus far, and at the ±50 ppm precision of these measurements, obtained using an MC-ICP-MS [2,3] smaller variations that may exist cannot be clearly resolved.

This study presents high-precision double spike TIMS data for ^{87}Sr/^{86}Sr (±5 ppm) ^{88}Sr/^{86}Sr (±10ppm) and ^{84}Sr/^{86}Sr (±20 ppm) for a suite of lunar basalts and highland rocks. These data indicate that there are significant and resolvable variations in δ^{88}Sr ranging from +0.30 for a ferroan anorthosite to +0.10 for a high-Ti Mare basalt. The lunar highland rocks (including anorthosites, troctolites and norites) possess a relatively small range of δ^{88}Sr values from +0.30 to +0.24 (0.06‰) whereas the mare basalts are distinctly lighter and encompass a larger range of δ^{88}Sr values, from +0.26 to +0.10 (0.16‰). The Mare basalts all possess negative Europium anomalies consistent with having been derived from a plagioclase depleted source, whereas the anorthosites are plagioclase rich. These observations suggest that the preferential incorporation of heavy Sr stable isotopes in plagioclase is the dominant mechanism controlling stable isotope fractionation in lunar basalts (similar to that seen in evolved terrestrial basalts [2]). Preliminary ^{84}Sr/^{86}Sr data suggests that the lunar rocks may possess slightly lighter compositions than terrestrial rocks, but this cannot be resolved at the present level of analytical precision. Taken together, these results clearly indicate that for the Moon primary igneous processes alone can generate significant variations in δ^{88}Sr, without the biological fractionation and recycling that may occur on Earth.

[1] Fietzke & Eisenhauer (2006), *Geochem. Geophys. Geosyst.* **7**, Q08009 [2] Charlier et al. *Earth Planet. Sci. Lett*. Submitted (2011) [3] Moynier et al. (2010) *Earth Planet. Sci. Lett***. 3-4,** 359-366

Exclusive use of a soil gas hydrocarbon geochemistry to vector towards mineral deposits

DALE SUTHERLAND

Activation Laboratories Ltd., Ancaster, Ontario, Canada, dalesutherland@actlabsint.com

This Soil Gas Hydrocarbon (SGH) geochemistry has been scientifically shown to detect those hydrocarbons released from the decomposition of bacteria at the end of their life cycle. From a "you are what you eat" perspective, the 162 specific hydrocarbons in the C5 to C17 carbon series range that are able to be detected provide an information rich forensic signature of identification from the bacteria that were directly growing on specific types of mineral deposits.

The forensic signature has been tested through projects administered by the Canadian Mining Industry Research Organization (CAMIRO) as well as those conducted by the Ontario Geological Survey. The use of the hydrocarbon signature has been able to differentiate between barren and ore bearing conductors and geophysical targets of mineralization or kimberlites from naturally occurring signals such as from granite gneiss.

Although the SGH name implies the exclusive use of soils, this geochemistry is also able to use other sample media such as humus, peat, sand, till, submerged sediment, and even snow. As these hydrocarbons are relatively neutral species the state of the flow of hydrocarbons that migrate and geochromatographically disperse through the overburden can be captured by the surface area of the sample media taken in a survey. This capability is vital in areas of difficult terrain where a complete sample survey may cover swamps, lakes, peaty areas as well as high ground. This multi-media survey can be processed and mapped together without data leveling, thereby significantly reducing the bias in interpretation represented by areas where sampling was formerly not warranted.

Several independent studies have also illustrated the successful depiction of blind mineralization that is shallow or to depths in excess of 700 metres. Figure 1 illustrates additional penetrating capability of this nano-scale geochemistry at dramatically delineating gold mineralization beneath a basalt cap. Similar results have been shown over areas of permafrost.

As a forensic signature the identification and vectoring capability of SGH provides a high level of confidence. The robustness of this geochemistry has allowed it to be used to discover new resources in not only greenfield applications but has also delineated mineralized extensions in brownfield surveys.

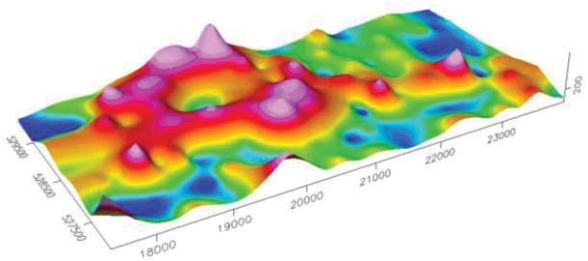

Figure 1: SGH gold anomaly below basalt cap, Mali, Africa

Viscosity of carbon dioxide-bearing silicate melt at high pressure

AKIO SUZUKI[1*]

[1]Department of Earth and Planetary Materials Science, Tohoku University, Sendai, Japan, a-suzuki@m.tohoku.ac.jp (* presenting author)

Knowledge of the viscosity of silicate melts at high pressure is of importance for modeling igneous processes in the Earth's interior. In natural magmas, volatiles are dissolved and affects physical properties. It has been known that volatiles reduce the viscosity of magmas. However, very few studies have been performed to investigate the effect of volatiles on the viscosity at mantle pressures. In the present study, the viscosity of carbon dioxide-bearing jadeite melt has been determined up to 4 GPa. We adopted the falling sphere method for viscometry. Experimental detail has been described elsewhere[1, 2]. X-ray radiography technique enables us to measure the falling velocity of a platinum sphere in situ. Experiments were performed at the NE7A station at the High Energy Accelerator Research Organization (KEK). We used a Kawai type multi anvil apparatus driven by a DIA type guide block installed on the MAX-III apparatus. A charge-coupled device (CCD) camera with a YAG:Ce fluorescence screen was used as an X-ray camera. The present study shows that an addition of carbon dioxide produces a viscosity decrease.

[1] Suzuki *et al*. (2002) *Phys. Chem. Miner*. **29**, 159-165. [2] Suzuki *et al*. (2011) *Phys. Chem. Miner*. **38**, 59-64.

Unveiling key players in the geological disposal environment

YOEHY SUZUKI[1*], AKARI FUKUDA[2], UTA KONNO[3], MARIKO KOUDUKA[3], HIROKI HAGIWARA[2], ANDREW MARTIN[4], NAOTO TAKENO[3], KAZUMASA ITO[3], TAKASHI MIZUNO[2]

[1]The University of Tokyo, Earth and Planetary Sciences, yohey-suzuki@eps.s.u-tokyo.ac.jp (* presenting author)
[2]Japan Atomic Energy Agency, mizuno.takashi@jaea.go.jp
[3]National Institute of Advanced Industrial Science and Technology, Institute of Geology and Geoinformation, n.takeno@aist.go.jp
[4]National Cooperative for the Disposal of Radioactive Waste, Andrew.Martin@nagra.ch

Introduction

It is well established that the speciation, distribution and transport of radionuclides is profoundly influenced by microbial activities in the shallow aquifer. However, it remains to be challenging to predict microbial influences on radionuclide migration in the deep aquifer for geological disposal of radioactive wastes. Currently, there are two major gateways to the deep biosphere through long vertical boreholes from the surface or short horizontal boreholes from the underground tunnel. Neither approach is exempt from the disturbance of the steady biogeochemical state and microbiological populations established through the long evolutionary history within the fracture networks. Despite the disturbance, it is very critical to identify indigenous microbial populations that potentially affect the long-term behavior of radionuclides (e.g. biosorption and redox transformation) and contaminant ones playing short-term roles during the recovery from the disturbance by consuming artificially introduced oxidants.

Underground research laboratories for comparison

The Grimsel Test Site (GTS), central Switzerland, has been in operation since 1984. The GTS provides 400-500-m deep granitic groundwater from boreholes that vary in age from 1 to 25 years. The Mizunami URL (MIU), which is being constructed in central Japan, provides 200-400-m deep granitic groundwater since 2007. The microbial comparison of the URLs associated with freshwater groundwater might result in the clarification of microorganisms commonly associated with the deep granitic subsurface.

Key indigenous and contaminant microbial populations

16S rRNA gene sequence analyses were conducted for groundwater samples from the GTS and the MIU. Sequences related to "*Candidatus* Magnetobacterium bavaricum" of Nitrospirae were predominant in all GTS boreholes, while β-proteobacterial sequences were only obtained from 1-2 year old GTS boreholes. Similarly, the predominance of β-proteobacterial sequences was gradually shifted to that of Nitrospirae sequences within several years after horizontal drilling at the MIU. The detection of the common microorganisms from the geographically distinct URLs suggests that these microbes are cosmopolitan in the granitic aquifer, radionuclide interactions with which should be clarified to provide general and reliable information for the safety of geological disposal in granitic repositories.

Acknowledgement

This study was supported by grants from the Nuclear and Industrial Safety Agency (NISA).

Cyanobacteria and photoferrotrophs: together again?

ELIZABETH D. SWANNER[1*] AND ANDREAS KAPPLER[1]

[1]University of Tübingen, Center for Applied Geoscience (ZAG), Geomicrobiology, Tübingen, Germany.
elizabeth.swanner@ifg.uni-tuebingen.de (* presenting author)

Phototrophs in a Ferrous Ocean

Anoxygenic phototrophs capable of metabolically oxidizing Fe^{2+} to Fe^{3+} are believed to be responsible for the deposition of mixed-valence Fe-containing Banded Iron Formations (BIF) in a Precambrian atmosphere of low O_2 [1]. The evolution of oxygenic photosynthesis by cyanobacteria has long been regarded as the primary mechanism for a rise in atmospheric O_2 in the Paleoproterozoic [2], and this O_2 would have further reacted with abundant aqueous Fe^{2+} to contribute to the deposition of BIF. As BIF were deposited across a wide range of Earth history and represent several distinct depositional settings, they potentially recorded changes in the makeup of the marine biosphere, particulalry among the anoxygenic photo(ferro)trophs and cyanobacteria. We ask what these changes were, and whether or not they are recorded in the style and substance of BIF deposition.

To address this, we report on our attempts to co-cultivate marine species of cyanobacteria and a photoferrotroph under conditions relevant to the hypothosized Precambrian ferrous ocean. Both strains will be independently evaluated to determine what chemical and physical factors imposed by changing ocean chemistry could have limited growth. These include light intensity, temperature and trace element availability. The results will be useful to compare with datasets reporting the calculated abundance of trace elements (e.g. Ni, Co) in the Precambrian ocean [3]. Then, the spatial distribution of trace metals and phosphorus to Fe and organic carbon from cell-mineral precipitates of Fe-containing co-culture experiments will be used for late-stage diagenesis experiments at temperature and pressure conditions observed in BIF to determine whether any trace element signatures associated with the phototrophic metabolisms in a ferrous ocean would be retained through time. A combination of fluorescence-based metal dyes in confocal microscopy and scanning transmission X-ray microscopy (STXM) will be used to assess these relationships both before and after simulated diagenesis.

Analogues for Precambrian Microbial Communities

As ferrous-rich marine environments today are scarce, analogue environments to study the phototrophic biosphere as occurred in the Precambrian and its implications for BIF are lacking. However, laboratory experiments are most useful if relevant to natural systems. Therefore we will compare the results of our data with the natural distribution of cyanobacteria and photoferrotrophs from a circumneutral Fe-rich freshwater lake. As most knowledge about photoferrotrophs is currently sourced from work with pure cultures, further molecular, chemical and cultivation-based studies of these organisms in natural environments is warranted.

[1] Kappler et al (2005) *Geology* **33**, 865-868. [2] Cloud (1968) *Science* **160**, 729-736. [3] Konhauser et al (2009) *Nature* **458**, 750-754.

An assessment of submarine groundwater discharge and its nearshore ecological impacts: Examples from the U.S. west-coast and Hawai'i

P.W. SWARZENSKI[1*], C.A. SMITH[2], P. M. GANGULI[3], J.A. IZBICKI[4] AND R.W. SHEIBLEY[5]

[1]USGS, Santa Cruz, CA (pswarzen@usgs.gov) (*presenting author)
[2]USGS, St. Petersburg, FL (cgsmith@usgs.gov)
[3]University of California, Santa Cruz, CA (pganguli@ucsc.edu)
[4]USGS, San Diego, CA (jaizbick@usgs.gov)
[5]USGS, Tacoma, WA (sheibley@usgs.gov)

The dynamic exchange of a coastal aquifer with sea water is a ubiquitous but still mostly inadequately quantified vector for nutrients and trace elements enroute to the sea. Biogeochemical reactions within this coastal aquifer/sea water mixing zone will transform many chemical species, including the redox sensitive- and microbially-mediated elements. As a result, this mixing zone can be a productive incubator zone for transformation products that rely on microbes or steep redox gradients. Geochemical and geophysical data from sites that extend from southern California to Puget Sound and Hawai'i will be used to assess submarine groundwater discharge (SGD) rates, scales, and constituent loadings. Unique geologic, climatic, and hydrologic characteristics define many west-coast U.S. and Hawaiian coastal systems. In these systems, the physical drivers and anthropogenic impacts on SGD are often unique and are assessed using a suite of naturally-occurring radionuclides (^{222}Rn and ^{223,224,226,228}Ra) and multi-channel electrical resistivity techniques. SGD is also evaluated as a sustained vector for nutrient (e.g., N and P) and trace element (e.g., Hg, U) loadings to nearshore environments and discussed in terms of ecosystem processes and impacts.

Coastal groundwater discharge near Kahekili Beach Park, Lahaina, Maui, Hawai'i

P.W. SWARZENSKI[1*], C.G. SMITH[2], C.D. STORLAZZI[1], L. DIAZ AND M.L. DAILER[3]

[1]USGS, Santa Cruz, CA (pswarzen@usgs.gov) (*presenting author)
[2]USGS, St. Petersburg, FL (cgsmith@usgs.gov)
[1]USGS, Santa Cruz, CA (cstorlazzi@usgs.gov)
[1]USGS, Santa Cruz, CA (ldiaz@usgs.gov)
[3]University of Hawai'i, Honolulu, HI (dailer@hawaii.edu)

This presentation describes a study conducted off Kahekili Beach Park, located just north of Lahaina on the west coast of Maui, Hawai'i, to better understand rates and drivers of coastal groundwater discharge and associated material transport into nearby coastal waters. This site has recently been well studied to examine how focused municipal wastewater plumes may be conveyed to the coastal waters by discharging groundwater [1, 2]. At this location there are multiple spring vents close to shore (water depth < 2m), where much lower salinity water can readily be observed discharging into the water column. There has also been a notable change in bottom type; this site was once dominated by corals and now is dominated by turf- or macro-algae [1]. This suggests a likely local nutrient imbalance that warrants further investigation. Previous reports have utilized dissolved nitrate - $\delta^{15}N$ records [1] as well as a suite of tell-tale organic pollutants [2] to infer focused municipal wastewater discharges at this location. Our study presents the first estimates of coastal groundwater discharge to this site based on the submarine groundwater discharge tracer, ^{222}Rn, and extends our understanding of the scales, magnitudes, and constituent loads conveyed by this submarine route.

[1] Dailer, Knox, Smith, Napier & Smith (2010) *Marine Pollution Bulletin*, **60**, 655-671. [2] Hunt & Rosa (2009) U.S.G.S. *Scientific Investigations Report*, 2009–5253, 166 p.

Pore scale CO_2-brine-mineral interactions in caprock

ALEXANDER M. SWIFT[1*], DAVID R. COLE[2], MICHAEL V. MURPHY[2], JULIA M. SHEETS[2], SUSAN A. WELCH[2]

[1] The Ohio State University, Columbus, Ohio, USA, swift.63@osu.edu (* presenting author)
[2] The Ohio State University, Columbus, Ohio, USA

Although the carbon sequestration capacity of the Mount Simon formation in western Ohio has been the subject of much published work, less is known about the ability of the overlying Eau Claire to serve as a caprock over geologic time. Predicting this involves a better understanding of how mineralogic heterogeneity controls the nature and extent of precipitation (pore-closing) and dissolution (pore-opening) in response to CO_2 perturbation. Preliminary study of select rock core indicates that the Eau Claire comprises subfacies on the scale of cm to m dominated by quartz-rich sandstone, shale and carbonate. At the pore scale (mm to microns), the relative abundance and pore-accessibility of reactive minerals such as illite, iron oxides, pyrite, and chlorite become key factors in controlling local geochemical regimes.

Results are presented here from *in situ*, temperature- and pressure-corrected kinetic models of CO_2-saturated brine in contact with rock that draw upon pore, rather than bulk, mineralogies. 2D mineral and pore scan raster maps of thin sections are obtained using a field emission gun scanning electron microscope (FEG-SEM) equipped with QEMSCAN software that compares backscattered electron (BSE) and characteristic x-ray signals against a database of standard mineral patterns. These methods permit the analysis of how micron-scale mineralogical heterogeneity varies over distances of tens of vertical meters. As quantifying the effective reactive pore surface area is a key step in improving the predictability of reactive transport models used to assess the fate of CO_2 in the subsurface, the surface area of pores down to micron scale is estimated by summing pore-non pore pixel edges. A sensitivity study is performed on parameters of particular relevance: CO_2 fugacity (8 – 32 MPa), mineral proportions (informed by sample composition), and brine chemistry (date, location, and depth-matched with rock samples).

Preliminary results indicate that, because of the relative abundance of Mg- and Fe-rich minerals at pore surfaces, CO_2-saturated brine-rock interactions exhibit greater reactivity and are more pH-fO_2-dependent than is predicted by models based on the same samples but considering only bulk mineralogy.

Work is performed by the Subsurface Energy Materials Characterization and Analysis Lab at The Ohio State University, and is sponsored by the Dept. of Energy "Nanoscale Control of Geologic CO_2" Energy Frontier Research Center. Core is provided by the Ohio Department of Natural Resources.

Fate of magnetite nanoparticles in leachate-impacted groundwater

A.L. SWINDLE[1*] AND A.S. MADDEN[1]

[1]University of Oklahoma, Norman, OK, USA, (aswindle@ou.edu, amadden@ou.edu)

Nano-scale iron oxides, particularly magnetite, have been suggested as potential reductants for a number of environmental contaminants such as heavy metals, radionuclides, and volatile organics. Experiments have generally shown that magnetite is a viable reductant of a number of contaminants in a laboratory setting [1], though effectivness is influenced by iron-oxide particle size and the presence of additional cationic and anionic species [2]. However, key questions remain about the fate of magnetite nanoparticles in groundwaters with complex chemistry.

Magnetite nanoparticles were synthesized in the laboratory by partial oxidation of ferrous iron sulfate in a basic medium. A combination of TEM and XRD were used to characterize the reation products. A custom-made nanoparticle holder was designed to be compatible with the existing 1" OD groundwater wells at the USGS Norman Landfill Site. By means of this nanoparticle holder, magnetite nanoparticles were deposited on TEM grids and then inserted into a groundwater monitroing well at the USGS Norman Landfill Site. The particles were reacted for 10 days, retrevied from the site, and then stored in an anearobic chamber prior to anaylsis. The reaction products were anaylzed via TEM and compared to the intial characterization. Total volumes were calculated for both the initial synthesis products and the reacted magnetite particles. These volumes were compared to determine the volume of material lost and to calculate an approximate dissolution rate.

TEM characterization of the synthesis products indicated euhedral magnetite with a size range of 250 to 11 nm, along with euhedral goethite particles. Mineralogies identified in synthesis products via TEM were confirmed by XRD analysis. TEM analysis of the reacted particles revealed that the particles were subhedral, indicating dissolution of the magnetite particles, primarily at the corners and edges. Bright field images also indicated a textured surface on the reacted magnetite surfaces, which is also indicative of dissolution of the iron oxide particles.

Experimental results indicate that the magnetite particles lost 10 to 30 percent of their total volume over the 10 day time period. Interestingly, no clear trend between particle size and total volume lost was apparent in the data. An approximate dissolution rate of 2.9 (0.9) x 10^{-9} nmol/m^2*day was obtained using the TEM images.

[1] Roh (2003) *Clay and Clay Minerals* **51**, 83-95. [2] Roonasi (2010) *Surface and Interface Analysis* **42**, 1118-1121.

Implications of noble gases in Stardust samples for the source of Earth's water

TIMOTHY D. SWINDLE

Lunar and Planetary Laboratory, University of Arizona, Tucson AZ USA, tswindle@lpl.arizona.edu

Comets as the Source of Earth's Water

Comets have long been considered a possible source of Earth's water. The compositions of comets would provide an obvious constraint, but the only compositional parameter that has been widely applied is the D/H ratio. Although most comets in which D/H have been measured have ratios a factor of two higher than Earth's oceans, a recent measurement of Comet Hartley 2 gave an Earth-like ratio [1], reviving interest in the idea of a cometary source.

Another compositional parameter that could prove powerful is the noble gas abundance in comets. Based on a spectroscopic measurement of the Ar/O in the coma of Comet Hale-Bopp [2], Swindle and Kring [3] argued that if comets had brought in the Earth's water, orders of magnitude more noble gas would be in Earth's atmosphere than there presently is. However, that measurement has not been replicated, and other measurements suggest much lower noble gas abundances in comets, giving only upper limits [4].

More recently, noble gases have been measured in samples returned from the coma of Comet Wild 2 by the Stardust mission, so it is appropriate to revisit the argument, considering only the noble gases in the dust.

Extrapolating Stardust measurements to Xe in comets

Marty et al. [5] measured He and Ne in Stardust samples, and concluded that the dust contained ~0.1 cm^3STP of Q-type ^{20}Ne per gram of dust (~9 x 10^{-5} g_{Ne}/g). If we conservatively assume that comets are 10% dust, that would mean that to bring in an amount of H_2O equivalent to the Earth's oceans, 3 x 10^{-4} of Earth's mass [6] would also bring in more than 1000 times as much Ne as is currently present in the atmosphere (~10^{-12} g_{Ne}/g). However, Ne is light enough that it is possible that it would not be retained during cometary impacts (although its molecular weight is higher than that of H_2O). If we consider Xe instead, the ^{20}Ne/^{132}Xe (molar) ratio in Q-type gas is 3.2, which would mean that an ocean's worth of cometary water would contain more than 10,000 times as much ^{132}Xe as the present atmosphere. It is difficult to envision ways to lose that amount of Xe, although the argument does depend on the identification of the Stardust Ne as Q-type. Furthermore, this argument only applies to the dust, and does not even consider the ice, which could have large amounts of noble gases as well.

Once again, noble gas abundances appear to be a problem for arguing for a cometary source for Earth's water, but more definitive measurements are clearly needed.

[1] Hartogh et al. (2011) *Nature* **478,** 218-220. [2] Stern et al. (2000) *Astrophys. J.* 544, L169-L172. [3] Swindle and Kring (2001) *11th Goldschmidt Conf.*, Abstract #3785. [4] Weaver et al. (2002) *Astrophys. J.* 576, L95-L98. [5] Marty et al. (2008) *Science* **319**, 75-78. [6] Abe et al. (2000) In *The Origin of the Earth and Moon*, 413-433.

Isotopic constraints on water and carbon fluxes in Langat Basin, Peninsular Malaysia: A Reconnaissance Study

MUHAMMAD.I.SYAKIR[1,2*], IAN.D.CLARK[1], JAN VEIZER[1]

[1]University of Ottawa, Dept. of Earth Sciences, Ottawa, Canada, misha104@uottawa.ca (*presenting author)
[2]Universiti Sains Malaysia, School of Industrial Technology, Penang, Malaysia

Introduction

Evapotranspiration is a nexus for planetary energy and carbon cycles, but it remains poorly constrained. Here we use stable isotopes of Oxygen and Hydrogen to partition flux of water due to plant transpiration from the direct evaporative flux from soils, water bodies and plant surfaces in the tropical watershed of Peninsular Malaysia.

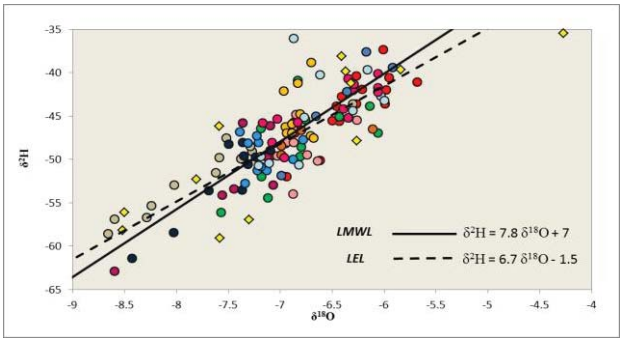

Figure 1 : Intersection of Local Meteoric Water Line (LMWL) and the Local Evaporative Line (LEL) in the Langat Basin.

Results and Conclusions

Mean annual rainfall, obtained from 30 years of hydrological data, is ~2078 mm. Tentatively, 45% of this precipitation returns to the atmosphere via transpiration (T), with 38% partitioned into discharge (R), 9% into interception (I_n), and 8% into evaporation (E_d), emphasizing the role of water cycle as a "conveyor belt" essential for nutrient transport in terrestrial ecosystems [1,2]. The flux of carbon from the atmosphere to the tropical ecosystem of the watershed, related to this transpiration water flux via water utilization factor (WUE), is about 505 g C m^{-2} yr^{-1}.

[1] Ferguson & Veizer (2007) *J.Geophys.Res.*, **122**, D24SO6
[2] Schulte et.al. (2011) *Earth-Science Review* **109**, 20-31.

Metagenomic Analysis of Inactive Hydrothermal Sulfides from Lau Basin

JASON B. SYLVAN[1*] AND KATRINA J. EDWARDS[2]

[1]University of Southern California, Los Angeles, CA, USA, jsylvan@usc.edu*

The East Lau Spreading Center (ELSC) and Valu Fa Ridge comprise a ridge segment in the southwest Pacific Ocean where rapid transitions in the underlying mantle lenses manifest themselves by gradients in seafloor rock geochemistry. At the spreading center in the north, basaltic host rock extrudes while the influence of subduction in the south creates mainly basaltic andesite host rock, with a continuous gradient between these two end members. We studied the geology and microbial diversity of seafloor silicate rock samples and inactive sulfide chimney samples collected along the ELSC and Valu Fa Ridge by X-ray diffraction, elemental analysis, thin section analysis, bacterial 16S rRNA sequencing and metagenomic analysis. Here, we discuss results from the inactive sulfides. On a chimney collected from the ABE vent field, the outside portion of the chimney was dominated by sulfur oxidizing Gammaproteobacteria in the SUP05 clade whereas the inside conduit of the same inactive chimney was dominated by the sulfate reducers in the deltaproteobacterial family Desulfobulbaceae. An inactive sulfide chimney sampled from Tui Malila vent field, where host rock is more strongly influenced by dewatering reactions from the subducting plate, hosted a starkly different bacterial community; sulfur oxidizing Epsilonproteobacteria in the genera *Sulfuromonas* and *Sulfurovum* were recovered from the same sample along with sulfate reducing Desulfobulbaceae and methane oxidizing Gammaproteobacteria in the order Methylococcales, indicating that this sample was either recently inactive or in the final stages of cessation of venting. We also present here the preliminary analysis of metagenomes sequenced from these samples using an Ion Torrent next generation sequencing machine.

The record of early crustal evolution preserved in detrital zircons from Mount Murchison metasedimentary rocks, Western Australia

P.J. SYLVESTER[1*], A.K. SOUDERS[1] AND J.S. MYERS[2]

[1]Department of Earth Sciences, Memorial University, St. John's, NL, Canada (*psylvester@mun.ca, kate.souders@mun.ca)
[2]Department of Applied Geology, Curtin University, Perth, WA, 6845, Australia (myersm@iinet.net.au)

The Mt. Narryer and Jack Hills metasedimentary belts of the Narryer Terrane of Western Australia have been the subject of intense study for almost thirty years because they contain ca. 4.35 Ga detrital zircons, which are the oldest minerals known on Earth. These rocks also contain numerous younger populations of Hadean and Archean detrital zircons of diverse provenance, preserving a rich archive of information on early crustal evolution. Largely ignored has been a third major sequence of metasedimentary rocks in the Narryer Terrane, located at Mt. Murchison, 27 km south-southeast of Mt. Narryer and 98 km southwest of the Jack Hills. The detrital zircon population at Mt. Murchison can provide insights into the extent of Hadean sources in the Narryer Terrane, and whether magmatic events that produced detrital zircons in this region were episodic or continuous during the Archean.

The Mt. Murchison metasedimentary belt is 5 km long and 2 km wide, and contains fuchsitic quartzite, bedded coarse-grained quartzite, glassy quartzite, and quartz pebble conglomerate that appear similar in appearance to mature clastic units at Mt. Narryer and the Jack Hills. We have determined the U-Pb ages of detrital zircons in a sample of fuchsitic quartzite from Mt. Murchison using laser ablation-inductively coupled plasma mass spectrometry. One-hundred-thirty-nine detrital zircon grains in the sample are concordant within 10%. Seventy percent of the grains have $^{207}Pb/^{206}Pb$ ages that fall within four populations: 3125 ± 40 Ma (16%), 3235 ± 40 Ma (23%), 3445 ± 40 Ma (18%) and 3540 ± 40 Ma (13%). The oldest grain has a $^{207}Pb/^{206}Pb$ age of 3955 ± 12 Ma (2s); the youngest grain is 3001 ± 20 Ma (2s).

The detrital zircon population of the Mt. Murchison sample differs from those of quartzites and conglomerates from Mt Narryer and the Jack Hills in the paucity of grains older than 3.6 Ga, and the presence of a large population of 3.1 – 3.2 Ga grains. On the other hand, the 3.4 Ga age peak in the Mt. Murchison sample is also a prominent detrital zircon age population in the Jack Hills, and 3.5 Ga sources contributed to all three metasedimentary belts. This suggests that while there was significant age heterogeneity in the detrital sources of the Narryer Terrane, there were also some common sources that linked the paleodrainage systems of the Mt. Murchison, Mt. Narryer and Jack Hills areas.

When combined, the detrital zircon age data for all three metasedimentary belts define a rather continuous record of major magmatism in the Narryer Terrane from *ca.* 3100 to 3650 Ma. This implies unusually long-lived and continuous (rather than episodic) magmatic processes for crustal growth in the early Archean. Reconstructing the record of ages of clastic sedimentary sources in ancient terranes requires analysis of multiple depositional units of paleodrainage systems.

PGE abundances in upper mantle xenoliths from the Carpathian-Pannonian Region

CSABA SZABÓ[1] KEIKO HATTORI[2], WILLIAM GRIFFIN[3] , SUE O'REILLY[3] AND LÁSZLÓ ELŐD ARADI[1]

[1]Lithosphere Fluid Research Lab, Eötvös University, Budapest, Hungary (cszabo@elte.hu)
[2]Department of Earth Sciences, University of Ottawa, Canada (khattori@uottawa.ca)
[3]GEMOC, Department of Earth and Planetary Sciences, Macquarie University, Australia

The contents of Os, Ir, Ru, Rh, Pt and Pd were determined in lherzolite xenoliths and their sulfide grains (up to 150 μm) from the Carpathian-Pannonian region (CPR) to evaluate the abundance of the highly siderophile elements in the subcontinental lithospheric mantle beneath the region of the Alpine-Mediterranean area. The studied locations include the Styrian basin (western CPR, Austria), Bakony—Balaton-Highland (central CPR, Hungary), Nógrád-Gömör (northern CPR, Hungary, Slovakia), and the East-Transylvanian basin (eastern CPR, Romania).

Total PGE contents range between 7 and 21 ppb regardless of location. Ir-type PGEs are overall high, 5-12 ppb, which confirms the residual mantle nature of the xenoliths. The ratio of Ir- and Pd-type PGEs varies between 0.83 and 2.83. Os/Ir ratios in xenoliths from Styrian and East-Tranylvanian basins are slightly below the chondritic ratio, whereas those from Bakony—Balaton-Highland are above the chondritic value. Ru/Ir is ca. 30 % higher than the chondritic value in the majority of xenoliths from Styrian and East-Transylvanian basins. In contrast, xenoliths from the Bakony—Balaton-Highland show chondritic Ru/Ir, except xenoliths most strongly depleted in Al. These PGE ratios do not show correlations with Al. Pt and Pd contents and their ratios with Ir-type PGEs correlated with Al, as expected, due to incompatible nature of Pt and Pd during partial melting in the Bakony—Balaton-Highland xenoliths, which have the widest range in Al contents. In situ PGE analyses on sulfide grains (mss, chalcopyrite and pentlandite) show positive correlations of Os, Ir, Ru and Rh, except in sulfides from the Bakony—Balaton-Highland and some sulfides from Nógrád-Gömör and East-Transylvania, whereas Pt and Pd correlate poorly with the Ir-type PGEs. The total concentrations of PGEs range between 4 and 796 ppm. The majority of the PGE patterns show high and variable abundances of Os, Ir, Ru and Rh, with decreasing abundance from Rh to Au and a strong negative Pt anomaly. Sulfides in xenoliths from the Bakony—Balaton-Highland, being basically mss, show a smooth negatively sloped PGE pattern from Os to Au.

Whole-rock and in situ sulfide grain analyses demonstrate that the upper mantle beneath the CPR shows a district-scale variation in PGE abundances. Although the xenoliths show no evidence for modal metasomatism, the variation can be explained by different degrees of partial melting and cryptic metasomatism.

Complex calc-alkaline volcanism recorded in Mesoarchaean supracrustal belts in SW Greenland

KRISTOFFER SZILAS[1*], J. ELIS HOFFMANN[3] AND ANDERS SCHERSTÉN[4]

[1]Geological Survey of Denmark and Greenland - GEUS, Copenhagen, Denmark ksz@geus.dk (* presenting author)
[2]Steinmann Institut, Abt. Endogene Prozesse, Universität Bonn, Germany hoffjoel@uni-bonn.de
[3]Department of Geology, Lund University, Sweden anders.schersten@geol.lu.se

Abstract

In this geochemical study we investigate the petrogenesis of three Mesoarchaean co-magmatic supracrustal belts (Ravns Storø, Bjørnesund and Perserajoorsuaq) situated in southern West Greenland. They comprise mainly amphibolites with a tholeiitic basaltic composition and leucoamphibolites with a calc-alkaline andesitic composition. Both lithological units are cut by aplite sheets of tonalite-trondhjemite-granodiorite (TTG) composition with U-Pb zircon ages of c. 2900 Ma. Lu-Hf and Sm-Nd isochrons based on whole rock samples yield ages of 2990 ±41 Ma and 3020 ±78 Ma, respectively. Leucoamphibolites from the three supracrustal belts show apparent chemical mixing trends between tholeiitic amphibolites and TTG gneisses end-members. By assimilation-fractional-crystallisation (AFC) modelling we can show that one group of leucoamphibolites can be explained by contamination of the parental melts by a TTG-like end-member and another group of high P_2O_5, La and Nb leucoamphibolites can be explained by contamination involving a hypothetical low-silica adakite (slab-melt) end-member. However, the leucoamphibolites are juvenile with $\varepsilon Nd_{(2970Ma)}$ from +2.1 to +3.5 and $\varepsilon Hf_{(2970Ma)}$ of +3.5 to +4.3. Thus, the mafic source of the felsic contaminant melts must have been derived from a depleted mantle source more or less at the same time (<60 Ma) as the volcanism took place. Contamination by older continental crust is not a viable explaining of the data.

Accordingly, our preferred interpretation of the geochemical and isotopic data is that the protoliths of the supracrustal rocks formed in an island arc setting, where early tholeiitic volcanism gave way to calc-alkaline volcanism in a maturing island arc. The apparent AFC trends are best explained by in-situ partial melting of basaltic arc crust to form juvenile TTG- and adakite-melts that mixed with mafic magmas or contaminated their mantle source to produce the calc-alkaline leucoamphibolite protolith. This model has important implications for the general interpretation of other Archaean supracrustal belts, because AFC and chemical mixing trends towards a TTG-like end-member are not uniquely diagnostic of crustal contamination, but may rather reflect processes operating at source levels in volcanic arcs such as melting-assimilation-storage-homogenisation (MASH) or slab-melt metasomatism of their mantle source. This study strongly argues for the operation of uniformitarian subduction zone processes as far back as at least 3000 Ma.

Understanding the formation and properties of Titan's aerosols with the PAMPRE laboratory experiment

C. SZOPA[1*], N. CARRASCO[1], J.J. CORREIA[1], E. HADAMCIK[1], P.R. DAHOO[1], T. GAUTIER[1], A. MAHJOUB[1], J. HE[2], A. BUCH[2], AND G. CERNOGORA[1]

[1]LATMOS, Univ. Pierre & Marie Curie Paris 6 and Univ. Versailles St Quentin, UMR CNRS 8190, IPSL, Paris, France, cyril.szopa@lamtos.ipsl.fr (* presenting author), nathalie.carrasco@lamtos.ipsl.fr, correia@lamtos.ipsl.fr, edith.hadamcik@lamtos.ipsl.fr, prd@lamtos.ipsl.fr, thomas.gautier@lamtos.ipsl.fr, ahmed.mahjoub@lamtos.ipsl.fr, guy.cernogora@lamtos.ipsl.fr
[2]Ecole Centrale Paris, Chatenay Malabry, France, arnaud.buch@ecp.fr, jing.he@ecp.fr

Type Section Heading Here [bold, 9pt font size]

In order to support the treatment and interpretation of data collected by the Cassini and Huygens instrumentation, our team developped in 2004 a laboratory experiment based on a radio-frequency reactive plasma to produce analogues of Titan's aerosols (or "tholins"). This experiment, named PAMPRE, enables to produce tholins under variable controlled conditions compatible with the present and past Titan's upper atmosphere ones. The originality of PAMPRE, compared with other experimental set-ups used to porduce tholins, comes from its capability to generate and maintain the tholins inside the plasma without any wall effects. This specificity thus allows to study the tholins production and growth directly in situ by using the appropriate analytical diagnostics.

The studies we do with PAMPRE can be shared in four distinct actions:

1. Study the physical and chemical properties of tholins. This part is originally the most important one since it is partly dedicated to produce reference data which can be compared with observational data. We also study the influence of the production conditions on the tholins properties to better understand the context in which Titan's aerosols can be produced.
2. Characterize the plasma chemistry in order to constrain the chemical pathways leading to the production of solid organic particles directly from the gaseous phase. This part is obviously correlated to the chemistry that occurs in Titan's atmosphere to generate the aerosols.
3. Characterize the physicla properties of the plasma. This original task is very important to understand the influence the context in which the tholins are produced in the experimental set-up. This makes easier the transposal of our results obtain in laboratory to the Titan's atmosphere.
4. More recently we started the study of the evolution in time of Titan's tholins we produce in the context of Titan's geological times.

The goal of this paper is to present an overview of results obtained in the different branches of study of Titan's tholins with the PAMPRE experiment, with an emphasize on the most recent ones.

Fluxes of sulfide-derived sulfate in the Rio Grande valley

ANNA SZYNKIEWICZ[1*], DAVID M. BORROK[1] AND DAVID VANIMAN[2]

[1]University of Texas at El Paso, Geological Sciences, El Paso TX, USA, aaszynkiewicz@utep.edu (* presenting author), dborrok@utep.edu

[2]Planetary Science Institute, Tuscon AZ, USA, dvaniman@psi.edu

Sulfide oxidation is an important weathering pathway in surface environments. However, few data are available to address the contributions and fluxes of sulfide-derived SO_4^{2-} in hydrologic systems. In order to better understand this process, we measured the seasonal fluxes of SO_4^{2-} and the $\delta^{34}S$-$\delta^{18}O$ of riverine SO_4^{2-} as well as sulfate-rich salt efflorescenses in three watersheds connected to the upper Rio Grande valley. In this region, the $\delta^{34}S$ of hydrothermal and biogenic sedimentary sulfides differ by 20-30 ‰ compared to S from evaporites. Therefore, the contribution and fluxes of sulfide-derived SO_4^{2-} can be estimated using S isotope mass balance constraints.

In the Red River, a small tributary to the Rio Grande within the Taos Plateau in northern New Mexico, sulfide-rich mineralization in the form of hydrothermal veins and disseminated pyrite undergoes oxidation in natural alteration scars and abandoned mine waste piles. In April and August of 2010, the measured $\delta^{34}S$ and $\delta^{18}O$ of riverine SO_4^{2-} varied from -2.5 to +1.3 ‰ and from -7.1 to -4.0 ‰, respectively. These variations were consistent with the previously reported $\delta^{34}S$ of pyrite (-13.6 to +2.7 %), and the $\delta^{34}S$ and $\delta^{18}O$ values of gypsum/jarosite (-12.1 to +2.6 ‰ and -9.3 to +3.1 ‰) formed by surface oxidation of hydrothermal sulfides. In the Red River valley, nearly 100 % of aqueous SO_4^{2-} appears to be sourced by sulfide oxidation. The measured flux of sulfide-derived SO_4^{2-} was higher during the snowmelt in April (19.3 tons/day) compared to baseflow conditions in August (15.2 tons/day).

In the Rio Chama and Rio Puerco, tributaries to the Rio Grande in western and central New Mexico, sulfides occur as biogenic pyrite in Cretaceous shale and coal formations. Sulfate-rich salt efflorescences are common weathering products in surface outcrops of these formations. Analysis by X-ray diffraction shows that these are largely Mg, Na, and Ca sulfates (e.g., starkeyite or hexahydrite, thenardite, and gypsum) and $\delta^{34}S$ analyses indicate that the sulfate in these phases formed by sulfide oxidation. Between 2009 and 2011, the contribution of sulfide-derived SO_4^{2-} to the total S load varied widely in the Rio Chama (from 48 to 95 %). S isotopes indicated mixing of SO_4^{2-} from the dissolution of salt efflorescence (-25.2 to -9.5 ‰) and Jurassic evaporites (+15.1 to +17.7 ‰). In the lower reaches of the Rio Chama, the fluxes of sulfide-derived SO_4^{2-} varied widely between Nov 2009 (10.5 tons/day) and Apr 2010 (134.3 tons/day). These variations, however, were to some degree controlled by water releases from upstream reservoirs. Similar contributions of sulfide-derived SO_4^{2-} were calculated for the semi-arid Rio Puerco (68 % of the total S load) during the snow melt season. Because less water is available in the Rio Puerco, the fluxes of sulfide-derived SO_4^{2-} were significantly lower (~3.8 tons/day) compared to the Rio Chama. This investigation indicates that much of the SO_4^{2-} (>50 %) in the upper Rio Grande valley is derived from sulfide oxidation in the surrounding watersheds.